

GREEN POLYMER CHEMISTRY:
SYNTHESIS OF POLY(DISULFIDE) POLYMERS AND NETWORKS

A Dissertation

Presented to

The Graduate Faculty of The University of Akron

In Partial Fulfillment

of the Requirements for the Degree

Doctor of Philosophy

Emily Quinn Rosenthal-Kim

December, 2013

**GREEN POLYMER CHEMISTRY:
SYNTHESIS OF POLY(DISULFIDE) POLYMERS AND NETWORKS**

Emily Quinn Rosenthal-Kim

Dissertation

Approved:

Advisor
Dr. Judit Puskas

Accepted:

Department Chair
Dr. Coleen Pugh

Committee Chair
Dr. Matthew L. Becker

Dean of the College
Dr. Stephen Z. D. Cheng

Committee Member
Dr. Abraham Joy

Dean of the Graduate School
Dr. George R. Newkome

Committee Member
Dr. Chrys Wesdemiotis

Date

Committee Member
Dr. Lingyun Liu

AKNOWLEDGEMENTS

I would like give sincere thanks to my advisor, Dr. Judit E. Puskas. She is the unequivocal embodiment of the high standards which she sets for all of her students, and working for her has been both inspirational and educational. I would like to thank my graduate committee members Dr. Matthew Becker, Dr. Abraham Joy, Dr. Chrys Wesdemiotis and Dr. Lingyun Liu for their time and guidance in helping me complete this research. I am also grateful to all the past and present members of the BioMERG research group who have always made it a joy to come to work. I would like to thank Dr. Agapov and Dr. Wilk for providing AFM images. I would also like to thank Dr. Adel Halasa for all his encouragement over the years.

My parents, Barbara and Rosey Rosenthal, deserve a multitude of thanks for teaching me the skill of creativity and for always letting me find my own path. Finally, I would like to thank my husband, Yong Min Kim, who is my unwavering champion.

ABSTRACT

The disulfide group is unique in that it presents a covalent bond that is easily formed and cleaved under certain biological conditions. While the ease of disulfide bond cleavage is often harnessed as a method of biodegradation, the ease of disulfide bond formation as a synthetic strategy is often overlooked. The objective this research was to synthesize poly(disulfide) polymers and disulfide crosslinked networks from a green chemistry approach. The intent of the green chemistry approach was to take advantage of the mild conditions applicable to disulfide bond synthesis from thiols. With anticipated use as biomaterials, it was also desired that the polymer materials could be degraded under biological conditions.

Here, a new method of poly(disulfide) polymer synthesis is introduced which was inspired by the reaction conditions and reagents found in Nature. Ambient temperatures and aqueous mixtures were used in the new method. Hydrogen peroxide, one of the Nature's most powerful oxidizing species was used as the oxidant in the new polymerization reaction.

The dithiol monomer, 3,6-dioxa-1,8-octanedithiol was first solubilized in triethylamine, which activated the thiol groups and made the monomer water soluble. At room temperature, the organic dithiol/amine solution was then mixed with dilute aqueous hydrogen peroxide (3% by weight) to make the poly(disulfide) polymers. The presence of a two phase system (organic and aqueous phases) was critical to the polymerization

reaction. As the reaction progresses, a third, polymer phase appeared. At ambient temperatures and above, this phase separated from the reaction mixture and the polymer product was easily removed from the reaction solution. These polymers reach $M_n > 250,000$ g/mol in under two hours. Molecular weight distributions were between 1.5 and 2.0. Reactions performed in an ice bath which remain below room temperature contain high molecular weight polymers with $M_n \approx 120,000$ g/mol and have a molecular weight distribution of around 1.15. However, the majority of the product consists of low molecular weight cyclic poly(disulfide) oligomers. In reactions maintained below 18°C, the organic components were miscible in the aqueous hydrogen peroxide and a milky emulsion was produced. The polymers were degraded using the disulfide-specific reducing agent, dithiothreitol

Poly(disulfide) polymer networks were also synthesized in a two-phase system. Due to the poor solubility of the crosslinker, trimethylolpropane tris(2-mercaptopropionate, organic solvents were required to obtain consistent networks. The networks were degraded using dithiothreitol in tetrahydrofuran. The networks were stable under aqueous reducing conditions.

The disulfide-bearing biochemical, α -lipoic acid, was investigated as monomer for the new method of poly(disulfide) polymer synthesis. It was also polymerized thermally and by a new interfacial method that proceeds at the air-water interface. Polymer products were often too large to be characterized by SEC ($M_n > 1,000,000$ g/mol). A poly(α -LA) polymer sample showed mass loss in aqueous solutions of glutathione at pH = 5.2 which was used to model cytosolic conditions. Poly(α -LA) was decorated with PEG (2,000 g/mol) in an esterification reaction catalyzed by Candida

antarctica lipase B (CALB). The decorated polymers were imaged using AFM which revealed branch-like structures.

To make new α -lipoic acid based monomers and macromonomers, CALB-catalyzed esterification, was used to conjugate α -lipoic acid to a variety of glycols including: diethylene glycol monomethyl ether, tetraethylene glycol, hexaethylene glycol, and poly(ethylene glycol). The products were verified using NMR spectroscopy and mass spectrometry.

TABLE OF CONTENTS

	Page
LIST OF TABLES	ix
LIST OF FIGURES	xiii
LIST OF SCHEMES.....	xxi
LIST OF ABBREVIATIONS.....	xxiii
CHAPTER	
I. INTRODUCTION	1
II. BACKGROUND.....	4
2.1. Poly(disulfide) polymers.....	4
2.2. Disulfide networks in biomaterials	17
2.3. Thiol oxidation in biological systems	22
2.4. Biomaterials using α -lipoic acid	27
III. EXPERIMENTAL.....	38
3.1. Materials and instrumentation.....	38
3.2. Methods.....	42
IV. RESULTS AND DISCUSSION.....	62
4.1. New oxidative polymerization of DODT using triethylamine and H_2O_2	62
4.2. Mechanism investigation	114
4.3. Copolymerization of DODT with ED	125
4.4. Disulfide network synthesis.....	142

4.5. Polymerization of α -lipoic acid and synthesis of α -lipoic acid derivatives.....	170
4.6. Synthesis of monofunctional α -LA derivatives via enzymatic catalysis.	210
V. CONCLUSIONS.....	217
REFERENCES	224
APPENDICIES	233
APPENDIX A. THIOKOL MONOMERS	234
APPENDIX B. MEASUREMENT OF DN/DC FOR POLY(DODT) IN THF	236
APPENDIX C. AFM IMAGES OF POLY(α -LA-PEG) and POLY(α -LA-PEG- <i>co</i> - α -LA)	239

LIST OF TABLES

Table	Page
3.2.1. Concentrations of reagents in kinetic studies with variation in triethylamine concentration.....	45
3.2.2. Concentration of reagents in the aqueous and two phase DODT polymerizations.....	48
3.2.3. Comonomer solutions of ED with DODT	50
3.2.4. Concentration of TMPTMP in each DODT/amine solution.....	53
3.2.5. Final concentration of reagents in optimized network reaction.....	54
3.2.6. Reaction conditions for the polymerization of R- α -LA using triethylamine and aqueous H ₂ O ₂	56
3.2.7. Reaction conditions for the synthesis of CH ₃ -DEG- α -LA.....	59
3.2.8. Reaction conditions HO-TEG- α -LA and HO-HEG- α -LA synthesis.....	59
3.2.9. Reagent concentration in the synthesis of HO-TEG- α -LA.....	61
4.1.1. Volume and moles of reagents used in preliminary studies with sonication	63
4.1.2. Volume and moles of reagents used in scouting reactions.	64
4.1.3. Volume and moles of reagents used in exploratory reactions.	65
4.1.4. Conditions and results of example polymerization reactions	68
4.1.5. SEC data for the room-temperature reactions listed in 4.1.4.....	75
4.1.6. Results of SEC analysis for polymerizations performed in an ice bath.....	79
4.1.7. The conversion data collected from the kinetic experiment where triethylamine and DODT were mixed in a 2.25:1 molar ratio.....	86

4.1.8. Results from SEC analysis of poly(DODT) in kinetic study where triethylamine and DODT were mixed in 2.25:1 molar ratio.....	87
4.1.9. Concentrations of reagents in kinetic studies with variation in triethylamine concentration.	89
4.1.10. SEC data from kinetic studies with variation in triethylamine concentration.....	90
4.1.11. SEC data from samples taken during high stir-rate polymerization of DODT in an ice bath.....	93
4.1.12. Estimated peak MW of fringe peaks in the 2 min aliquot of the DODT polymerization with $[H_2O_2] = 0.375\text{ M}$	96
4.1.13. SEC results from the DODT polymerization with $[H_2O_2] = 0.375\text{ M}$	97
4.1.14. Material recovered from each sample in the chain extension study.	100
4.1.15. SEC results from chain extension study	105
4.1.16. Molecular weights of oxidized polymers compared to starting polymers.....	110
4.1.17. SEC results for oxidized polymers compared to starting polymers.....	110
4.2.1. Concentration of reagents in two DODT polymerizations.	119
4.2.2. Relative amount of oligomers found in each sample by ESI-MS.....	120
4.2.3. Results from SEC analysis of poly(DODT) samples.....	125
4.3.1. FTIR assignments for ED and poly(ED)	128
4.3.2. Results from copolymerization survey of ED with DODT.	130
4.3.3. Copolymer compositions in mole fraction ED based on NMR integrations	133
4.3.4. Thermal transitions of homopolymers and copolymers.....	136
4.3.5. Copolymer decomposition temperatures and residual mass for each copolymer. T_2 and T_{50} are 2% and 50% mass loss temperatures.	138
4.3.6. Results from SEC analysis of copolymers from reactions with different stirring rates.	141

4.4.1. Scouting studies for poly(disulfide) network synthesis.....	143
4.4.2. Scouting studies for poly(disulfide) network with variation thiol:amine molar ratio.....	144
4.4.3. Final concentration of reagents in small and large scale network synthesis.....	147
4.4.4. Results from a series of networks made using optimized method.....	148
4.4.5. Results from THF swelling study using small samples from optimized recipe.....	157
4.4.6. Results from DI H ₂ O swelling study using small standardized samples.....	157
4.4.7. Group molar attraction constants (F) and DODT unit molar attraction constant.....	158
4.4.8. Solubility parameters for calculated poly(DODT) repeat unit.	159
4.4.9. M _c calculated from Flory-Rehner Eq (Eq. 2.1).....	159
4.4.10. Solubility parameter for poly(DODT) repeat unit.	161
4.4.11. Results from GSH (Aq) degradation in acidic buffer (pH = 5.2).	165
4.4.12. Results from poly(DODT) network exposure to digestive system model.....	166
4.5.1. Thermal transitions of R- α -LA and DL- α -LA.....	174
4.5.2. Reaction conditions and conversions the polymerization of R- α -LA using triethylamine and aqueous H ₂ O ₂	175
4.5.3. Reaction conditions and conversions for the thermal polymerization of α - LA under vacuum	184
4.5.4. Results from SEC analysis of thermally polymerized α -LA monomers	189
4.5.5. Molding conditions for α -LA monomers and observations.....	202
4.5.6. Yield and conversion data for the three precipitation polymers.	207
4.5.7. SEC data for polymers synthesized by precipitation (dn/dc = 0.109 mL/g).....	208
4.6.1. Conversion results from reaction of CH ₃ -DEG and α -LA after 14 hours at 55°C.....	210

4.6.2. Reagent concentrations and conversions for α -LA-TEG-OH and α -LA-HEG-OH synthesis.....	213
--	-----

LIST OF FIGURES

Figure	Page
2.1.1 Dithiol monomer polymerized by Wang <i>et al.</i> ²⁴	14
2.3.1. Diagram of the glutathione enzyme system. ⁵⁶	27
2.4.1. (R)- α -lipoic acid.....	26
2.4.2. Protein adsorption onto ethanethiol-tethered SAMs (A, left) is compared to α -LA-tethered SAMs (B, right) using SPR. Reproduced from Karamanska, R.; Mukhopadhyay, B.; Russell, D. A.; Field, R. A., <i>Chemical Communications (Camb)</i> 2005 , 26, 3334-3336, with permission of The Royal Society of Chemistry.....	30
2.4.3. Structure of poly(α -LA) (A) and poly(thio-1-oxo-6- mercaptopoctamethylene) (B).....	33
2.4.4. Structure of copolymers of α -LA and cyclic phosphonites (TPO followed by SPO). ⁽⁸⁰⁾	34
2.4.5. Poly(α -LA- <i>co</i> -DT) synthesis and crosslinking. Reprinted by permission from Macmillan Publishers Ltd: <i>Polymer Journal</i> , Yamanaka, T.; Endo, K., <i>Polymer Journal</i> 2007 , 39, 1360-1364. Copyright (2007).	36
3.1.1. Dithiol monomers: a. 1,2-ethanedithiol, b. 3,6-dioxa-1,8-octanedithiol	38
3.1.2. Trithiol reagents: a. trimethylolpropane tris(2-mercaptopropionate), b. trimethylolpropane tris(2-mercptoacetate).....	39
4.1.1. ^1H NMR spectrum of DODT and poly(DODT)(Sample 10-120-55). (500 MHz; CDCl_3 ; 12 s relax; 128 trans.)	70
4.1.2. ^1H NMR spectrum poly(DODT)(Sample 10-9-70). (500 MHz; CDCl_3 ; 12 s relax; 128 trans.)	71
4.1.3. ^{13}C NMR spectrum of DODT (A) and poly(DODT) (B; Sample 10-120-55). (500 MHz; 10 s relax.; 1024 trans.)	72

4.1.4. FTIR spectra from DODT and poly(DODT) sample 10-120-55: (a) 2557 cm ⁻¹ , S-H stretch; (b) 667 cm ⁻¹ , C-S from thiols; (c) 1042 cm ⁻¹ , C-O asymmetric ether stretch; (d) 644 cm ⁻¹ , C-S stretch of disulfides; (e) 467 cm ⁻¹ , S-S stretch. Reprinted with permission from { Rosenthal, E. Q., Puskas, J.E.; Wesdemiotis, C. <i>Biomacromolecules</i> , 2011 , <i>13</i> , 154-164}. Copyright {2011} American Chemical Society..	74
4.1.5. Light scattering (LS), refractive index (RI) and UV chromatograms from SEC analysis of poly(DODT) sample 10-120-55.....	76
4.1.6. Refractive index (RI) chromatograms from SEC analysis of poly(DODT) samples 10-25-Ice (top) and 160-25-Ice (bottom). Reprinted with permission from { Rosenthal, E. Q., Puskas, J.E.; Wesdemiotis, C. <i>Biomacromolecules</i> , 2011 , <i>13</i> , 154-164}. Copyright {2011} American Chemical Society	78
4.1.7. MALDI-ToF MS spectrum for low MW fraction of poly(DODT) sample 10-120-55 showing oligomers from hexamer (1103.4 m/z) to 26-mer (4707.5 m/z).....	80
4.1.8. Isotope distribution for hexamer from poly(DODT) sample 10-120-55 (A), isotope distribution pattern predicted using ChemCalc software for cyclic poly(DODT) hexamer (B). ⁸⁸	81
4.1.9. Mass spectrum for sample 10-25-Ice	82
4.1.10. Emulsion formed in reaction 10-60-15 after 1 day at room temperature.	83
4.1.11. ESI-MS spectrum of emulsion formed in reaction 10-60-15.....	83
4.1.12. The monomer consumption is plotted against reaction time past 90 % conversion where triethylamine was present in a 2.25:1 molar ratio with DODT.	86
4.1.13. M _n conversion plot for the oxidative polymerization of DODT where triethylamine was present in a 2.25:1 molar ratio relative to DODT.....	87
4.1.14. Monomer consumption is plotted against time for the polymerization reaction where triethylamine was present in a 2:1 molar ratio relative to DODT..	88
4.1.15. The monomer consumption with time is plotted for studies which compared low (0.306 M) and high (1.833 M) triethylamine concentrations.....	90
4.1.16. The M _n is plotted against conversion for DODT polymerizations with low (0.306 M) and high (1.833 M) triethylamine concentrations.....	91

4.1.17. M_n (solid) and (M_w/M_n) (dashed) are plotted against time for the high stir rate polymerization in an ice bath.....	93
4.1.18. RI trace from the 35 min and 120 min samples taken from the DODT polymerization with mechanical stirring	94
4.1.19. RI traces from timed samples from reaction where $[H_2O_2] = 0.375\text{ M}$	96
4.1.20. MALDI-ToF spectrum of 2 min sample from reaction where $[H_2O_2] = 0.375\text{ M}$	98
4.1.21. MALDI-ToF spectrum of 35 min sample from reaction with $[H_2O_2] = 0.375\text{ M}$	98
4.1.22. 1H NMR spectra from the chain extension experiment (12s relax, 64 trans.; 500 MHz; $CDCl_3$). Reprinted with permission from { Rosenthal, E. Q., Puskas, J.E.; Wesdemiotis, C. <i>Biomacromolecules</i> , 2011 , <i>131</i> , 154-164}. Copyright {2011} American Chemical Society.	101
4.1.23. ^{13}C NMR spectrum of the final polymer from the chain extension experiment.(12 s relax; 64 trans.; $CDCl_3$; 500 MHz). Reprinted with permission from { Rosenthal, E. Q., Puskas, J.E.; Wesdemiotis, C. <i>Biomacromolecules</i> , 2011 , <i>131</i> , 154-164}. Copyright {2011} American Chemical Society	103
4.1.24. Solid state ^{13}C NMR spectrum of insoluble fraction from final product of chain extension study. Reprinted with permission from { Rosenthal, E. Q., Puskas, J.E.; Wesdemiotis, C. <i>Biomacromolecules</i> , 2011 , <i>131</i> , 154-164}. Copyright {2011} American Chemical Society.	104
4.1.25. RI SEC traces from the chain extension study.....	105
4.1.26. Disulfide reduction of a poly(DODT) sample 10-120-55 by dithiothreitol (DTT) (32 trans.; 300 MHz; $CDCl_3$). Reprinted with permission from { Rosenthal, E. Q., Puskas, J.E.; Wesdemiotis, C. <i>Biomacromolecules</i> , 2011 , <i>131</i> , 154-164}. Copyright {2011} American Chemical Society	107
4.1.27. The DSC trace of poly(DODT) for sample 10-120-55 showing T_g . (2 nd heating; heating rate = $10^\circ\text{C}/\text{min}$).....	108
4.1.28. The TGA decomposition profile of Sample 10-120-55. (N_2 atmosphere; heating rate of $10^\circ\text{C}/\text{min}$). Reprinted with permission from { Rosenthal, E. Q., Puskas, J.E.; Wesdemiotis, C. <i>Biomacromolecules</i> , 2011 , <i>131</i> , 154-164}. Copyright {2011} American Chemical Society.	109
4.1.29. Mark-Houwink-Sakurada constants derived from slope and intercept of log $[\eta]/\log M_w$ plot.....	112

4.1.30. Catenane proposed by Ishida and coworkers for their poly(disulfide) polymer from 1,2-dithane. Reprinted by permission from Macmillan Publishers Ltd: Polymer Journal,[Ishida, H.; Kisanuki, A.; Endo, K. <i>Polymer Journal</i> , 2009 , <i>41</i> , 110-117. Copyright (2009).	113
4.1.31. ^1H NMR spectrum of iodine-oxidized poly(DODT) sample (30 min) (12 s relax.; 64 trans; CDCl_3 ; 300 MHz)	114
4.2.1. ^1H NMR spectrum of DODT in D_2O (3 s relax.; 64 scans; 300 MHz; D_2O)	115
4.2.2. ^1H NMR spectrum of DODT with triethylamine in D_2O shows improved aqueous solubility of ionized DODT. (3 s relax.; 64 scans; 300 MHz; D_2O).....	116
4.2.3. ^1H NMR spectrum of organic phase in CDCl_3 after the addition of H_2O_2 . (3 s relax.; 64 scans; 300 MHz; CDCl_3)	118
4.2.4. Mass spectrum of reaction solution from the aqueous solution system.....	121
4.2.5. ESI mass spectrum of DODT dimer showing cyclic and linear species.....	122
4.2.6. ^1H NMR spectrum of polymer from pre-dissolved system in CDCl_3 . (500 MHz; 10 s relax.; 128 scans)	123
4.2.7. ^{13}C NMR spectrum of polymer from pre-dissolved system in CDCl_3 . (1 s relax.; 1024 scans; 500 MHz)	124
4.2.8. RI traces from SEC analysis of poly(DODT) samples prepared from aqueous and two-phase systems.....	125
4.3.1 Comparison of ED (<i>solution</i> ; CDCl_3) and polyED (<i>solid state</i>) ^{13}C NMR spectra.	126
4.3.2: Comparison of ED and poly(ED) FTIR spectra.	127
4.3.3. DSC second heating cycle for poly(ED) from polymerization with 24 hr reaction time.....	129
4.3.4. FTIR spectra for all ED-DODT copolymers in survey.....	131
4.3.5 ^1H NMR spectra from soluble copolymers and poly(DODT) (12 s relax; 128 trans.; 300 MHz; CDCl_3)	132
4.3.6. ^{13}C NMR spectrum for copolymer sample ED-5-S. (10 s relax. 1024 trans.; 500 MHz; 1024 trans.; CDCl_3)	134
4.3.7. DSC traces for poly(ED) and poly(ED-co-DODT) samples.	135

4.3.8. The Fox plot for ED-DODT copolymers is compared to the experimental data.....	137
4.3.9. Stress-strain curves for CB-filled poly(DODT) and poly(ED-co-DODT) (Extension rate = 50 mm/min)	139
4.3.10. ^1H spectra of Mag-ED-3 and Mech-ED-3 are compared.(1 s relax; 64 trans.; 500 MHz; CDCl_3)	141
4.3.11. SEC traces (LS and RI) for Mag-ED-3 and Mech-ED-3.....	142
4.4.1. Crosslinker, trimethylolpropane tris(2-mercaptopropionate) (TMPTMP)	142
4.4.2. Small-scale networks at 72 hrs reaction time (in order of decreasing [TMPTMP]).	148
4.4.3. Small-scale networks extracting in acetone (in order of decreasing [TMPTMP]).	149
4.4.4. Large-scale networks swollen with THF	150
4.4.5. Large-scale networks are shown after purification and drying.....	150
4.4.6. ^1H NMR spectrum of swollen poly(DODT) network with 50:1 crosslinker ratio (10 s relax; 128 trans.; THF-d_8 ; 300 MHz;)	151
4.4.7. ^{13}C NMR spectrum of swollen poly(DODT) network with 50:1 crosslinker ratio. (THF-d_8 ; 300 MHz; 6 s relax; 4096 trans.)	152
4.4.8. Solid-state, ^{13}C NMR of 100:1 network (1024 s; 400 MHz).....	153
4.4.9. DRIFTS spectra for three networks with three different crosslinker ratios	154
4.4.10. Mass gain for networks swollen in THF (error bars are propagated error values).....	156
4.4.11. Mass gain for networks swollen in DI H_2O (error bars are propagated error values).....	156
4.4.12. Cartoon of DODT polymerization with organic solvent mixture used in network synthesis.....	160
4.4.13. RI and LS traces from poly(DODT) polymer sample Top	160

4.4.14. ^1H NMR of Top polymer sample (12 s relax.; 128 trans.; 500 MHz; CDCl_3).....	162
4.4.15. ^{13}C NMR of Top polymer sample (1 s relax.; 1024 trans.; 500 MHz; CDCl_3).....	163
4.4.16. Network samples before and after exposure to HCl (A) and bile salt solutions (B = 4.5 mg/mL and C = 200 mg/mL)	166
4.4.17. Network conversions at 4 days with and without sodium pyrophosphate.....	167
4.4.18. Poly(DODT) network conversion with time using the $\text{Na}_4\text{P}_2\text{O}_7/\text{H}_2\text{O}_2$ system	169
4.5.1. ^1H NMR spectra of DL- α -LA (top) and R- α -LA (bottom) (3s relax; 128 scans; 500 MHz; CDCl_3)	171
4.5.2. ^{13}C spectrum of R- α -LA (2s relax; 8192 scans; 500 MHz; CDCl_3);	172
4.5.3. Full DSC heating cycles for DL- α -LA and R- α -LA; Heating rate: 2.5°C/min	174
Figure. 4.5.4. ^1H NMR of R-Ox-23 (12 s relax.; 128 scans; methanol- d_4 ; 300 MHz).	177
4.5.5. Possible monomer configurations in polymer backbone of poly(α -LA).	179
4.5.6. ^{13}C NMR of R-Ox-23 (300 MHz; 12 s relax.; 2400 scans; methanol- d_4)	179
4.5.7. A) FTIR spectrum α -lipoic acid from SBDS* B) FTIR spectra of R-Ox-23 and R-Ox-0. (64 scans)	181
4.5.8. DSC chromatograms of 2 nd and 3 rd heating cycles for sample R-Ox-0 (heating rate = 10°C/min).....	183
4.5.9. ^1H NMR spectra of samples DL-T-90-A and R-T-90 (10 s relax.; 512 scans; 500 MHz; methanol- d_4)	185
4.5.10. ^1H NMR of sample R-T-80-1 st PPTN (15 s relax; 32 scans; 300 MHz; DMSO-d_6)	187
4.5.11. SEC chromatograms from R-T-100.....	188
4.5.12. SEC chromatograms from R-T-80-1 st PPTN (top) and R-T-80-2 nd PPTN (bottom) are compared.....	188

4.5.13. Amplification strategies for AFM visualization of poly(α -LA) chains.	190
4.5.14. ^{13}C NMR spectrum of PEG-decorated poly(α -LA). (6 s relax.; 5000 scans; CDCl_3 ; 300 MHz)	191
4.5.15. The FTIR spectrum of PEG-decorated poly(α -LA) product.	192
4.5.16. The LS (red), RI (blue) and UV (green) traces from SEC analysis of the poly(α -LA)-PEG product are shown.....	194
4.5.17. AFM image of a 0.11mg/mL solution of poly(α -LA) sample R-T-100 decorated with 2000 g/mol PEG in chloroform spuncast onto mica.	195
4.5.18. Detail of AFM image of a 0.11mg/mL solution of poly(α -LA) sample R-T-100 decorated with 2000 g/mol PEG in chloroform spuncast onto mica. Height profile taken from area indicated by white horizontal line. Branch indicated by arrow is 290 nm long.....	196
4.5.19. MALDI-ToF MS spectrum of CALB-catalyzed PEG- α -LA conjugation reaction at 1 hr.	198
4.5.20. MALDI-ToF MS spectrum of CALB-catalyzed PEG- α -LA conjugation product at 24 hrs.....	199
4.5.21. The progression for CALB-catalyzed PEG- α -LA conjugation at 60°C under vacuum.....	200
4.5.22. Detail of MALDI-ToF MS spectrum of from uncatalyzed reaction of α -LA and PEG at 24 hrs shows only trace amounts of conjugated product.....	201
4.5.23. Compression molded sheets of DL-CM-90 (A) and R-CM-90 (B).....	203
4.5.24. Tensile curves from sample DL-CM-95 (extension rate = 500 mm/min)	204
4.5.25. The degradation of DL-CM-95 by GSH(50 mM in acetate buffer; pH = 5.2; 37°C) with time is shown.....	205
4.5.26. Tensile curves from samples DL-CM-90 and R-CM-90 at 37°C (extension rate = 500 mm/min)	206
4.5.27. SEC traces (LS and RI) from poly(α -LA) samples R-PPTN-65 and R-PPTN-100	208
4.5.28. Poly(α -LA) filament is pulled from R- α -LA precipitated onto H_2O at 25°C	209
4.6.1. ESI mass spectra for the products of α -LA and DEG esterification.....	211

4.6.2. ^1H NMR spectrum of sample DEG-LA-Bulk (3 s relax.; 64 scans; 500 MHz; CDCl_3)	212
4.6.3. ESI mass spectrum from the product of α -LA and TEG esterification in bulk.	214
4.6.4. ESI mass spectrum from the product of α -LA and HEG esterification.	215
4.6.5. Proton NMR spectra are compared for the TEG and HEG product. (3 s relax, 64 scans in CDCl_3).....	216
5.1. Proposed mechanism for new method of oxidative dithiol polymerization includes both chain-growth and step-grow pathways.....	220

LIST OF SCHEMES

Scheme	Page
2.1.1. Traditional poly(sulfide) polymer synthesis developed by Patrick and Mnookin.....	5
2.1.2. The three fundamental steps in thiol oxidation to disulfides.....	7
2.1.3. Mechanism for base-catalyzed thiol oxidation (adapted from Oae. ¹⁰)	7
2.1.4. Triethylamine-catalyzed, solution polymerization of dithiol monomers under pure oxygen atmosphere reported by Choi <i>et al.</i> ¹⁹	10
2.1.5. Synthesis of disulfide polymers reported by Ishida <i>et al.</i> ²¹	11
2.1.6. Oxidation reaction of two thiols by DMSO to create a disulfide bond. ¹⁰	12
2.1.7. Polymerization of hexane dithiol reported by Goethals and Sillis in 1968. ²²	12
2.1.8. Polymerization of aromatic dithiols using reported by Meng <i>et al.</i> (²³)	13
2.1.9. Oxidation of thiols past the disulfide group to the sulfonic acid. ¹⁰	14
2.2.1. Multi-step synthesis of disulfide crosslinked hyaluronic acid and gelatin hydrogels. ³⁷	20
2.3.1. Cysteine coupling to form cystine followed by the mechanism of disulfide bond reduction by cysteine..	24
2.3.2. Flavin-catalyzed thiol oxidation to disulfides at room temperature. ^{10, 50}	23
4.1.1. Poly(DODT) synthesis with triethylamine and dilute aqueous H ₂ O ₂	67
4.1.2 Disulfide reduction by dithiothreitol (DTT)	106
4.5.1. Redox pathway between dihydrolipoic acid and α -lipoic acid.	170

LIST OF ABBREVIATIONS

α -LA	α -lipoic acid
DEG	diethylene glycol methyl ether
DODT	3,6-dioxa-1,8-octanedithiol
DRIFTS	diffuse reflectance infrared Fourier transform spectroscopy
DSC	differential scanning calorimetry
ED	1,2-ethane dithiol
ESI	electrospray ionization
Et_3N	triethylamine
FTIR	Fourier transfer infrared spectroscopy
GSH	glutathione
GSSG	oxidized glutathione
HEG	hexaethylene glycol
MALDI	matrix assisted laser desorption/ionization
M_c	average molecular weight between crosslinks
M_n	number average molecular weight
M_w	weight average molecular weight
NMR	nuclear magnetic resonance
PEG	poly(ethylene glycol)
SEC	size exclusion chromatography

TEG	tetraethylene glycol
THF	tetrahydrofuran
TMPTMP	trimethylolpropane tris(2-mercaptopropionate)
ToF	time of flight.

CHAPTER I

INTRODUCTION

The antiseptic and healing properties of sulfur have been recorded for thousands of years, but in the growing field of biomaterials, sulfur has the opportunity to play new and important roles. In recent years the chemistry of the disulfide bond has garnered renewed interest because of its active role in biological systems. Thiol-disulfide interchange is a common and constant bioreaction that is critical to protein folding, enzyme activity and the regulation of oxidation potentials within organisms. The oxidation-reduction reactions that drive the thiol-disulfide interchange hold keys to improved processes and materials.

The focus of this research was not only to synthesize new, useful disulfide-bearing materials, but to develop synthetic processes that comply with green chemistry guidelines set out by Anastas and Warner.¹ In nature, both the synthesis and reduction of disulfide bonds proceed under mild reaction conditions that are in line with green chemistry practices. Our aim was to synthesize disulfide-bonded materials in a manner inspired by biological conditions.

By emulating Nature's approach to synthesis in the laboratory, the guidelines of green chemistry fall into place almost automatically. For example, in nature there is an enzyme to catalyze almost every reaction inside an organism, and use of catalysis is the ninth principle of Green Chemistry. Another example is that biochemical reactions

usually proceed at ambient (or near ambient) temperatures. This meets the 6th guideline set by Anastas and Warner—“Design forenergy efficiency.”

Following a green chemistry approach to biomaterials is helpful on many levels. First, it reduces the possibility of accidents (both human or chemical) at the research level. Second, it reduces pollution and energy consumption at the manufacturing level. Lastly, it diminishes concern over the presence of harmful extractables in the final end product of the biomaterial. As the fields of biomaterials and medicine merge closer together, the responsibility to “do no harm” falls as much on the academic researcher as it does on the medical practitioner. Only by following a mindful approach to synthesis can biomaterials researchers uphold that responsibility.

Poly(sulfide) polymers were among the first synthetic polymers created with a patent issued to J. C. Patrick in 1929, however they remain a relatively under-characterized class of polymers and have received a little academic attention. As an example, only two paragraphs are allotted to poly(sulfide) and poly(disulfide) polymers in George Odian’s 811 page text, *Principles of Polymer Chemistry*, neither of which attribute the invention to Patrick.²

Here we report a new method of poly(disulfide) polymer synthesis which was applied to dithiol monomers, as well as to a cyclic disulfide monomer. This method uses mild reaction conditions like ambient temperatures and aqueous mixtures that were directly inspired by disulfide bond synthesis in biological systems. We report a variation of this method to synthesize poly(disulfide) polymer networks. Additionally, a new method for the polymerization of α -lipoic acid is described.

Of equal importance to the newly developed methods, is the investigation into poly(disulfide) polymers as whole. This work uncovers new or forgotten questions about the structure of poly(disulfide) polymers, the mechanism of polymerization and the role of multiphase reaction systems. It is hoped that the findings reported here will foster more detailed investigation into this interesting class of polymers.

CHAPTER II

BACKGROUND

The objective of this research was to apply the principles of green chemistry to the synthesis of poly(disulfide) polymers and networks with anticipated applications as biodegradable biomaterials. A brief history of poly(disulfide) polymers, as well as background helpful in understanding the role of sulfur in biochemistry is provided in the following sections.

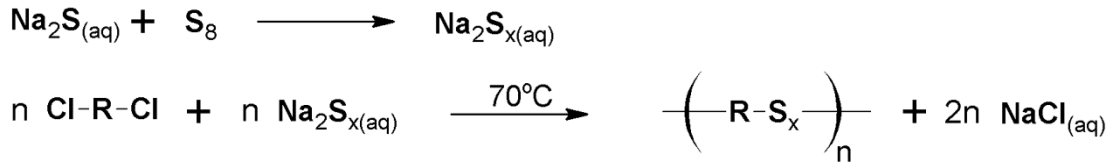
2.1. Poly(disulfide) polymers

2.1.1. Thiokols

Polysulfide polymers were first introduced in the patents of J.C. Patrick and N.M. Mnookin in the late 1920s.^{3, 4,5} Based on their research, Thiokol Corporation was founded, and today the term ‘Thiokol’ is often used interchangeably for polysulfide polymers.² During the next decades, research into polysulfide polymers was dominated by the researchers at Thiokol, and the topic went seemingly unnoticed in academic investigation. Over thirty patents concerning polysulfide polymers were awarded to Thiokol based on the work of Patrick, Mnookin, Fettes, Davis and many others. A visual list of the many monomers polymerized using their methods is given in Appendix A.

In the first step of the Thiokol synthetic route, short sulfur chains of varying lengths were created *in situ* by reacting aqueous sodium sulfide with elemental sulfur. In the second step, α,ω -dihalogenated linear organic compounds³ were added to the sodium

sulfur salt solution and reacted while heating.^{3,4, 5} The sulfur rank (or number of consecutively linked sulfur atoms) of the sulfur salts in step one varies from 1 to 5. Later adaptations varied the reaction conditions to control the average sulfur rank. For example, sulfur salts synthesized from sodium hydroxide, sodium hydrosulfide and elemental sulfur create salts with an average sulfur rank between 1 and 2.⁶ Sodium hydroxide and sulfur alone produce salts with ranks between 2 and 4.5. Some side products produced in the first step, such as sodium thiosulfate, must undergo additional reactions with iodine or hydrogen peroxide to become useful reagents.⁶ Dibrominated and dichlorinated species have both been used in the second step. Monohalides may also be added the reaction to tailor the molecular weight or add terminal functional groups.^{6,7} Thiol terminal groups are produced by the partial reduction of polymers. Higher rank polysulfide bonds may also be reduced to disulfide bonds after the polymer has been made.⁶ The two steps of traditional polysulfide polymerization are shown in Scheme 2.1.1.⁷



Scheme 2.1.1. Traditional poly(sulfide) polymer synthesis developed by Patrick and Mnookin.

The synthetic methods developed at Thiokol became both industrial and academic standards for polysulfide polymer preparation. In 2009, the use of phase transfer catalysts was reported by Ramakrishnan and coworkers⁸ and by Kalaee and coworkers.⁹

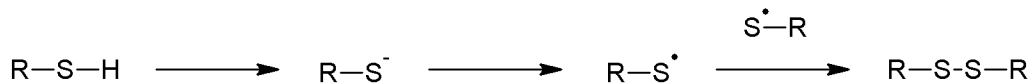
They showed the synthesis of two new polysulfide polymers, using a dihalide and sodium polysulfide reaction and the phase transfer catalyst tetra-*n*-butylammonium bromine (TBAB).⁸ Despite the addition of the TBAB they obtained poor product return (25-30%) compared to the traditional method which generally delivers greater than 80% conversion.⁷

When following synthetic routes that first create sodium salts, the average rank of the sulfur bonds may be controlled to varying specificity, but exclusive formation of disulfide bonds is not expected. Other methods have been developed to produce solely disulfide linkages.

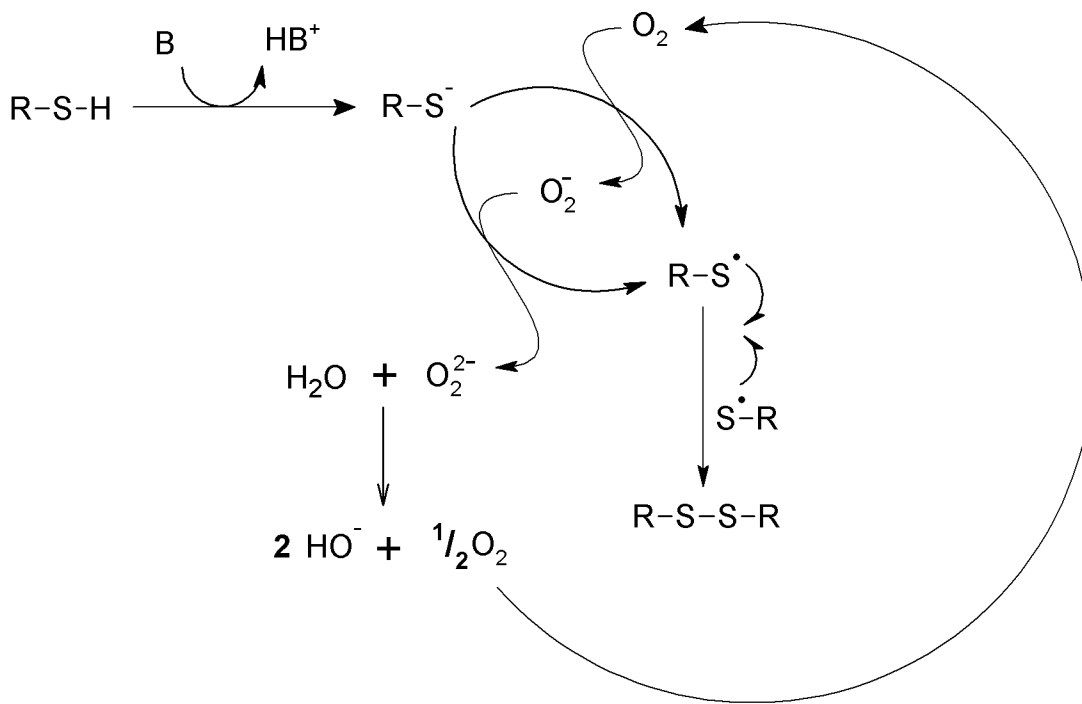
2.1.2. Polymerization of dithiols with oxygen

The oxygen, or air, oxidation of thiols to disulfides is a well-known reaction.¹⁰ The mechanism of the reaction varies depending on the catalyst; however, two common reactive species exist in all oxygen oxidation pathways: the thiolate anion, and the thiyl radical (Scheme 2.1.2).¹⁰ The first step in the reaction is the formation of a thiolate anion by removal of its acidic proton. Thiols are generally more acidic than their alcohol analogues. For example, the pKa of ethyl mercaptan is 10.5,¹¹ while the pKa of ethyl alcohol is 16.¹² The thiolate anion is subsequently converted to a thiyl radical in a single electron transfer to a reducible species (*eg.* an oxygen molecule or oxidized metal cation). Thiyl radicals then couple to form a disulfide. Each oxygen molecule may undergo two reduction reactions thereby oxidizing one thiolate anion per oxygen atom.¹⁰ Reduced oxygen molecules also act as bases and abstract protons from thiols further promoting the reaction. A more detailed mechanism of the base-catalyzed reaction is shown in Scheme

2.1.3. The mechanism of metal-catalyzed reactions is not certain, but it is proposed that the oxygen removes electrons from the metal, which in turn oxidizes the thiolate anion.



Scheme 2.1.2. The three fundamental steps in thiol oxidation to disulfides.



Scheme 2.1.3. Mechanism for base-catalyzed thiol oxidation (adapted from Oae.¹⁰).

In the 1950s, Marvel and Olson published academic research on the synthesis of disulfide polymers. Taking a different approach from the scientists at Thiokol Corporation, they selected α,ω -alkanedithiols as the starting material. The dithiols were suspended in an aqueous solution of lauric acid and potassium hydroxide. Compressed

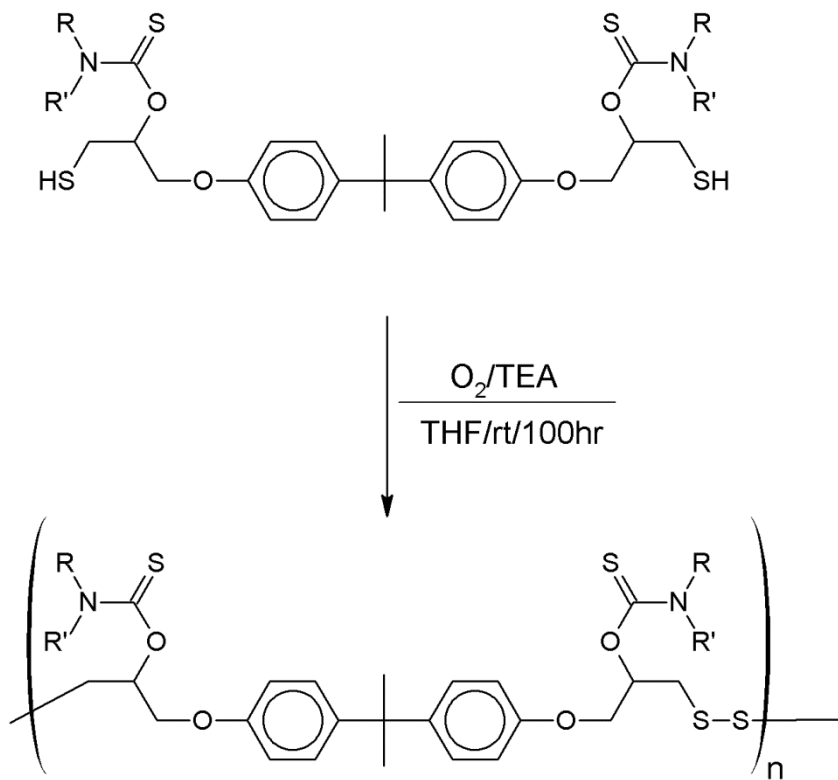
air was bubbled through the emulsion for one to four days. Several other oxidizing agents (bromine, nitric acid, and ferric chloride) were investigated, but they found that air oxidation produced the best results.¹³ They also discovered the utility of selenious acid as a catalyst for the reaction.¹³ Lauric acid and potassium hydroxide were added to create surfactant molecules in a one-pot process, however hydroxide ions also have the power to oxidize thiol groups and a slight stoicheometric imbalance could additionally promote polymerization. In a subsequent publication, they analyzed the effect of temperature on the oxidative polymerization and concluded that increasing temperatures lead to higher molecular weights up to 80°C. Above 80°C, specific dithiol monomers underwent crosslinking reactions to form gel.¹⁴

Many preparative methods for air oxidation of thiols have developed with variations in solvent and catalyst system. Whistler and Hoffman polymerized a sugar dithiol using three different oxidative reagents: oxygen, ammonium persulfate, hydrogen peroxide.¹⁵ The oxygen oxidation was performed in both an aqueous emulsion and pyridine solvent. Like Marvel and Olson, they used potassium hydroxide and lauric acid to make an emulsifier *in situ* for reactions performed in aqueous media. The catalysts, selenium dioxide, and potassium hydroxide were added to both the aqueous and pyridine reactions. Hydrogen peroxide and ammonium persulfate oxidations were only performed in pyridine. The highest molecular weight polymers were achieved in pyridine with pure oxygen gas as the oxidizing agent.¹⁵

Meng *et al.* have applied the use of a copper catalyst to the oxygen oxidation of a wide variety of dithiol monomers including aliphatic, aromatic, and arylene dithiols and their copolymers.^{16, 17} An oxidative solution of copper chloride, *N,N,N',N'*-

tetramethylethylene diamine (TMEDA) and pyridine were vigorously mixed while oxygen was bubbled into the solution. To the solution, dithiol dissolved in pyridine was added dropwise over 1.5 to 3 hours and then allowed to stir for an additional hour. The copper catalyst was removed by filtration through alumina, and hydrochloric acid was added to the filtered solution and reacted for an hour. The dilute conditions, (1.0g dithiol/35mL pyridine) lead to cyclic oligomers which rarely had more than five repeat units.¹⁶ The cyclic oligomers were later subjected to ring opening polymerizations at temperatures between 180°C and 250°C.¹⁸ Molecular weights were not reported.

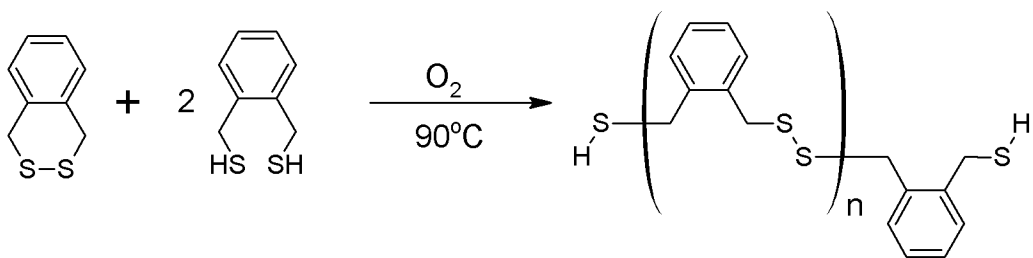
Choi *et al.* oxidized their unique dithiol monomer with oxygen in the presence of triethylamine (Scheme 2.1.4).¹⁹ In this one-pot process, the monomers were synthesized in tetrahydrofuran before triethylamine (2.5 equivalents) was added to the reaction vessel in the oxidation step. The reaction was then stirred under an oxygen atmosphere for 100 hours at ambient temperature. Kinetic studies of one of their polymerizations showed that 80% conversion was reached after 10 hours. The polymerizations were also attempted without triethylamine. The resulting polymer was produced in near quantitative yields, but it had a lower M_n of 3,700g/mol.¹⁹ The same monomer polymerized with the addition of triethylamine yielded a polymer with a number average molecular weight of 20,200g/mol. The present literature investigation has uncovered efficient methods of air oxidation, however, the addition of catalysts; bases, metal ions, or metal complexes have invariably been required.¹⁰



Scheme 2.1.4. Triethylamine-catalyzed, solution polymerization of dithiol monomers under pure oxygen atmosphere reported by Choi *et al.*¹⁹

2.1.3. Ring-opening polymerization of disulfides

Ring-opening polymerization is a useful, conventional method for the synthesis of poly(sulfide) polymers, such as polypropylene sulfide (PPS),^{7,20} but it is less frequently seen in poly(disulfide) polymer synthesis. The ring opening polymerization reported by Ishida *et al.* is a thermally initiated process that proceeds in bulk.²¹ The cyclic disulfide and its dithiol analogue were reacted under vacuum in a sealed test tube. The test tube was kept at a constant temperature above the melting point of the monomers, α,α' -mercapto-o-xylene (XDT) and 1,4-dihydro-2,3-benzodithiine (XDS). The reaction conditions for the reaction with the highest yield are shown in Scheme 2.1.5.

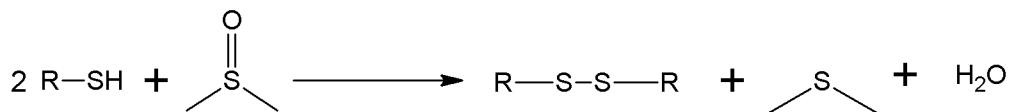


Scheme 2.1.5. Synthesis of disulfide polymers reported by Ishida *et al.*²¹

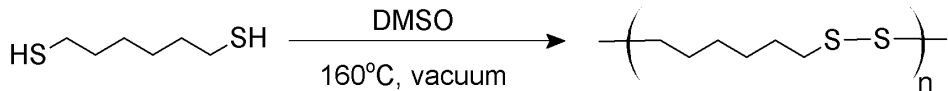
Another ring-opening polymerization was performed by Song *et al.*¹⁸ who started with cyclic disulfide oligomers, like those mentioned previously. To prepare the macrocycles for polymerization, they were compression molded at $140^\circ C$ for 40min. The compressed samples were then heated to temperatures ranging from $180^\circ C$ to $250^\circ C$. Two different atmospheres were examined: air and nitrogen. Polymerization progressed under both atmospheres, although the polymers produced were not equivalent. As the reaction temperature increased, the presence of thiosulfonates within the polymer also increased. The amount of thiosulfonates was also increased by an air atmosphere. It was postulated by the authors that the presence of thiosulfonates increased the glass transition of the compounds from $70.4^\circ C$ to $71.0^\circ C$.¹⁸ However, the variation of less than one degree in the glass transition temperature may not represent a statistically significant difference. Disulfide ring-opening polymerizations represent the only examples poly(disulfide) polymer synthesis in bulk.

2.1.4. Oxidative polymerization with DMSO

The oxidation of thiols to disulfides by sulfoxides is another well-documented reaction. An advantage to sulfoxide reactions are that sulfhydryl groups are not oxidized past the disulfide.¹⁰ The general equation of sulfoxide oxidation (Scheme 2.1.6),¹⁰ indicates that the removal of water will encourage reaction progression. The oxidative properties of dimethyl sulfoxide was applied to the synthesis of poly(disulfide) polymers as early as 1968 by Goethals and Sillis (Scheme 2.1.7).^{7,22} They reported the polymerization of a several aliphatic dithiols. The maximum reported Mn = 10,500 g/mol was reached in 6 hrs with hexane dithiol as the monomer.

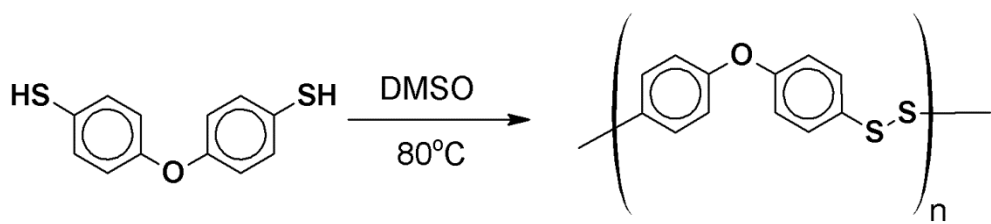


Scheme 2.1.6. Oxidation reaction of two thiols by DMSO to create a disulfide bond.¹⁰



Scheme 2.1.7. Polymerization of hexane dithiol reported by Goethals and Sillis in 1968.²²

Later, Meng *et al.* reported the synthesis of an aromatic disulfide polymer by heating their aromatic monomer, 4,4'-oxybis(benzenethiol), in DMSO for 8 hours at 80°C (Scheme 2.1.8).²³ The mole ratio of thiol groups to moles of DMSO was about 1:5. Due to the insolubility of the polymer, its molecular weight was not determined, however, the reaction formed a polymer solid enough to be “cut into small pieces”.²³



Scheme 2.1.8. Polymerization of aromatic dithiols using reported by Meng *et al.*²³

More recently, DMSO was used by Wang *et al.* to polymerize a large dithiol (Figure 2.1.1).²⁴ The monomer, 38mg, was dissolved in 100 μ L of DMSO which corresponds to 8.4×10^{-5} mol of sulphydryl groups in 1.4×10^{-3} mol of DMSO (1:16 ratio). The solution was incubated at 37°C for five days before the polymer was precipitated in acetone. The polymer had an average molecular weight of 6,200 g/mol. The polymer had similar buffering ability as compared to PEI (polyethyleneimine), but with decreased cytotoxicity. The intended purpose of the polymer was as a gene delivery system. The polymer forms nanoparticle complexes with DNA and siRNA and then releases the nucleic acids upon introduction to a reducing environment.

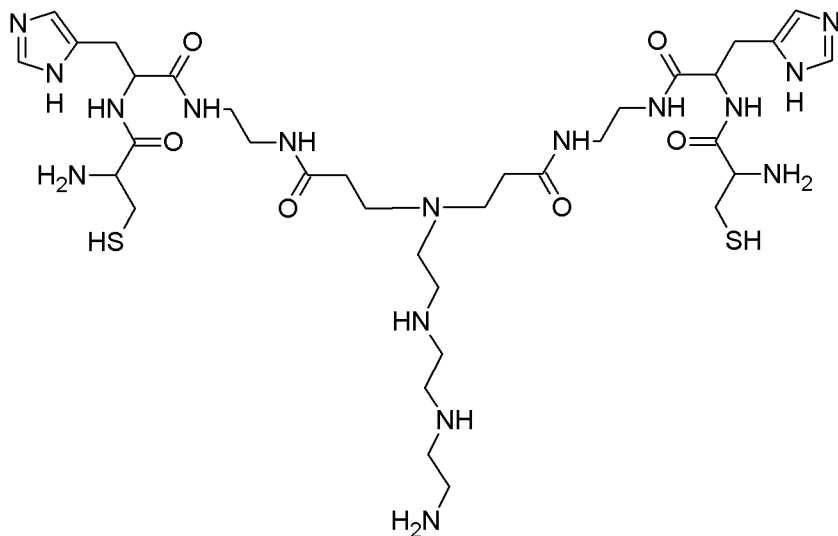
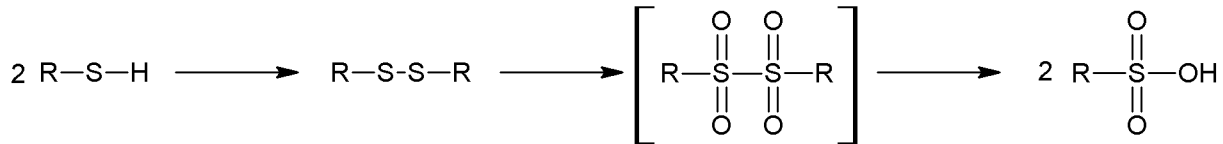


Figure 2.1.1 Dithiol monomer polymerized by Wang *et al.*²⁴

2.1.5. Polymerization with hydrogen peroxide

Hydrogen peroxide is used as an oxidizing agent in many synthetic organic chemistry reactions, including the oxidative polymerization of aniline²⁵ and phenols²⁶ and the oxidation of thiols. In the oxidation of thiols, the reaction does not stop at the disulfide, and they are readily over oxidized to form a sulfonic acid (Scheme 2.1.9).^{10, 27} The intermediate in Scheme 2.1.9 is not readily isolated.²⁷ Pascal and Tarbell performed kinetic studies on the hydrogen peroxide reaction and concluded that the presence of dissolved oxygen contributed to the rate of the reaction.²⁸



Scheme 2.1.9. Oxidation of thiols past the disulfide group to the sulfonic acid.¹⁰

Supale and Gokavi present a solution to the over oxidation of thiols by the addition of a chromium(III) catalyst.²⁹ Aromatic and aliphatic sulfides were dissolved in a solution of 40% aqueous chromic potassium sulfate and 60% methanol. To the solution, an excess of 30% H₂O₂ was added drop-wise while stirring. Acetone, acetonitrile and ethanol were also tested as solvents but produced lower yields.²⁹ As mentioned previously, Whistler and Hoffman attempted to polymerize a sugar dithiol with hydrogen peroxide in pyridine and were unsatisfied with the results.¹⁵

Hanhela and Mazurek polymerized 2,2'-thiodiethanethiol and 2,2'-oxydiethanethiol with hydrogen peroxide in order to modify Thiokol prepolymers. Twenty milliliters of 3 M hydrogen peroxide was added dropwise to a solution containing 0.04 moles of dithiol in 50mL of 1.6 M sodium hydroxide. The mixture was allowed to react for one hour and then filtered, rinsed with water and dried. To purify the product, it was extracted with chloroform, washed with water and dried over magnesium sulfate. The oxidation of 2,2'-thiodiethanethiol formed a white residue (solid) which became a viscous liquid after purification. The product of 2,2'-oxydiethanethiol was viscous liquid without the formation of a white residue.³⁰

2.1.6. Other methods of polymerization

Tatsuma *et al.* electrochemically polymerized 2,5-dimercapto-1,3,4-thiadiazole in methanol with an iodine catalyst.³¹ An electrochemical process for the polymerization of α,ω -alkane dithiols has been introduced in the past decade by Endo *et al.*³² Acetonitrile³², and dichloromethane³³ were the chosen solvents for this reaction for their ability to dissolve the polymers formed. Monomers were dissolved in the chosen solvent (previously distilled) to create highly dilute solutions (3.2×10^{-2} M) and cooled to 0°C

under a nitrogen atmosphere. The highest M_n (13,000 g/mol) was reported for propanedithiol, but returned only 8% polymeric product.³²

2.1.7. Other methods of disulfide synthesis

Countless methods of thiol oxidation exist that have not been applied to polymerization reactions. The following subsection include methods of thiol oxidations that are good candidates for polymerization reactions or coupling reactions in biomaterials.

Thiols are not oxidized to disulfides by ultrasonic waves on their own, but ultrasound promotes radical reactions through the chemical and physical effects of ‘cavitation.’³⁴ Because air oxidation of thiols proceeds through a radical intermediate (Scheme 2.1.2), it is a good candidate for ultrasound activation. García and coworkers reported that the use of sonication greatly increased the rate of thiol oxidation by atmospheric oxygen.³⁵ Their procedure still required triethylamine to catalyze the reaction, but sonication further decreased the reaction time. The research centered on the synthesis of symmetric disulfides in DMF at above ambient temperatures.³⁵ As only reagents with a single thiol group were analyzed, the possibility of polymerization was not investigated. In addition to the radical intermediate, oxidative polymerization of dithiols by air is a good candidate for ultrasound activation for another reason. While Garcia noted the positive effects of polar aprotic solvents in thiol oxidation, the oxidation of thiol may also be performed in water. Water forms small amounts of oxidative radical species upon the application of ultrasound³⁴ which will further promote the reaction. Homolytic bond cleavage in peroxides is also increased by sonication.³⁴

Iodine will quantitatively oxidize thiols to disulfides producing two moles of HI.¹⁰ Cerritelli *et al.*,²⁰ Choi *et al.*,¹⁹ and Tatsuma *et al.*³¹ have all employed iodine oxidation in their research.

2.2. Disulfide networks in biomaterials

2.2.1. Synthetic approaches to disulfide networks

Disulfide bonds are introduced into crosslinked polymer networks by three general approaches. In the first approach oligomers or shorter linear polymers are coupled through oxidation of thiol end groups, or by a disulfide-containing coupling agent. The long polymer chains are then crosslinked in a subsequent reaction. The second approach is to introduce a disulfide-containing crosslinking agent. Cystamine, 3,3'-dithiopropionic acid and 3,3'-dithiobis(propionic hydrazide) have all been reported as disulfide-containing crosslinkers.^{36, 37} Here, the crosslinking reaction is often an amidation or esterification reaction. In both of the described approaches, disulfide functionality is present before the polymer network is crosslinked.

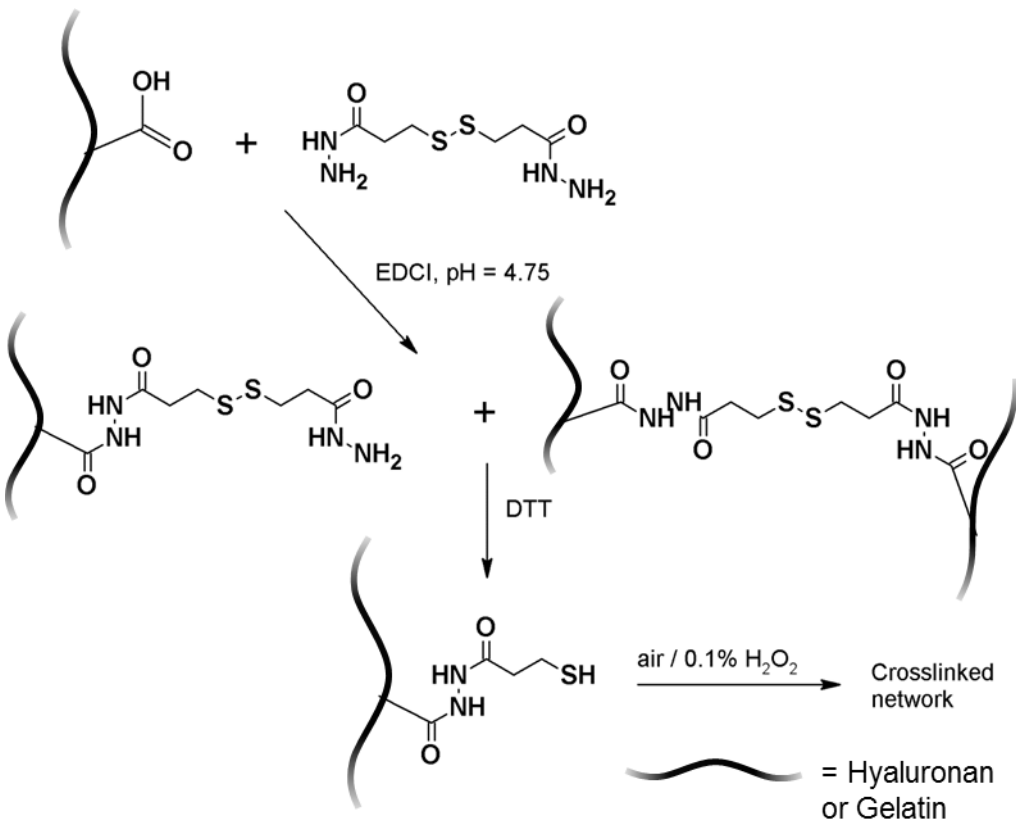
This section focuses of the third approach where networks are crosslinked through the oxidation of thiols to disulfides. In this approach, disulfide functionality is not present until the networks are synthesized. From a green chemistry perspective, the advantage of the third approach stems from the mild reaction conditions in which disulfide crosslinks can be formed. Networks are created by the oxidation of pendant thiol groups attached directly to the polymer chain, the oxidation of thiol endgroups in multiarm polymers or by the coupling of thiol endgroups with a multifunctional thiol compound.³⁸ Exposure of free thiol groups to DMSO or to oxygen are the two most common methods of disulfide bond formation in the preparation of hydrogel biomaterials.

A poly(ethylene glycol) hydrogel was synthesized by Koo *et al.*^{40, 39} using a α,ω -thioacetate-functionalized low molecular weight PEG ($M_n = 600$ g/mol) and trifunctional thioacetate crosslinker. Thioacetate groups were added to either end of the purchased PEG in a series of steps. PEG was tosylated by reacting it in a solution of dichloromethane with dimethylamino pyridine, *p*-toluenesulfonyl chloride and triethylamine for 3 hrs. The tosylated polymer was purified in chloroform, washed with water and dried. It was then redissolved in DMF and reacted with potassium thioacetate overnight to add thioacetate groups to either end. The trifunctional thioacetate crosslinker was synthesized by adding S-acetylmercaptosuccinic anhydride in DMF to tris(t-aminoethyl)amine, also dissolved in DMF. An ammonia/methanol mix was used to deprotect both the polymer and the crosslinker. Preliminary crosslinking was performed with an aqueous solution of DMSO that was stirred for 2 days. To finish the crosslinking, the solutions were incubated at varying temperatures.

Rheometry was used to analyze how the solution crosslinked with an increase in temperature. Glutathione was used as the reducing agent in the reduction reaction. The glutathione reduction mechanism is the same as that presented later in Scheme 2.3.1 for cysteine. The presence of glutathione greatly increased the rate of degradation over the control (distilled water). In turn, this increased the rate of drug release. The authors report no cytotoxicity for the polymer or degradation product.⁴⁰

Shu and coworkers developed another method of adding sulfhydryl groups to polymers through amidation of pendant carboxylic acid groups.³⁷ The biopolymers, gelatin and hyaluronan, were dissolved in water and reacted with DTP (dithiobis(propionic hydrazide)) while maintaining a pH of 4.75 with aliquots of 1.0 M

HCL. Solid EDCI (1-ethyl-3-[3-(dimethylamino)propyl] carbodiimide) was added to the solution. DTP could form amide bonds at either of its terminal amine groups, thereby crosslinking the polymers, however, the authors proposed that only one end of the difunctional molecule reacted. The reaction was terminated by adding 1.0 M NaOH solution until the pH reached 7.0. Dithiothreitol (DTT) was added to cleave the disulfide bond in DTP and expose a sulfhydryl group. The polymer was purified, lyophilized, and dissolved in buffer (pH=7.4). Polymer solutions were poured into Petri dishes and allowed to crosslink by exposure to air for 24 hours. The crosslinking process was completed by immersing the gels in highly dilute hydrogen peroxide solution (0.1%). Scheme 2.2.1 details the reactions used to form the thiolated polymers.



Scheme 2.2.1. Multi-step synthesis of disulfide crosslinked hyaluronic acid and gelatin hydrogels.³⁷

2.2.2. Calculation of network crosslink density

The molecular weight between crosslinks can be calculated using the Flory-Rhener equation (Eq. 2.1).^{41, 42, 43} First the polymer network must be swollen in a good solvent. It is helpful to use a well characterized solvent so that solvent parameters such as density and the Hildebrand constant may be found in the literature. From the mass gain of the swollen polymer, the average molecular weight between crosslinks (M_c) is calculated.

$$\bar{M}_c = -V\rho_p \frac{(\phi_p^{1/3} - \phi_p/2)}{[\ln(1-\phi_p) + \phi_p + \chi\phi_p^2]} \quad (\text{Eq. 2.1})$$

Where:

M_c = average molecular weight between crosslinks

V = molar volume of solvent

ρ_p = polymer density

ϕ_p = volume fraction of polymer in swollen gel

χ = Flory-Huggins interaction parameter between solvent and polymer

$$\phi_p = \frac{1}{\frac{M_s \rho_p}{M_p \rho_s} + 1} \quad (\text{Eq. 2.2})$$

Where:

M_s = mass of solvent in gel (g)

M_p = mass of polymer in gel (g)

ρ_s = density of solvent (g/cm^3)

The χ solubility parameter, or Flory-Huggins interaction parameter, must be calculated when it is not available in the literature. Equation 2.3 is used to calculate χ , however, for new or undercharacterized polymers, the Hildebrand constant must be estimated based on the additive properties of each functional group in the repeat unit molecule, as shown in Eq. 2.4.^{43, 44, 45, 46}

$$\chi = 0.34 + \frac{V}{RT} (\delta_s - \delta_p)^2 \quad (\text{Eq. 2.3})$$

Where:

χ = Flory-Huggins solvent/polymer interaction parameter

$$\chi = \chi_S + \chi_H$$

$$\chi_S \approx 0.34$$

V = Molar volume of solvent

δ_s = Hildebrand constant of solvent (MPa^{1/2})

δ_p = calculated Hildebrand constant of polymer repeat unit (MPa^{1/2})

$$\delta_p = \frac{\sum F}{\sum V} = \frac{\sum F}{V_m} \quad (\text{Eq. 2.4})$$

Where:

F = Molar attraction constant of chemical group ((MPa)^{1/2}•cm³•mol⁻¹)

V = Molar volume of chemical group (cm³•mol⁻¹)

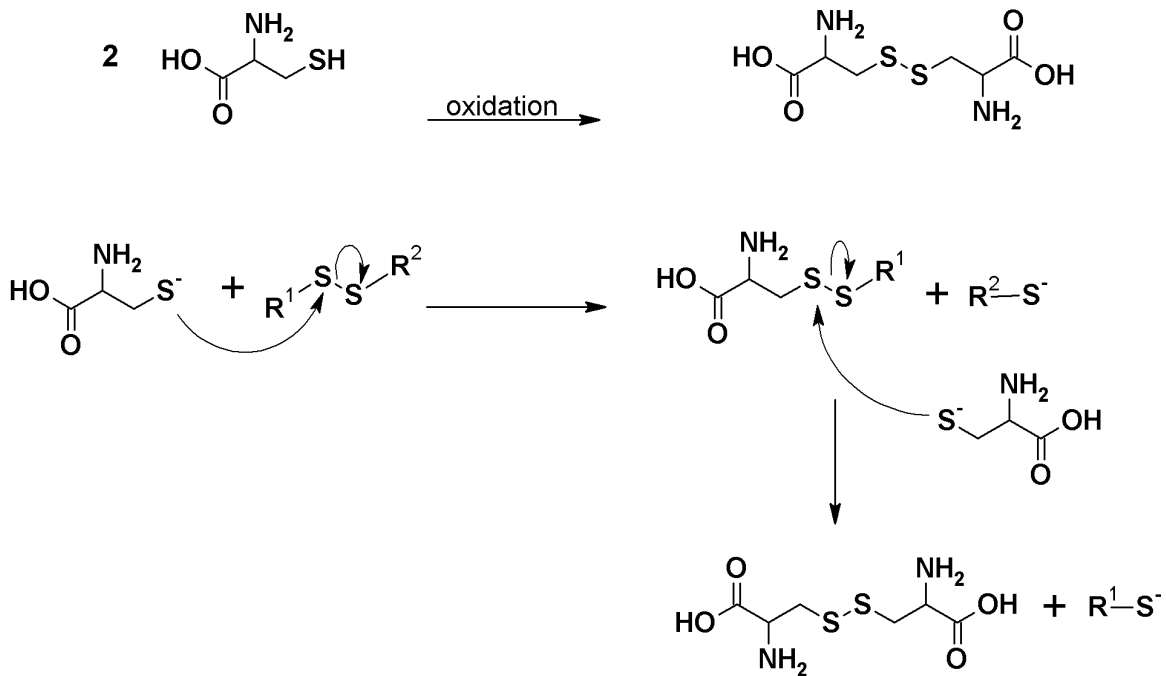
V_m = Molar volume of polymer repeat unit (cm³•mol⁻¹)

2.3. Thiol oxidation in biological systems

As mentioned in the introduction, thiol-disulfide oxidation-reduction reactions provide an essential route in biochemical pathways. In biological systems the most important oxidizer of thiols to disulfides are other disulfides, which are subsequently reduced to thiols. This constant exchange between thiols and disulfides is called shuffling,⁴⁷ and it is crucial to the regulation of cellular oxidation potentials.⁴⁸ A diagram

describing an abridged version of the complex biochemical pathways of sulfur compounds was published by Jacob *et al.*⁴⁹ The disulfide bond is placed at the very center of the diagram because of the many reactions that pass through the disulfide redox state.

Disulfide molecules in biological systems are most often the result of the homogeneous coupling of two cysteine residues through their sulfhydryl groups. The coupling of free cysteine to form cystine, and the proposed reaction mechanism⁴⁹ using a generic disulfide bond are shown in Scheme 2.3.1. Cysteine is the only amino acid that contains sulfhydryl groups which form disulfide bridges in protein folding. Exposed disulfide bridges may serve as oxidizing agents, which is how many enzymes function. An advantage to utilizing disulfides to create new disulfides is the elimination of possible over oxidation.

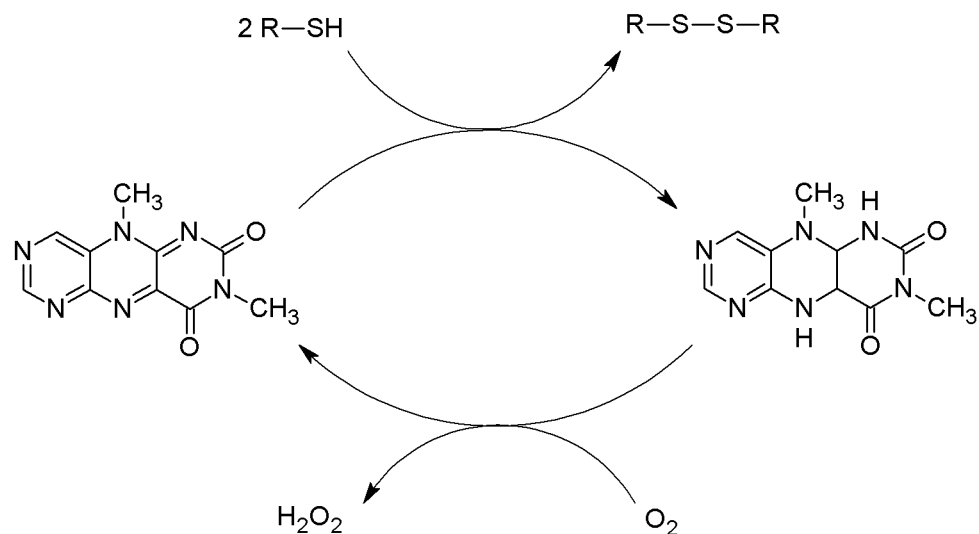


Scheme 2.3.1. Cysteine coupling to form cystine followed by the mechanism of disulfide bond reduction by cysteine.

2.3.1. Oxidation-reduction reactions of enzymes and related compounds

Flavin compounds are often attached to enzymes as cofactors, however, they are also known to oxidize disulfides on their own.^{10, 50} Yano *et al.* have developed a highly oxidizing flavin derivative that shows particular effectiveness towards thiols (Scheme 2.3.2) and nitroalkanes.⁵⁰ The effect of pH on the reaction rate was studied at room temperature, and the highest rate constant was seen at a pH of 9.5, which corresponded to the pKa of the thiol (mercapto ethanol, pKa 9.5).⁵¹ Regeneration of the original flavin derivative was achieved by exposing the reduced flavin to oxygen gas.⁵¹ Holden and Main showed that riboflavin (vitamin B₂) showed a negligible catalytic effect on the oxidation of thiols under anaerobic conditions.⁵² The reactions were performed in

solution under anaerobic (note: this is not clear, as the title says aerobic and the body of the paper declares anaerobic) conditions and monitored using UV-Vis spectroscopy.



Scheme 2.3.2. Flavin-catalyzed thiol oxidation to disulfides at room temperature.^{10, 50}

Metal ions in biological complexes have been shown to catalyze the air oxidation of thiols faster than their non-biological counterparts. The Fe(III) ion in heme, for example increased the rate of oxidation by seven times over iron sulfate.¹⁰ Within a cell, the purpose of metal complexes, like heme and vitamin B₁₂, is to absorb and transfer oxygen which makes them ideal catalysts for oxidative reactions.

Enzyme oxidations are essentially disulfide shuffling reactions using strategically placed disulfide bridges. Thioredoxin enzymes are common to a wide variety of organisms and are expressed in a variety of protein configurations. The thioredoxin system consists of the enzyme thioredoxin (Trx), thioredoxin reductase (TrxR or TR) and NAPDH. As the name suggests, the role of thioredoxin reductase is to reduce the disulfide bond in thioredoxin. NAPDH and a proton are also reactants in this process. As

a result of the reduction, NAPD⁺ is produced and the thioredoxin becomes a strongly reducing enzyme that will transfer electrons to the disulfide bridge of another protein without further catalytic assistance.⁵³ The reducing power of the system was harnessed by Farris *et al.* to reduce the disulfide bridges in soy flour protein.⁵⁴ They found the enzyme system to be an effective and efficient method of disulfide bond cleavage that could be applied to an industrial process. The current cost of the enzyme system seems prohibitive of a large-scale reaction since no mention of enzyme recovery was discussed. While thioredoxin reductase works as part of an enzymatic system, it has also been shown to reduce smaller molecules, such as quinonoid compounds, ascorbate, S-nitroso glutathione and lipid hydroperoxides, on its own.⁵⁵ Bindoli includes a third enzyme in the thioredoxin system, peroxiredoxin. Peroxiredoxin is one of many enzymes and proteins that may receive electrons from reduced thioredoxin and is important in the regulation of cellular hydrogen peroxide concentrations.⁴⁸

In concert with the thioredoxin enzyme system, the glutathione enzyme system regulates the concentration of thiols, disulfides and hydrogen peroxide within an organism.⁴⁸ The glutathione system includes glutathione reductase (GR), glutathione (GSH or GSSG) and glutathione peroxidase (GPx) and hydrogen peroxide. Figure 2.3.1 presents a diagram of the glutathione enzyme system. NADPH transfers two protons to GR across its active disulfide bridge to create two thiol groups. The thiols then reduce GSSG to GSH as they couple back into the disulfide bridge. GSH removes and couples with glutathione tethered to the selenium cofactor in GPx. Free GSH is attached to GPx through H₂O₂-catalyzed oxidative coupling to selenium which produces water.

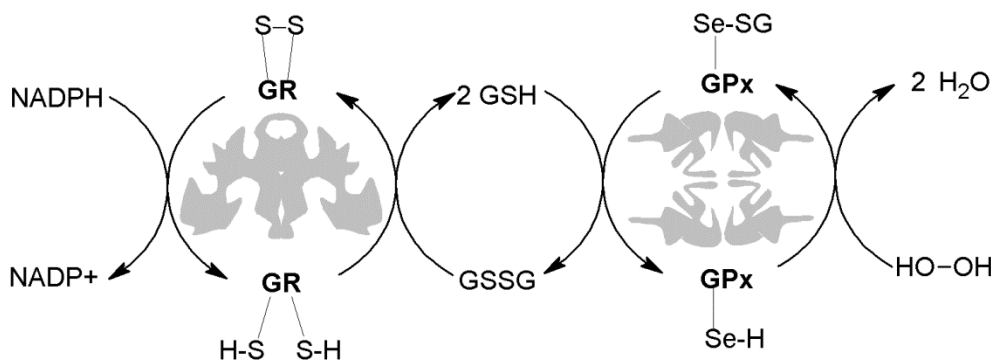


Figure 2.3.1. Diagram of the glutathione enzyme system.⁵⁶

Oxidase enzymes are a class of enzymes that include sulfhydryl oxidases and peroxidases, both which have the ability to oxidize thiols. In his 1946 publication, Randal demonstrated that the oxidation of thiols by hydrogen peroxide was catalyzed by horseradish peroxidase.⁵⁷ Horseradish peroxidase has established itself as an efficient catalyst in organic chemistry.⁵⁸ Sulfhydryl oxidases are a subclass of enzymes that specifically oxidize thiols using a flavin cofactor. The flavin cofactor and two sulfur-containing residues work in concert to form a protein disulfide bridge from two thiol-containing residues.

2.4. Biomaterials using α -lipoic acid

The structure α -lipoic acid, with disulfide ring attached by a four-carbon chain to a carboxylic acid group, provides the molecule with unique biological activity. The amphiphilicity of the molecule allows it to penetrate lipid bilayers, including the blood-brain barrier while remaining limitedly soluble in aqueous environments. A-LA is one of the most powerful biological antioxidants and readily reduces reactive oxidant species in biological systems.^{59, 60} Additionally, it plays a vital role in the enzymatic redox systems.

The disulfide group readily complexes with metals and is a demonstrated chelating agent. Taking advantage of both the antioxidant and chelating properties, α -LA-palladium complexes are being used to protect against radiation poisoning.⁶¹

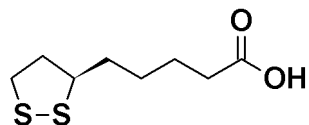


Figure 2.4.1. (R)- α -lipoic acid.

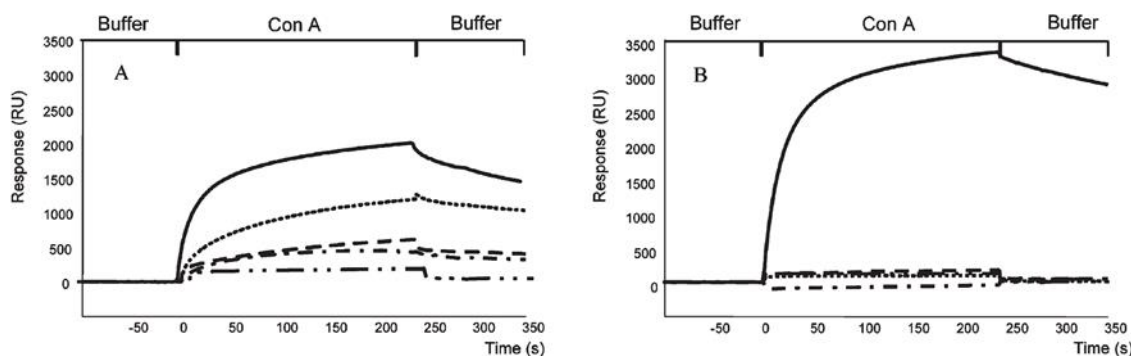
2.4.1. Self-assembled monolayers on gold surfaces

α -LA and its derivatives serve as an alternative to alkanethiol compounds in the preparation of self-assembled monolayers on gold substrates. The sulfur atoms adhere to the gold substrate in the same way as their thiol counterparts, and the method of preparation is the same. Pre-cleaned, gold-coated substrates are soaked in a dilute ethanolic solution of α -LA for about 8 to 24 hours. Another method which allows the ethanolic solution to dry has also been investigated and gave comparable protein adsorption results.⁶² SAMs prepared from α -LA alone result in a surface rich in carboxylic acid groups, and so, they are capable of hydrogen bonding. It has been shown that SAMs with hydrogen-bonding sites can form a second layer of molecules on top of the first.⁶³ For α -LA SAMs, this would leave the biologically active (and redox-sensitive) thiolane ring exposed on the surface which could, in turn, affect subsequent testing (both biological and electrochemical). The problem of a second layer of α -LA is mute in most reports because α -LA is usually modified through esterification or amidation of the carboxylic acid group before monolayer preparation.

Two studies have been found that compare the properties of alkanethiol and α -LA-tethered SAMs. Using AFM, Langry and coworkers were able to measure that the tensile force required to remove α -LA from a gold surface was 0.31 ± 0.13 nN, while the force required to remove an alkane thiol from the gold substrate was 1.05 ± 0.29 nN.⁶⁴ They suggest that the reduced strength of the α -LA-Au bond stems from the spatial constraint of the two sulfur atoms which allows for a concerted reaction where S-Au bonds break as S-S bonds form simultaneously.⁶⁴ The work of Dijksma *et al.* reports that alkanethiol SAMs provide better coverage of the gold substrate and are more stable than α -LA SAMs when not exposed to light. Upon exposure to light, they found that the α -LA SAM deteriorated more slowly than the alkanthiol SAM.⁶⁵

Despite the reduced surface-bonding strength, α -LA-tethered SAMs show improved biological results. Karamanska and coworkers prepared SAMs of α -D-mannopyranoside and α -1,3-D-mannopyranosyl(α -1,6-D-mannopyranosyl)- α -D-mannopyranoside-based tethered by either ethanethiol ($-\text{CH}_2-\text{CH}_2-\text{SH}$) or the ethylamide of α -LA ($-\text{CH}_2-\text{CH}_2-\text{NH}-\text{CO}-\text{CH}_2-\text{CH}_2-\text{CH}_2-\text{CH}_2-\text{thiolane}$).⁶⁶ They then exposed the gold-SAM to solutions of proteins and used surface plasmon resonance (SPR) to measure the mass of proteins adsorbed to the surface. SPR compares the plasmonic resonance of the thin gold film underneath the SAM before and after exposure to the protein solution. The change in plasmonic resonance can be converted to adsorbed protein mass. SPR analysis showed lower non-specific binding in four out of the five proteins analyzed for the α -LA tethered SAMs. The one protein (Concanavalin A) which showed high adsorption on α -LA-based SAMs is known to have an affinity for the carbohydrate tethered and thought to be specifically bound. The longer tether provided

by the ethalamide of α -LA allows for a more ordered SAM which is thought to affect the protein adsorption. Ideally, an alkanethiol tether of similar length would be compared to the α -LA-based SAM, however, the authors wanted to compare a readily available thiol carbohydrate with the α -LA functionalized carbohydrate. Figure 2.4.2 shows the SPR data presented in the literature. Other research into α -LA-functionalized carbohydrate SAMs have also been reported to prevent the adsorption of serum proteins when used as a post-adsorption blocking agent.⁶⁷ The α -LA structures were not compared to thiolalkane counterparts.



Solid = Concanavalin A; Dash-dot = *Tetragonolobus purpureas* lectin; Dash-dot-dot = *Ricinus communis* agglutinin; Dotted = Fibrinogen; Dashed = Cytochrome C.

Figure 2.4.2. Protein adsorption onto ethanethiol-tethered SAMs (A, left) is compared to α -LA-tethered SAMs (B, right) using SPR. Reproduced from Karamanska, R.; Mukhopadhyay, B.; Russell, D. A.; Field, R. A., *Chemical Communications (Camb)* 2005, 26, 3334-3336, with permission of The Royal Society of Chemistry

Gold to sulfur binding is not limited to flat, gold-coated surfaces. A-LA has also been used to attach functionality to gold nanoparticles. Andres and coworkers designed tumor imaging agents by attaching folate-functionalized poly(ethylene glycol) to gold

nanoparticles using α -LA.⁶⁸ The PEGylated particles were soluble in aqueous solutions and were brought into the targeted cancer cells with over-expressed folate receptors. α -LA has also been used to attach RGD functionality to gold nanoparticles adhered to thiol-functionalized SAMs blocked with BSA.⁶⁹ The RGD-functionalized nanoparticles were used to probe the effect of “sticky-spot” spacing on cell adhesion.

2.4.2. Surface modification using α -lipoic acid

In α -LA-tethered SAMs and nanoparticles the biologically active thiolane ring is hidden from cells and proteins. One example of exposed α -LA thiolane rings comes from Song and coworkers.⁷⁰ Using carbodiimide-activated amidation, α -LA was attached to exposed amine groups on surface of a crosslinked 1,2-diaminocyclohexane coated stent. Platelet adhesion tests using AFM showed that very few platelets adhered to the α -LA-functionalized surfaces compared to the bare metal surface. The authors also discuss that the platelets on the α -LA-functionalized surface are not aggregated and therefore would be less prone to clotting *in vivo*.⁷⁰ These results are supported by a previous study that indicates α -LA inhibits the expression of adhesive molecules in some cells.⁷¹ Platelet adhesion to the crosslinked polymer before α -LA functionalization was not shown.

2.4.3. Reduction-sensitive vesicles

Redox-sensitive disulfide bonds are an invaluable tool in the design of drug delivery vesicles. The disulfide bond may form or maintained under mildly oxidizing conditions, such as those found in the slightly basic bloodstream. In reducing environments, such as those found in the cell cytosol and lysosome compartments,

disulfide bonds are cleaved to form thiol groups. Disulfide cleavage is accelerated in these environments by enzymes specific to disulfide cleavage. In drug delivery, this means that therapeutic agents maybe trapped inside vesicles under mild conditions, continue to be protected while circulating in the body and then be released upon endocytosis. Additionally, crosslinking of self-assembled vesicles, like micelles and liposomes, reduces susceptibility to shear-induced disassembly. The importance of reduction-sensitive vesicles is demonstrated by several review papers.^{20, 72, 73}

The resulting reactive thiolate anions formed upon reduction may, however be harmful to the cell. A-LA presents a unique solution to the problem; upon reduction of α -LA crosslinks the resulting dithiolate compound readily reforms the disulfide ring while at the same time reducing a neighboring oxidized species. Separated by four methylene groups from the thiolane ring, the sterically unhindered carboxylic acid group facilitates conjugation to a wide variety of molecules, including peptides, carbohydrate polymers⁷⁴ and phospholipids.⁷⁵

Balakirev and coworkers functionalized a DNA-complexing quaternary amine (cationic) with two reduced α -LA ligands (dihydrolipoic acid or DHLA).⁷⁶ The cationic monomer compound was exposed to DTT in order to initiate polymerization through sulfur-sulfur bonds. Micelle formation around DNA was visualized using SEM and the cell uptake of the polymeric DNA structures was demonstrated by visualizing the fluorescent dyed complexes.

2.4.4. Polymers from α -lipoic acid

Biochemists L. J. Reed and C.-I. Niu first reported the presence of poly(DL- α -LA) in 1955 where it was a byproduct in their synthesis of DL- α -lipoic acid.⁷⁷ The following year, Thomas and Reed published an account of the purposeful, thermally-induced polymerization of the disulfide, however the focus of the paper was on the subsequent depolymerization of the polymer to desired DL- α -LA rather than the characterization of the polymer.⁷⁸ DL- α -lipoic acid was heated to at 65°C for fifteen minutes to produce a colorless polymer. The reaction reached monomer conversion of 52%. The next report of α -LA polymerization is from 1980 and used tributylphosphine (TBP) with α -LA in an acetonitrile solution. Rather than polymerize through the disulfide bonds as shown in Figure 2.4.3. A., this reaction forms poly(thio-1-oxo-6-mercaptopoctamethylene) in which the α -LA units are connected via a thioester bond (Figure 2.4.3. B) The pendant thiol group was acetylated to prevent crosslinking through oxidation. Based on polystyrene standards, the number average molecular weight (M_n) of the acetylated polymer was 8,400 g/mol.⁷⁹

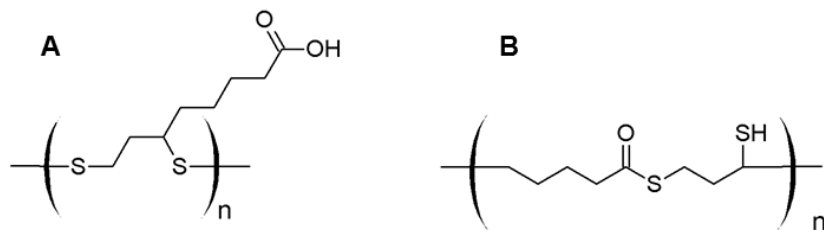


Figure 2.4.3. Structure of poly(α -LA) (A) and poly(thio-1-oxo-6-mercaptopoctamethylene) (B).

α -LA was also copolymerized with salicylyl phenylphosphonite (SPO) or trimethylene phenylphosphonite (TPO) to produce alternating copolymers.⁸⁰ Equal volumes of 2.00 M solutions of α -LA and cyclic phosphonite monomer in chloroform were mixed under nitrogen at -30°C and kept at room temperature for a specified number of days before purifying by precipitation into diethyl ether. The two copolymers are formed by two distinct mechanisms and so produce polymers with differing monomer linkages (Figure 2.4.4). The copolymerization of α -LA-TPO produced a polymer with pendant thiol groups that were subsequently protected by an acylation reaction. While the acylated copolymer reached M_n of 16,000 g/mol with 82% conversion, the SPO polymer only reached 1,500 g/mol with 88% conversion. Molecular weights were determined by vapor pressure osmometry. Balakirev and coworkers polymerized their lipoic acid derivative monomer (200 μmol) under nitrogen atmosphere in 1:10 DMSO:TNE buffer (pH= 8.5) solution for 48 hours at 37°C . Dithiothreitol (0.06 μmol) was used to initiate polymerization. No characterization of the polymer was reported.

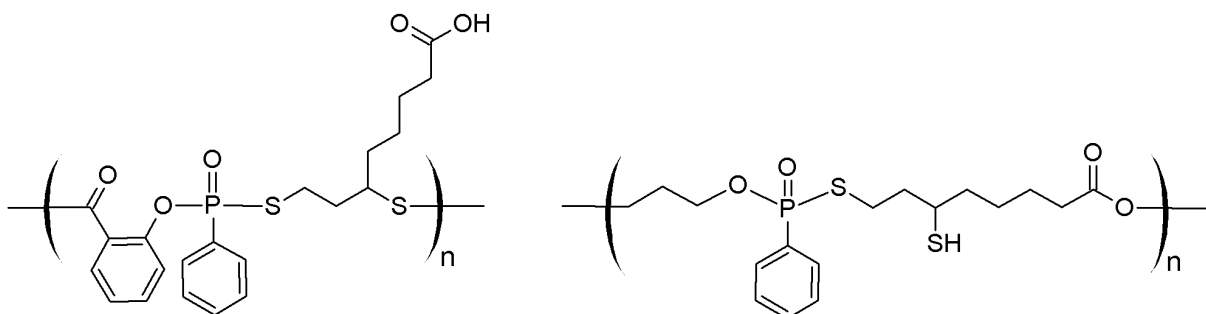


Figure 2.4.4. Structure of copolymers of α -LA and cyclic phosphonites (TPO followed by SPO).⁸⁰

The group of Kiyoshi Endo has been investigating the ring-opening polymerization of cyclic disulfides, including α -LA, for the last decade. Copolymers of α -LA and 1,2-dithiane (DT) of varying molar ratios were thermally polymerized in bulk conditions under high vacuum.⁸¹ Monomer conversion, molecular weights and polydispersity index all increased with increasing α -LA monomer content. An exception to the trend was a slight decrease in M_n for the 100% α -LA homopolymer which reached 416,000 g/mol. The highest molecular weight was found for the 70% α -LA copolymer which had a M_n of 550,000 g/mol (based on polystyrene standards). The authors propose a catenane structure for the copolymers with the interlocking cyclic structures averaging about 5,000 g/mol. These copolymers were later dissolved in pyridine and crosslinked with zinc (II) acetate at room temperature.⁸² The copolymerization and subsequent crosslinking is shown in Figure 2.4.5.

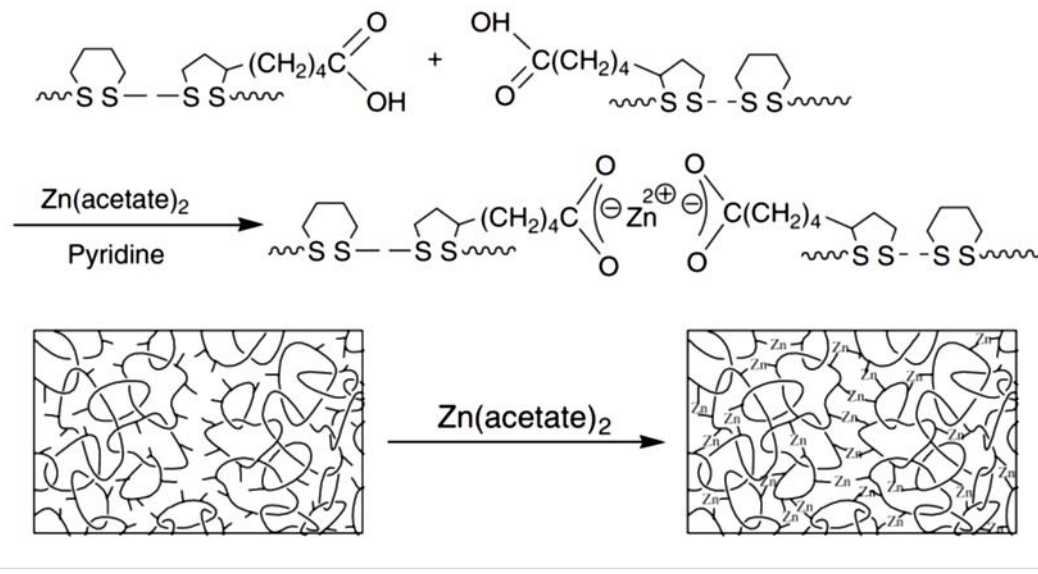


Figure 2.4.5. Poly(α -LA-*co*-DT) synthesis and crosslinking. Reprinted by permission from Macmillan Publishers Ltd: Polymer Journal, Yamanaka, T.; Endo, K., *Polymer Journal* **2007**, *39*, 1360-1364. Copyright (2007).

Endo and coworkers also investigated the homopolymerization of α -LA on its own.⁸³ The thermal polymerization was again carried out under high vacuum in bulk conditions. Polymers were not obtained below the melting temperature of the crystalline monomer, but readily polymerized at elevated temperatures with conversion and molecular weight increasing with increasing temperature. Polymers from the reaction carried out at 90°C reached M_n of 1,370,000 g/mol with a PDI of 1.5 and 66.8% conversion. The catenane structure proposed for the polymer consists of interlocking cyclic polymers of $M_n = 12,000$ g/mol. Their assessment of the cyclic ring stems from the GPC analysis of the UV degradation products of higher molecular weight polymers

and from polymerizing α -LA in the presence of cyclic poly(ethylene glycol) derivatives.⁸³

CHAPTER III

EXPERIMENTAL

3.1. Materials and instrumentation

3.3.1. Materials

The dithiol monomers, 1,2-ethanedithiol ($\geq 98.0\%$) (ED; CAS # 54-36-6) and 2-[2-(2-sulfanylethoxy)ethoxy] ethanethiol (95%) (DODT; CAS # 14970-87-7; common name: 3,6-dioxa-1,8-octanedithiol), and trithiol reagents, trimethylolpropane tris(2-mercaptopropionate) ($\geq 95\%$) (TMPTMP; CAS # 33007-83-9) and trimethylolpropane tris(2-mercaptoproacetate) (technical grade) (TMPTMA; CAS # 10193-96-1) were purchased from Sigma Aldrich.

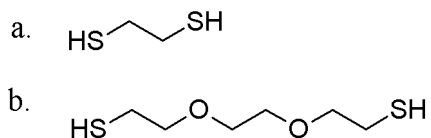


Figure 3.1.1. Dithiol monomers: a. 1,2-ethanedithiol, b. 3,6-dioxa-1,8-octanedithiol.

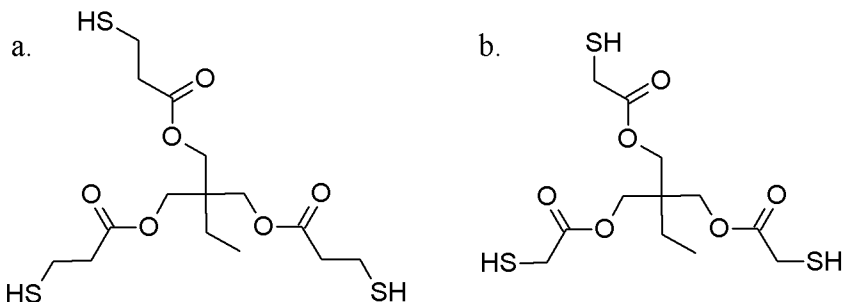


Figure 3.1.2. Trithiol reagents: a. trimethylolpropane tris(2-mercaptopropionate), b. trimethylolpropane tris(2-mercptoacetate).

Triethylamine ($\geq 99\%$) (TEA; CAS # 121-44-8) was purchased from Sigma-Aldrich and kept under nitrogen atmosphere until reacted. Hydrogen peroxide solution (3% by weight; 0.88 M) (CAS # 7722-34-1) was purchased from both Fisher Scientific and J.T.Baker. The solution from J.T.Baker contained 0.05% N-(4ethoxyphenyl)acetamide preservative (CAS # 62-44-2; common name: phenacetin). No reactivity difference between the two solutions was observed. Hydrogen peroxide solution (30% by weight; 9.73 M; stabilized) was purchased from Sigma-Aldrich and stored at 2°C until used.

(\pm)- α -lipoic acid ($\geq 99\%$; CAS # 1077-28-7) purchased from Sigma-Aldrich was used as received. (*R*)- α -lipoic acid ($>98\%$; CAS # 1200-22-2) purchased from TCI was purified by one of the following methods: 1) Recrystallization from 75/25 hexanes/pentanes,⁸⁴ 2) Dissolution in chloroform to precipitate the poly(α -LA) impurities. Diethylene glycol methyl ether (CH₃-DEG) and hexaethylene glycol (HEG) were purchased from Sigma Aldrich and used as received. Tetraethylene glycol (TEG) was purchased from TCI USA and used as received. CH₃-PEG-OH (Sigma-Aldrich; M_n = 2,000 g/mol (reported); M_n = 1,829 g/mol, M_w = 1,852 g/mol by MALDI-ToF MS)

was dried before use by applying vacuum and heat until all bubbling subsided. Enzyme catalyst was purchased also purchased from Sigma-Aldrich (*Candida antarctica* lipase B recombinant from yeast on Immobead 150; Lot # BCBD9402V = 3325 U/g; Lot # 1388469 = 5865 U/g).

Deuterated solvents (deuterium oxide, chloroform-d, methanol-d₃, acetone-d₆, tetrahydrofuran-d₈) were purchased from Cambridge Isotope Laboratories. THF was dried in an MBraun column purification system. Common laboratory solvents such as acetone, chloroform, ethyl acetate, hexanes, heptanes, methanol, isopropanol, tetrahydrofuran, toluene, were purchased from Fisher Scientific or Sigma-Aldrich and were all ACS reagent grade or above and used as received.

3.1.2. Instrumentation

3.1.2.1. Nuclear magnetic resonance (NMR) spectroscopy

¹H and ¹³C NMR spectroscopy was performed using a Varian Mercury 300 MHz instrument and a Varian INOVA 500 instrument. Analysis of the spectra was performed using a 1D NMR Processor software produced by Advanced Chemistry Development.

3.1.2.2. Infrared spectroscopy

Fourier transform infrared spectroscopy (FTIR) was carried out using a Digilab Excalibur Series FTS 3000 instrument. THF-soluble samples were dissolved in THF and cast onto a KBr crystal for analysis. Non-soluble samples were mixed with powdered KBr (approximately 4 mg sample in 100 mg KBr) and pressed into pellets for analysis. Data was recorded and processed using Win-lab software. Diffuse reflectance infrared

Fourier transform spectroscopy (DRIFTS) was carried out using a Nicolet 6700 instrument from ThermoScientific with a Harrick Praying Mantis DRIFTS attachment. Data was collected using OMNIC software and processed in Microsoft Excel.

3.1.2.3. Size exclusion chromatography (SEC)

Molecular weights and molecular weight distributions were determined by SEC on a system equipped with six Waters Styragel® columns, a Waters 2487 dual absorbance UV detector, a Wyatt Optilab DSP interferometric refractometer, a Wyatt DAWN EOS multi-angle laser light scattering detector and a Wyatt Viscostar viscometer. Tetrahydrofuran continuously distilled over calcium hydride under N₂ atmosphere was used as the mobile phase. Data collected from SEC were processed using Astra Software Version 5.3.4.14.

3.1.2.4. Mass spectrometry

Matrix assisted laser desorption/ionization time-of-flight mass spectrometry (MALDI-ToF) was performed on a Bruker UltraFlex-III time-of-flight mass spectrometer equipped with a Nd:YAG laser emitting at 355 nm. Mass spectra were measured in positive reflectron mode, using T-2-(3-(4-t-Butyl-phenyl)-2-methyl-2-propenylidene) malononitrile (DCTB) as matrix and sodium trifluoroacetate (NaTFA) as cationizing salt. Polymer, matrix, and cationizing salt were dissolved in anhydrous THF at concentrations of 1 mg/mL, 20 mg/mL, and 10 mg/mL, respectively. The DCTB and NaTFA solutions were mixed in the ratio 10:1 (v/v). Sample preparation involved depositing 0.5 µL of matrix/salt mixture on the wells of a 384-well ground-steel plate, allowing the spots to

dry, depositing 0.5 μ L of polymer on top of the dry matrix spot, and adding another 0.5 μ L of matrix/salt on top of the dry sample (sandwich method). Electrospray Ionization Mass Spectrometry (ESI-MS) was performed using a Bruker Daltonics Esquire-LC or HCT Ultra II ion trap mass spectrometer. Samples were typically dissolved in THF. Sodium trifluoroacetate (NaTFA) was used as the cationizing agent. Both forms of mass spectrometry were performed in the laboratory of Dr. C. Wesdemiotis at the University of Akron.

3.1.2.5. Thermal analysis

Differential Scanning Calorimetry (DSC) was carried out on a TA Q2000 DSC using a heat-cool-heat thermal cycle. A typical thermal cycle started by heating the sample from 40°C to 175°C at 10°C/min to remove any previous thermal history. In the second step of the cycle, the sample was cooled at 10°C/min to reach -100°C. The third step of the cycle heated the sample from -100° to 175°C at 10°C/min. Thermal Gravimetric Analysis, (TGA) was performed on a TA 5000 TGA using a heating rate of 10°C/min from room temperature to 500°C under nitrogen atmosphere. Analysis of the thermal data was performed using the Universal Analysis 2000 software.

3.2. Methods

3.2.1. New polymerization of DODT using triethylamine and H₂O₂

3.2.1.1. Polymerization of DODT and characterization of poly(DODT)

In preparation for polymerization, triethylamine and DODT were mixed, typically in between a 2:1 and 2.5:1 molar ratio depending on indicated monomer concentration.

In most polymerizations, the monomer/amine solution was then reacted with 2.0 equivalents of hydrogen peroxide (Aq.; 3% by wt). The final concentrations of reactants in example polymerizations are listed Table 4.1.4. The final concentrations of other reactions are given in their Results and Discussion Section. It is important to note that the reactions proceed in a multi-phase system. In most reactions an aqueous and organic phase are present. Additionally, a polymer phase begins to separate from the reaction mixture after the addition of one equivalent of H₂O₂ is added to the reaction flask. The rate of hydrogen peroxide addition was controlled in order to maintain reaction temperatures below the values specified in the table.

Air was incorporated into the reaction mixture by bubbling dry air through a 15 gauge needle or with vigorous stirring in an open environment. The polymers were removed from the reaction mixture and rinsed with deionized water, methanol or acetone. The polymers were then extracted in methanol/acetone solution or acetone until translucent (24 to 72 hrs) to remove residual water and triethylamine. Longer extraction times were required for more viscous polymers. After extraction in acetone, polymers were dried until a constant mass was reached. In ice bath reactions, all reagents were pre-chilled to 2°C, and the reaction vessel was submerged in an ice bath where the dithiol/triethylamine solution was allowed to chill further to 0°C. Polymer products were characterized by NMR, FTIR, SEC, MALDI-ToF MS, DSC and TGA.

3.2.1.2. Kinetic studies of DODT polymerization using triethylamine and H₂O₂.

In a round-bottomed flask 14.5299 g (0.0797 mol) DODT and 25.00 mL (0.1794 mol) triethylamine were stirred for about 20 min to make a 2.09 M stock solution

of DODT in triethylamine. Into 6 glass vials, 6.92 mL (6.09 mmol) H₂O₂ was added, followed by 1.54 mL of the stock solution (3.23 mmol DODT) and allowed to react for a specified time (1, 5, 10, 30, 120 and 240 min). The final concentrations of DODT, triethylamine and hydrogen peroxide in each vial were 0.381 M, 0.858 M and 0.720 M respectively. Reactions were stopped by pouring the reaction mixture into methanol and removing the precipitated product. The polymer product was transferred to massed aluminum pans and placed in a vacuum oven until a constant mass was reached. Four samples (1, 5, 30 and 120 min) were selected for SEC analysis and further experiments.

A kinetic study was later repeated in triplicate under similar reaction conditions. Triethylamine and DODT were mixed in a 2:1 molar ratio. To a round bottomed flask 11.1618 g (0.0612 mol) DODT and 17.00 mL (0.1220 mol) triethylamine were added to produce a 2.27 M solution of DODT. To massed vials filled with 2.86 mL H₂O₂ (2.51 mmol), 0.75 mL of the stock solution (1.70 mmol DODT) was added, capped and shaken vigorously for 15 s. Final concentrations of DODT, triethylamine and hydrogen peroxide in each vial were 0.471 M, 0.938 M and 0.697 M respectively. The vials were then placed on an orbital shaker (300 rpm) until the predetermined reaction time was over. The content of the vials was then poured (if possible) into 10 mL of methanol held in a 20 mL glass vial (massed). The reaction vial was then rinsed with 10 mL of methanol which was added to the precipitation vial. The precipitation vial was centrifuged for 1 min at 1,700 rpm, then decanted, refilled with 10 mL methanol and centrifuged and decanted again. Both sets of vials were dried in a vacuum oven until a constant mass was reached (1 week).

Another set of kinetic studies were performed with variations in the concentration of triethylamine. The final concentrations of the reagents in the reaction mixture are shown in Table 3.2.1. To maintain the same concentration of DODT and H₂O₂ between the two studies, H₂O₂ was diluted with DI H₂O in the 1:1 molar ratio study. To massed vials charged with indicated volume of oxidizing solution, DODT/triethylamine solution was added at once and shook at 300 rpm on an orbital shaker. Reactions were stopped at timed intervals by adding 10 mL of a 50/50 acetone and methanol solution. The vials were then placed in a centrifuge at 1,700 rpm for 1 min after which the solvent decanted. This process was repeated before allowing the reactions to dry in a vacuum oven until a constant mass was reached. Reactions were performed in triplicate for each time interval.

Table 3.2.1. Concentrations of reagents in kinetic studies with variation in triethylamine concentration.

Study	DODT/Et ₃ N	H ₂ O ₂ (mL)		Final Concentrations (M)		
	(mL)	0.67 M	0.88 M	DODT	Et ₃ N	H ₂ O ₂
Et ₃ N 1:1	0.50	4.9	---	0.306	0.306	0.611
Et ₃ N 6:1	1.65	---	3.75	0.306	1.833	0.611

3.2.1.3. Chain extension with ED

In a round bottomed flask, a solution of previously synthesized poly(DODT) in THF was prepared (0.5008g in 10 mL THF) and placed in an oil bath thermostated at 25.0°C. From the mass of the polymer added, it was calculated that the solution had a DODT *repeat unit* concentration of 0.28 M. Using a syringe, 2.72mL of a 2.31 M ED solution in triethylamine was added to the DODT solution (0.5915g ED, 6.28mmol ED)

and stirred for 10 minutes. The concentration of DODT repeat units and ED monomer in the solution was 0.22 M and 0.49 M respectively. Aqueous H₂O₂ solution (2.68 mL; 3.1 mmol) was added over 1.5 minutes while stirring vigorously. The temperature of the reaction flask peaked at 30.2°C following the addition of hydrogen peroxide. Aliquots were taken at 4 and 30 minutes. The oil bath temperature was then raised to 55°C and kept at this temperature for 40min before bringing the reaction to reflux at 70°C. The flask was removed from heat at the onset of reflux and allowed to stir for 16 hours.

3.2.1.4. Degradation of DODT using dithiothreitol.

In 100 mL of THF, 0.3123 g polymer (1.7 mmol repeat units) were dissolved. To THF solution, 40 mL of a 50.05 mM dithiothreitol (Aq) (DTT) solution were added (2.00 mmol DTT). The mixture was stirred vigorously with a magnetic stir bar. Aliquots (10mL) were taken at timed intervals for NMR analysis. The reduction reaction of each aliquot was terminated by adding 5 mL CDCl₃ and 5 mL saturated NaCl solution which separated both polymer and monomer from the water-soluble DTT. The organic phase was then dried over MgSO₄ and analyzed by NMR.

3.2.1.5. Conformational analysis using SEC

Samples of poly(DODT) from the kinetic study (1, 5, 30 and 120 min) were each dissolved in 10mL of chloroform at a concentration of about 13 mg/mL. Using a glass pipet 17.2 mM solution of I₂ in chloroform was added drop-wise to the polymer solutions until they turned pale yellow and did not clear (<1 mL). The solutions were stirred for 2 hrs. Each solution was then washed with a dilute sodium thiosulfate solution, followed by washing with 0.1 N HCl and finally with DI water. The organic phase was then dried

over magnesium sulfate and the solvent was allowed to evaporate. Final drying was performed in a vacuum oven for 18 hours.

3.2.2. Mechanism investigation.

3.2.2.1. Solubility of reagents and model experiments.

In a small glass vial, 0.50 mL (3.06 mmol) of DODT and 1.00 mL of D₂O were mixed and allowed to equilibrate. The D₂O layer was then analyzed by ¹H NMR. To another glass vial, 0.50 mL(3.06 mmol) of DODT, 1.00 mL (7.17 mmol) triethylamine and 1.00 mL of D₂O were mixed and allowed to equilibrate. The D₂O layer was then analyzed by ¹H NMR. In a third glass vial, 0.50 mL(3.06 mmol) of DODT and 1.00 mL (0.88 mmol) of H₂O₂ (3% aq soln) were mixed and a sample of the organic layer was quickly removed. The organic layer was then analyzed by ¹H NMR in CDCl₃.

To determine the effect of temperature on solubility, 10.00 mL cold (2°C) triethylamine and cold (2°C) 20.00 mL DI H₂O were added to a 50.00 mL burette and mixed. The mixture was allowed to equilibrate at 2°C. The mixture was then observed as it slowly warmed to room temperature. In a 50.00 mL burette, 10.00 mL of a 2.26 M(1:1 equiv. ratio) solution of DODT in triethylamine and 20.00 mL of DI H₂O were mixed.. The volume of each layer was recorded at room temperature and at 2°C. The saturation concentration of the ionic DODT/triethylamine complex was determined by adding 21.3 mL of 1.95 M DODT solution in triethylamine (1:1.25 equivalent ratio of DODT to Et₃N) to a burette and mixing it with 17.00 mL of water at room temperature (above 18°C). After mixing and equilibrating overnight, the volume of the organic and aqueous layers was recorded.

3.2.2.2. Polymerization starting from aqueous solution of DODT and triethylamine.

A fresh ionic solution was made by combining 8.5 mL DI H₂O with 15.65 mL of 2.26 M DODT stock solution. A 10.00 mL aliquot of the solution was added to a round-bottomed flask followed by 12.0 mL 1.35 M H₂O₂. The mixture was allowed to react for 5 min before the polymer was removed and placed in methanol to extract water and triethylamine. To another round-bottomed flask, 3.59 mL of 2.26 M DODT solution in triethylamine was added, followed by 18.4 mL of 0.88 M H₂O₂. After 5 min reaction time the polymer product was removed and soaked in methanol. The final concentrations of reagents are provided in the table below. The polymers were placed in a vacuum oven until a constant mass was reached. Residual reaction solution for each polymerization was reserved and analyzed by ESI-MS.

Table 3.2.2. Concentration of reagents in the aqueous and two phase DODT polymerizations.

System	[DODT] (mol/L)	[Et ₃ N] (mol/L)	[H ₂ O ₂] (mol/L)
Aqueous Solution	0.39	0.77	0.74
Two-phase	0.37	0.74	0.74

3.2.3. Polymerization of ED and ED-DODT copolymerization using triethylamine and H₂O₂.

3.2.3.1. Homopolymerizations of ED

A 2.0 M solution of ED (0.012 mol; 1.00 mL) in triethylamine (0.036 mol, 5.00 mL) was prepared. To the ED/amine solution, 13.6 mL (0.012 mol) aqueous H₂O₂ (3% by weight) was added and stirred vigorously. Final concentrations of ED, triethylamine and H₂O₂ in the mixture were 0.61 M, 1.84 M and 0.61 M, respectively. The precipitate product was allowed 24 hours to flocculate in the solution before filtering and rinsing with cold water and cold methanol. The product was dried in a vacuum oven until a constant mass was reached.

For the poly(ED) sample prepared for comparison to the survey of copolymers, ED (0.119 mol; 10.000 mL; 11.23 g) and triethylamine (0.268 mol; 37.39 mL; 27.145 g) were mixed to create a 2.5 M stock solution of the ED. To a 100 mL round-bottomed flask equipped with a magnetic Teflon stir bar and charged with 7.95 mL ED stock solution, 0.040 mol (45.45 mL) H₂O₂ was added all at once. The temperature inside the reaction flask was monitored using a thermometer. After 10 min, the reaction was stopped by diluting the reaction solution with methanol and filtering out the polymer precipitate. The precipitate was dried until a constant mass was reached. A portion of the crude product was purified by mixing it with THF and letting it sit overnight. The product was then filtered and dried in a vacuum oven. A sample of the THF filtering solution was reserved and analyzed by ESI-MS.

3.2.3.2. Survey of ED-DODT copolymerizations.

ED (0.119 mol; 10.000 mL; 11.23 g) and triethylamine (0.268 mol; 37.39 mL; 27.145 g) were mixed to create a 2.5 M stock solution of the ED. DODT (0.122 mol; 20.000 mL; 22.28 g) and triethylamine (0.275 mol; 27.82 g; 38.32 mL) were mixed to create a 2.1 M stock solution of the DODT. The monomer stock solutions were stirred for about 40 min at 1100 rpm.

Comonomer solutions were mixed in 100 mL round-bottomed flasks equipped with magnetic Teflon stir bars, and stirred at 400rpm for several minutes. The mixing speed was then increased to 850 rpm and 0.040 mol (45.45 mL) H₂O₂ was added all at once. The temperature inside the reaction flask was monitored using a thermocouple probe. The numbers in the sample IDs refer to the mole fraction of ED in the comonomer solution. For example, the copolymer with an ED mole fraction of 0.9 is labeled ED-9.

Table 3.2.3. Comonomer solutions of ED with DODT.

Sample	Monomer concentration in Et ₃ N (mol/L)		Conc. Monomer in Final Mixture (mol/L)		Mole Fraction ED
	ED	DODT	ED	DODT	
ED-9	2.21	0.25	0.34	0.04	0.9
ED-7	1.66	0.71	0.26	0.11	0.7
ED-5	1.14	1.14	0.18	0.18	0.5
ED-3	0.66	1.54	0.11	0.26	0.3
ED-1	0.21	1.92	0.04	0.33	0.1

After 10 minutes, the reactions were stopped by removing the products from the reaction solutions. The product of ED-9 was removed by filtration. All other products were removed from the reaction flasks with tweezers, rinsed with methanol and transferred to massed aluminum pans for drying. When a constant mass was achieved the

samples were removed and weighed. Dried samples were dissolved in THF and precipitated in methanol. Insoluble copolymers were filtered from the THF and rinsed with methanol. All products were dried in the vacuum oven until a constant mass was reached.

3.2.3.3. Tensile testing of poly(DODT) and poly(ED-*co*-DODT)

Poly(ED-*co*-DODT) was synthesized by mixing 12.00 mL 2.5 M solution of ED in triethylamine with 18.00 mL of 2.5 M DODT in triethylamine in a 500 mL round bottomed flask to make a comonomer mixture with an ED fraction of 0.4. The comonomer mixture was then reacted with 170.45 mL aqueous H₂O₂ (3% by wt) for 2 hours. Poly(DODT) by the same method as described previously. After purification by precipitation, the two products were dissolved separately in 250 mL chloroform with 30 phr carbon black (Degussa/Evonik 234). The chloroform was allowed to evaporate from the polymer/carbon black mixtures in Teflon pans.

Using laboratory press (Carver Laboratory Press with Omega CN 9000 Temperature Controller), the carbon black was dispersed into the polymer by a ‘micromixing’ technique. The poly(DODT) sample was micromixed at 80°C, and the poly(ED-*co*-DODT) was mixed at 120°C. After 25 cycles of compression and folding, the samples were molded into small tensile pads and allowed to anneal by cooling from the molding temperature to room temperature under pressure for 24 hours. Standard microdumbbells were then cut from each pad, the thickness measured using a micrometer and tested on an Instron 5567 tensiometer with an extension rate of 50 mm/min.

3.2.3.4. Effect of mixing rate ED-DODT copolymerization.

Two copolymers were prepared from comonomer/triethylamine solution containing an ED mole fraction of 0.3. The first copolymer was made using a magnetic stir bar (Mag-ED-3). The second copolymer was mixed using an overhead mechanical stir rod equipped with a teflon paddle (Mech-ED-3). Reactions were stopped after 2 hrs. The oxidizing mixtures were decanted and the products were purified by dissolution in chloroform, followed by precipitation in a 50:50 methanol/acetone mix. The products of the two reactions were analyzed by proton NMR and SEC.

3.2.3. DODT-based disulfide networks

3.2.3.1. New network synthesis using DODT and TMPTMP

DODT (2.05 mL; 12.54 mmol, 0.34 M) was combined with TMPTMP (0.03 mL; 0.08 mmol; 0.002 M) and triethylamine (1.71 mL; 12.35 mmol; 0.34 M). To the thiol/amine solution, 3.0 mL tetrahydrofuran and 5.0 mL ethyl acetate were added. Hydrogen peroxide was then added (about 25 mL of 3% (aq); 22.0. mmol; 0.60 M), and air was bubbled into the reaction beaker for 5 min. After the bubbling, the reagents were allowed to react undisturbed for 16 hours. The rubbery gel disk that formed was soaked in acetone for 6 hours and then dried in a vacuum oven for 24 hours.

3.2.3.2. Method optimization for network synthesis

In the standardized method of DODT network synthesis stock solutions of TMPTMP with DODT and triethylamine were prepared. TMPTMP was weighed into 4 glass vials in varying amounts. To the vials, 3.30 M DODT in triethylamine (1:1 molar

ratio) was added. An example of the final concentrations of TMPTMP, and its molar ratio to DODT for a solutions used in a typical reaction is listed in Table 3.2.4

Table 3.2.4. Concentration of TMPTMP in each DODT/amine solution.

[TMPTMP] (mol/L)	DODT:TMPTMP
0.5532	6.0 : 1.0
0.1342	24.6 : 1.0
0.0640	51.6 : 1.0
0.0331	99.7 : 1.0

To synthesize a small-sized network, 0.50 mL of a TMPTMP-DODT-triethylamine solution was added to a 4.0 mL glass vial, followed by 0.50 mL THF, 0.83 mL ethyl acetate 2.00 mL of H₂O₂ (3% aq.). Large sized networks were made in 20.0 mL vials to which 2.17 mL of stock solution, 2.17 mL THF, 3.60 mL of ethyl acetate and 8.6 mL H₂O₂ were added. The final concentrations of each reagent for the 4 standard networks are listed below. In the standard synthesis vials were capped and shaken vigorously for 2.0 min then allowed to react undisturbed for 3 to 4 days. Networks were removed from the vials and extracted in acetone, then extracted in THF followed by drying for 1-2 days in a chemical hood and drying in a vacuum oven until a constant mass was reached.

Table 3.2.5. Final concentration of reagents in optimized network reaction.

DODT:TMPTMP	[TMPTMP] (mol/L)	[DODT] (mol/L)	[Et ₃ N] (mol/L)	[H ₂ O ₂] (mol/L)
6:1	0.072	0.431	0.431	0.460
25:1	0.018	0.431	0.431	0.460
50:1	0.008	0.431	0.431	0.460
100:1	0.004	0.431	0.431	0.460

3.2.3.3. Swelling and crosslink density

Network samples were cut with razor blades into pie-shaped wedges. Incongruent or defective portions of networks which contained bubbles or air pockets were not included. Dry mass of cut samples was recorded before placing them into glass vials with 3 mL of swelling solvent (DI H₂O, THF or hexane). After 72 hrs, swollen samples were removed from vials, firmly patted dry with a Kimwipe, and massed while swollen. Each sample was returned to the swelling solvent. Each measurement was repeated 5 times.

The molecular weight between crosslinks was calculated using the Flory-Rhener equation (Eq. 2.1). The polymer density was estimated using the monomer density (1.14 g/mL) and by group addition. Solvent parameters were found in the literature.

3.2.3.4. Reduction of networks

3.2.3.4.1. Network reduction using dithiothreitol

A 50 mM solution of DTT in THF was mixed in a 25 mL volumetric flask. To one vial, 10.0 mL 50 mM DTT solution was added to a 0.0126 g network sample. To another vial, 5.0 mL 50 mM DTT and 5.0 mL DI H₂O were added 0.0207 g network

sample. The network was stored in the reducing medium in a dark 37°C and checked every 24 hrs.

3.2.3.4.2. Network reduction in aqueous environments

In the glutathione degradation experiment, 50 mM solution of glutathione (GSH) in 5.2 pH acetate buffer was prepared. Acetate buffer was used to mimic lysosomal conditions and to prevent base-catalyzed GSH oxidation to GSSG. To a series of 4 vials, 3.0 mL of the GSH solution was added followed by the network sample. Vials were stored in a windowless oven set at 37°C. The samples were periodically removed from the oven and massed. They were then replaced in the glutathione/buffer solution.

In the digestive model study, stomach acid was represented by HCl (Aq) solution with pH ≈ 2.09 recorded using a pH probe. The small intestines were represented by two aqueous mixtures of bile salts (cholic acid-deoxycholic acid sodium salt mixture) with different concentrations. To make a 4.15 mg/mL mixture, 0.4162 g bile salts were added to 100 mL D.I. water and shaken. A pH probe recorded pH = 7.23. The second bile salt mixture was made by mixing 1.9991 g bile salts with 100 mL DI H₂O. A pH probe recorded pH = 6.50. To a series of 3 vials, 10.0 mL each solution was added followed by a wedge cut from the 1:50 network sample. Vials were stored in a dark oven set at 37°C. The samples were periodically removed from the oven and massed. They were then replaced in the solution and returned to the oven.

3.2.5. Polymerization of α -lipoic acid and α -lipoic acid derivatives.

3.2.5.1. Polymerization of α -LA

3.2.5.1.1. Polymerization of α -lipoic acid with triethylamine and H_2O_2

To a round bottomed flask, triethylamine (0.40 mL) and DI H_2O (0.60 mL) were added. In R-Ox-0 the aqueous amine solution was allowed to equilibrate in an ice bath. Next, α -lipoic acid was added slowly. H_2O_2 was added to the flask and allowed to stir for 2 hrs. The reaction was stopped by adding HCl to the reaction solution which coagulated the polymer product. Reaction conditions and reagent concentrations are listed in Table 3.2.6.

Table 3.2.6. Reaction conditions for the polymerization of R- α -LA using triethylamine and aqueous H_2O_2 .

Sample	Temp. (°C)	[R- α -LA] (mol/L)	[Et ₃ N] (mol/L)	[H ₂ O ₂] (mol/L)
R-Ox-23	23	0.304	0.399	0.758
R-Ox-0	0	0.333	0.399	0.758

3.2.5.1.2. Thermal polymerizations of α -LA

In a typical thermal polymerization, α -LA was added to a round bottomed flask attached to a Schlenk line. The flask was then placed in an oil bath thermostated to a given temperature above the melting point of α -LA and vacuum was applied. After the allotted time, the flask was removed from heat, and the contents of the flask dissolved in 10 mL-15 mL of THF. The polymer was then precipitated in diethyl ether or chloroform.

In compression molding experiments, α -LA monomer was added directly to the heated tensile pad mold and allowed to melt thoroughly before closing the mold. For

annealed samples, the filled mold was then placed in the compression press between 90°C and 95°C, brought up to 5,000 psi for 2-5 min, then bumped 3 times and returned to 10,000-15,000 psi compression. The sample was heated for 2 hrs, then allowed to cool to room temperature under pressure. Non-annealed samples were first melted in the tensile pad mold, then molded quickly under 2,000 psi-5,000 psi and removed from the press while still hot.

3.2.5.1.3. Post-polymerization functionalization of poly(α -LA) with PEG-CH₃

Poly(α -LA) synthesized previously (sample R-T-100; 0.1168 g; 0.56 mmol acid groups) and 1.0967 g (of PEG-CH₃ (2000 g/mol; 0.55 mmol) were dissolved in 12.0 mL of THF. To the solution 180.5 mg of CALB were added. The flask was placed under nitrogen in an oil bath set to 65°C for 47.5 hrs. The product was then dissolved in 25 mL of chloroform and the enzyme was filtered out through MgSO₄ and activated carbon to remove any water and free α -LA. Solvent was removed by rotary evaporation and then the flask was placed in a vacuum oven until dry. In a 100 mL volumetric flask, 0.0110g of product was added, then it was filled to the line with chloroform, and allowed to dissolve overnight. The solution was spincoated onto both silica wafers and freshly cleaved mica chips and imaged using AFM.

3.2.5.1.4. Synthesis of α -LA-PEG-CH₃

To a round-bottomed flask attached to a Schlenk line and equipped with a magnetic stir bar, 3.7215 g (2.00 mmol; 3.38 mL) CH₃-PEG-OH were added. The flask was placed in an oil bath thermostated at 60°C, and vacuum was applied all bubbling had

subsided from the melted polymer (about 40 min). To the PEG melt, 0.4555 g (2.21 mmol;) of recrystallized α -LA and 80 mg CALB were slowly added. When the α -LA was thoroughly melted, the flask was returned to vacuum and allowed to react for 24 hours. Aliquots of the reaction were taken at timed intervals during the reaction (65 min, 3 hrs, 6 hrs, 18 hrs, and 24 hrs). At 24 hrs, the reaction was diluted with acetone. After removing the enzyme by filtration, the product was precipitated into cold diethyl ether and allowed to flocculate overnight. The product was recovered by filtration and dried in a vacuum oven until a constant mass was achieved. The procedure was repeated with CALB omitted.

3.2.5.1.5. Polymerization of α -lipoic acid by precipitation (with water).

A 0.562 M of α -LA solution in THF was prepared. Then 0.5 mL of the solution was dropped into a crystallization dish filled with water at room temperature. The process was repeated using water at 65°C and 100°C. Polymeric products were collected from the air/water interface using a glass rod and dried in a vacuum oven until a constant mass was reached.

3.2.5.2. Synthesis of monofunctional α -lipoic acid derivatives via enzymatic catalysis.

3.2.5.2.1. Synthesis of α -LA-DEG-CH₃

Three reactions were run in capped test tubes equipped with a magnetic stir bar at ambient pressures. The mass and concentration of reagents is shown in Table 3.2.7. The test tubes were then placed in an oil bath at 55°C and allowed to react for 14 hrs. At 13 hrs, a drop of HCl was added to each reaction. The samples were removed from heat,

diluted with chloroform and filtered into a separatory funnel. The reaction solution was washed with 3 portions of DI water, dried over MgSO₄ and the solvent was removed by rotary evaporation.

Table 3.2.7. Reaction conditions for the synthesis of CH₃-DEG-α-LA.

Sample	α-LA		DEG-CH ₃			THF (mL)	V _{total} (mL)	CALB (mg)	
	Mass (g)	mmol	Conc. (mol/L)	Vol (mL)	mmol				
DEG-Bulk	0.4126	2.00	0.50	4.00	33.96	8.49	0.00	4.00	80
DEG-1	0.4136	2.00	0.50	0.47	3.99	1.00	3.52	3.99	80
DEG-.5	0.4127	2.00	0.50	0.23	1.95	0.48	3.80	4.03	80

3.2.5.2.2. Synthesis of α-LA-TEG-OH and α-LA-HEG-OH

TEG was added to a round bottomed flask using a pipet. HEG was added to a separate flask using a syringe. To the flasks, α-LA and CALB were added slowly in the amounts indicated in Table 3.2.8. The flasks were evacuated and refilled with N₂ gas 3 times and left under N₂ atmosphere in an oil bath at 55°C.

Table 3.2.8. Reaction conditions HO-TEG-α-LA and HO-HEG- α-LA synthesis.

α-LA		Glycol					CALB
Mass (g)	mmol	Conc. (mol/L)		Vol (mL)	Mass (g)	Conc. (mol/L)	(mg/mL)
0.5164	2.50	0.25	TEG	10.00	10.20	52.52	5.25
0.1053	0.50	0.25	HEG	2.00	1.03	3.65	1.83

After 4 hours, the reactions were removed from heat, diluted with THF, filtered, rotavaped and then redissolved in chloroform. The product was purified by washing with

5 to 6 portions of acidified water ($\text{pH} \approx 4.5$). The organic phases were dried with MgSO_4 , then filtered with #2 paper into a massed round bottomed flask from which solvent was removed by rotary evaporation.

The effect of α -LA concentration on the rate of CALB-catalyzed TEG functionalization was investigated by comparing reactions with two concentrations of α -LA. Using a pipet, 10.00 mL of TEG was added to each round-bottomed flask attached to a Schlenk line and equipped with a magnetic stir bar. The flasks were placed under vacuum in an oil bath at 55°C for 20 min to dry the TEG. The flasks were then removed from heat and vacuum, and α -LA was slowly added while stirring. When α -LA was completely dissolved, the immobilized enzyme was added (purchased from Sigma-Aldrich; *Candida antarctica* lipase B recombinant from yeast on Immobead 150; Lot # BCBD9402V = 3325 U/g; Lot # 1388469 = 5865 U/g Let me confirm which lot# it was). The amounts and concentration of each reagent are listed in Table 3.2.9.

The flasks were placed in the oil bath and returned to vacuum. Aliquots were taken for ESI-MS analysis at 20 min, 30 min, 55 min and 6.5 hrs. The flasks were then removed from the bath and vacuum and allowed to cool. The reactions were diluted with 30 mL of chloroform and the enzyme was filtered out. The chloroform solution was washed with nine 100 mL portions of dilute HCl (Aq) ($\text{pH} = 4.0$). The organic phase was then dried over MgSO_4 and the chloroform was removed by rotary evaporation.

Table 3.2.9. Reagent concentration in the synthesis of HO-TEG- α -LA.

Sample	a-LA			TEG			CALB (mg)
	Mass (g)	mol	Conc. (mol/L)	Vol (mL)	Mol	Conc. (mol/L)	
LA-TEG-0.4	0.8263	0.00400	0.4005	10.00	0.0579	5.7921	202.1
LA-TEG-0.2	0.4128	0.00200	0.2001	10.00	0.0579	5.7921	202.5

CHAPTER IV

RESULTS AND DISCUSSION

The objective of this research was to synthesize poly(disulfide) polymers and networks using a green chemistry approach. Anticipating applications as reduction-sensitive biomaterials, the new method developed employed mild reaction conditions, low toxicity solvents and recyclable catalysts. Additionally, with rising concerns over energy sources and costs, many reactions were performed at ambient temperatures, which improves energy efficiency over traditional synthetic methods that require heating.

4.1. New oxidative polymerization of DODT using triethylamine and H₂O₂.

4.1.1. Scouting experiments

García-Ruano *et al.*³⁵ reported the use of sonication to promote the triethylamine-activated, air-oxidation of monothiol compounds dissolved in dimethylformamide (DMF) to form symmetric disulfide compounds. Building on their sonication method, two dithiol compounds were selected for oxidation, with the intent of synthesizing disulfide-bonded polymers. The two dithiols selected as compounds for the reaction were 3,6-dioxa-1,8-octanedithiol (DODT) and 1,2-ethanedithiol (ED). A series of small-scale preliminary reactions were performed which varied the volume of triethylamine and DMF. Table 4.1.1 lists the volume and moles of reagents used in the preliminary study.

Table 4.1.1. Volume and moles of reagents used in preliminary studies with sonication.

Reaction	Dithiol			Triethylamine		DMF
Vial No.	Dithiol	mL	mmol	mL	mmol	mL
P1	DODT	0.2	1.2	0.16	1.2	1.0
P2	DODT	0.2	1.2	0.33	2.4	1.0
P3	DODT	0.2	1.2	0.16	1.2	1.0
P4	DODT	0.2	1.2	0.33	2.4	1.0
P5	DODT	0.2	1.2	0.33	2.4	---
P6	DODT	0.2	1.2	0.33	2.4	---
P7	ED	0.1	1.2	0.16	1.2	---
P8	ED	0.1	1.2	0.34	2.4	---

After reacting under sonication for 50 min, no visible reaction was observed in any of the 8 reaction vials. However, when excess aqueous H₂O₂ was added to the failed reactions in vials P2, P4, P6 and P7, an immediate, exothermic reaction was observed which caused a visible change in the vial contents from a clear solution to a milky white mixture. The reaction mixtures in vials P2, P4 and P6 were poured into aluminum dishes. A polymeric mass developed in P6 within a few minutes. Vial P7 formed a chunky white precipitate that was not soluble in acetone nor methanol, and it appeared to be very slightly soluble in THF and chloroform. After reacting overnight polymeric products were observed in vials P2 and P4. No change was seen in vials P1 or P5 after 24 hrs. Based on the conditions which quickly produced the polymer mass in vial P6, a new series of scouting reactions was performed.

In vial P6 of the preliminary reactions, the molar ratio of triethylamine to DODT was 2:1, and no DMF was used. It was particularly desirable to eliminate DMF because it

is a known teratogen. Following this strategy, a series of reactions were performed to further investigate the role of triethylamine and the addition of H₂O₂.

The scouting reactions are summarized in Table 4.1.2. Reactions S1 and S2 were stirred for three hours. Reactions S3 and S4 were heated for 1 hr and then allowed to react overnight. Reactions S5 and S6 were also allowed to react overnight. Observations were made the following day.

Table 4.1.2. Volume and moles of reagents used in scouting reactions.

Trial No.	DODT		Triethylamine		H ₂ O ₂		PBS		Polymer Product?
	mL	mmol	mL	Mmol	mL	mmol	mL	Heat	
S1	3.0	18.3	---	---	20.8	18.3			No
S2	3.0	18.3	---	---	10.4	9.2			No
S3	1.0	6.1	1.7	12.2	---	---	6.0	×	No
S4	1.0	6.1	1.7	12.2	“Excess” ≈15 mL /13 mmol			×	Yes
S5	1.0	6.1	1.7	12.2	---	---	6.0		No
S6	1.0	6.1	1.7	12.2	“Excess” ≈15 mL/13 mmol				Yes

In reactions S1 and S2 a white substance evolved in the flasks almost immediately upon the addition of hydrogen peroxide, however, with time the reaction mixture became an opaque white liquid. No polymer phase was observed. Reactions S3 and S5 showed three liquid phases. The top phase was milky white, the middle phase was clear and the bottom phase was a translucent white liquid that balled up into a sphere.

From the scouting experiments, it was found that no polymeric substance was formed without triethylamine or H₂O₂. A series of 9 exploratory reactions was performed varying the ratios of DODT, triethylamine and hydrogen peroxide. The conditions for

the exploratory reactions are summarized in Table 4.1.3. Using a syringe, DODT and triethylamine were added to each vial. The hydrogen peroxide was added in successive 0.5mL increments with constant swirling of the reaction vial.

Table 4.1.3. Volume and moles of reagents used in exploratory reactions.

Reaction	DODT		Triethylamine		H_2O_2	
No.	mL	mmol	mL	mmol	mL	mmol
E1	1.00	6.1	2.55	18.3	1.74	1.5
E2	1.00	6.1	2.55	18.3	3.47	3.1
E3	1.00	6.1	2.55	18.3	6.94	6.1
E4	1.00	6.1	1.70	12.2	1.74	1.5
E5*	1.00	6.1	1.70	12.2	3.47	3.1
E6	1.00	6.1	1.70	12.2	6.94	6.1
E7	1.00	6.1	1.28	9.2	1.74	1.5
E8	1.00	6.1	1.28	9.2	3.47	3.1
E9	1.00	6.1	1.28	9.2	6.94	6.1

*Reaction spilled; no observations.

The reactions with 1.5 mmol of hydrogen peroxide (E1, E4, E7) would briefly turn white upon the addition of H_2O_2 , but after swirling, the reaction would return to a clear solution. Viscous liquids separated to the bottom of the vials in reactions E2 and E7. Reactions E3, E6 and E9 each formed a globular polymeric product which separated to the bottom of the reaction mixture. The remaining liquid was decanted, and the product was rinsed in fresh DI water followed by methanol. The products from reactions E3, E6 and E9 were placed in aluminum pans where they were allowed to soak in acetone to extract residual water and starting materials. The solvent was decanted, and the

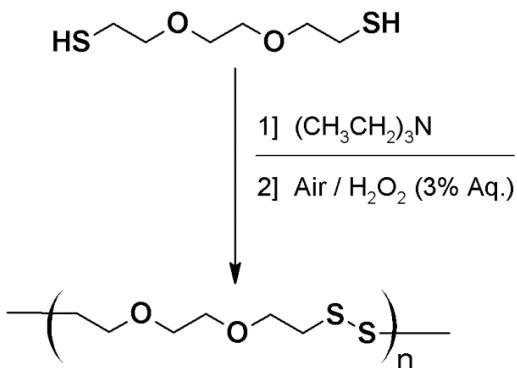
products were dried overnight. The resulting products were sticky, gooey masses. Thin layer chromatography of the products was used to determine if column purification was necessary. Silica plates were used with varying ratios of ethyl acetate and hexanes as the mobile phase. The products' chromatograms showed only one spot that did not correspond to the R_f values of the starting materials (DODT and triethylamine).

Reaction E5 was knocked over slightly while adding H_2O_2 , as the stoichiometry was already thrown off, so an additional 15 mL of H_2O_2 was added to the reaction. A polymer product with the consistency of fresh mozzarella cheese formed in the next few minutes. It did not become sticky after soaking in acetone and drying. From the results of the E5 reaction, it was apparent that a molar excess of H_2O_2 relative to moles of DODT were required to form a solid polymer. To E1, E4, and E7, 12 mL of additional H_2O_2 were added and allowed to react. All three reactions formed polymer products. The reaction in E7, which contained the least triethylamine, formed a gooey mass while the products of reactions E1 and E4 were non-sticky polymers.

From the results of the scouting experiments, it was observed that solvent (DMF) was a hindrance to polymerization, that a molar excess of triethylamine to DODT was necessary for polymerization, and that at least a 2:1 molar ratio of triethylamine to DODT was preferred. It was also observed that to achieve non-sticky polymers, thought to be higher molecular weight, a 2:1 molar ratio of H_2O_2 to DODT was necessary.

Scheme 4.1.1 displays the polymerization system. In the first step of the polymerization system, the dithiol monomer (DODT is shown) is dissolved in triethylamine. In the second step, dilute, aqueous hydrogen peroxide is added and air is

incorporated into the reaction mixture by bubbling through a needle and/or by vigorous stirring.^{85, 86}



Scheme 4.1.1. Poly(DODT) synthesis with triethylamine and dilute aqueous H_2O_2 .

4.1.2. Effect of reaction conditions

Table 4.1.4 lists the conditions and results of DODT polymerization under varying conditions. The reactions in Table 4.1.4 are identified by three numbers. The first number represents the length of time (in min) of the premixing step (DODT with Et_3N) the second number represents the length of time of the oxidative step (in min). The oxidative time starts as soon as the first drop of H_2O_2 reaches the reaction flask. The third number represents the maximum temperature reached in the reaction flask (T_{\max}). The maximum temperature reached inside the reaction flask was controlled by the rate of H_2O_2 addition; slower addition of H_2O_2 translated to a lower maximum temperature reached in the flask. It was later determined that adding H_2O_2 in a steady stream from a burette allows for an average addition rate of 0.5 mL/s (30 mL/min). At this rate the maximum reaction temperature was maintained below 55°C when the reaction was started at room temperature.

Table 4.1.4. Conditions and results of example polymerization reactions.

Reaction	Premixing	Oxidative	Temp (°C) Start//Max	Final Concentrations (M)			% Conv.
	(min)	(min)		DODT	Et ₃ N	H ₂ O ₂	
10-9-70	10	9	RT // 70	0.39	0.88	0.72	73%
10-120-70	10	120	RT // 70	0.39	0.88	0.72	80%
10-5-55	10	5	RT // 55	0.37	0.74	0.74	80%
10-10-55	10	10	RT // 55	0.36	0.80	0.73	67%
10-120-55	10	120	RT // 55	0.36	0.90	0.72	90%
10-25-Ice	10	25	0 // ≈20-25	0.35	0.69	0.75	88%
160-25-Ice	160	25	0 // ≈20-25	0.35	0.69	0.75	87%
10-60-15	10	60	0 // 15	0.35	0.69	0.75	Emulsion

The reaction mixtures immediately changed from clear to translucent white upon the addition of H₂O₂. The opacity of the solution increased as more H₂O₂ was added. After the addition of approximately 1 molar equivalent of H₂O₂ to DODT, a liquid polymer product began to separate from the reaction mixture. The time and volume at which one molar equivalent of H₂O₂ reached the reaction flask was dependent on the scale of the reaction, however, the time was usually under 1 min.

With the addition of more than one molar equivalent of H₂O₂, the liquid polymer phase became more viscous. The polymer phase continued to increase in viscosity with increased reaction time. At the same time, the once-opaque reaction mixture cleared to a slightly hazy translucent aqueous phase. A thin layer of triethylamine was observed on top of the aqueous phase when stirring was stopped. Although the polymerization reactions proceed in a multi-phase system, reported concentrations were calculated assuming a homogeneous system.

The temperature inside the reaction flasks increased abruptly as soon as H₂O₂ was added to the dithiol/amine solution. The maximum temperature (T_{max}) reached in the reaction flask was controlled by varying the rate of H₂O₂ addition. In the reactions which reached 70°C (10-9-70 and 10-120-70), the full volume of H₂O₂ (166 mL) was added at once from a 250 mL graduated cylinder. In the synthesis of sample 10-120-55, H₂O₂ (145 mL) was added in 10 mL aliquots over about 5 min (averaged rate = 29 ml/min). H₂O₂ (12 mL) was added more slowly to the ice bath reaction (10-25-Ice, 160-25-Ice, 10-25-15) with 1 mL aliquots being added over a period of about 2 min (averaged rate = 6 ml/min).

The length of the premixing step had no significant effect on the monomer conversion, as can be seen by comparing reactions 10-25-Ice and 160-25-Ice (Table 4.1.4). The highest conversion was reached in reaction 10-120-55. Higher T_{max} values provide a slight increase in conversion in short reaction times (10-10-55 v. 10-9-70), but they result in lower conversion rates when the reaction is allowed to continue to longer reaction times (10-120-70 v. 10-120-55). Because some loss of low molecular weight species is possible during the purification process, the % conversion values may be slightly lower than the actual value. Some variance in conversion must also be attributed to the variation in concentration. For example, 10-120-55 has the highest triethylamine concentration.

The ¹H NMR spectra of the DODT monomer and the poly(DODT) polymer from reaction 10-120-55 are compared side-by-side in Figure 4.1.1. In the monomer spectrum (A) the signal from the sulphydryl proton appears as a triplet (*d*, 1.58 ppm) as it is split by the two neighboring methylene protons (*c*). In turn, these sulfur adjacent methylene

protons (*c*, 2.71 ppm) appear as a quartet after their signal is split by both the thiol proton and the two oxygen-adjacent methylene protons (*b*, 3.61 ppm). The central, equivalent methylene protons have equivalent vicinal hydrogen neighbors and appear as a singlet (*a*, 3.62 ppm). In the polymer spectrum, the sulfur-adjacent methylene protons have shifted downfield to 2.91 ppm (*c*) and appear as a triplet since the signal is split by only their methylene neighbors. The triplet from the oxygen adjacent protons has also shifted downfield to 3.75 (*b*). The central protons were least affected by polymerization reaction, and their singlet signal shifts only slightly downfield to 3.65 ppm (*a*).

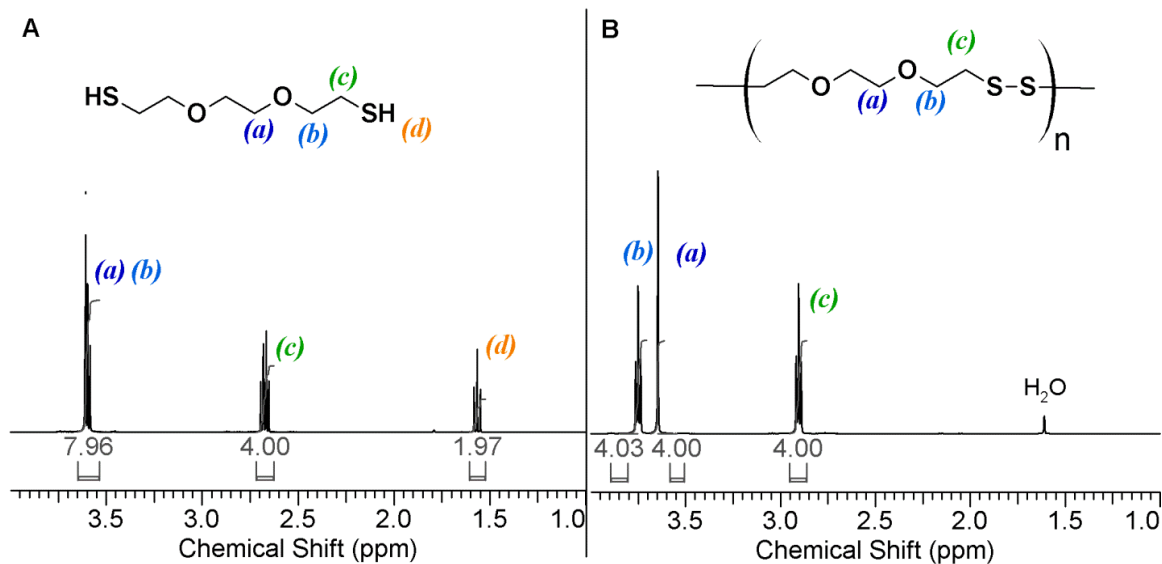


Figure 4.1.1. ^1H NMR spectrum of DODT and poly(DODT) (Sample 10-120-55).
(500 MHz; CDCl_3 ; 12 s relax; 128 trans.)

Surprisingly, $-\text{SH}$ end group protons were not detected in this sample. However thiol end groups were detected in the two reactions that reached high temperatures. The ^1H NMR spectra of samples of 10-9-70 and 10-120-70 showed $-\text{SH}$ proton signals (*e*)

(Figure 4.1.2.). Integration based on the proton signal from the thiol end groups relative to the main chain protons was used to calculate the molecular weight of sample 10-9-70 as $M_n = 15,500$ g/mol, which is somewhat higher than the $M_n = 13,000$ g/mol value measured by SEC (Table 4.1.5.). For sample 10-120-70 NMR integration calculations gave $M_n = 39,000$ g/mol which is below the $M_n = 48,000$ g/mol measured by SEC. Because polymer samples from the ice bath reactions are dominated by the low molecular weight species, the ^1H NMR spectra show a multitude of overlapping peaks corresponding to the oligomers and polymer. However, no triplet of $-\text{SH}$ end group protons was seen between 1.60 ppm and 1.50 ppm.

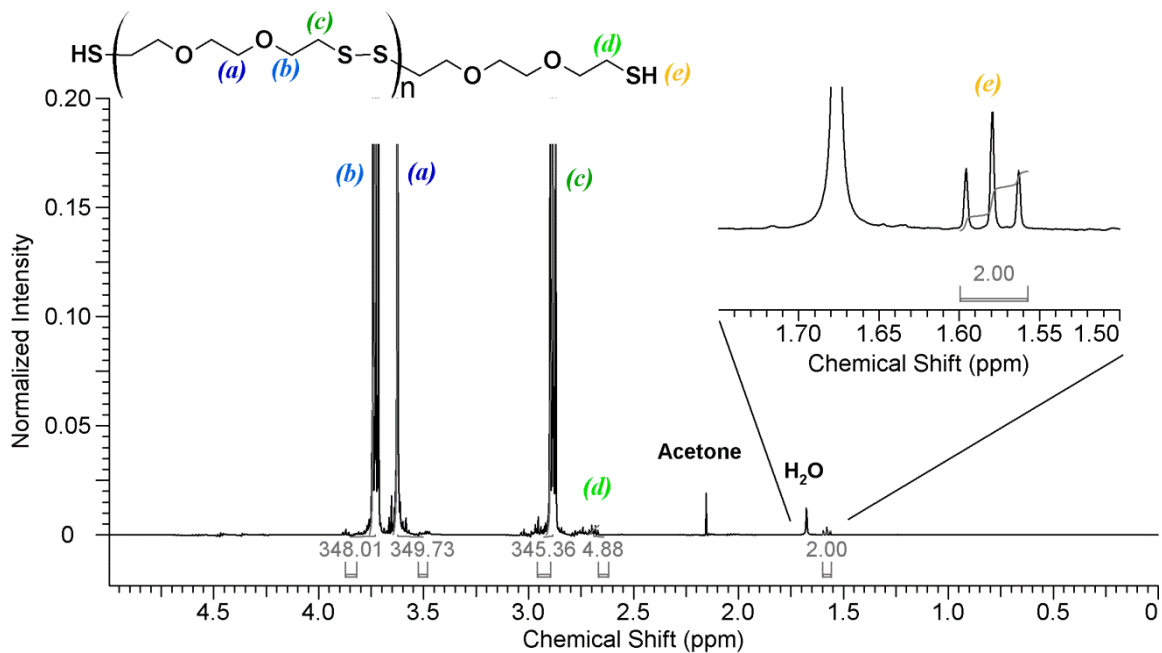


Figure 4.1.2. ^1H NMR spectrum poly(DODT)(Sample 10-9-70). (500 MHz; CDCl_3 ; 12 s relax; 128 trans.)

The ^{13}C NMR spectrum of the starting material and polymer product of reaction 10-120-55 are shown in Figure 4.1.3. Large changes in chemical shift distinguish the monomer and polymer spectra. The sulfur-adjacent carbon (C) signal, which shifts from 24.39 ppm in the dithiol starting material to 38.39 ppm in the polymer, shows the greatest change in after polymerization because the sulfur atom is less shielding in the disulfide state. The oxygen-adjacent carbon (B) signal moves upfield from 72.82 ppm to 70.32 ppm and the central carbon atom's signal (A) moves upfield slightly from 70.13 ppm to 69.95 ppm in the less polar polymer molecule.

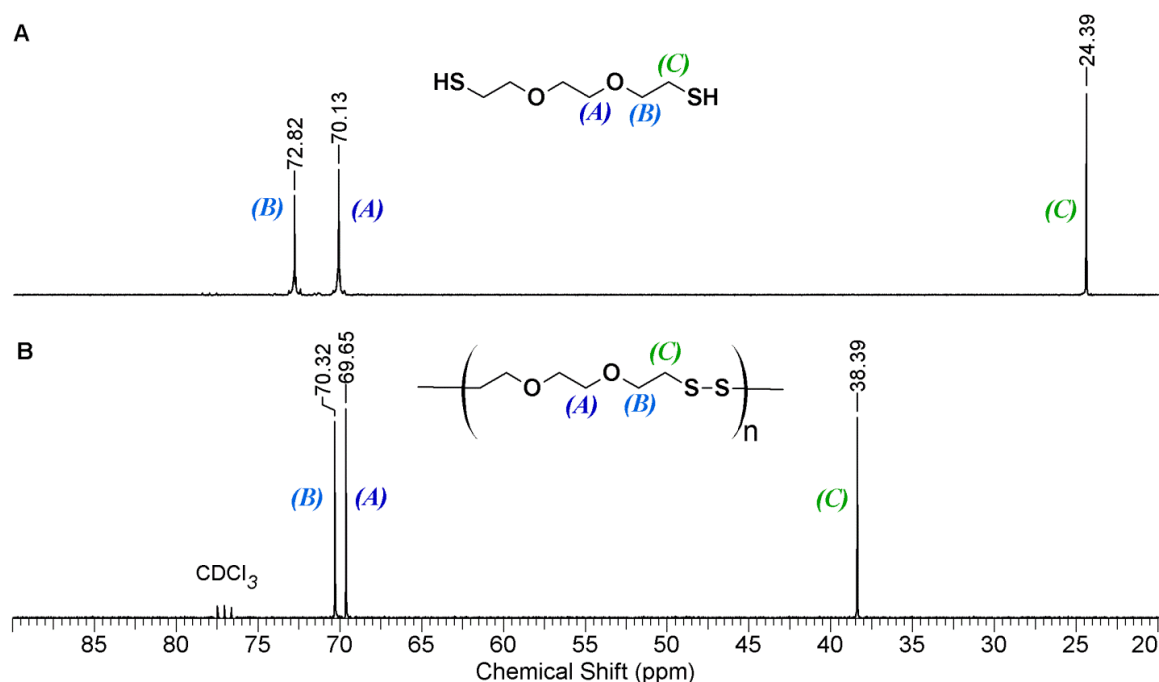


Figure 4.1.3. ^{13}C NMR spectrum of DODT (A) and poly(DODT) (B; Sample 10-120-55). (500 MHz; 10 s relax.; 1024 trans.)

The ^{13}C NMR of the 10-120-55 polymer verified the absence of thiol end groups in the polymer.

In Figure 4.1.4, the infrared spectra of the monomer and poly(DODT) sample 10-120-55 are compared. The strong peak at 2557 cm^{-1} (a) in the monomer spectrum which corresponds to S-H stretch of DODT thiol groups is absent in the polymer spectrum. A sharp peak in the fingerprint region of the monomer spectrum (b; 667 cm^{-1}) corresponding to the C-S bond vibration in thiols also disappears after polymerization. In its place, a weak C-S stretching signal appears at 644 cm^{-1} (d) which corresponds to the C-S stretch in disulfide compounds. Due to their symmetry, disulfide bond signals are inherently weak in IR and only a small signal corresponding to the S-S bond can be seen in the polymer spectrum at 467 cm^{-1} (e). A signal at 1042 cm^{-1} (c) from C-O-C symmetric stretching evolves from a shoulder in the monomer spectrum to a strong peak the polymer spectrum. Strong peaks in this region are seen in other compounds with multiple ether bonds. The C-H stretching signals from 2800 cm^{-1} to 3000 cm^{-1} appear in both spectra, as does the strong asymmetric C-O-C signal at 1113 cm^{-1} . Other poly(DODT) samples have very similar spectra, and even polymers which display a thiol peak in ^1H NMR do not present a characteristic thiol peak.

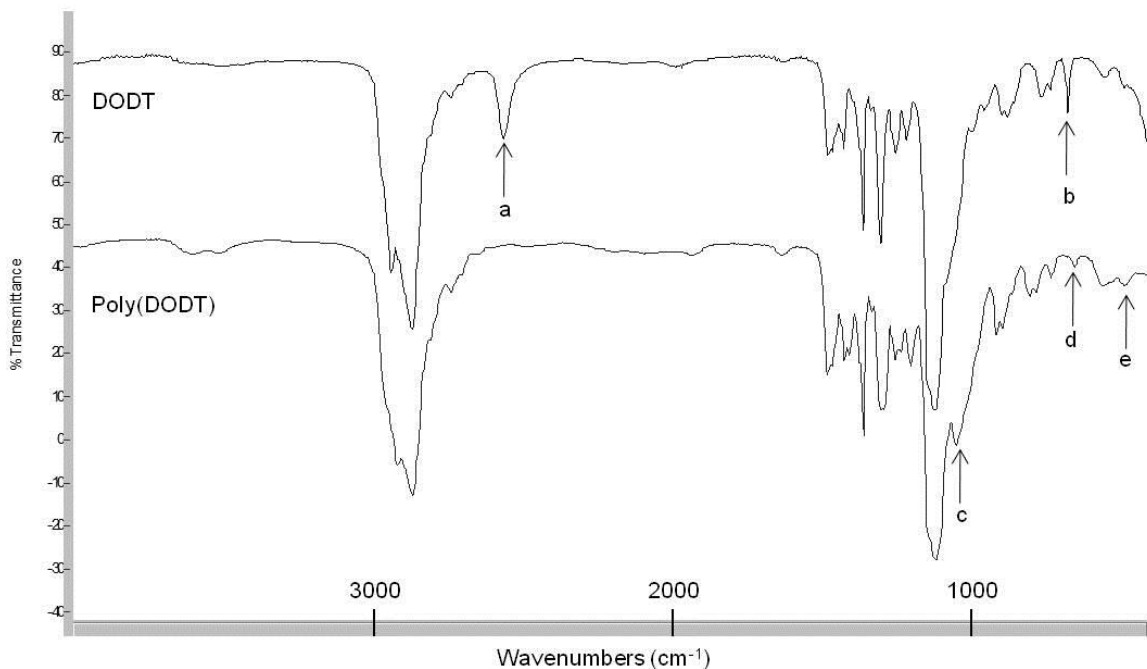


Figure 4.1.4. FTIR spectra from DODT and poly(DODT) sample 10-120-55: (a) 2557 cm^{-1} , S-H stretch; (b) 667 cm^{-1} , C-S from thiols; (c) 1042 cm^{-1} , C-O asymmetric ether stretch; (d) 644 cm^{-1} , C-S stretch of disulfides; (e) 467 cm^{-1} , S-S stretch. Reprinted with permission from {Rosenthal, E. Q., Puskas, J.E.; Wesdemiotis, C. *Biomacromolecules*, **2011**, *13**1*, 154-164}. Copyright {2011} American Chemical Society.

Previous work from Park *et al.* based poly(DODT) molecular weight values on PEG standards. Drawn on paper the monomer DODT resembles PEG, but its visual appearance is misleading because the sulfur atoms do not behave like their chalcogen neighbor, oxygen. In fact, the electronegativity of sulfur (2.58) is nearly the same as that of carbon (2.55). The dn/dc value for poly(DODT) in THF was measured using a series of solutions with varying polymer concentration and the calibration curve is shown in

Appendix B. The polymer sample used for the measurement was 10-120-55. The measured dn/dc for poly(DODT), 0.132 mL/g is much different from the literature dn/dc value of PEG (6,700 g/mol) in THF which is 0.068 mL/g.⁸⁷ The dn/dc value of the same polymer sample was also calculated from my 100% mass recovery of the analyzed peak in the SEC to be 0.125 mL/g. The dn/dc values of polymer samples calculated from 100% mass recovery are listed in Table 4.1.5.

The molecular weight values listed in Table 4.1.5 were obtained using the measured dn/dc value (0.132 mL/g). The dn/dc calculated from 100% mass recovery for each sample are also included in the table. Following the table, Figure 4.1.5 shows the light scattering (LS), refractive index (RI) and UV chromatograms for poly(DODT) sample 10-120-55. The reactions which start at room temperature show one large peak in the LS and RI traces. The molecular weights for these peaks are listed in Table 4.1.5. Removed from the main peak, the RI and UV traces, show a small peak in the low molecular weight region of the chromatogram. Here species are too small to be detected by LS. These low molecular weight species were later analyzed by MALDI-ToF MS.

Table 4.1.5. SEC data for the room-temperature reactions listed in Table 4.1.4.

Sample	M _n (g/mol)	M _w (g/mol)	(M _w /M _n)	dn/dc (mL/g)	R _{gz} (nm)	R _{hw} (nm)	[η] _w (mL/g)
10-9-70	13,000	18,000	1.43	0.124	13.6	3.7	19.6
10-120-70	48,000	83,000	1.74	0.129	14.4	8.3	49.1
10-5-55	92,000	192,000	2.09	0.120	27.2	12.7	79.8
10-10-55	139,000	248,000	1.78	0.107	27.6	14.9	98.0
10-120-55	207,000	332,000	1.60	0.125	34.6	17.4	117.0

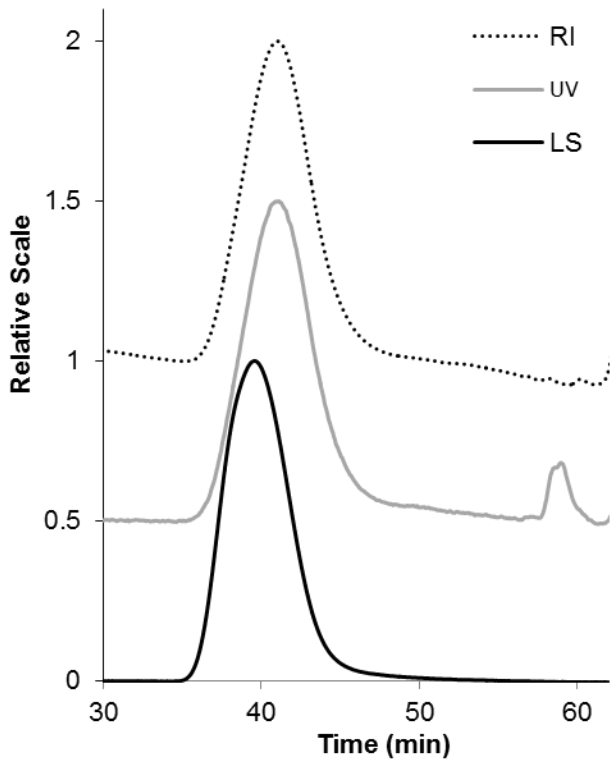


Figure 4.1.5. Light scattering (LS), refractive index (RI) and UV chromatograms from SEC analysis of poly(DODT) sample 10-120-55.

The two reactions which were started at 0°C that reached 20-25°C display a different pattern in SEC analysis. The RI traces show a high molecular peak followed by a series of equally large low molecular weight peaks (Figure 4.1.6). These low molecular weight peaks make up 41.5% of sample 10-25-ice and 59.5% of 120-25-ice. The high molecular weight peaks were integrated separately from the low molecular weight peaks, and comparison of the two reactions shows that the premixing time did not affect their molecular weights. Additionally, the high molecular weight peaks show very narrow molecular weight distributions ($M_w/M_n = 1.15$). Adjusting for mass of the low molecular weight fraction, the $d\eta/dc$ of the high molecular weight peak was calculated from 100%

mass. The results of SEC analysis of the two ice bath reactions are summarized in Table 4.1.6. The low molecular weight peaks are below the range of LS detector, and their molecular weights and approximate degree of polymerization were estimated from a calibration curve derived from the retention time. The signal to noise ratio in the RI trace in Figure 4.1.6 is poor due to the low concentration of polymer in the sample.

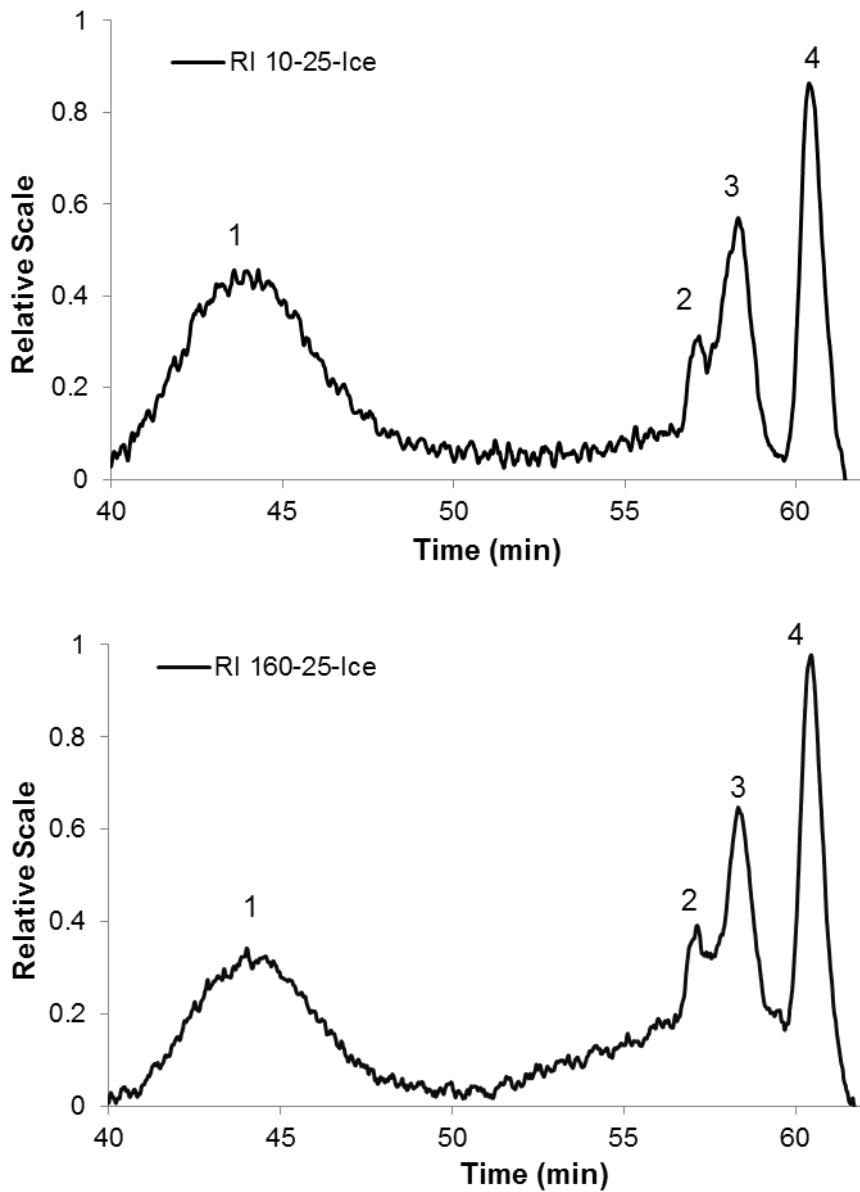


Figure 4.1.6. Refractive index (RI) chromatograms from SEC analysis of poly(DODT) samples 10-25-Ice (top) and 160-25-Ice (bottom). Reprinted with permission from { Rosenthal, E. Q., Puskas, J.E.; Wesdemiotis, C. *Biomacromolecules*, **2011**, *13*, 154-164}. Copyright {2011} American Chemical Society.

Table 4.1.6. Results of SEC analysis for polymerizations performed in an ice bath.

10-25-Ice	Peak	Molecular Weight		PDI (M_w/M_n)	dn/dc (mL/g)
		M_n (g/mol)	M_w (g/mol)		
	1	113,000	130,000	1.15	0.039
	Retention Time (min)	Peak M.W. (g/mol)		Approx.DP	
	2	57.1	1100	6	
	3	58.3	800	4	
	4	60.5	400	2	
160-25-Ice		Molecular Weight		PDI (M_w/M_n)	dn/dc (mL/g)
		M_n (g/mol)	M_w (g/mol)		
	1	116,000	133,000	1.15.	0.043
	Retention Time (min)	Peak M.W. (g/mol)		Approx.DP	
	2	57.2	1000	6	
	3	58.3	800	4	
	4	60.4	400	2	

Figure 4.1.7 shows the MALDI-ToF mass spectrum of the ionizable portion of sample 10-120-55. The spectrum shows peaks at repeating intervals of 180 m/z which corresponds to the predicted mass of the repeating DODT units (Figure 4.1.7). The mass of the monoisotopic peaks indicates the absence of thiol (or any other) end groups. From the absence of end groups it is concluded that the low molecular weight polymers are cyclic. Further support for cyclic poly(DODT) species is given by comparing the experimental isotope distribution pattern (Figure 4.1.8) to the pattern predicted for cyclic

DODT. The two patterns are nearly identical, and if linear species were also present, small peaks at about 1110 and 1111 m/z would visible.

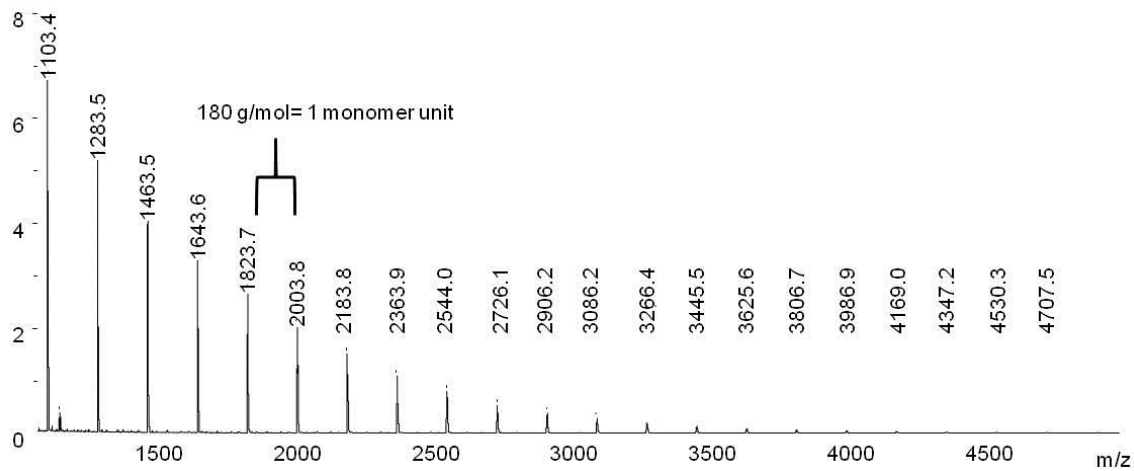


Figure 4.1.7. MALDI-ToF MS spectrum for low MW fraction of poly(DODT) sample 10-120-55 showing oligomers from hexamer (1103.4 m/z) to 26-mer (4707.5 m/z).

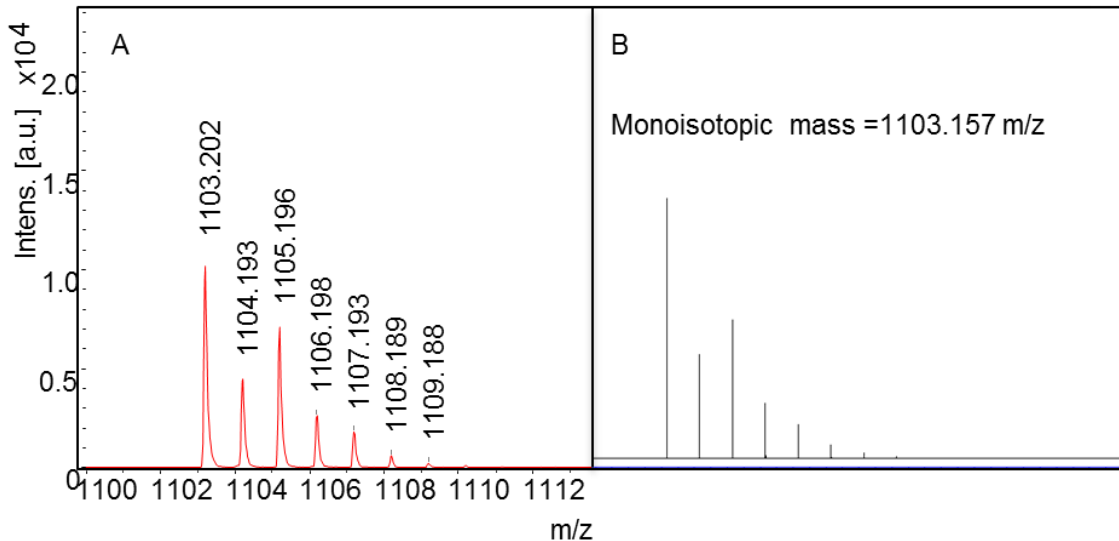


Figure 4.1.8. Isotope distribution for hexamer from poly(DODT) sample 10-120-55 (A), isotope distribution pattern predicted using ChemCalc software for cyclic poly(DODT) hexamer (B).⁸⁸

The mass spectra from the samples 10-25-Ice and 160-25-Ice show a distribution peaks corresponding to the mass of cyclic oligomers. The spectrum for 10-25-Ice is shown in Figure 4.1.9 and is representative of 160-25-Ice as well. The peak representing the cyclic dimer (382.8 m/z) is the dominant peak followed in intensity by the trimer and tetramer peaks. Oligomers beyond the 10-mer (1823.2 m/z) are not detected.

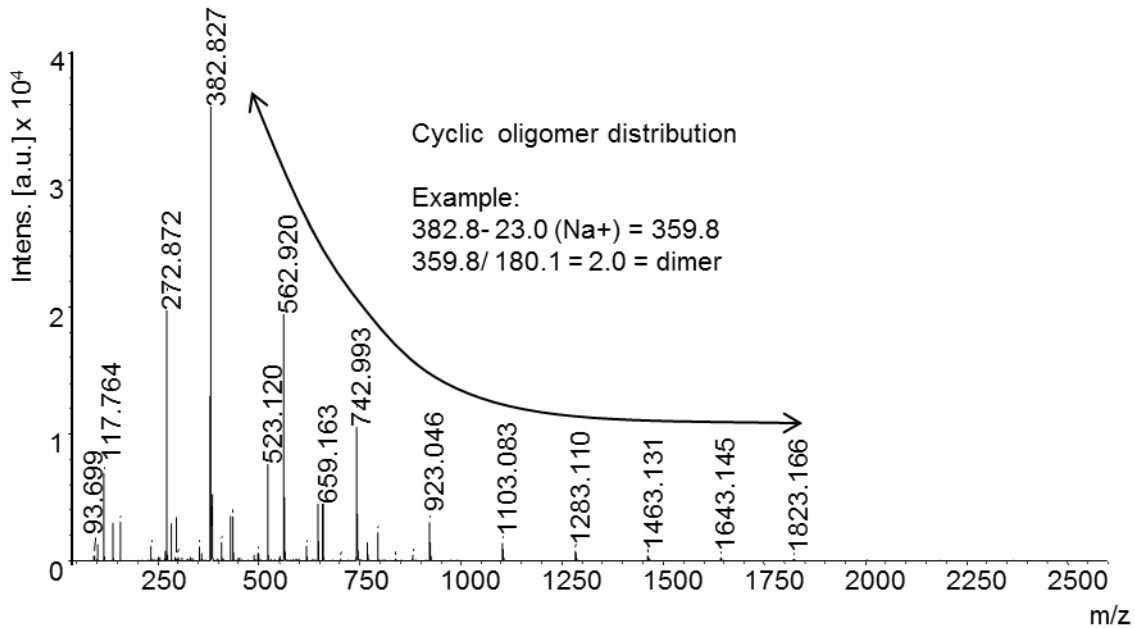


Figure 4.1.9. Mass spectrum for sample 10-25-Ice

Reaction 10-60-15 was started at 0°C and hydrogen peroxide was added slowly over 2 min to prevent the reaction from exceeding 18.7°C, which is the temperature at which triethylamine becomes immiscible with water. This reaction showed no polymer phase separation; instead a milky emulsion was formed. The emulsion persisted even after the reaction was allowed to equilibrate to room temperature. Figure 4.1.10 shows the emulsion formed in reaction 10-60-15. ESI-MS analysis of the emulsion was performed within the subsequent week. Figure 4.1.11 shows the ESI-MS spectrum. Cyclic dimers, trimers and tetramers are seen.



Figure 4.1.10. Emulsion formed in reaction 10-60-15 after 1 day at room temperature.

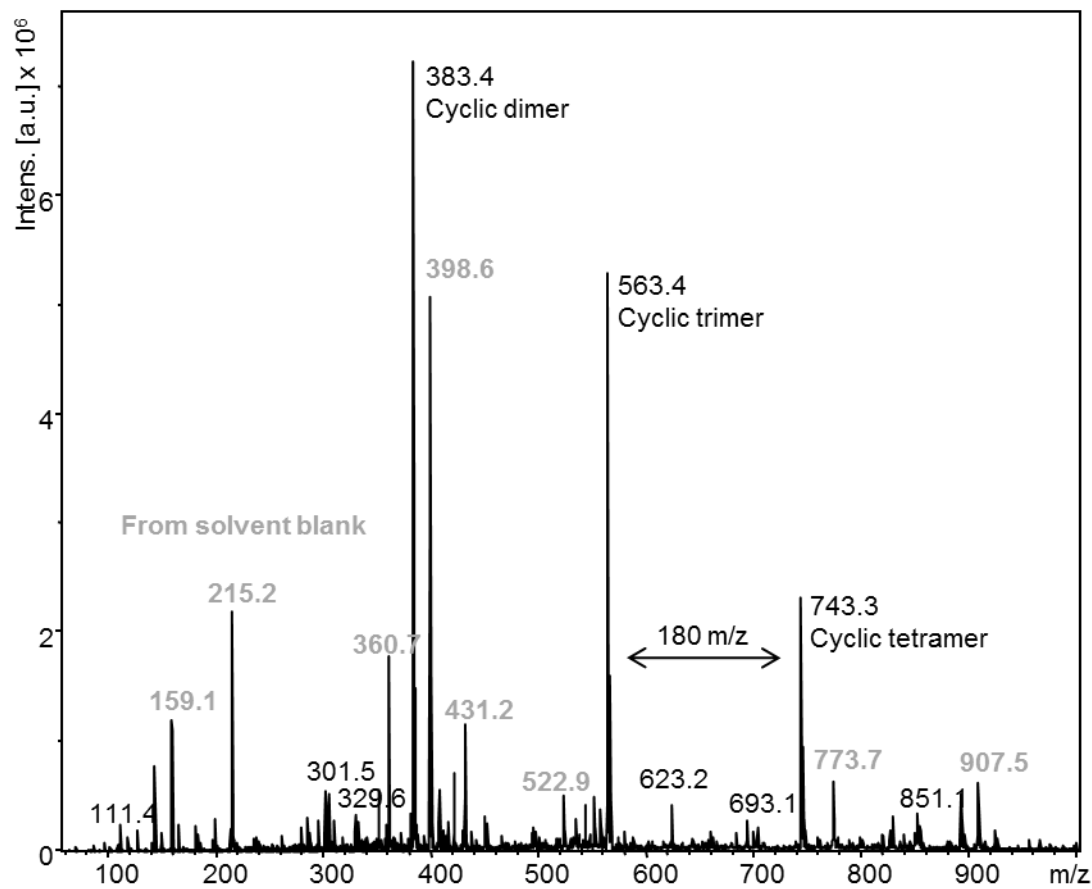


Figure 4.1.11. ESI-MS spectrum of emulsion formed in reaction 10-60-15.

In summary, the reaction temperature has a significant effect on the polymer products. Of particular importance is the temperature at which triethylamine and water become immiscible, 18.7°C. The reaction which was started at 0°C and reached 15°C (did not exceed 18.7°C) formed only cyclic dimers, trimers and tetramers. Products of reactions which were started at 0°C and surpassed 18.7°C during the reaction contain high molecular weight and low molecular weight fractions. SEC analysis shows that low molecular weight fraction of these reactions is between 40-60% of the total polymer sample. MALDI-ToF analysis indicates that the low molecular weight fraction consists of *cyclic* oligomers which were mostly cyclic dimers, trimers and tetramers. Oligomers beyond the 10-mer (decimer) were not detected. The high molecular weight polymer fraction of the low temperature reactions had a narrow molecular weight distribution ($M_w/M_n = 1.15$). Thiol protons were not detected by proton NMR, which indicates that the high molecular weight polymers may also be cyclic. Reactions which were started at room temperature and did not exceed 55°C reached molecular weights above 200,000 g/mol. A small fraction (<10%) of low molecular weight species were detected in the SEC RI trace, and MALDI-ToF analysis showed that the low molecular weight species were cyclic. Thiol proton signals were not detected by proton NMR, which indicates that the high molecular weight polymers may also be cyclic. Reactions which were started at room temperature and reached 70°C during the reaction also have a small fraction of low molecular weight species. The MALDI-ToF spectrum showed a distribution of cyclic oligomers. Thiol proton signals were detected by proton NMR indicating the presence of linear polymers with thiol end groups.

4.1.3. Kinetic studies of DODT polymerization

The time dependence of the new thiol oxidative polymerization was investigated under various conditions. Because the reaction mixture is not homogeneous, aliquots cannot be taken. Instead, each data point is represented by a separate polymerization reaction or by an average of three reactions stopped at the same time. H₂O₂ was added first to each reaction vial, then the DODT/triethylamine solution was added in one shot which begun the reaction timer. In these small scale reactions, the internal reaction temperature does not exceed 55°C when the reagents are mixed. The volume of DODT/triethylamine solution used in each experiment was under 2.0 mL and could conveniently be added in one aliquot with a syringe or volumetric pipet to minimize variation data.

In the first kinetic study triethylamine and DODT were mixed in a 2.25 to 1 molar ratio. Final concentrations of DODT, triethylamine and hydrogen peroxide in each reaction vial were 0.381 M, 0.858 M and 0.720 M respectively. The plot of % conversion versus time shows that the polymerization proceeds in two stages (Figure 4.1.12). During the first 10 min, the conversion is very fast, with over 75% of the monomer converted in the first 5 min. During this first stage, the semi-logarithmic rate plot is nearly linear. During the second stage, conversion rate slows down. However, despite the slowed conversion rate, the molecular weight increases more rapidly than in the first stage (Table 4.1.7).

Table 4.1.7. The conversion data collected from the kinetic experiment where triethylamine and DODT were mixed in a 2.25:1 molar ratio.

Time	% Conv.
1 min	39.68
5 min	75.88
10 min	88.40
30 min	88.91
120 min	93.70
240 min	98.24

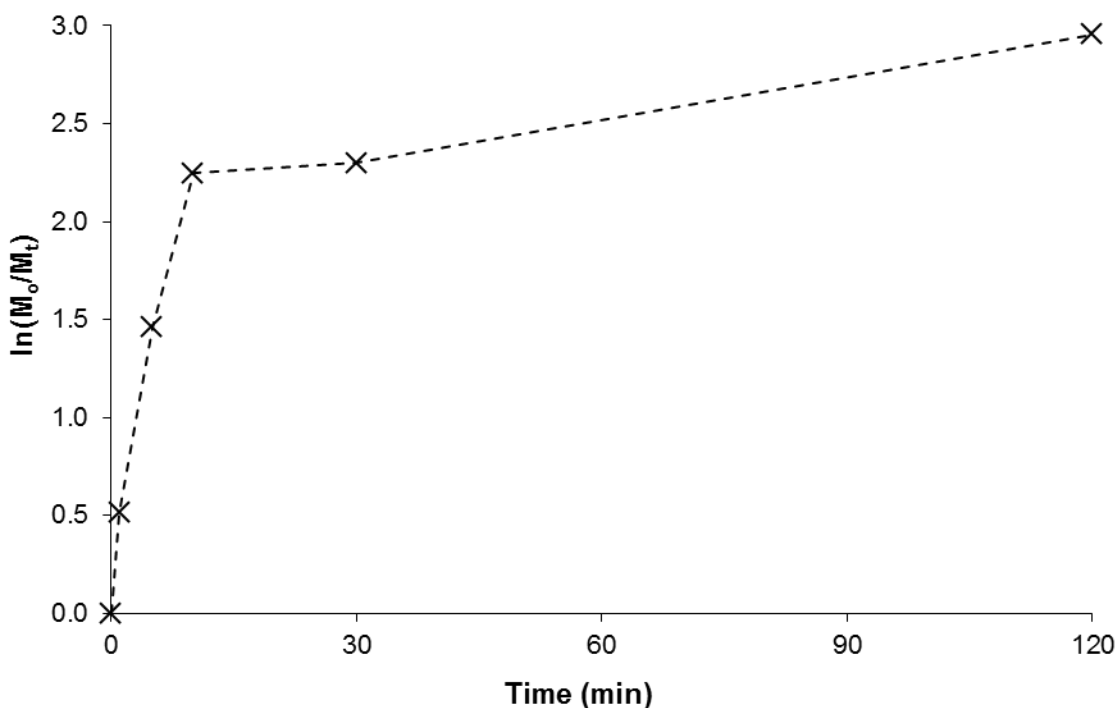


Figure 4.1.12. The monomer consumption is plotted against reaction time past 90 % conversion where triethylamine was present in a 2.25:1 molar ratio with DODT.

Four polymers from the kinetic study were analyzed by SEC and the data collected is shown in Table 4.1.8. The PDI remains under 2, hovering around 1.5. The plot of molecular weight against time conversion is also shown. The graph displays an

exponential growth with conversion, indicating chain-chain coupling in the second stage. The $M_w/M_n \approx 1.5$ also indicates chain-chain coupling, typical in radical polymerizations having termination by radical recombination.²

Table 4.1.8. Results from SEC analysis of poly(DODT) in kinetic study where triethylamine and DODT were mixed in 2.25:1 molar ratio.

Time (min)	M_n (g/mol)	M_w (g/mol)	M_n/M_w	dn/dc (mL/g)	R_{gz} (nm)	R_{hw} (nm)	$[\eta]_w$ (mL/g)
1	37,000	56,000	1.51	0.127	12.9	---	35.9
5	197,000	287,000	1.46	0.102	30.1	16.6	109.6
30	187,000	312,000	1.67	0.117	35.9	16.5	106.3
120	253,000	367,000	1.45	0.109	37.3	18.3	119.2

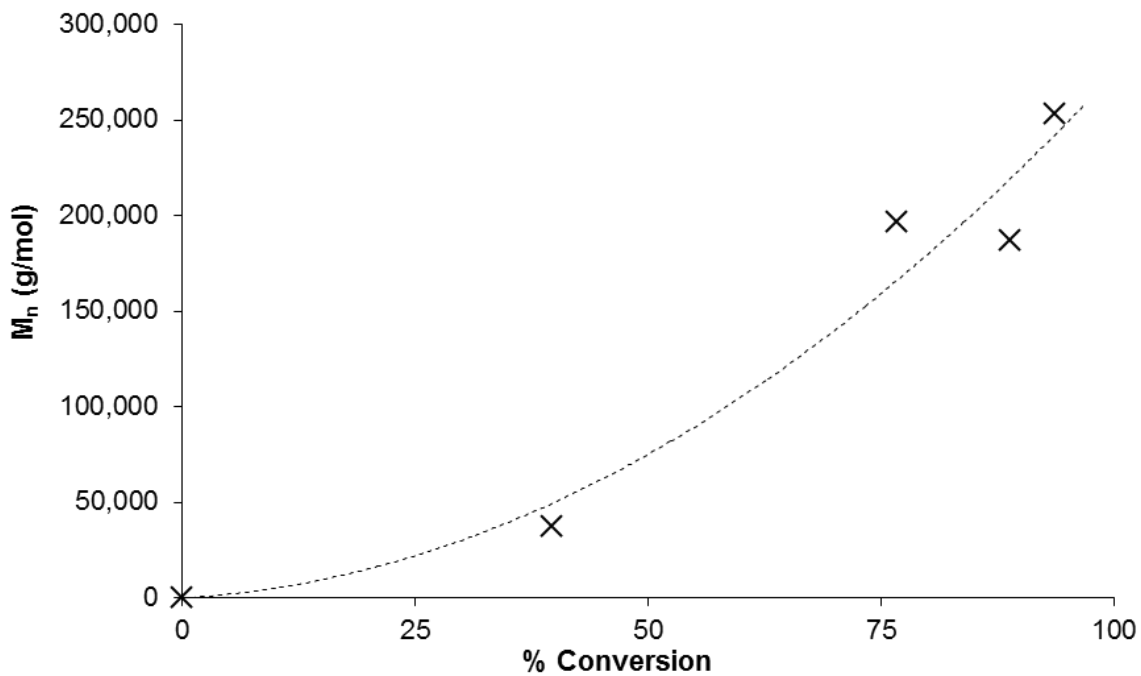


Figure 4.1.13. M_n conversion plot for the oxidative polymerization of DODT where triethylamine was present in a 2.25:1 molar ratio relative to DODT.

A similar kinetic study was then repeated in triplicate with a 2:1 molar ratio of triethylamine to DODT. The final concentrations of DODT, triethylamine and H₂O₂ were 0.368 M, 0.737 M and 0.737 M respectively. The semilogarithmic rate plot is shown in Figure 4.1.14. It also shows over 90% monomer conversion in the first 5 min. A dip in monomer conversion is also seen in the plot at 10 min. The dip, if it is significant, is likely due to chain scission by lower molecular weight species still present in the reaction mixture. The monomer conversion returns to above 90% by 30 min.

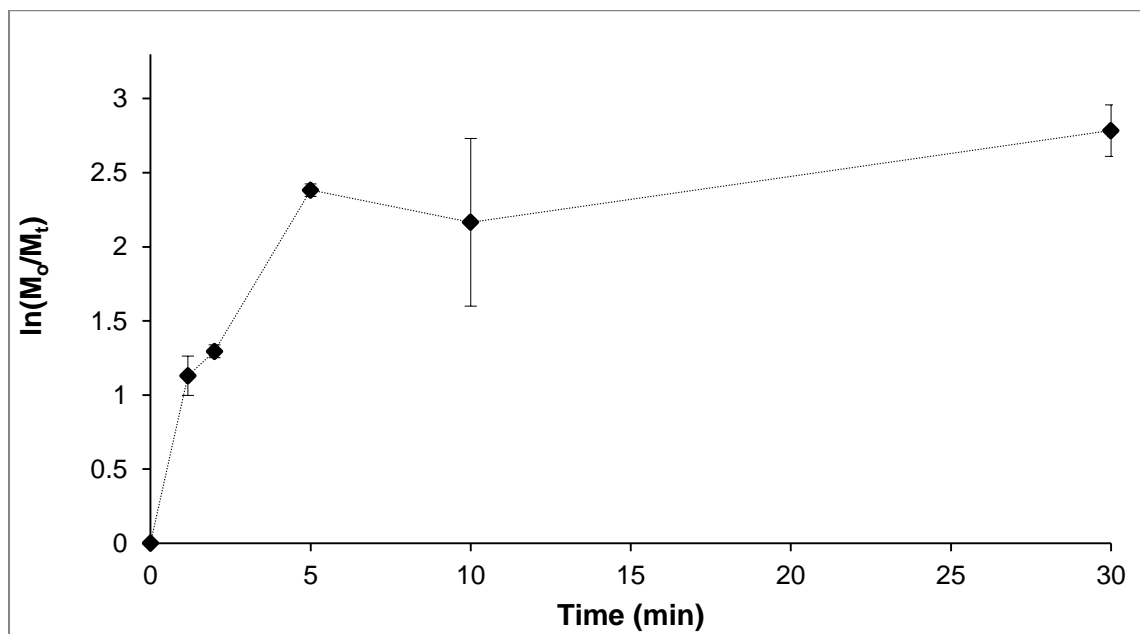


Figure 4.1.14. Monomer consumption is plotted against time for the polymerization reaction where triethylamine was present in a 2:1 molar ratio relative to DODT.

Two additional kinetic studies were performed which varied concentration of triethylamine in two extremes. The first study looked at a reaction where triethylamine and DODT were present in equal concentration (1:1 molar ratio). The second study

looked at a reaction where there were 6 moles of triethylamine to every mole of DODT (6:1 molar ratio). The final concentrations of the reagents in the reaction mixtures are listed in Table 4.1.9. To maintain the concentration of DODT and H₂O₂ consistent between the two reactions, H₂O₂ was diluted in the 1:1 molar ratio reaction. All reactions were performed starting at room temperature (23-24°C). To massed vials filled with H₂O₂, an aliquot of DODT/triethylamine solution was added and reacted for a specified time on an orbital shaker. After purification and drying, the samples were analyzed by SEC and NMR.

Table 4.1.9. Concentrations of reagents in kinetic studies with variation in triethylamine concentration.

Study	DODT/Et ₃ N	H ₂ O ₂ (mL)		Final Concentrations (M)		
	(mL)	0.67 M	0.88 M	DODT	Et ₃ N	H ₂ O ₂
Et ₃ N 1:1	0.50	4.9	---	0.306	0.306	0.611
Et ₃ N 6:1	1.65	---	3.75	0.306	1.833	0.611

Table 4.1.10. SEC data from kinetic studies with variation in triethylamine concentration.

Study	Time (min)	M_n	M_w	M_w/M_n	% Conv.
Et ₃ N 1:1 [Et ₃ N] = 0.306 M	1	6,000	9,000	1.51	41.4
	2	15,000	26,000	1.74	50.3
	4	23,000	39,000	1.74	45.4
	8	22,000	55,000	2.18	44.4
	16	24,000	41,000	1.76	46.0
	30	29,000	49,000	1.68	46.5
Et ₃ N 6:1 [Et ₃ N] = 1.833 M	0.5	49,000*	87,000*	1.79*	26.0
	2	51,000	79,000	1.54	70.1
	37	48,000	73,000	1.52	81.8

*One measurement; All other data are an average of 3 measurements from three different reactions.

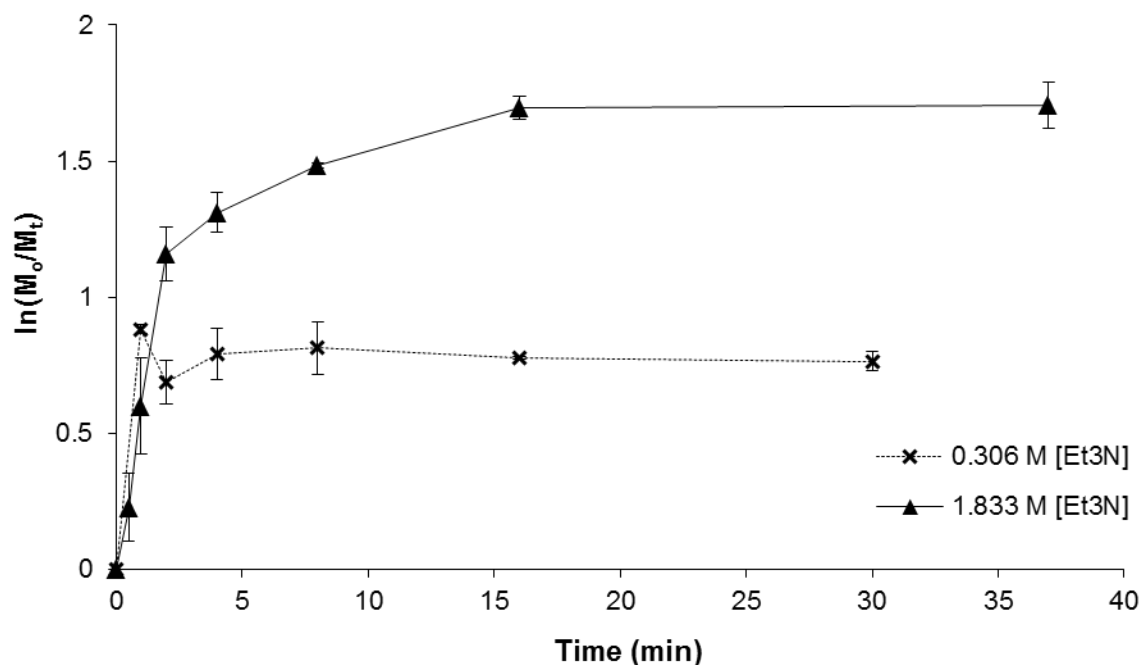


Figure 4.1.15. The monomer consumption with time is plotted for studies which compared low (0.306 M) and high (1.833 M) triethylamine concentrations.

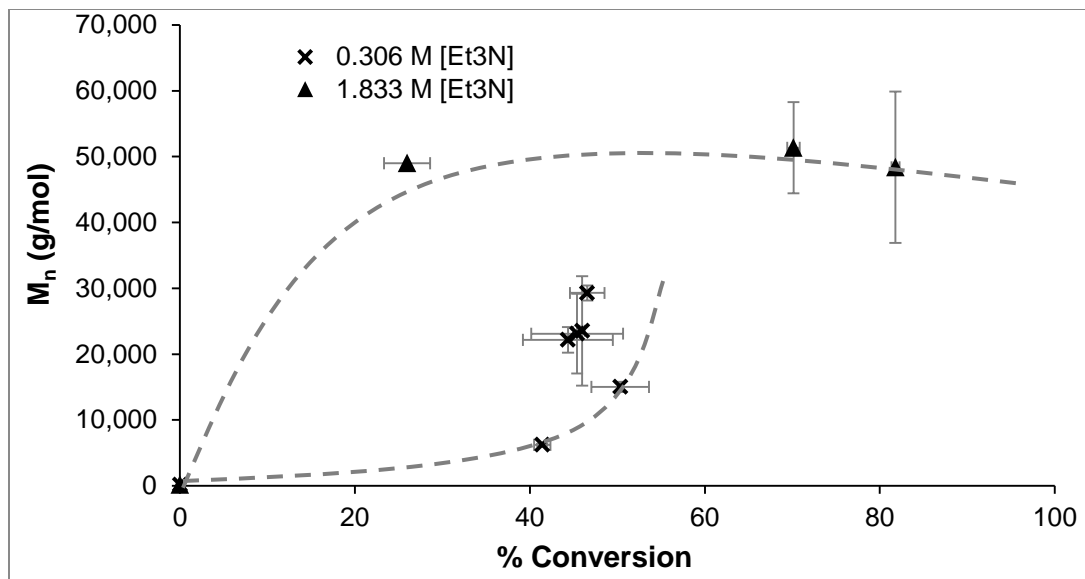


Figure 4.1.16. The M_n is plotted against conversion for DODT polymerizations with low (0.306 M) and high (1.833 M) triethylamine concentrations.

In the study with 0.306 M triethylamine, the maximum conversion, 50.3%, was reached at 2 min. In the following samples, the conversion decreased slightly and remained below 50% even after 30 min reaction time (Table 4.1.10). The M_n of the polymers from the 0.306 M triethylamine reaction remained below 30,000g/mol after 30 min. In this study the M_n v. conversion plot shows exponential growth in M_n even after the conversion has slowed or reverted. The exponential curve, however, is more pronounced in this plot than in the plot from the kinetic study shown previously (Figure 4.1.13) which used a 2.25:1 triethylamine to DODT ratio. If this curve were shifted to the 100% conversion mark, it would more closely resemble the theoretical curve for a step polymerization mechanism. Investigation into the kinetics under these and other conditions are ongoing.

The kinetic study performed with 1.833 M triethylamine reached 81.79 % after 30 min. In these reactions the conversion increased rapidly during the first 2 min to 70%. In the second stage the % conversion continued to steadily increase but at a reduced rate. The M_n reached 49,000 g/mol after 30 s and maintained approximately the same M_n for the following 36.5 min. In this study the M_n v. conversion plot resembles a plot for an uncontrolled radical polymerization. Interestingly, previous reactions which used triethylamine concentrations in between these low and high extremes, the M_n v. conversion plot is more linear and resembles that of a controlled radical polymerization.

Experiments were also carried out with mechanical (high shear) stirring. DODT-triethylamine solution was added to a round bottomed flask and placed in an ice bath, with an overhead mechanical stirring rod. H_2O_2 was added by burette at an average rate of 0.5 mL/s. The final concentrations DODT, triethylamine and H_2O_2 were 0.375 M, 0.638 M and 0.751 M respectively. The temperature of the reaction peaked at 30°C at 1 min. The mechanical stirring lead to the formation of a persistent milky emulsion during the polymerization. After 1 min a polymer phase began to separate from the emulsion, but the emulsion phase did not clear. Samples of the *polymer phase* were taken at timed intervals and analyzed by SEC. Conversion data for the samples taken during the reaction was not possible due to the presence of two phases.

The initial sample, taken at 1.5 min, had a M_n of 62,000 g/mol and molecular weight distribution (M_w/M_n) of 1.75 (Table 4.1.11). By 120 min reaction time, the M_w/M_n had increased to nearly 3. There was also severe drop in M_n between the 35 min sample and 120 min sample. The $M_n = 121,000$ g/mol at 35 min drops to 52,000 g/mol

at 120 min (Figure 4.1.1). Stirring was stopped after 2 hrs. Over the subsequent 22 hrs the M_n recovers to 79,000 g/mol and the M_w/M_n narrows slightly from 2.74 to 2.40.

Table 4.1.11. SEC data from samples taken during high stir-rate polymerization of DODT in an ice bath.

Time (min)	M_n (g/mol)	M_w (g/mol)	(M_w/M_n)	R_{gz} (nm)	R_{hw} (nm)	$[\eta]_w$ (mL/g)
1.5	62,000	108,000	1.75	15.9	12.8	59.8
35	121,000	274,000	2.26	34.3	24.9	101.0
120	52,000	141,000	2.72	24.9	---	72.1
1440	79,000	189,000	2.40	27.5	19.8	83.2

^aNot calculated in Astra..

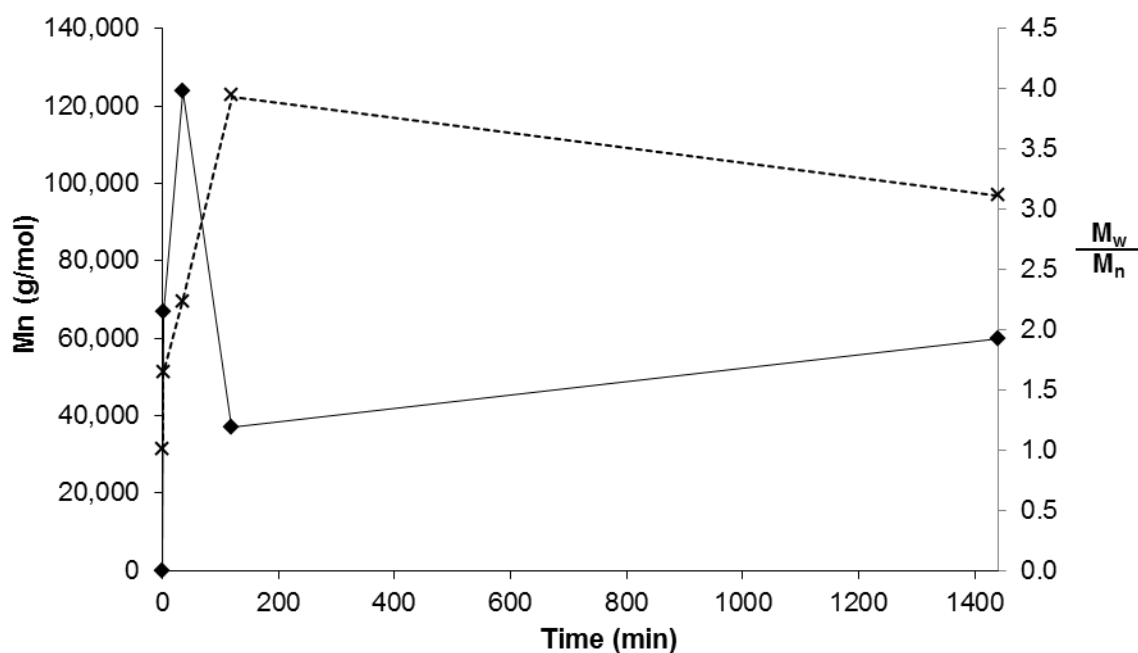


Figure 4.1.17. M_n (solid) and (M_w/M_n) (dashed) are plotted against time for the high stir rate polymerization in an ice bath.

The mechanically mixed reaction showed M_n at 35 min comparable to the magnetically stirred ice-bath reactions, 10-25-Ice and 160-25-Ice (which only ran for 25 min). However, the M_w/M_n of the mechanically stirred reaction is twice as broad ($M_w/M_n = 2.26$). When comparing the two reactions, however, it is important to note that the magnetically stirred Ice reactions had a triethylamine to DODT ratio of 2.0:1.0 while this reaction (mechanically stirred) had a triethylamine to DODT ratio of 1.7:1.0.

Interestingly, in the mechanically stirred polymerization, low molecular weight species do not dominate the RI traces as seen in the magnetically stirred ice bath reactions. The low molecular weight species only comprise about 7.5% of the separated polymer phase sample at 35 min (Figure 4.1.18). The low molecular weight fraction of the polymer phase increased to 19.0% in the 2 hr sample

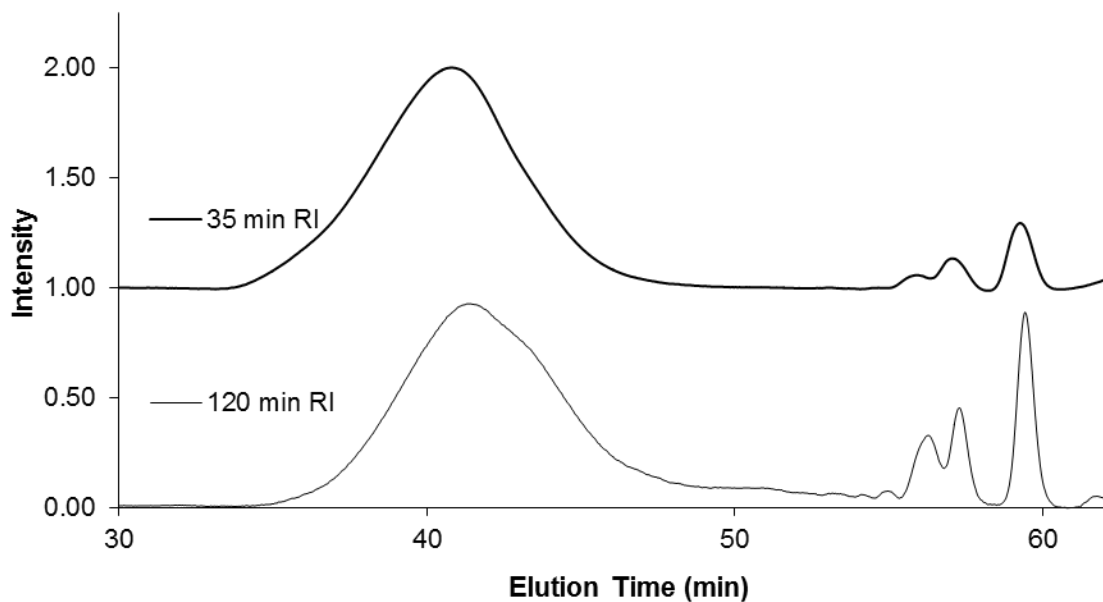


Figure 4.1.18. RI trace from the 35 min and 120 min samples taken from the DODT polymerization with mechanical stirring.

A drop in M_n after the initial fast stage of polymerization was observed for mechanically stirred DODT polymerizations. Similar results have been reported for oxidative polymerizations of dithiols in solution. For example, Koo *et al.*³⁹ report the polymerization of oligoethylene glycol dithiol (12 glycol units) dissolved in a methanol and ammonia mix using a pure oxygen bubble. The peak molecular weight of $M_n = 140,000$ g/mol was reached at 6 hrs reaction time. The M_n then decreased to about 30,000 g/mol by 48 hrs. Thiolate anions and/or thiyl radicals from low molecular weight species can act as disulfide-reducing agents. Under mechanical stirring conditions, the interface between the three phases is increased. The polymer phase is prevented from separating to the bottom of the flask and is forced into contact with both triethylamine organic phase and the aqueous oxidative phase.

The effect of decreased H_2O_2 concentration was investigated under mechanical stirring conditions in an ice bath. The final concentrations of reagents were DODT, triethylamine and H_2O_2 were 0.375 M, 0.638 M and 0.375 M respectively. With reduced H_2O_2 concentration, the polymer phase (liquid) was less viscous than reactions run with standard 2:1 molar ratio of H_2O_2 . SEC analysis of the polymer samples gives insight into the growth of the high molecular weight peak.

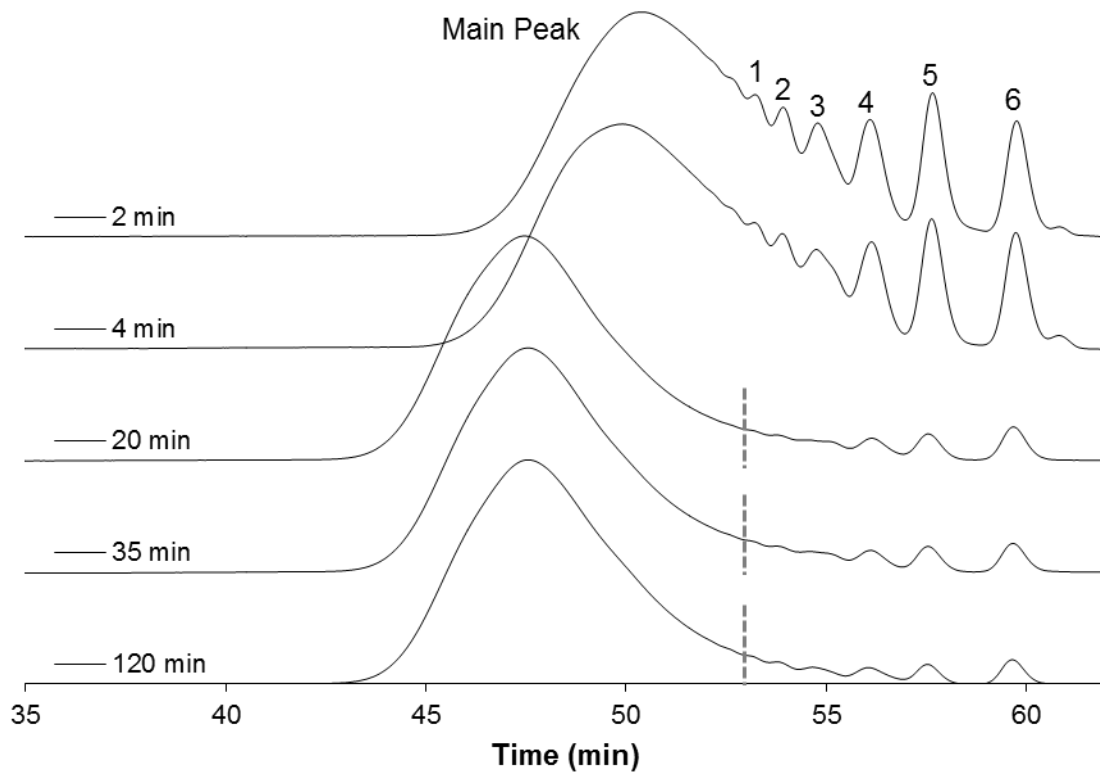


Figure 4.1.19. RI traces from timed samples from reaction where $[H_2O_2] = 0.375\text{ M}$.

Table 4.1.12. Estimated peak MW low MW peaks in the 2 min aliquot of the DODT polymerization with $[H_2O_2] = 0.375\text{ M}$

Peak #	Retention Time (min)	Estimated Values	
		MW (g/mol)	D_{P_n}
6	59.7	150	1
5	57.6	320	2
4	56.1	550	4
3	54.7	920	6
2	53.9	1230	8
1	52.1	2360	15
Main Peak			
2 min	50.3	4500	25
4 min	49.8	5500	31

Table 4.1.13. SEC results from the DODT polymerization with $[H_2O_2] = 0.375\text{ M}$

	M_n	M_w	PDI
20 min	5,000	8,600	1.73
35 min	4,700	8,200	1.73
120 min	5,000	8,100	1.60

Early in the polymerization, the RI trace displays a series of peaks trailing from the principle peak to the low molecular weight region. With time these low molecular weight peaks shrink, and the principle peak shifts to shorter elution times. In addition to the main peak in the 2 min sample, six peaks can be identified in the RI traces and their peak molecular weight can be estimated based on retention times. The labeled peaks are shown in Figure 4.1.18 and the estimated peak molecular weights are listed in Table 4.1.12. The molecular weights at 20 min, 35 min and 120 min were calculated by separating the high MW peaks as shown in Figure 4.1.19. The SEC data is displayed in Table 4.1.13. There was no significant change in molecular weight after 20 min reaction time.

The decrease in H_2O_2 concentration significantly affects the molecular weight of the poly(DODT). After 2 hrs reaction time the M_n of the polymer sample from the reaction with $[H_2O_2] = 0.375\text{ M}$ was 5,000 g/mol. Under the same reaction conditions except with $[H_2O_2] = 0.751\text{ M}$ the M_n was 52,000 g/mol. Reducing the concentration of H_2O_2 by a factor of 2 resulted in a decrease in the M_n by a factor of 10. However the M_w/M_n for the 0.375 M product was narrower ($M_w/M_n = 1.73$) than that of its 0.751 M counterpart ($M_w/M_n = 2.72$).

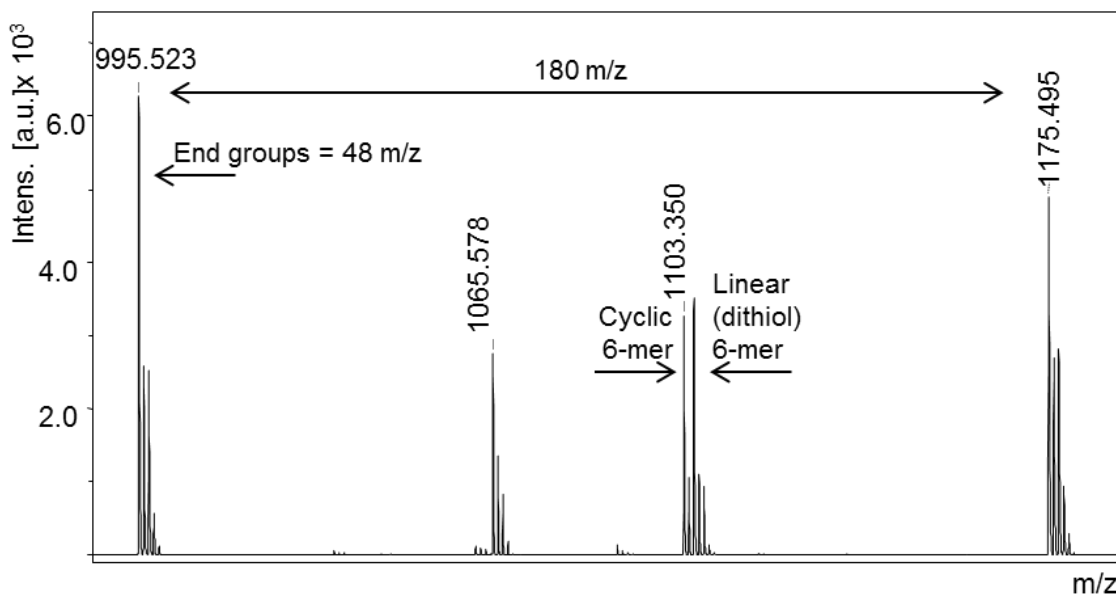


Figure 4.1.20. MALDI-ToF spectrum of 2 min sample from reaction where $[H_2O_2] = 0.375\text{ M}$.

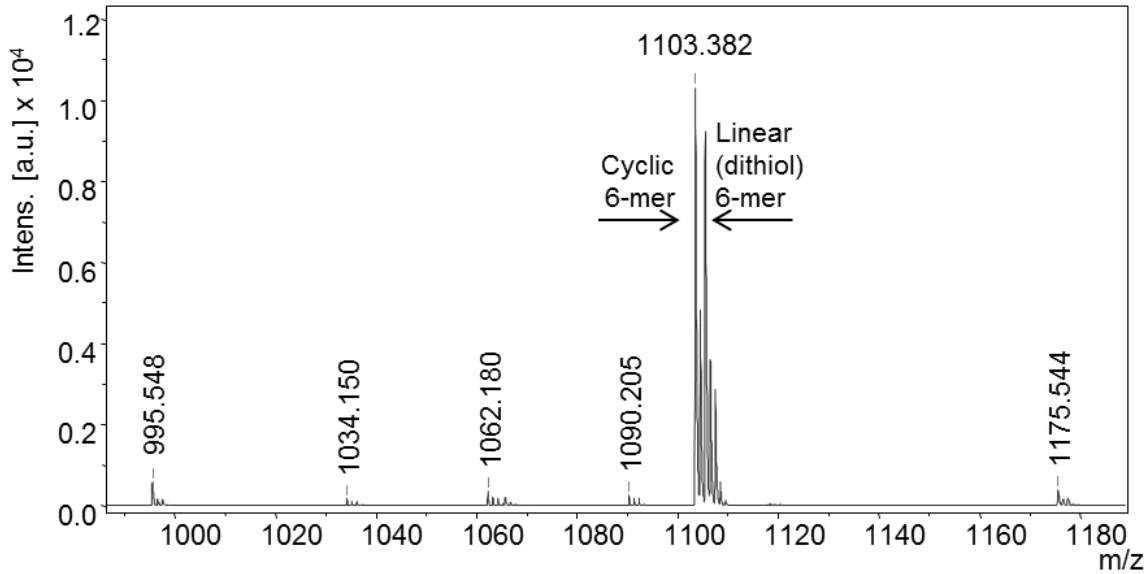


Figure 4.1.21. MALDI-ToF spectrum of 35 min sample from reaction with $[H_2O_2] = 0.375\text{ M}$.

MALDI-ToF analysis of the low H₂O₂ concentration, mechanical stirring reactions show multiple distributions. In the 2 min sample (Figure 4.1.20), the distribution of cyclic oligomers is less than 1% of the total sample, but by the 35 min the cyclic oligomers dominate and the other distributions are negligible (0.05% of total sample) (Figure 4.1.21). The difference between cyclic oligomer distribution and main distribution in the 2 min sample is 72 m/z. The peaks in the main distribution of the 2 min sample indicate the possibility of end groups other than thiol groups. An alternative explanation to end groups with is that a temporary THF adduct is formed during the MALDI process. Investigation into the origin of the multiple distributions is on going. Multiple distributions have not been seen in the magnetically stirred, room temperature reactions with [H₂O₂] ≈ 0.7.

4.1.4. Chain extension.

Living characteristics displayed by the new oxidative polymerization were further tested in a chain extension experiment of poly(DODT) sample 10-9-70 with 1,2-ethanedithiol (ED). Immediately upon the addition of hydrogen peroxide to the poly(DODT)-ED solution, small white chunks appeared in the solution. Using a syringe without a needle, aliquots of the reaction mixture were taken at 4 min (0.5 mL) and 30 min (1.0mL). They were immediately diluted with water to stop the reaction. The small white chunks (insoluble) were filtered from the liquid sample and rinsed with methanol. The remaining liquid sample was also poured into methanol. No precipitate was seen in the methanol portion. Similarly, the insoluble fraction of the final polymer product was filtered out and rinsed with methanol. All fractions, insoluble and soluble,

were dried until a constant mass was reached. The percentage of soluble and insoluble material recovered from each sample is listed in the Table 4.1.14.

Table 4.1.14. Material recovered from each sample in the chain extension study.

	Insoluble	Soluble	Conv.
4 min	18.9%	81.10%	92.50%
30 min	27.80%	72.20%	82.30%
24 hrs	65.50%	34.50%	92.60%

The total soluble fraction the final product was 0.345 g, which is less than the starting amount (0.5005 g). This indicates that some of the original poly(DODT) was converted to insoluble, high ED-content copolymer by ED. Copolymers with $f_{ED} > 5$ are insoluble in THF.

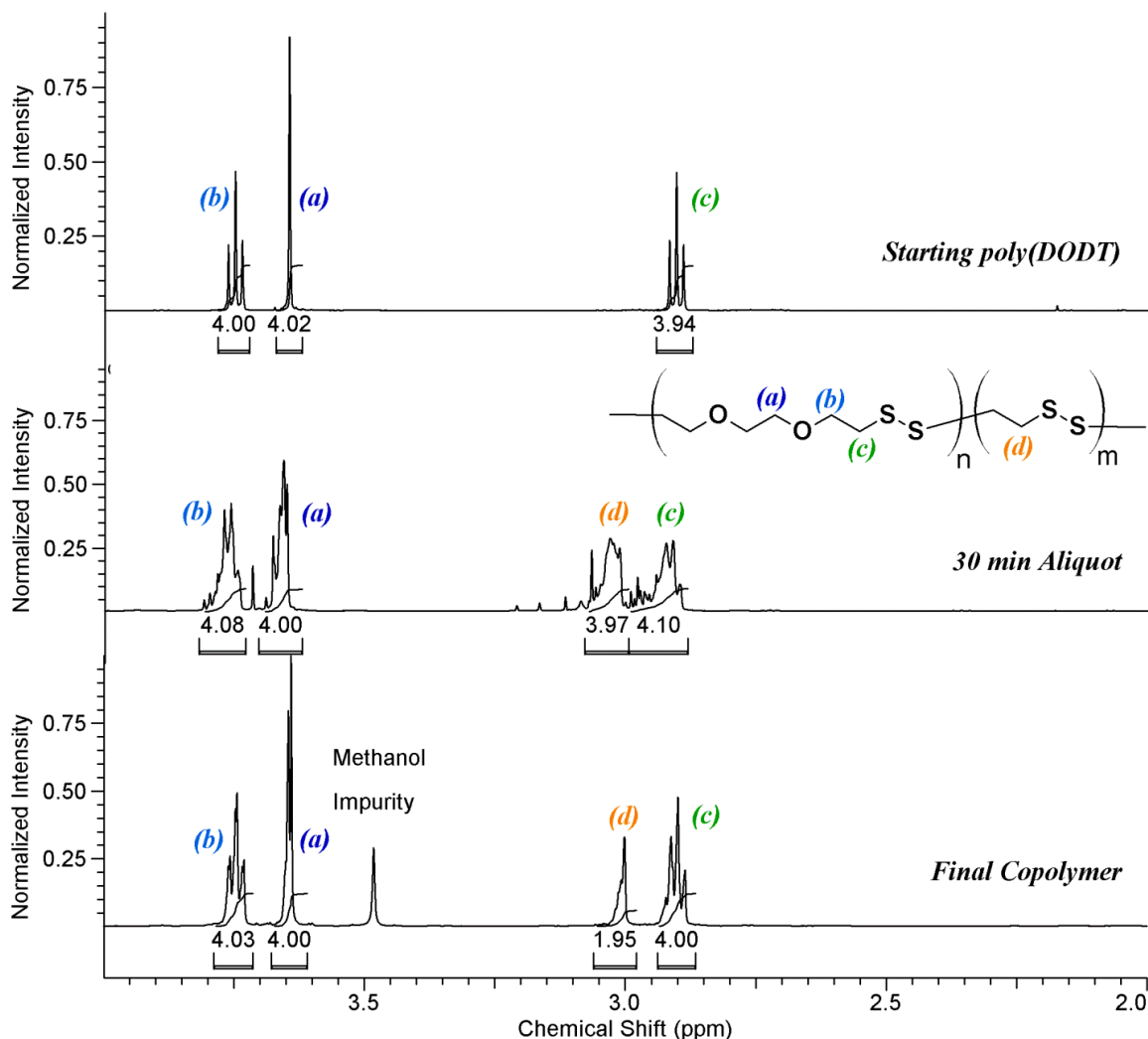


Figure 4.1.22. ^1H NMR spectra from the chain extension experiment (12s relax, 64 trans.; 500 MHz; CDCl_3). Reprinted with permission from { Rosenthal, E. Q., Puskas, J.E.; Wesdemiotis, C. *Biomacromolecules*, **2011**, *13*(1), 154-164}. Copyright {2011} American Chemical Society.

The ^1H NMR spectra starting polymer(poly(DODT)), the 30 minute aliquot and the final polymer are compared in Figure 4.1.22. Peaks from the starting material at 3.75ppm (b), 3.65ppm (a) and 2.90ppm (c) are retained in the product spectrum, except they are dramatically broadened and show more irregular splitting patterns. A new peak

also appears in the two product spectra at 3.02 ppm (*d*) which corresponds to the methylene protons in ED units. The broad peak area and multiplet splitting pattern suggest that neighboring repeat units are not consistent and switch between ED units and DODT units. A small thiol triplet is seen in the final polymer sample at 1.60 ppm. Integration of the peaks corresponding to main chain protons relative to the thiol protons gives a calculated molecular weight of 14,400 g/mol, which is significantly less than the M_n measured by SEC.

The solution NMR data conclusively demonstrate that ED incorporated into the poly(DODT) to form a copolymer. Interestingly, the ratio of DODT peaks (*a*, *b*, *c*) to the ED peak (*d*) changes from about 1:1 in the 30 min spectrum to almost 2:1 in the final polymer sample. At first this looks like ED units are leaving the polymer chains, however as ED adds to the poly(DODT) chains, the chains become more and more insoluble and are therefore no longer present in the soluble fraction. Only the chains with fewer ED units remain in the soluble fraction. The mass decrease of the soluble portion of the polymer relative to the starting poly(DODT) supports this conclusion.

The carbon NMR spectrum of the soluble portion of the final product shows the three peaks corresponding to poly(DODT) methylene carbons (*A*, *B*, *C*). The new peak at 37.39 ppm (*D*) corresponds to the two equivalent carbon atoms found in ED units. The ^{13}C spectrum again demonstrates that ED incorporated into the poly(DODT).

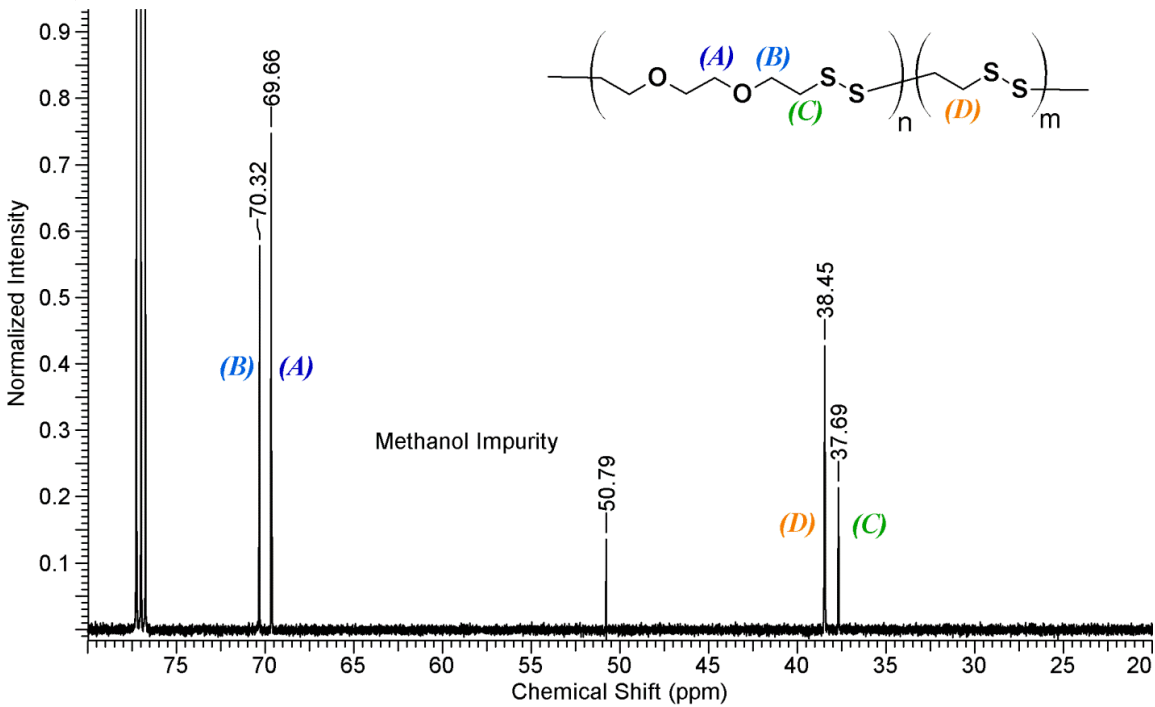


Figure 4.1.23. ^{13}C NMR spectrum of the final polymer from the chain extension experiment.(12 s relax; 64 trans.; CDCl_3 ; 500 MHz). Reprinted with permission from { Rosenthal, E. Q., Puskas, J.E.; Wesdemiotis, C. *Biomacromolecules*, **2011**, *13*, 154-164}. Copyright {2011} American Chemical Society

The solid-state carbon NMR of the insoluble fraction of the final polymer shows two broad peaks (Figure 4.1.24). The first peak appears at 71.67 ppm and corresponds to oxygen-adjacent carbons, so is attributed to DODT units. The second peak falls at 37.06 ppm and corresponds to disulfide-adjacent carbons. Because the larger peak is centered at 37 ppm (like poly(ED)) rather than at 38 ppm (found in poly(DODT)), it appears that the majority of the disulfide-adjacent carbons come from ED units. If the insoluble fraction were only poly(ED), the spectrum would show a single peak at

37.06 ppm. Thus the solid state NMR verified that the insoluble fraction is also demonstrates a copolymer.

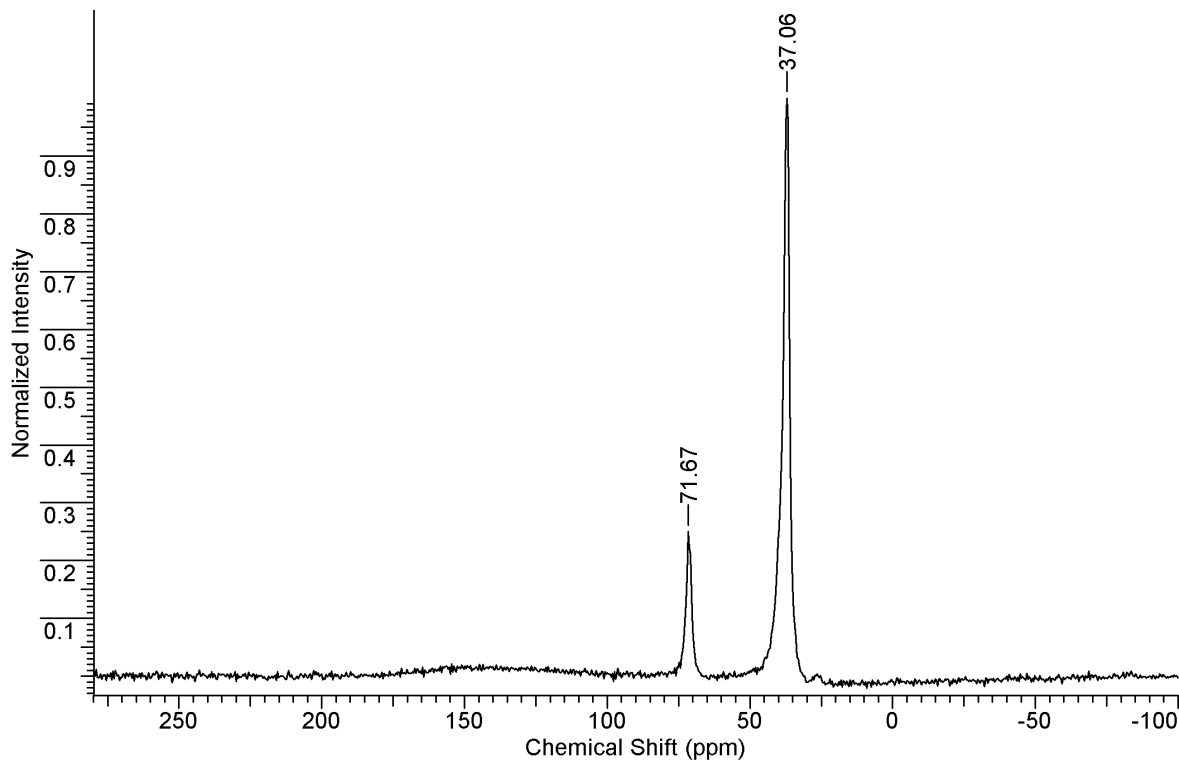


Figure 4.1.24. Solid state ^{13}C NMR spectrum of insoluble fraction from final product of chain extension study. Reprinted with permission from { Rosenthal, E. Q., Puskas, J.E.; Wesdemiotis, C. *Biomacromolecules*, **2011**, *13**1*, 154-164}. Copyright {2011} American Chemical Society.

Figure 4.1.25 shows the SEC RI traces of the starting material, 30 min aliquot and the final polymer product. The RI trace of the final product shows a shift towards higher molecular weight. Because no dn/dc value is available for the copolymer, the SEC data is based on 100% mass recovery of the injected sample. With this, the final product had

$M_n = 120,000$ g/mol. The SEC data for the chain extension study is summarized in Table 4.1.15.

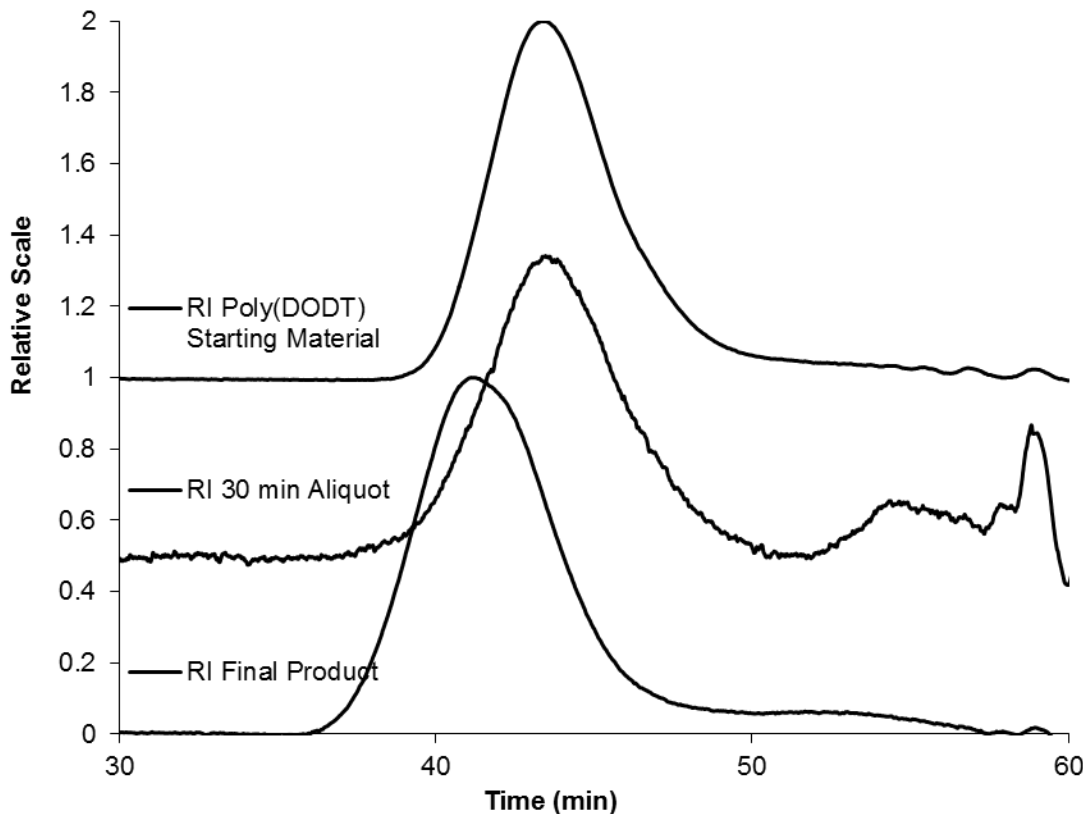


Figure 4.1.25. RI SEC traces from the chain extension study.

Table 4.1.15. SEC results from chain extension study.

Sample	M_n (g/mol)	M_w (g/mol)	M_w/M_n	R_{gz} (nm)	dn/dc used (mL/g)
Poly(DODT)	18,000	34,000	1.89	10.1	0.132
30 min Sample	68,000	89,000	1.33	16.9	0.080*
Final Product	107,000	199,000	1.86	15.5	0.073*

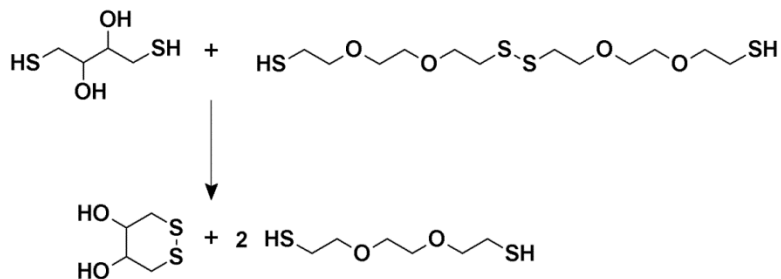
*from 100% mass recovery

4.1.5. Degradation of DODT using dithiothreitol.

Dithiothreitol (DTT) is specifically used to cleave disulfide bonds to thiols.

Reduction by DTT demonstrates both the exclusive presence of disulfide bonds in the polymer backbone and the possibility for biodegradation in reducing environments.

Scheme 4.1.2 shows the reduction reaction of DODT dimer to DODT monomer by DTT.



Scheme 4.1.2 Disulfide reduction by dithiothreitol (DTT).

The reduction of poly(DODT) disulfide bonds by DTT was visualized by following ^1H NMR signal of the sulfur adjacent methylene group (Figure 4.1.26). In the polymer spectrum, this group appeared as a triplet at 2.91 ppm, however as the polymer was degraded the quadruplet corresponding to the thiol adjacent methylene group began to appear at 2.71 ppm. With continuing exposure to DTT, the methylene triplet disappeared and was replaced by the monomer's methylene quartet. The polymer was almost completely degraded by 33 hours. A small triplet signal is also seen downfield, adjacent to the polymer triplet. This triplet is attributed to the small amount of residual DTT in the sample.

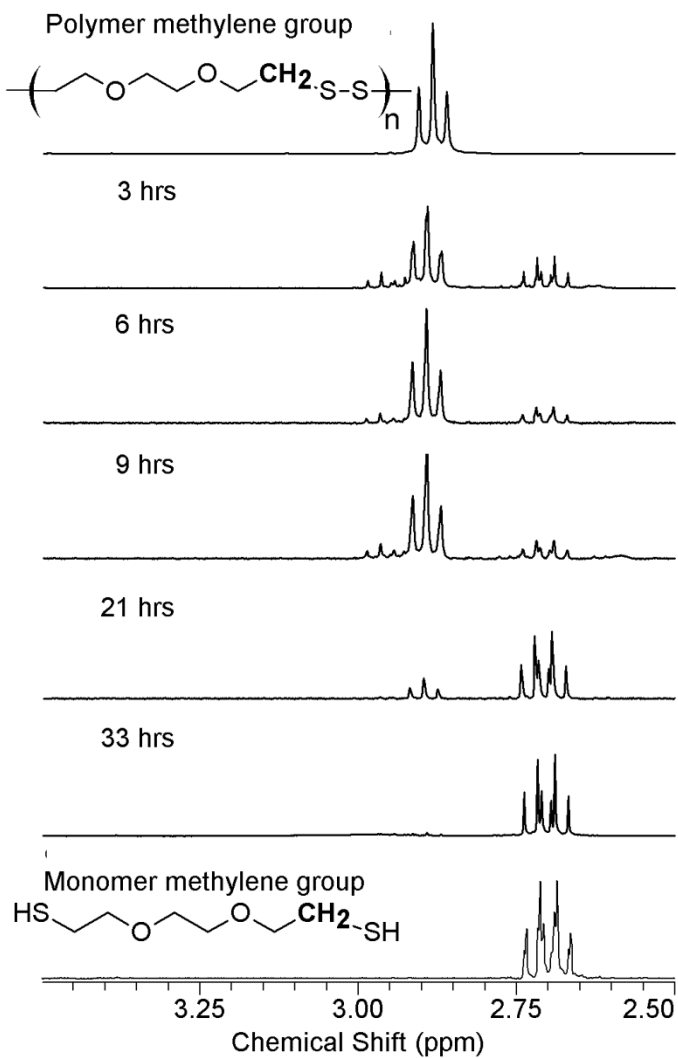


Figure 4.1.26. Disulfide reduction of a poly(DODT) sample 10-120-55 by dithiothreitol (DTT) (32 trans.; 300 MHz; CDCl_3). Reprinted with permission from { Rosenthal, E. Q., Puskas, J.E.; Wesdemiotis, C. *Biomacromolecules*, **2011**, *13*, 154-164}. Copyright {2011} American Chemical Society.

Degradation of the polymer DTT shows that the polymer backbone exclusively contains disulfide bonds. The presence of disulfide bonds allows for the degradation of the polymers under specific biological conditions, and shows that the bond cleavage

reaction can be catalyzed by the powerful disulfide reducing enzymes found in biological systems.

4.1.6. Thermal characterization

Sample 10-120-55 was characterized by DSC and TGA. The polymer presented a strong glass transition between -53°C and -49°C (Figure 4.1.27). No other transitions were observed within the analysis range of -150°C to 150°C . The TGA decomposition trace of sample 10-120-55 shows 2% mass loss at 236.3°C , 50% mass loss at 297.9°C and the decomposition profile plateaus at 356.8°C (Figure 4.1.28). The thermal degradation temperature as calculated by the Universal Analysis software was 283.7°C .

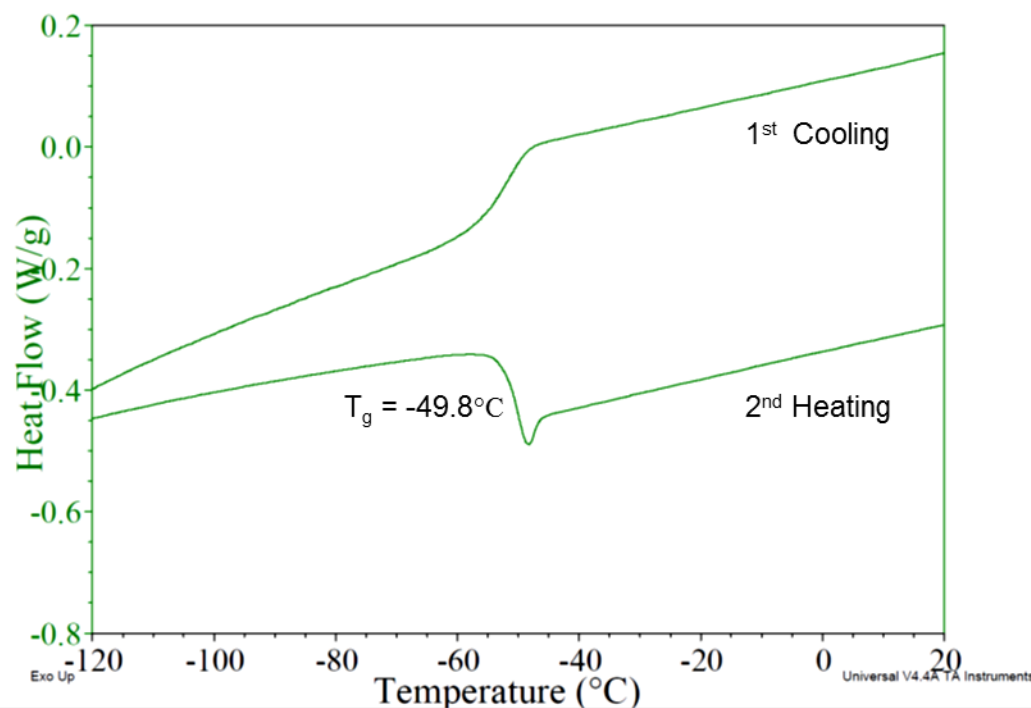


Figure 4.1.27. The DSC trace of poly(DODT) for sample 10-120-55 showing T_g . (2nd heating; heating rate = $10^{\circ}\text{C}/\text{min}$).

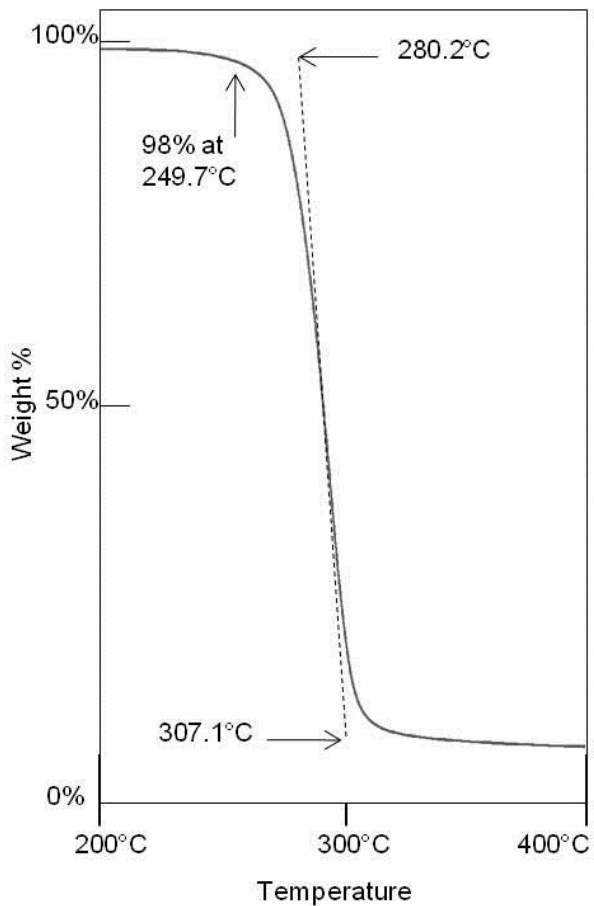


Figure 4.1.28. The TGA decomposition profile of Sample 10-120-55. (N_2 atmosphere; heating rate of $10^\circ\text{C}/\text{min}$). Reprinted with permission from { Rosenthal, E. Q., Puskas, J.E.; Wesdemiotis, C. *Biomacromolecules*, **2011**, *13*, 154-164}. Copyright {2011} American Chemical Society.

4.1.7. SEC conformational analysis

Polymers from the kinetic study were analyzed by SEC (reported in Table 4.1.8). Subsequently, the samples were further oxidized in a 1.7 mM (approximate) solution of I_2 in chloroform. Sample concentration in the solution was approximately 13 mg/mL. After a work-up with sodium thiosulfate solution followed by an acidic H_2O wash, the polymers were dried and analyzed by SEC (Table 4.1.16).

Table 4.1.16. Molecular weights of starting polymers (from kinetic study) are compared to the oxidized polymers.

Starting Polymer				Oxidized Polymer			
Sample	M _n	M _w	M _w /M _n	Sample	M _n	M _w	M _w /M _n
1-min	37,000	56,000	1.51	1-min-Ox	179,000	335,000	1.87
5-min	197,000	287,000	1.46	5-min-Ox	304,000	444,000	1.46
30-min	187,000	312,000	1.67	30-min-Ox	347,000	498,000	1.44
120-min	253,000	367,000	1.45	120-min-Ox	316,000	465,000	1.47

Table 4.1.17. SEC results of starting polymers (from kinetic study) are compared to the oxidized polymers.

Starting Polymer				Oxidized Polymer					
Sample	Conf. Slope*	[η] _w (mL/g)	R _{gz} (nm)	R _{hw} (nm)	Sample	Conf. Slope*	[η] _w (mL/g)	R _{gz} (nm)	R _{hw} (nm)
1-min	0.50	35.9	12.9	---	1-min-Ox	0.28	86.2	37.0	15.6
5-min	0.42	109.6	30.1	16.6	5-min-Ox	0.37	129.7	40.4	20.1
30-min	0.51	106.3	35.9	16.5	30-min-Ox	0.33	137.9	44.0	21.3
120-min	0.46	119.2	37.3	18.3	120-min-Ox	0.34	128.1	42.8	20.3

*log (nm)/log (g/mol)

The conformation slope (log (rms radius) v. log(molar mass)) provides a guide for polymer shape. Random coils usually have a conformation slope between 0.5-0.6 log(nm)/log(g/mol), while conformation slope for a sphere is approximately 0.33 and a rod would have a conformation slope of about 1.0.⁸⁹ The slope of the log(R_g) v. log(M_i) plot (conformational slope or scaling factor R_g - N^v) of the starting samples ranges from 0.41-0.51. Simulations showed a static scaling factor of v = 0.42 for rings and 0.50 for linear chains in the melt. In dilute solution the value of the simulated scaling

factor was similar for rings and linear chains at $\nu = 0.6$.⁹⁰ Scaling factors for linear chains have been measured by SEC and are 0.55-0.60.⁹¹ There is no measured value for high molecular weight rings in the literature. The $\nu < 0.6$ scaling factors measured in our samples indicate rings, in agreement with the NMR data showing no end groups.

All of the polymers increased in molecular weight after iodine oxidation, indicating intermolecular coupling leading to chain growth. Only the low molecular weight starting sample (1 min; $M_n = 37,000$ g/mol) showed an increase in M_w/M_n after oxidation. All other polymers maintained a distribution value around 1.5.

Here, the samples with the most similar molecular weights are 30-min ($M_w = 312,000$ g/mol) and 1-min-Ox ($M_w = 335,000$ g/mol). Comparing the intrinsic viscosity of the oxidized polymer sample (86.3 mL/g) to the intrinsic viscosity of the starting polymer (106.3 mL/g), we find that the viscosity decreased upon oxidation. However, the R_g/R_h values remained around 2 in both the starting and the oxidized materials.

After iodine oxidation, the conformation slope of the polymers were all between 0.28-0.37 log(nm)/log(g/mol). The decrease in conformation slope of the polymers after oxidation indicates that the oxidized polymers are more compact than the starting polymers and agrees with the decrease in viscosity.

Information about the conformation of the polymer may be interpreted from the Mark-Houwink-Sakurada equation (Eq. 4.1). Plotting the $\log[\eta]$ vs $\log(M_w)$ the Mark-Houwink-Sakurada constants (**K** and **a**) were calculated for poly(DODT) in THF at 35°C, and the plot is shown in Figure 4.1.29. The values of **K** and **a** for the starting polymers are 5.93×10^{-2} mL/g (5.93×10^{-4} dL/g) and **0.617** respectively. The values of **K** and **a** for

the oxidized polymers are 3.1×10^{-4} mL/g (3.1×10^{-6} dL/g) and **1.013** respectively. It is generally accepted that a random coil in a good solvent will have an **a** value between 0.5-0.8, while stiff *coils* will have an **a** value of 1.0. (Rigid rods will have an **a** value between 1.8-2.0) One interpretation is that upon oxidation the polymers have entangled into a catenane fashion or formed compact branching structures. A catenane structure has been proposed for other disulfide polymers produced in the research group of K. Endo. Their proposed structure is shown in Figure 4.1.30.

$$[\eta] = KM_v^a \approx KM_w^a \quad [\text{Eq. 4.1}]$$

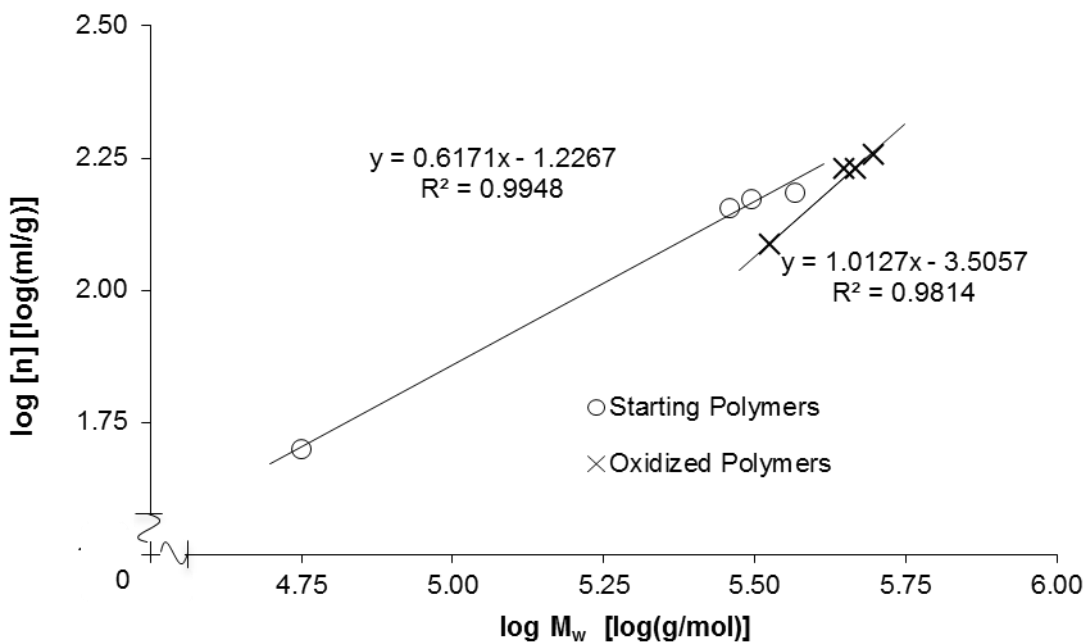


Figure 4.1.29. Mark-Houwink-Sakurada constants derived from slope and intercept of $\log [\eta]/\log M_w$ plot.

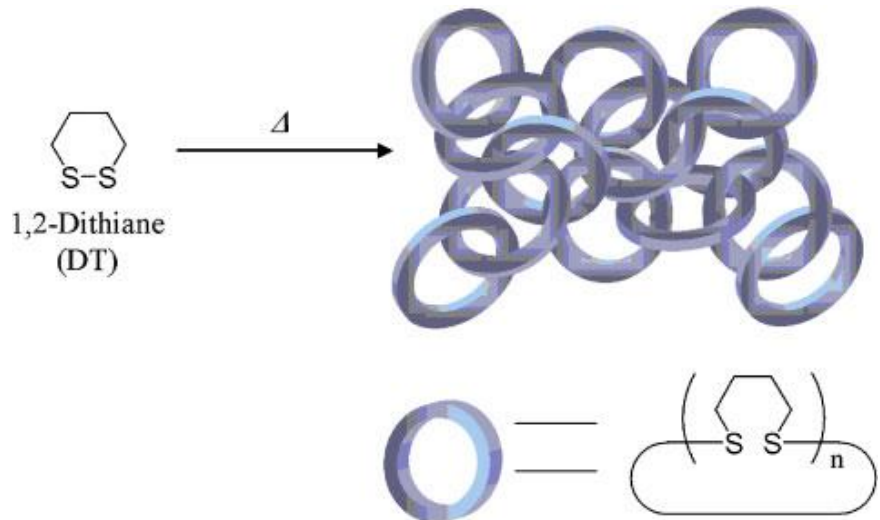


Figure 4.1.30. Catenane proposed by Ishida and coworkers for their poly(disulfide) polymer from 1,2-dithiane. Reprinted by permission from Macmillan Publishers Ltd: Polymer Journal,[Ishida, H.; Kisanuki, A.; Endo, K. *Polymer Journal*, **2009**, *41*, 110-117. Copyright (2009).

Comparison of the of ^1H NMR spectra for the 30 min polymer sample before and after oxidation showed a slight broadening of the peaks which was result of the broadened molecular weight distribution (Figure 4.1.31). A thiol triplet was not seen in either spectrum. A very small singlet peak appears at 1.25 ppm and is not attributed to the polymer, but to trace solvent residue from cleaning the NMR tube.

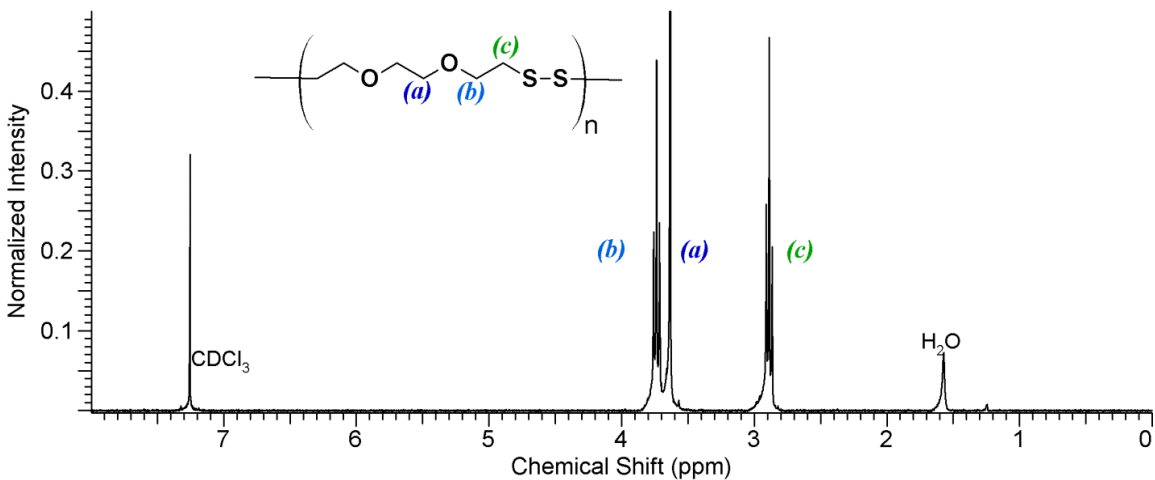


Figure 4.1.31. ^1H NMR spectrum of iodine-oxidized poly(DODT) sample (30 min)
(12 s relax.; 64 trans; CDCl_3 ; 300 MHz)

4.2. Mechanism investigation

4.2.1. Model experiments

The new dithiol polymerization system always displays more than one phase, when the temperature is above 18.7°C , and it is hypothesized that the presence of multiple phases plays an important role in the polymerization mechanism. The solubility of the dithiol monomer and triethylamine catalyst was investigated using ^1H NMR. D_2O was used as model for the aqueous phase of the polymerization reaction. DODT (0.50 mL (3.06 mmol)) and 1.00 mL of D_2O were mixed, then a sample of the D_2O phase was analyzed by ^1H NMR. The proton NMR the D_2O phase (Figure 4.2.1) shows that only a trace amount of the monomer is soluble in the aqueous phase. The protonated contamination in D_2O (HDO) is the strongest signal in the spectrum (relative intensity = 1) and is used as an internal standard to qualitatively determine the limited solubility of DODT in D_2O phase. The DODT spectrum in D_2O shows peaks with similar chemical

shifts as in d-chloroform, but with a different splitting pattern. The singlet for the central methylene protons and for the methylene protons neighboring oxygen atoms appear at 3.63 ppm and 3.61 ppm respectively. As seen previously, the two signals are overlapped. The deuterium-hydrogen exchange is very fast in D₂O and a peak representing the thiol protons is not observed. With the influence of the thiol proton absent, the sulfur adjacent methylene proton displays a triplet peak (split by 2 neighboring protons) rather than the quartet peak seen in CDCl₃ (splitting from three neighboring protons).

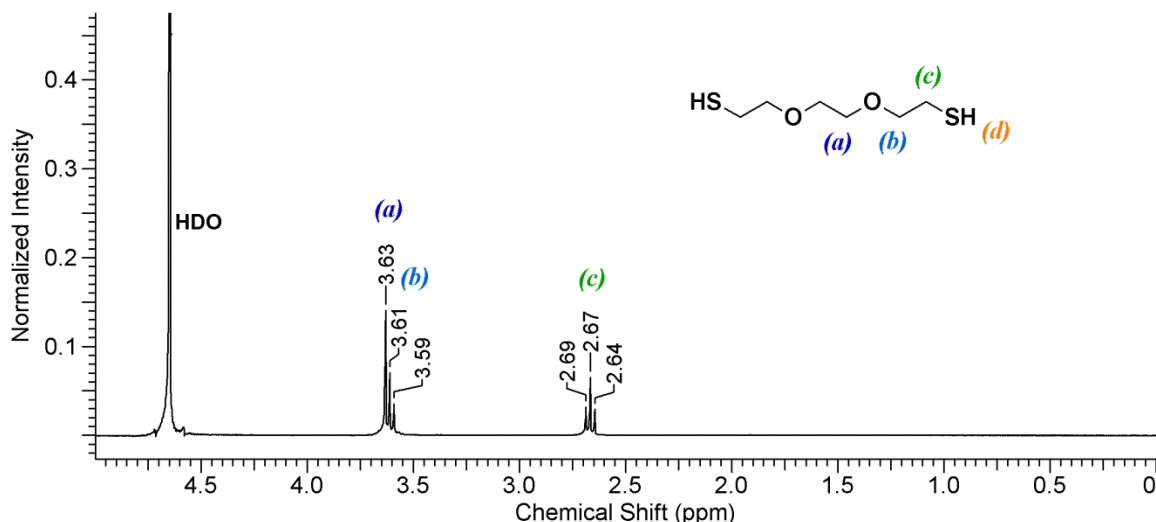


Figure 4.2.1. ¹H NMR spectrum of DODT in D₂O (3 s relax.; 64 scans; 300 MHz; D₂O).

When DODT was mixed with D₂O in the presence of slightly more than 2 molar equivalents of triethylamine, the solubility of DODT, and the resulting ¹H spectrum (Figure 4.2.2) changes significantly. The triethylamine methyl proton signals are now the strongest signal. The maximum intensity of the HDO peak is only 0.74 arbitrary intensity units (au) relative to the triethylamine methyl peaks. The intensity of the DODT peaks relative to the internal standard signal nearly triples, with the singlet corresponding to the

central methylene protons increasing from 0.17 au to 0.43 au. Signals representing DODT have all shifted up field. The singlet peak representing the central methylene protons (a) and the triplet peak representing oxygen adjacent protons (b) are no longer overlapped. Change in chemical shifts from the DODT-only spectrum indicates that the thiol protons have been abstracted and DODT is present in a new, ionic form. In addition to the DODT signals, a quartet at 2.94 ppm and a triplet at 1.06 ppm represent the ethyl substituents of the amine. Neat triethylamine is immiscible with water at room temperature, however it becomes miscible once ionized. In the organic phase there was approximately 2.34 mol amine for every 1 mol DODT. Integration values show that in the aqueous phase there are about 1.86 mol amine to every 1 mol DODT. This indicates that most DODT ions carry two negative charges and migrate into the aqueous phase as an ionic trio with two accompanying protonated triethylamine cations.

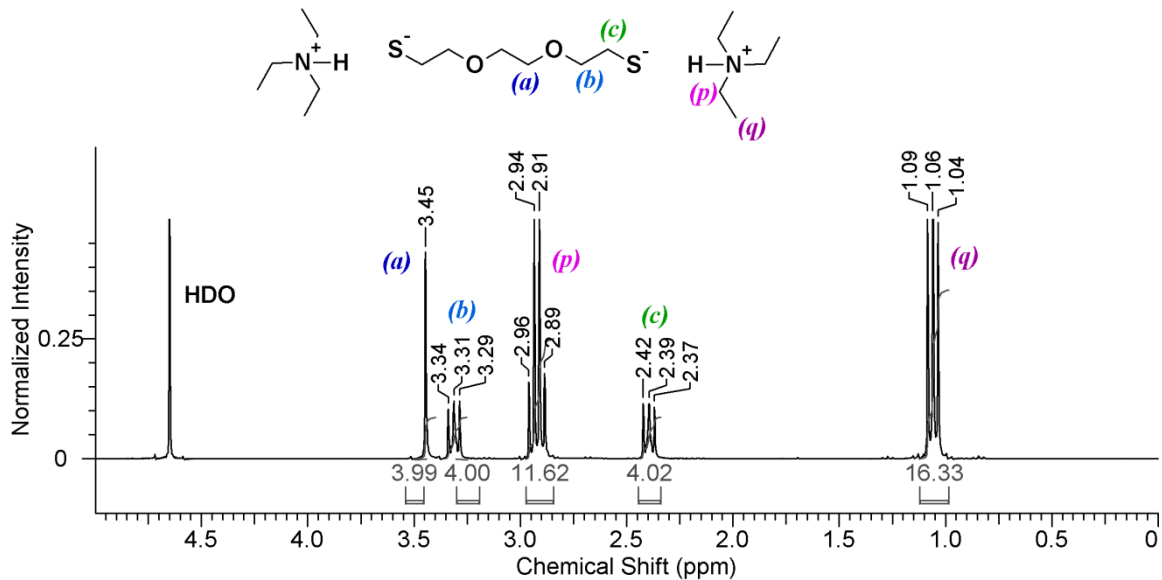


Figure 4.2.2. ^1H NMR spectrum of DODT with triethylamine in D_2O shows improved aqueous solubility of ionized DODT. (3 s relax.; 64 scans; 300 MHz; D_2O)

To determine what species are present in the organic phase during the polymerization reaction, DODT, triethylamine and H₂O₂ were mixed in a vial and a sample of the organic layer was immediately taken and diluted in CDCl₃. We will call this system “two-phase”. The ¹H NMR spectrum (Figure 4.2.3) of this sample shows signals from the triethylamine (labeled *p* and *q*) at about 1.0 ppm and 2.5 ppm. Again, signals from non-ionic DODT (labeled in grey *a*, *b* and *c*) appear at 3.6 ppm (singlet and triplet) and at 2.6 ppm (triplet). New peaks with shifts identical to those seen in the poly(DODT) spectrum also appear. A triplet at 3.70 ppm (turquoise *b*) represents the oxygen-adjacent methylene protons, and a triplet at 2.85 ppm (green *c*) is characteristic of disulfide-adjacent methylene protons. The singlet corresponding to the methylene protons (blue *a*) central to the DODT unit are hidden under the stronger peak at about 3.6 ppm from the dithiol monomer. Poly(DODT) is not soluble in triethylamine, so these new signals must arise from small molecules with the same structure. No thiol proton signals (around 1.5 ppm) are seen for any species which could indicate a complex with excess triethylamine, or cyclization.

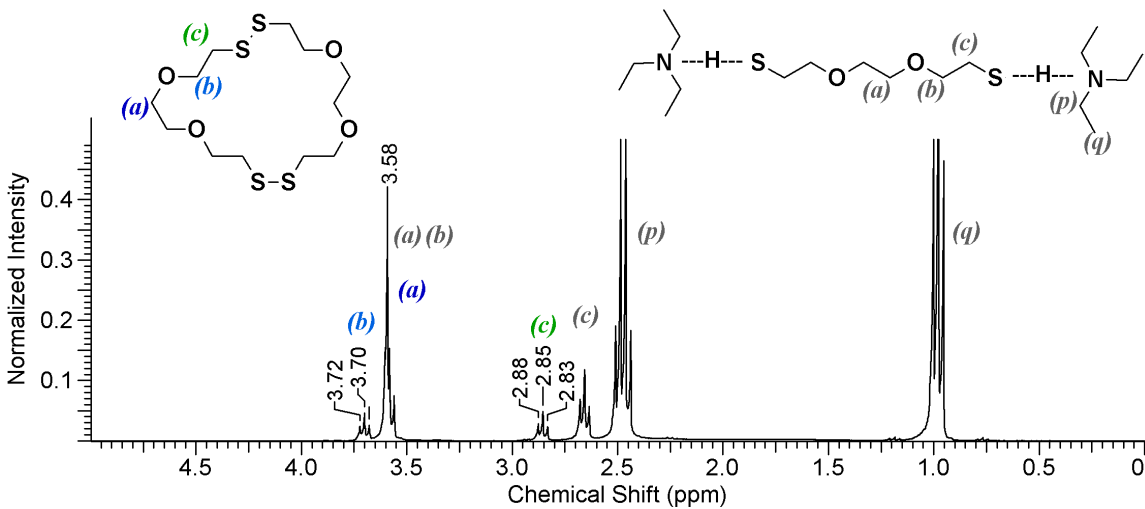


Figure 4.2.3. ^1H NMR spectrum of organic phase in CDCl_3 after the addition of H_2O_2 .

(3 s relax.; 64 scans; 300 MHz; CDCl_3)

The immiscibility of triethylamine with water above 18.7 °C was confirmed by observing the separation of the amine from the DI H_2O upon gradual heating from 2°C to 20°C. At 20°C, the aqueous-organic interface was not well defined, but two phases were distinguishable. A cloudy central layer formed with slight perturbation and required over 20 min to return to the unperturbed state. The same trial performed with the 2.26 M DODT/amine solution in place of neat triethylamine, showed no separation at lower temperatures, but at room temperature a small organic layer formed at the top of the liquid with a volume of 1.3 mL. This small organic layer is attributed to non-ionized triethylamine. This supports the ^1H NMR data indicating that not all DODT species are accompanied by 2 triethylamine units.

Repeated extractions of a 1.95 molar DODT/amine solution with DI H_2O were used to determine the saturation level of the organic compounds in aqueous solution. Calculating from the volume loss of the organic phase, the solubility of the DODT/amine

solution is 0.50 mL/mL H₂O. From the NMR data, it was calculated that about 1.86 moles of triethylamine accompany every mole of DODT into the aqueous phase. In the presence of triethylamine, saturated concentration of DODT in H₂O was calculated to be 0.85 mol/L

4.2.2. Polymerization starting from saturated aqueous solution of DODT and triethylamine.

DODT in triethylamine were dissolved in DI H₂O up to their saturation point (0.85 M DODT; 1.56 M Et₃N). An aliquot of this solution was used in the oxidative polymerization of DODT by H₂O₂. We will call this the pre-dissolved system. In this aliquot there was no excess triethylamine phase. Initial calculations for the pre-dissolved system were based the assumption that DODT and triethylamine ions migrate to the aqueous phase as an ionic trio in a 1:2 ratio. From NMR, the actual ratio was found to be 1:1.86, close to the theoretical value. To keep the final concentrations similar, a 1.35 M aqueous solution of H₂O₂ was prepared for the pre-dissolved system.

Table 4.2.1. Concentration of reagents in two DODT polymerizations.

System	[DODT] (mol/L)	[Et ₃ N] (mol/L)	[H ₂ O ₂] (mol/L)
Pre-dissolved	0.39	0.77	0.74
Two-phase (10-5-55)	0.37	0.74	0.74

The mixtures remaining after the polymers were removed were analyzed by ESI-MS because they looked different from one another. Mixture from the pre-dissolved system was slightly hazy, while the mixture from the two-phase system was opaque

milky white. Results from ESI analysis of the two residual mixtures revealed that the solutions had similar compositions. Cyclic dimers, trimers and tetramers of DODT were found in each, but the ratio of the species varied between the two samples. Table 4.2.1 shows the ratio of dimer, trimer and tetramer in each sample calculated from the intensity of the mass peak.

Table 4.2.2. Relative amount of oligomers found in each residual mixture by ESI-MS.

System	% Dimer	% Trimer	% Tetramer
Aqueous	44.04	52.88	3.08
Two-phase (10-5-55)	56.33	39.61	4.06

Figure 4.2.4 shows the mass spectrum of the reaction solution from the aqueous system sample, and is also representative of the spectrum from the two-phase system (except with changes in relative amounts.). The inset detail of the isotope distribution shows that the dimer is present in the cyclic form rather than in the linear dithiol form. Its first and principle peak appears at 382.9 m/z this corresponds to the mass of the monoisotopic peak (360.05 Da) plus the mass of the sodium counter ion (22.9 Da). Small peaks at 388 m/z nor 389 m/z would indicate the presence of linear dimer, but these peaks are not observed. All oligomeric peaks (383, 563 and 743 m/z) show isotope patterns indicating cyclic oligomers. The monoisotopic masses of each cyclic species are shown in the figure. All other prominent peaks (i.e. 142.9, 214.9 and 398.2 m/z) were also found in the solvent blank.

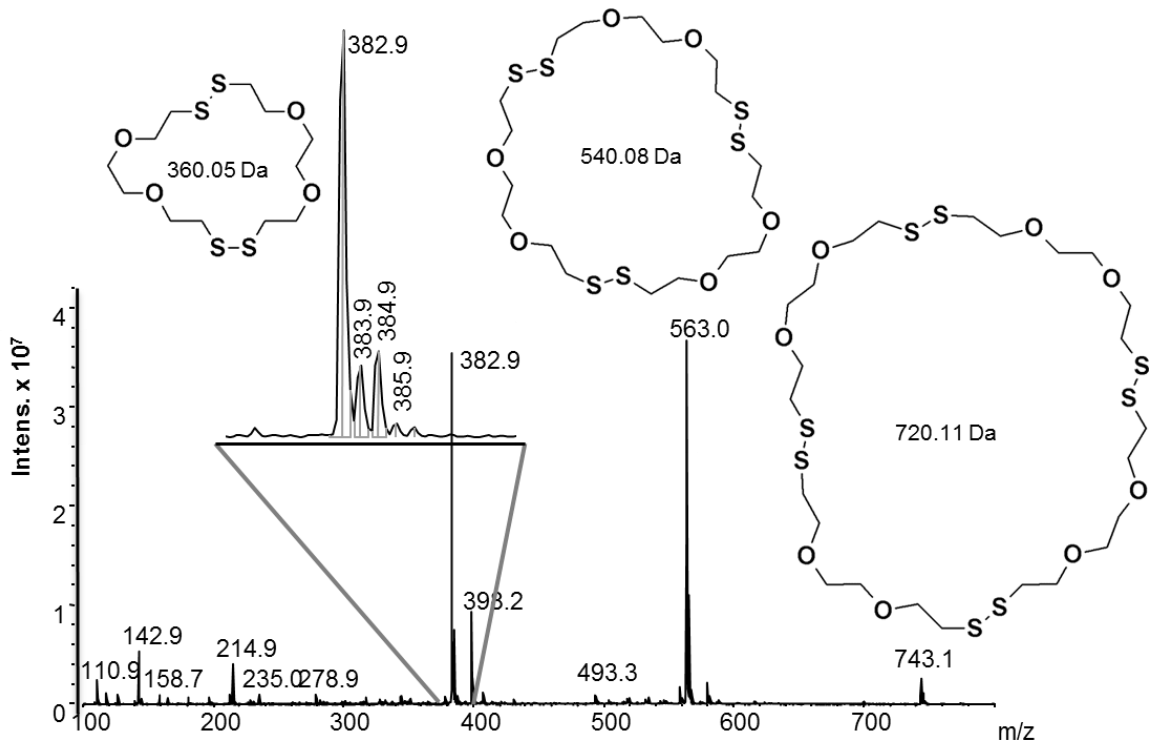


Figure 4.2.4. Mass spectrum of reaction solution from the aqueous solution system.

Interestingly, attempts to synthesize and isolate the cyclic dimer under less oxidizing conditions produced a mixture of cyclic and linear species. A solution of DODT, triethylamine and H_2O_2 in acetone were mixed. The final concentrations in acetone were 0.99 M, 0.51 M and 0.23 M. Before purification, the reaction solution was analyzed by ESI-MS. Monomer, dimers, trimers, tetramers were detected. A detail of the ESI-MS spectrum showing the dimer product is displayed in Figure 4.2.5.

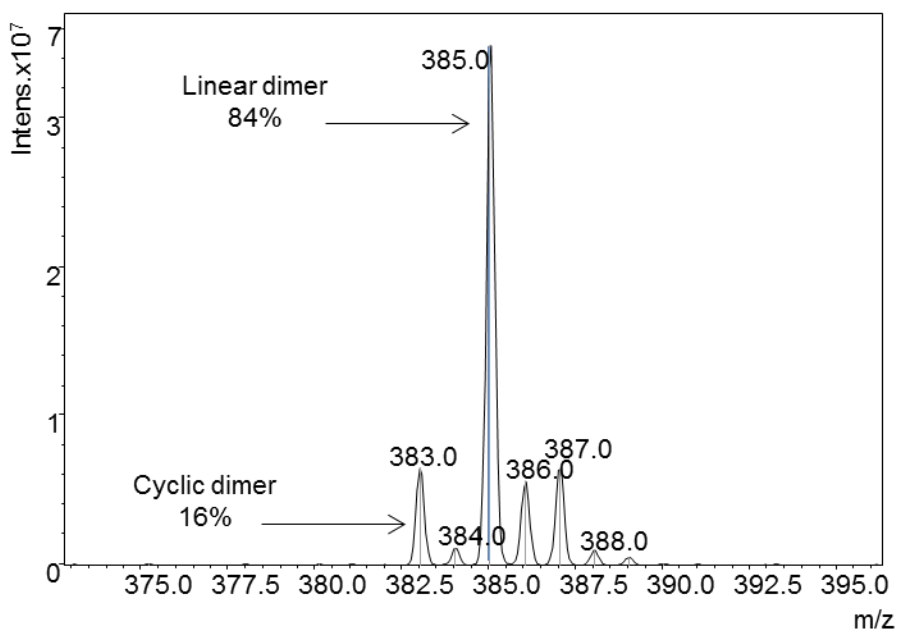


Figure 4.2.5. ESI mass spectrum of DODT dimer showing cyclic and linear species.

The aqueous solution system reached 94.8% conversion in 5 min, while the two-phase system reached only 80.1% conversion in 5 min. The ^1H spectrum of the pre-dissolved system displays the typical poly(DODT) peaks at 3.74 ppm (**b**, triplet), 3.64 ppm (**a**, singlet) and 2.90 ppm (**c**, triplet). It also shows a thiol proton peak at 1.59 ppm and a thiol adjacent methylene quartet at 2.70 ppm. Using the thiol-adjacent methylene signal as the basis for integration, the molecular weight of the polymer product would be 124,000 g/mol if all polymers are linear with thiol end groups. The measured $M_n = 55,000$ g/mol (Table 4.2.3.)

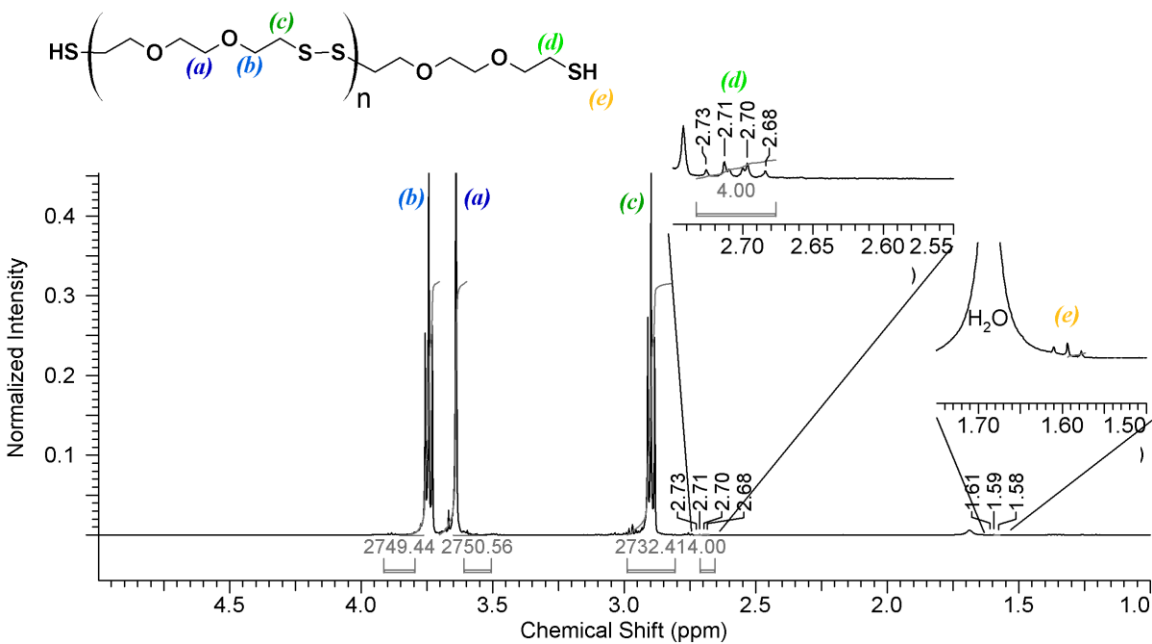


Figure 4.2.6. ^1H NMR spectrum of polymer from pre-dissolved system in CDCl_3 .
(500 MHz; 10 s relax.; 128 scans)

The carbon NMR spectrum (Figure 4.2.7) shows the peaks associated with poly(DODT) at 70.32 ppm (**B**), 69.65 ppm (**A**) and 38.45 ppm (**C**). No peak around 24 ppm, which would represent a thiol adjacent carbon is seen. However, the sample spectrum does show peaks at 68.39 ppm, 40.26 ppm and 39.20 ppm. Peaks around 39 to 40 ppm are characteristic of methylene carbons neighboring sulfur atoms present in a higher oxidation state, like the sulfone, thiosulfonate or sulfonic acid. All of which are shown in Figure 4.2.7. Similarly, the peak at 68.39 ppm may correspond to methylene carbons that are separated from the sulfur functional group by one carbon atom.

Investigation into polymers from a pre-dissolved system is on-going.

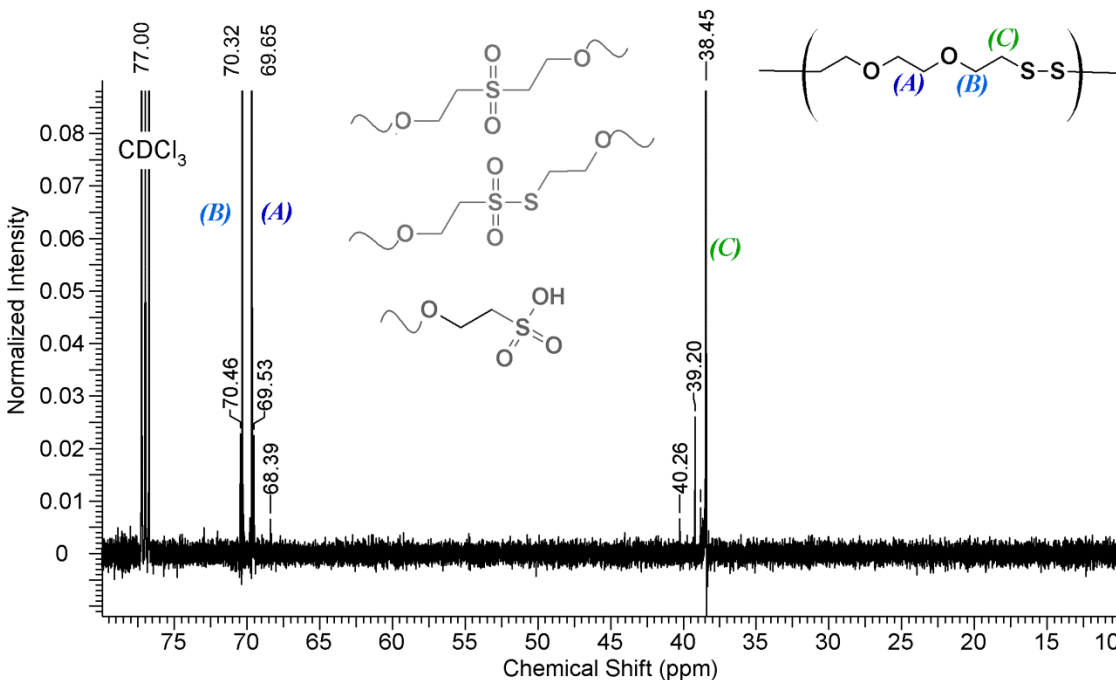


Figure 4.2.7. ^{13}C NMR spectrum of polymer from pre-dissolved system in CDCl_3 . (1 s relax.; 1024 scans; 500 MHz)

Results from SEC analysis of the polymers from the aqueous and two-phase system are compared in the table below. Refractive index (RI) and light scattering (LS) traces of each polymer are shown in Figure 4.2.8. The polymer from the two-phase system has molecular weights nearly double that of the pre-dissolved system with $M_n = 92,700 \text{ g/mol}$ compared to $M_n = 56,700 \text{ g/mol}$. The molecular weight distribution of the two-phase polymer is just over 2, and it is broader than the that of the pre-dissolved system, which was 1.71. They both show nearly identical low molecular weight peak pattern in the RI trace (Figure 4.2.8).

Table 4.2.3. Results from SEC analysis of poly(DODT) samples.

System	M_n (g/mol)	M_w (g/mol)	PDI	R_{gz} (nm)	R_{hw} (nm)	$[\eta]_w$ (mL/g)
Two-phase (10-5-55)	92,000	192,000	2.09	27.2	12.7	79.8
Pre-dissolved	55,000	96,000	1.76	15.0	9.2	59.1

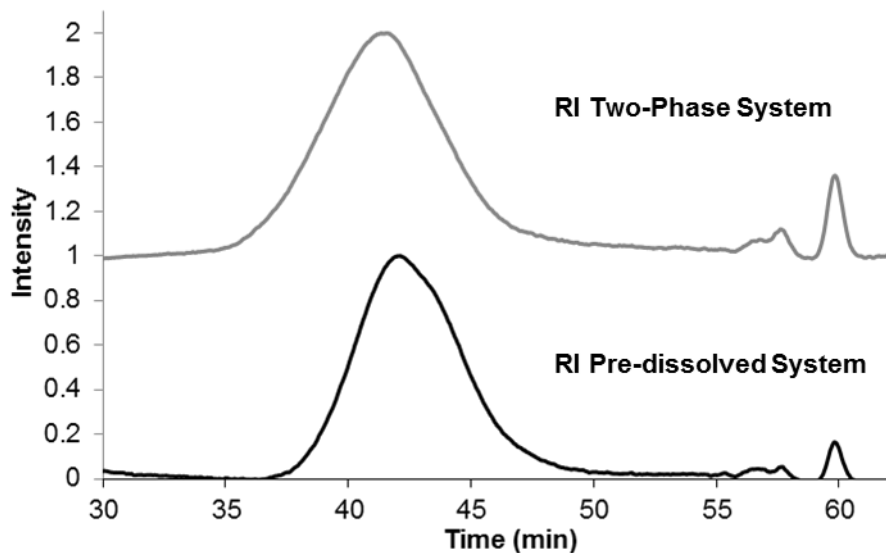


Figure 4.2.8. RI traces from SEC analysis of poly(DODT) samples prepared from aqueous and two-phase systems.

4.3. Homopolymerization of ED and copolymerization of ED with DODT

4.3.1. Homopolymerization of ED and characterization of poly(ED)

Homopolymerization of ED using the new system produced a very fine powdered product with monomer conversions up to 95.5%. The powdered product was rinsed with methanol and then extracted in THF. ESI analysis the THF purification step revealed no ED derivatives, indicating that all oligomers or impurities were washed away in the methanol rinse.

The ED homopolymer was not soluble in available deuterated solvents so it was analyzed by solid state NMR. Figure 4.3.1 compares the solution ^{13}C NMR of ED to the solid state ^{13}C NMR spectrum of poly(ED). Both show only one peak, however there is a shift from 28.77 ppm in the monomer to 36.20 ppm in the polymer spectrum.

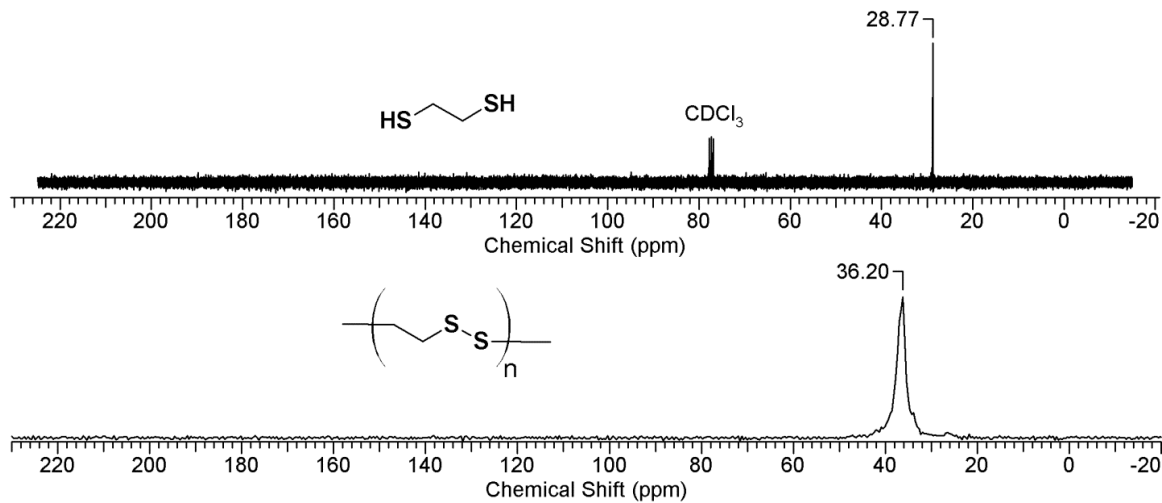


Figure 4.3.1 Comparison of ED (*solution*; CDCl_3) and polyED (*solid state*) ^{13}C NMR spectra.

The list of FTIR peak assignments for ED and poly(ED) are listed in Table 4.3.1. The spectra are compared in Figure 4.3.2. In the poly(ED) spectrum the strong peak at 2548 cm^{-1} , assigned to the S-H stretching of the thiol groups in ED,⁹³ disappeared. The C-S stretching band in the fingerprint region shifted from 692 cm^{-1} in the monomer to 677 cm^{-1} and the S-S band at 457 cm^{-1} appeared after the polymerization reaction. It should be noted that bands corresponding to disulfide bonds are weak due to the symmetry of the bond.⁹⁴

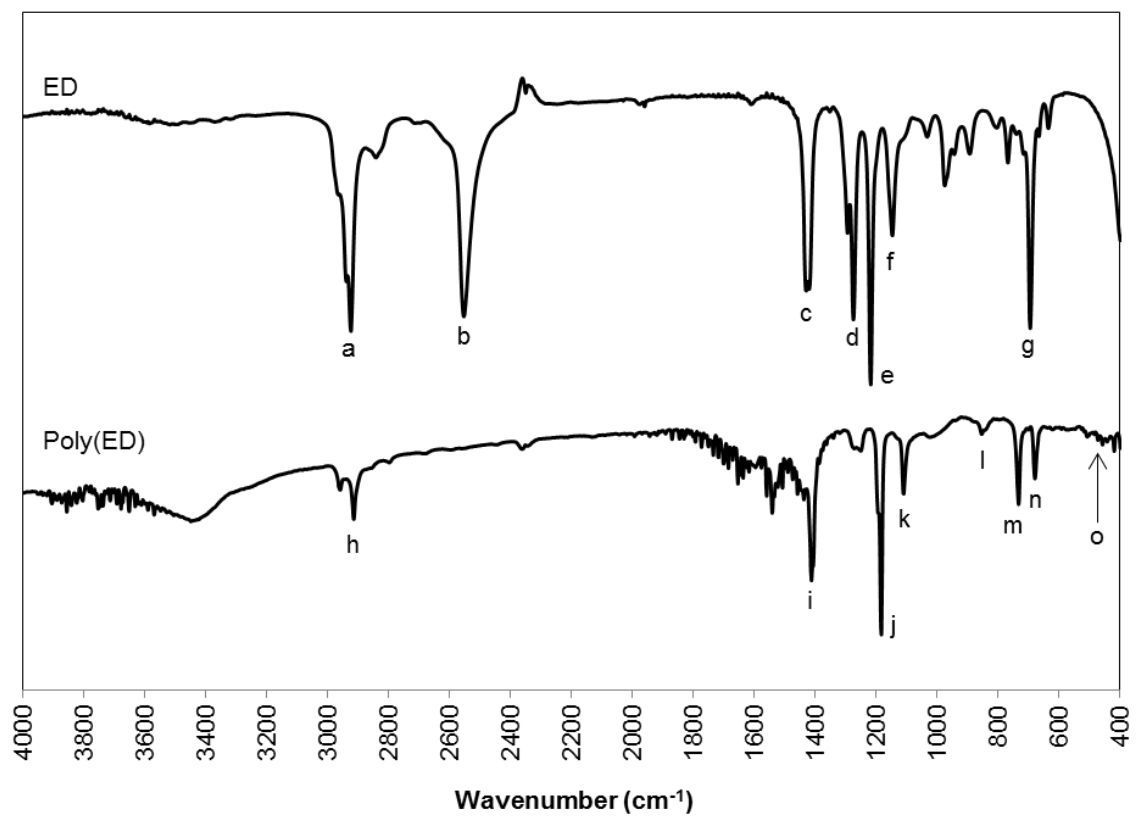


Figure 4.3.2: Comparison of ED and poly(ED) FTIR spectra.

Table 4.3.1. FTIR assignments for ED and poly(ED).

Band	Band (cm ⁻¹)	Assignment
ED		
A	2900	C-H stretch ^a
B	2548	S-H stretch
C	1431-1415	CH ₂ bend ^a
D	1273	CH ₂ wag ^a
E	1217	CH ₂ wag ^a
F	1147	CH ₂ twist ^a
G	692	C-S stretch ^a
Poly(ED)		
H	2995-2914	C-H stretch
I	1411	CH ₂ wag
J	1182	CH ₂ twist
K	1110	C-C asym. stretch
L	854	C-H rock ^b
M	734	C-S stretch ^b
N	677	C-S stretch ^a
O	457	S-S stretch ^b

a. ER-213 b. ER-212

Figure 4.3.3 presents the DSC traces of poly(ED). During the second heating ramp, poly(ED) shows a very weak T_g at -13.9°C and a melting peak at 132.90°C with two distinct shoulders at 122.8°C and 136.2°C. Poly(ED) was reported to be a semicrystalline polymer, with T_m between 159.5°C and 165.6°C.⁹⁵ It has also been reported that poly(ethylene disulfide) is only 14% crystalline.⁷ The very weak T_g suggests that the polymer produced by the new method is more crystalline than

amorphous, while the melting peak shoulders suggest the existence of more than one crystalline phases. DSC analysis of the homopolymer reacted for only 10 min shows a strong bimodal melting peak with maxima at 130.9°C and 139.3 C (Figure 4.3.3). It is proposed that with increased reaction time the two distinct crystalline phases, which form the two peaks, become more and more similar and the melting peaks merge.

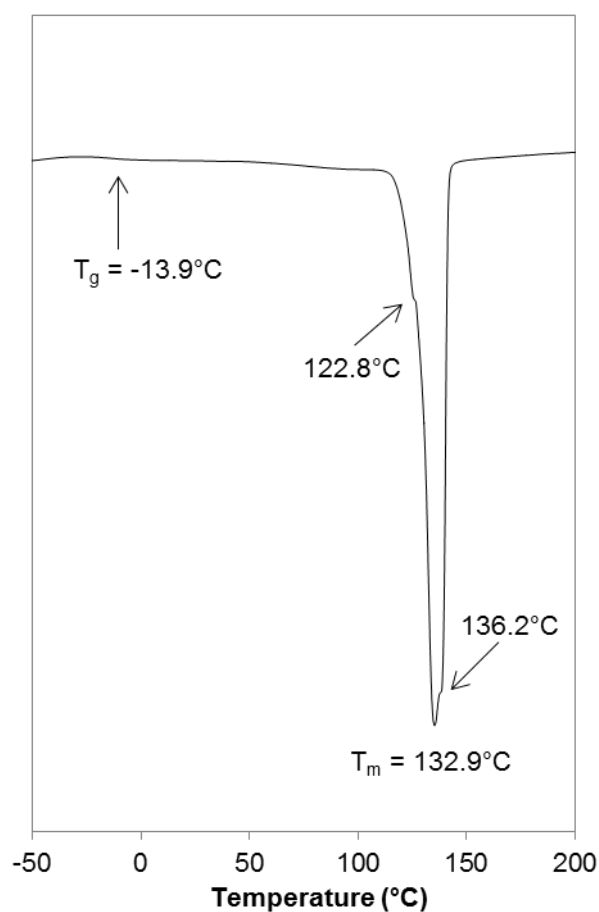


Figure 4.3.3. DSC second heating cycle for poly(ED) from polymerization with 24 hr reaction time.

4.3.2. Survey of ED-DODT copolymerizations.

4.3.2.1. Effect of Comonomer Composition

Kinetic studies of the DODT polymerization show that the conversion rate begins to plateau at around 10 min reaction time. For this reason all products in the copolymerization survey, including the ED and DODT homopolymers synthesized for comparison were removed from the oxidizing reaction solution after 10 min.

Table 4.3.2. Results from copolymerization survey of ED with DODT.

Sample	% Conv.	Appearance	After Methanol Wash/Precipitation	
			% Conv.	Appearance
Poly(ED)	95.5	Fine white powder		Fine white powder
ED-9	86.3	Fine white powder	81.5	Fine white powder
ED-7	87.9	Small rubbery curds	79.0	Chunky white powder
ED-5	82.9	White rubbery mass	53.2	White powder ^a 52 % Clear elastomer ^b 48 %
ED-3	85.5	Clear elastomer	72.1	Clear elastomer
ED-1	85.7	Clear elastomer	64.3	Clear elastomer
Poly(DODT)	67.9	Clear elastomer	57.8	Clear elastomer

^a THF insoluble; ^b THF-soluble

The FTIR spectra of all copolymers were compared (Figure 4.3.4). As the ED content of the comonomer mixture decreased, the intensity of the sharp peaks at 1411 cm^{-1} , 1182 cm^{-1} , 734 cm^{-1} and 677 cm^{-1} , the characteristic C-S stretch signals in poly(ED) also decreased. At the same time the intensity of the bands at 2861 cm^{-1} and 1106 cm^{-1} , characteristic of C-H and C-O stretches in poly(DODT) increased.

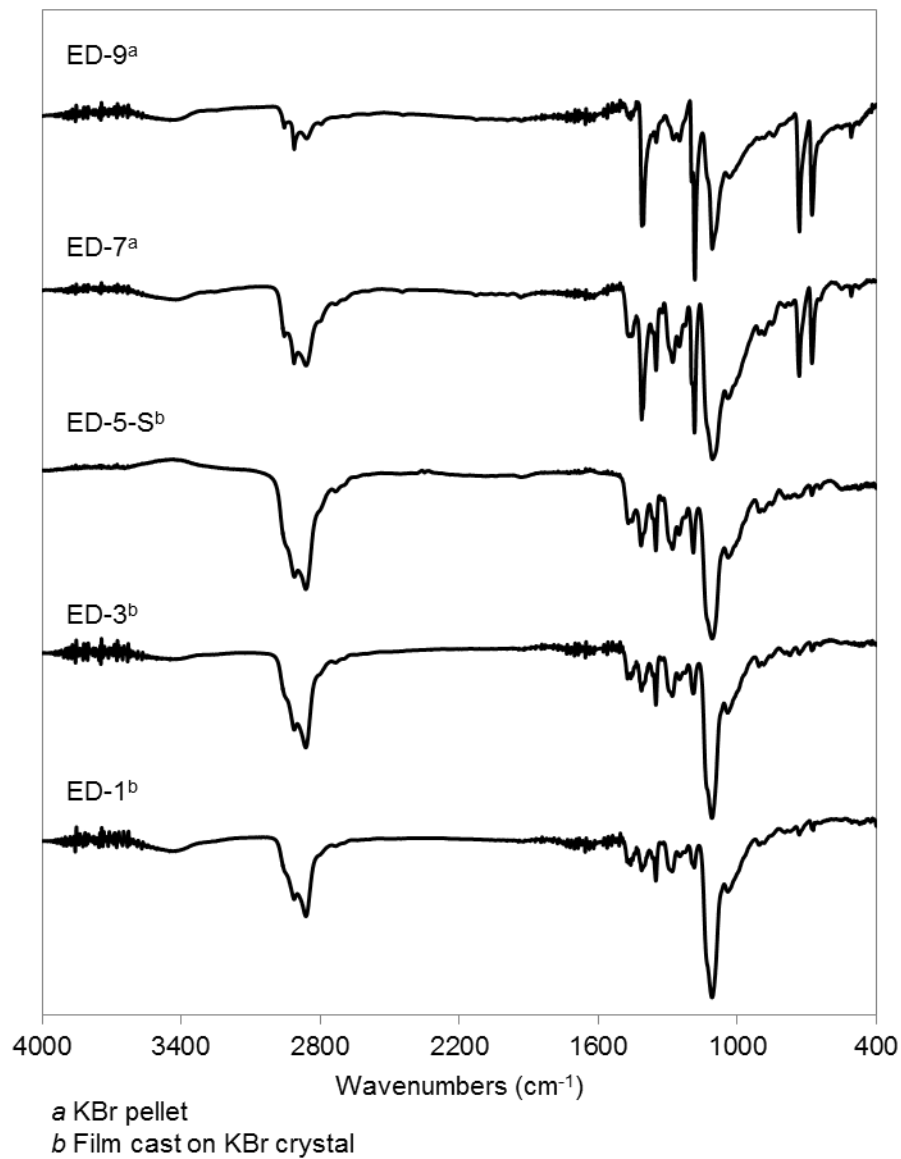


Figure 4.3.4. FTIR spectra for all ED-DODT copolymers in survey.

Figure 4.3.5 shows the ^1H NMR spectra of the soluble copolymer samples together with the DODT homopolymer. Poly(DODT) shows three proton peaks at 3.73 ppm, 3.63 ppm and 2.88 ppm. The two peaks furthest downfield correspond to the methylene protons adjacent to the oxygen atoms, with the singlet arising from the 4 equivalent methylene protons at the center of the molecule. The triplet at 2.88 ppm

corresponds to the sulfur-adjacent methylene units. The copolymers display all three peaks characteristic of poly(DODT) as well as a fourth peak at 3.00 ppm. Meng and coworkers found one singlet peak at 2.99 ppm corresponding to the 4 equivalent methylene protons of soluble cyclic oligomers of ED.¹⁶ Based on Meng's data the fourth peak at 3.02 ppm in the copolymer spectra is assigned ED methylene units found in the polymer.

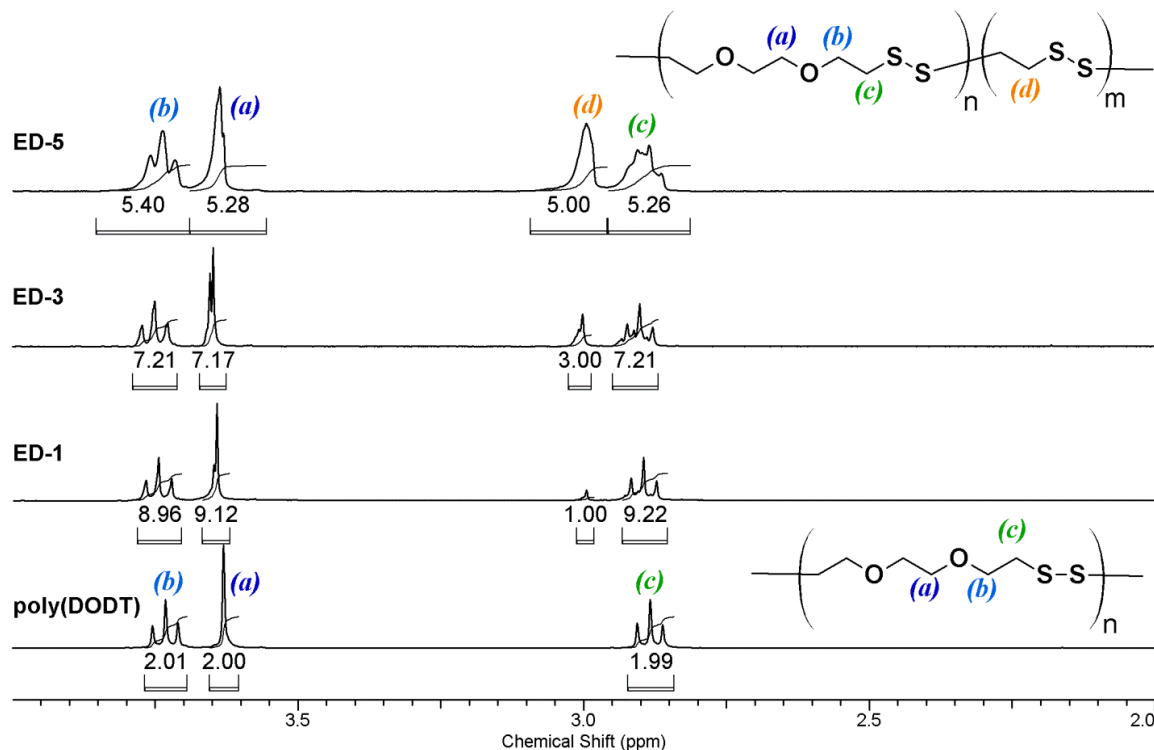


Figure 4.3.5 ^1H NMR spectra from soluble copolymers and poly(DODT) (12 s relax; 128 trans.; 300 MHz; CDCl_3).

The peak at 3.00 ppm corresponds to the sulfur-adjacent methylene protons from ED. The copolymer composition data obtained from NMR are listed in Table 4.3.4. The

copolymer compositions are practically equal to the feed composition. This indicates ideal copolymerization behavior.

Table 4.3.3. Copolymer compositions in mole fraction ED based on NMR integrations.

Sample	f_{ED} in feed	f_{ED} in copolymer
ED-5-S	0.34	0.32
ED-3	0.18	0.18
ED-1	0.05	0.05

The peaks in the copolymer spectra are broadened in comparison to the DODT homopolymer. Where the DODT homopolymer contains two distinct triplets (3.73 ppm and 2.88 ppm) and one singlet (3.63 ppm), the copolymer spectra contain multiple overlapping peaks in these regions corresponding to DODT units adjacent to ED units as well as DODT units adjacent to other DODT units. None of the spectra show a triplet near 1.5 ppm that is characteristic of a thiol proton.

Broadening of 1H NMR peaks is particularly noticeable in sample ED-5-S and this is also reflected in the ^{13}C spectrum (Figure 4.3.6). Peaks from 70.36 ppm to 70.39 ppm represent DODT carbons adjacent to oxygen atoms at either end of the monomer unit. In the DODT homopolymer the central carbon atoms are equivalent and appear as one single peak at 69.65 ppm, however in the copolymer two peaks at 69.69 ppm and 69.65 ppm are seen. A broad signal with peaks at 38.54 ppm and 38.48 ppm represents sulfur-adjacent carbons in DODT units. Finally, the broad peak at 37.72 represents the carbons atoms from ED. No other peaks are seen in the spectrum (except the solvent triplet at 77.16 ppm). The appearance of peaks near 28 ppm or

24 ppm would indicate carbons adjacent to ED or DODT thiols respectively, but they are not observed. Cyclic or catenane in structures have been suggested for disulfide polymers.²¹

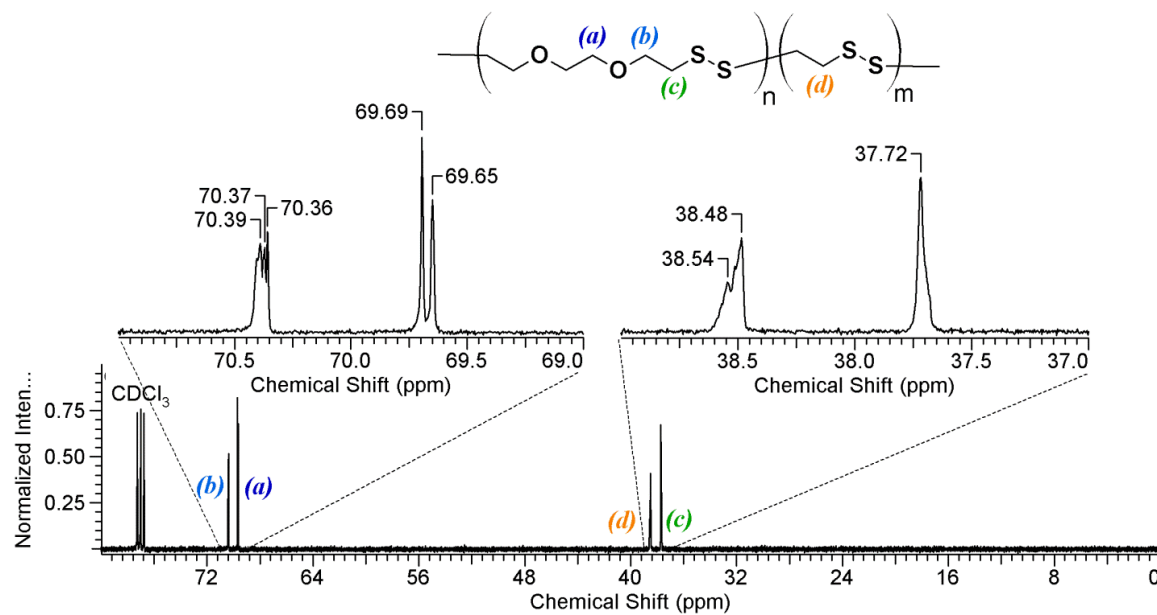


Figure 4.3.6. ^{13}C NMR spectrum for copolymer sample ED-5-S. (10 s relax. 1024 trans.; 500 MHz; 1024 trans.; CDCl_3)

4.3.1.2. Thermal Analysis

Figure 4.3.7 shows the DSC traces of the second heating cycle for all copolymer samples and poly(ED) reacted for 10 min. Table 4.3.4 lists the thermal transitions for the copolymers as well as the two homopolymers. Sample ED-9 shows sharp melting temperatures at 115.84°C and 124.52°C and a T_g at -30.01°C . This pattern is similar, but shifted from the poly(ED) sample with the same reaction time (10 min). Additionally, the T_g in the copolymer sample is much stronger. Sample ED-5 provides the most interesting results. The insoluble fraction displays thermal behavior that more closely resembles

ED-7, displaying a T_g at -43.5°C and broad melting peak at 62.3°C , while the soluble fraction behaves more closely to ED-3 showing only a T_g at -46.8°C .

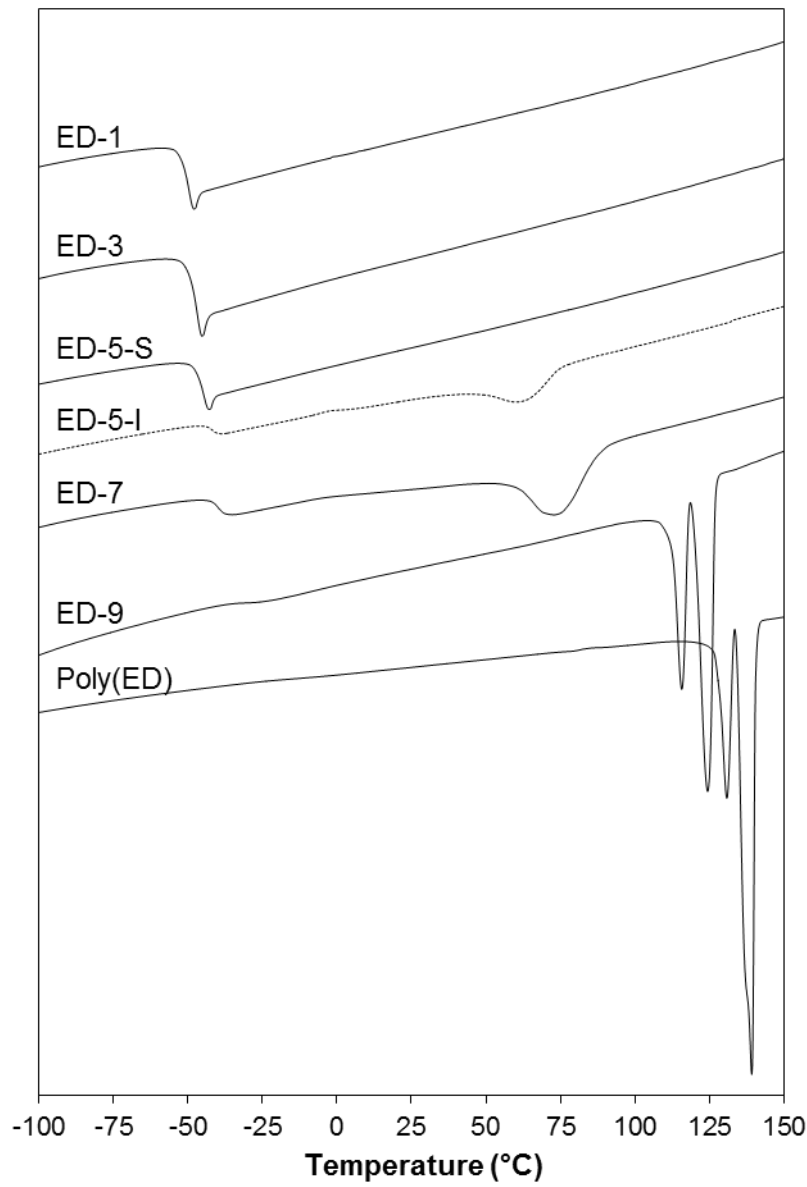


Figure 4.3.7. DSC traces for poly(ED) and poly(ED-co-DODT) samples.

Table 4.3.4. Thermal transitions of homopolymers and copolymers.

Sample	T_g (°C)	T_m (°C)	
		Peak 1	Peak 2
Poly(ED)	-13.71	130.90	139.30
ED-9	-30.01	115.84	124.52
ED-7	-39.91	74.11	---
ED-5-I	-43.53	62.27	---
ED-5-S	-44.92	---	---
ED-3	-46.84	---	---
ED-1	-49.82	---	---
Poly(DODT)	-49.84	---	---

Literature values for the T_g of poly(ED) and poly(DODT) were not available, so the experimental T_g values for poly(ED) and poly(DODT) were used when plotting the *theoretical* values of the Fox equation (Figure 4.3.8). The curvature in the theoretical Fox plot stems from the large mismatch in molecular weight of the two monomers, with DODT monomer being nearly twice the molecular mass of ED monomer. The experimental copolymer T_g values, determined by DSC, were plotted and compared to the theoretical values calculated using the Fox equation. The copolymer T_g deviate slightly below the predicted T_g for random copolymers or blends as calculated from the Fox equation. The weight fraction of the copolymers was based on the comonomer feed composition, which NMR has shown to be a good estimate for copolymer composition. However, the deviation of the experimental from theoretical curve can also be explained by the presence of ED-rich and DODT-phases. It could also be an indication of slightly preferential DODT incorporation into the copolymer. The degree of deviation below theoretical increases with increasing ED weight fraction, indicating that the

flexible DODT chains have a greater influence over the copolymer T_g than the much shorter ED units. There is very good agreement between theoretical and experimental values.

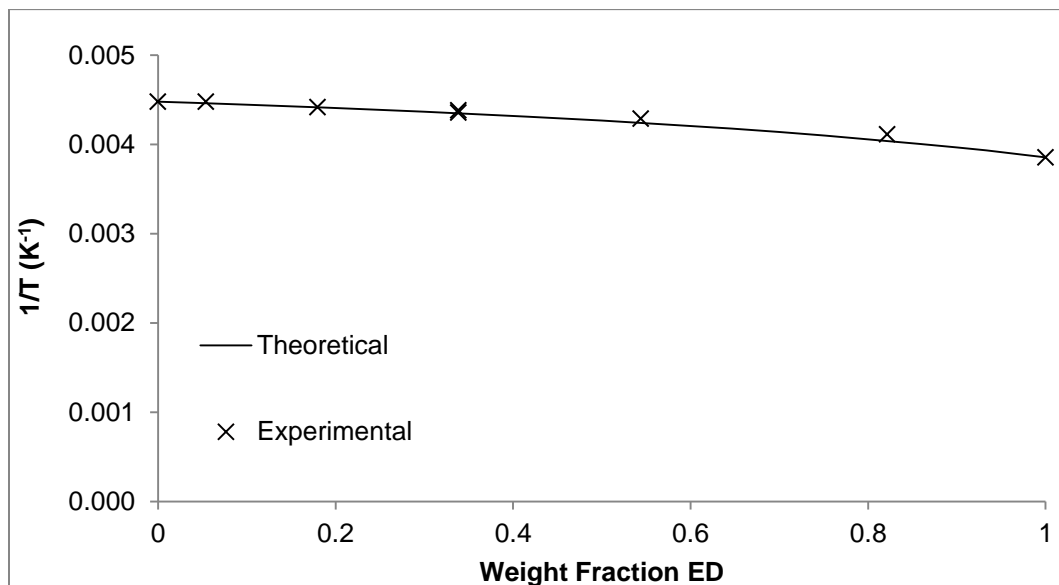


Figure 4.3.8. The Fox plot for ED-DODT copolymers is compared to the experimental data.

The DSC traces of ED-5-I, ED-7 and ED-9 represent blocky two phase systems with two strong transitions (T_g and T_m), so the copolymers are not random as asserted earlier.⁹⁶ Samples ED-3 and ED-1 show only the low T_g characteristic of poly(DODT), suggesting that ED blocks are not long enough to form crystalline regions. However, even small amounts of DODT incorporation disrupts the poly(ED) chain to produce a strong glass transition.

In TGA, copolymers ED-9 and ED-7 display small mass losses (1.14% at 94.96°C and 1.54% at 113.32°C) that could be due to residual solvents and/or low MW fractions.

As the mole fraction of ED decreased, the onset decomposition temperature increased from 263.0°C for ED-9 to 276.3°C for ED-1 (sample ED-7 breaks the trend slightly with an onset decomposition temperature of 260.7°C). The residual mass at 600°C also increased with decreasing poly(ED) content. This may be caused by the production of sulfur oxides from the decomposition of the oxygen-containing DODT units. However, poly(ED) homopolymer shows higher onset degradation temperature, T_{50} and residual mass than several of the copolymers. Table 4.3.5 summarizes the data collected from TGA.

Table 4.3.5. Copolymer decomposition temperatures and residual mass for each copolymer. T_2 and T_{50} are 2% and 50% mass loss temperatures.

Sample	T_2 (°C)	Onset T (°C)	T_{50} (°C)	Residual Mass
Poly(ED)	180.03	273.24	277.73	4.25%
ED-9	207.48	263.03	267.73	1.51%
ED-7	202.15	260.73	269.28	0.97%
ED-5-I	237.05	262.97	274.29	3.17%
ED-5-S	248.34	263.81	280.87	4.35%
ED-3	251.88	268.51	285.71	5.52%
ED-1	256.95	276.29	291.16	5.62%
Poly(DODT)	250.13	278.53	293.63	5.56%

4.3.1.3. Tensile testing of poly(disulfide) polymers

Poly(DODT) and poly(ED-co-DODT) with $f_{ED} = 0.4$ were filled with 30 phr food-grade carbon black (Black Pearls® 4350, Cabot). Both samples show low tensile strength. The results, however, are artificially low because the extension rate was

50 mm/min rather than the ASTM standard value of 500 mm/min. Early, unfilled samples were too delicate to be tested at 500 mm/min, so the strain rate was reduced. For consistency, the same rate was applied to the unfilled samples. Despite this disparity, the data is still useful to demonstrate the copolymers' superior strength over the DODT homopolymer. The copolymer shows about 3 times the maximum tensile strength of the DODT homopolymer suggesting that hard crystalline phases from the ED content are present.

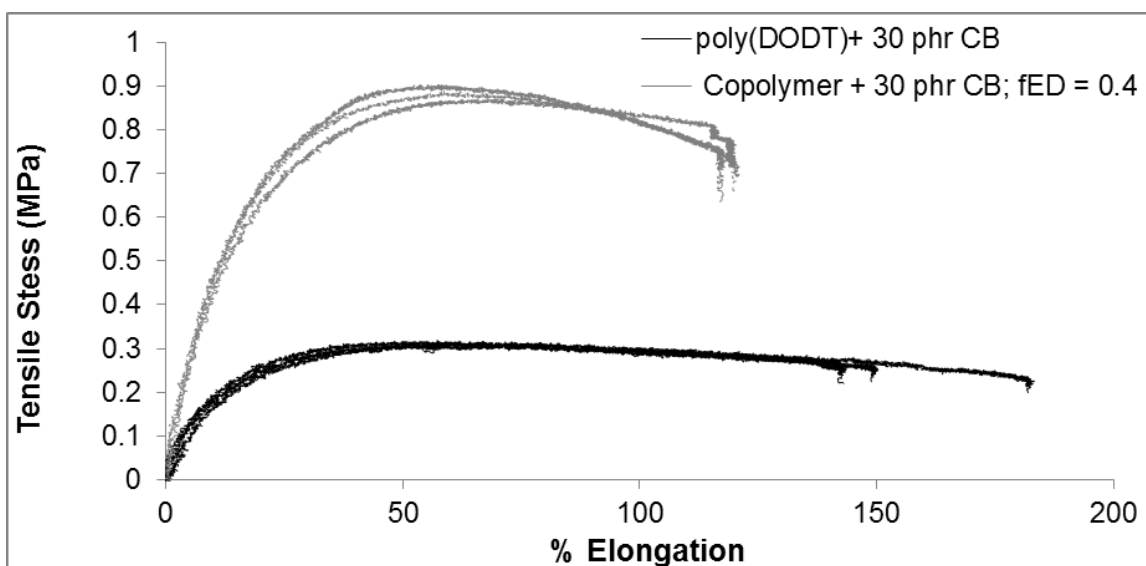


Figure 4.3.9. Stress-strain curves for CB-filled poly(DODT) and poly(ED-co-DODT)
(Extension rate = 50 mm/min)

4.3.2. Effect of mixing rate in ED-DODT copolymerization.

The effect of mixing was demonstrated in the copolymerization of ED with DODT. The magnetic stir bar provided thorough mixing of homogeneous solution, but was slowed by the presence of a polymeric phase. The product began to separate after

addition of half of the hydrogen peroxide. The Mag-ED-3 reaction mixture cleared during the reaction, leaving only the white, rubber polymer product. The lump of product was easily removed from the oxidizing mixture for purification.

After purification, the Mag-ED-3 product showed 90.5% conversion. The overhead mechanical mixer provided fast, steady mixing that was unaffected by the evolution of polymer precipitate. The mechanically stirred reaction formed a foamy, opaque white dispersion that did not clear as the reaction progressed. A liquid product separated to the bottom and sides of the reaction flask, but remained liquid even after two hours of oxidation. The Mech-ED-3 showed a monomer conversion of 63.4%.

A detail of the proton NMR spectra of the two copolymers are compared in Figure 4.3.10. The integration value of the ED methylene peak, **d** (3.01 ppm & 3.00 ppm), was fixed at 3.00 to reflect molar ratio of ED in the comonomer feed stock. In spectrum from Mag-ED-3, all three DODT methylene peaks (3.75 ppm, 3.65 ppm and 2.90 ppm) integrate to about 7 indicating the monomers incorporate into the backbone in the same ratio as found in the feed stock. In the spectrum from Mech-ED-3 the DODT methylene proton signals each integrate to around 12 showing that DODT was preferentially incorporated into the copolymer. A distinct thiol triplet is seen in the ¹H NMR spectrum of Mag-ED-3, but none is seen in the Mech-ED-3 spectrum.

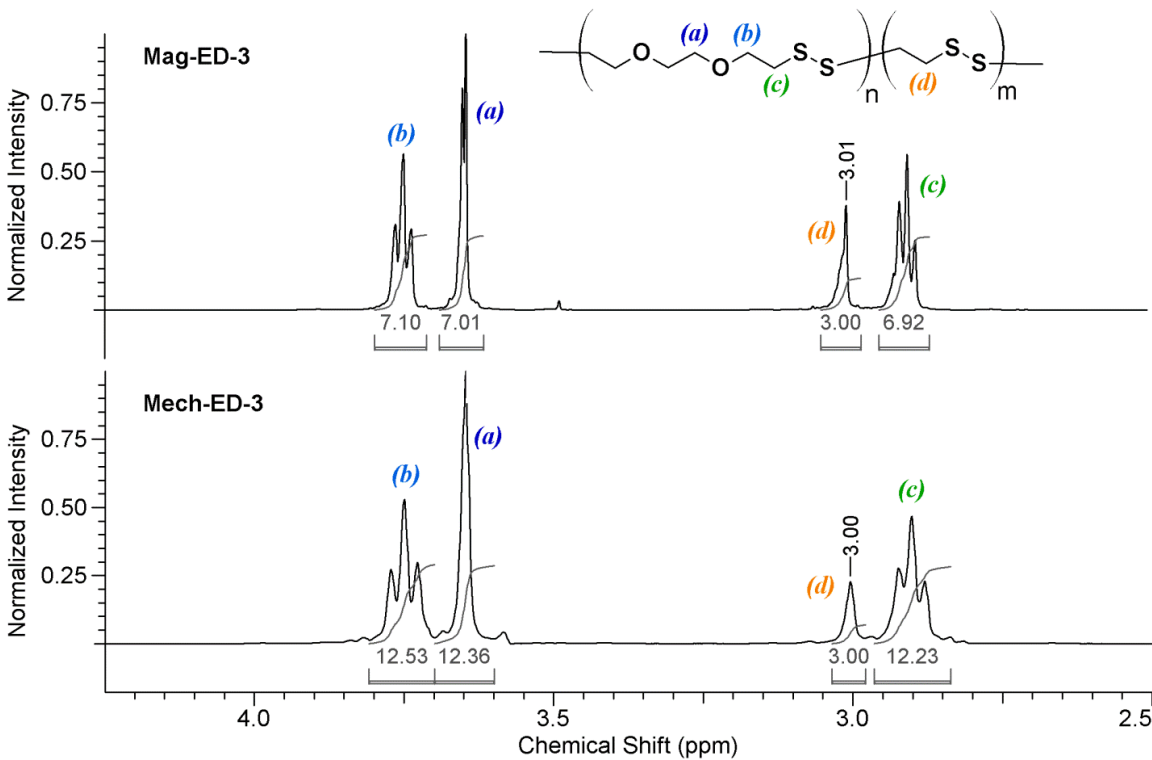


Figure 4.3.10. ^1H spectra of Mag-ED-3 and Mech-ED-3 are compared.(1 s relax; 64 trans.; 500 MHz; CDCl_3)

SEC analysis of the two copolymers showed that the magnetically stirred copolymer has a M_n six times greater than the M_n of the mechanically stirred polymer (Table 4.3.6). Additionally, Mag-ED-3 has a narrower molecular weight distribution.

Table 4.3.6. Results from SEC analysis of copolymers from reactions with different stirring rates.

	M_n (g/mol)	M_w (g/mol)	PDI
Mag-ED-3	263,700	511,800	1.94
Mech-ED-3	41,600	95,300	2.29

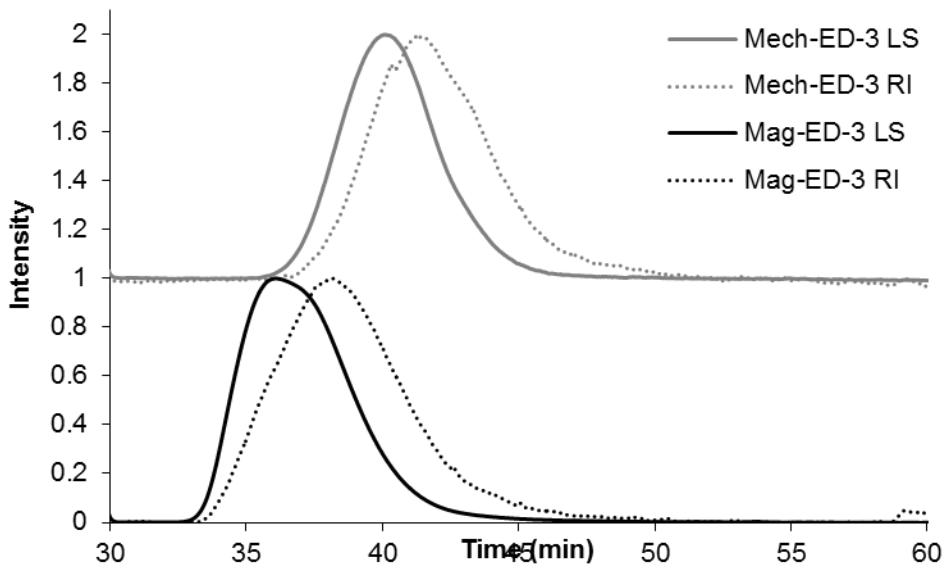


Figure 4.3.11. SEC traces (LS and RI) for Mag-ED-3 and Mech-ED-3.

4.4. Poly(disulfide) polymer networks

4.4.1. Scouting experiments

The dithiol monomer (DODT) and the trithiol compound, trimethylolpropane tris(2-mercaptopropionate) or TMPTMP, were used to synthesize poly(disulfide) polymer networks.⁸⁵

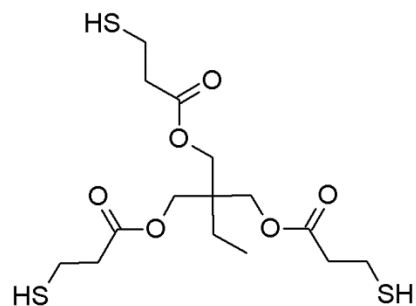


Figure 4.4.1. Crosslinker, trimethylolpropane tris(2-mercaptopropionate) (TMPTMP).

Early attempts to make networks without the addition of any organic solvent mixture formed sticky, heterogeneous masses. Scouting trials which varied the volume of organic solvent mixtures and hydrogen peroxide are shown in Table 4.4.1. These reactions were bubbled or mixed for 2-5 min and then reacted in open vessels. Other scouting trials, which varied triethylamine concentration, made networks with many bubbles and were fragile and spongy in texture and are listed in Table 4.4.2. These networks were shaken for only 20 s, then capped and allowed to react. Visible porosity increased with increasing amine concentration.

Table 4.4.1. Scouting studies for poly(disulfide) network synthesis.

Trial	[TMPTMP] (mol/L)	[DODT] (mol/L)	[Et ₃ N] (mol/L)	[H ₂ O ₂] (mol/L)	THF	EtOAc	Reaction Vessel	Observations
N-1	0.0030	0.464	0.483	0.419	3.00	5.00	25 mL beaker	Did not solidify
N-2	0.0033	0.513	0.534	0.371	3.00	5.00	20 mL vial	Did not solidify
N-3	0.0030	0.464	0.483	0.419	0.00	8.00	25 mL beaker	Did not solidify
N-4	0.0018	0.343	0.338	0.611	3.00	5.00	40 mL beaker	Rubbery disk
N-5	0.0018	0.278	0.273	0.733	3.00	0.00	40 mL beaker	Thin network floating on white emulsion

Table 4.4.2. Scouting studies for poly(disulfide) network with variation thiol:amine molar ratio.

Trial	[TMPTMP] (mol/L)	[DODT] (mol/L)	[Et ₃ N] (mol/L)	[H ₂ O ₂] (mol/L)	Molar Ratio Thiol:Et ₃ N	Observations
N-A1	0.058	0.316	0.806	0.429	1.0:1.0	Hat-shaped; Solid
N-A2	0.046	0.249	2.153	0.338	1.0:3.4	Hat-shaped; Small pores
N-A3	0.041	0.224	2.657	0.304	1.0:4.7	Hat-shaped; Visible pores; Fragile
N-A4	0.036	0.194	3.266	0.263	1.0:6.6	Visible pores; Fragile
N-A5	0.029	0.159	3.975	0.216	1.0:9.8	Visible pores; Crumbly

It was hypothesized that one reason for network heterogeneity in networks produced without organic solvents could be that TMPTMP is poorly soluble in both triethylamine and water, and therefore is not exposed to the oxidative aqueous phase at the same rate as the DODT monomer. Ethyl acetate was added to solubilize TMPTMP, DODT and triethylamine without being miscible with water. Tetrahydrofuran was added as a compatibilizer that allowed the organic and aqueous hydrogen peroxide to mix slowly. This mix of solvents produced two phases: an organic emulsion and an aqueous phase. This apparently slowed down the reaction, in comparison with the DODT homopolymerization. The slowed reaction time lead to networks with a more uniform texture. Also, it was found that decreasing the concentration of triethylamine from 2:1 molar ratio used in the homo- and copolymerizations of DODT to 1:1 molar ratio, improved the homogeneity of the networks.

A relatively good solid network was synthesized by first mixing DODT, TMPTMP and triethylamine in a 3:5 THF: ethyl acetate solution (Table 4.4.1. N-4). To the solution, 25 mL of H₂O₂ was added and air was bubbled into the mixture. Final

concentration of the DODT, TMPTMP, triethylamine and H₂O₂ were 0.34 M, 0.002 M, 0.34 M and 0.60 M respectively if a homogeneous system is assumed. The DODT-TMPTMP network had a conversion of 59.3% (dry mass = 1.3550 g). The purified network was a solid rubbery disk which was slightly smaller in diameter than the reaction vessel. It also had several internal air pockets and crater-like wells in the surface.

DSC analysis of the network showed $T_g = -49.64^\circ\text{C}$. TGA of the network showed no mass loss before 100°C and 2 % mass loss at 233°C. The decomposition temperature calculated by Universal Analysis software was 270.25°C. A 1 mg sample of the same network was soaked in DI H₂O for 4 hrs, patted dry and analyzed again by TGA. The sample was more white and opaque than before soaking. The TGA trace displayed 2.24% mass loss before 100°C. The decomposition temperature as calculated by the software was 269.71°C. Based on these data, poly(DODT) network shows displays thermal properties nearly identical to the uncrosslinked polymer. Like the polymer it is also relatively hydrophobic. Opacity of the water-soaked sample and mass-loss before 100°C seen in TGA are most likely the result of adsorbed water.

4.4.2. Method optimization for network synthesis

The optimized method for DODT network synthesis was similar to the method described in 4.4.1. It was found that mixing DODT and triethylamine in a 1:1 molar ratio produced the most homogeneous networks. It was found in mechanistic studies of DODT homopolymerization that about a 2:1 molar ratio was needed to activate the two -SH groups of DODT and bring them into the aqueous phase where they were subsequently oxidized. In the network synthesis, 1:1 molar ratio allowed only some of the DODT and

TMPTMP units to be activated by triethylamine. After the activated thiolate anions formed disulfide bonds, the triethylamine was released to activate thiol groups in the remaining DODT and TMPTMP. In this way, the rate of the disulfide coupling reaction was further decreased which appears to improve the homogeneity of the resulting network.

It was also found that the mix of THF and EtOAc was necessary for synthesizing internally flawless networks. Another important factor in preventing two networks from forming in the same reaction vessel (at the top and bottom of the vessel) was to keep the vial capped during the reaction, this prevented a second, film-like network from forming at the air interface. In combining these three factors, the optimized method created networks with a uniform relatively texture.

In the optimized method of DODT network synthesis, stock solutions of TMPTMP with DODT and triethylamine were prepared for each crosslinker ratio. The reagents and organic solvents were added to each reaction vessel before adding aqueous H₂O₂ and capping the vials. After shaking the vials, the final concentration of each reagent in the network synthesis reactions is listed in Table 4.26. The concentrations were calculated assuming a homogeneous system, however it is important to note that two phases (organic emulsion and aqueous) formed in the reaction system. Using the optimized system, the polymer network formed in the organic phase.

The network synthesis was performed in two different scales. The small scale reactions were made in 4 mL vials, and the total volume the reactions was 3.83 mL. The large scale reactions were performed in 20 mL glass vials, and the total reaction volume was 16.54 mL. Because the reaction depends on the mixing of the two phases, the ratio

of phase volume to interfacial area is critical. The reaction vials were selected because they maintained the approximate volume dimensions between each scale reaction. Ratio of cross sectional area (circular) to volume (cylindrical) for the small scale reaction was 1:33.86, and the same ratio for the large scale reaction was 1:33.81. The total solution height in each scale was approximately 34 mm and the approximate depth of THF was approximately 4.4 mm. Because THF was added as a compatibilizer between the organic and aqueous phases, care was taken to maintain the same ratio of the dimensions (height(or depth) and area). A large-scale 6:1 ratio network was not synthesized.

Table 4.4.3. Final concentration of reagents in small and large scale network synthesis.

DODT:TMPTMP	Rxn Scale	[TMPTMP] (mol/L)	[DODT] (mol/L)	[Et ₃ N] (mol/L)	[H ₂ O ₂] (mol/L)
6:1	Small	0.072	0.431	0.431	0.460
	Large	---	---	---	---
25:1	Small	0.018	0.431	0.431	0.460
	Large	0.018	0.433	0.433	0.458
50:1	Small	0.008	0.431	0.431	0.460
	Large	0.008	0.433	0.433	0.458
100:1	Small	0.004	0.431	0.431	0.460
	Large	0.004	0.433	0.433	0.458

In all trials the network with the lowest concentration of crosslinker, also had the lowest % conversion. The optimized method required reaction times of 96 hours or more to ensure higher than 50% of the theoretical monomer conversion. Reaction time was particularly important for the networks which had low TMPTMP concentration, and four days reaction time was needed for these networks to retain their shape after purification.

Table 4.4.4. Results from a series of networks made using optimized method.

DODT:TMPTMP	% Conversion		
	Small-Scale		Large-scale
	3 days	4 days	3 days
6:1	68%	76%	n/a
25:1	62%	81%	68%
50:1	62%	66%	67%
100:1	47%	65%	55%

The networks formed in the organic-rich layer of the vial. The depth of the network in the vial decreased with decreasing TMPTMP concentration and the bottom of the surface of the network in the reaction vial was convex. During synthesis, the opacity of the network also increased with increasing TMPTMP concentration (Figure 4.4.2). The figure also shows that small beads of DODT network formed at the bottom of the vials with the highest concentration of crosslinker (A, B).

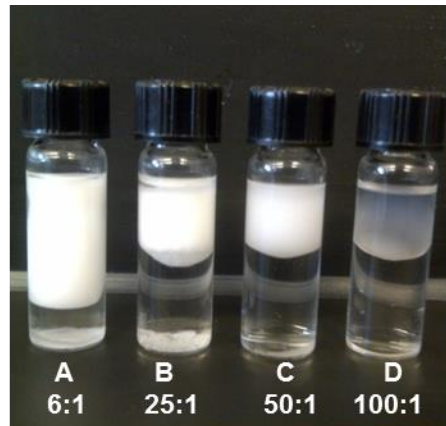


Figure 4.4.2. Small-scale networks at 72 hrs reaction time (in order of decreasing [TMPTMP]).

During the purification processes macroscopic flaws, like internal bubbles or fissures, could be seen because the networks became either translucent, for 1:6 recipe (A), or transparent, for 1:100 recipe (D). The figure below (Figure 4.4.3) shows the networks recovered from the vials in Figure 4.4.2 soaking in acetone. The bubbles which formed at the bottom of the 1:25 network were made more prominent in the swollen state as can be seen in Figure 4.4.3. In acetone, the networks all nearly doubled in volume and became more translucent.

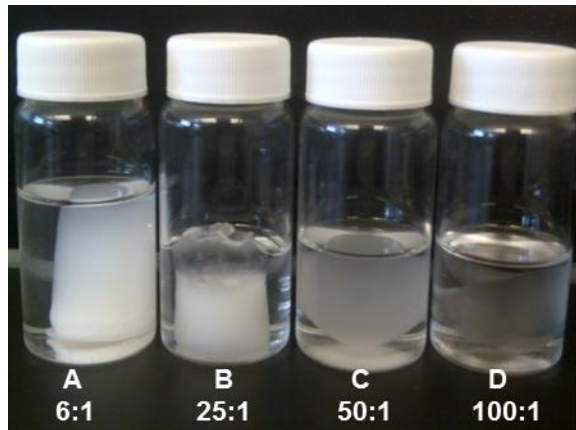


Figure 4.4.3. Small-scale networks extracting in acetone (in order of decreasing [TMTMP]).

The second step of purification (extraction in THF) was intended to extract any non-crosslinked DODT polymers, which are highly soluble in THF. THF swells the networks to several times their original volume. Both the small and large scale 1:100 networks swelled larger than their containers in THF, the larger networks were moved to different containers. Figure 4.4.4 shows the THF-swollen large-scale networks. Figure 4.4.5 shows the dry large-scale networks. The reaction time for the networks in Figures

4.4.4 and 4.4.5 was 3 days. The 100:1 network became flat and with an irregular shape after the second purification step. The 25:1 and 50:1 networks retained their shape.

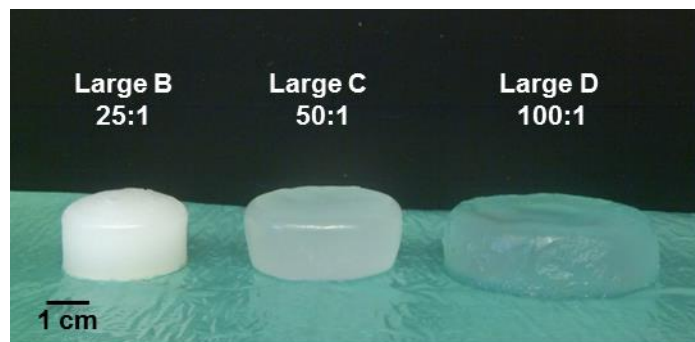


Figure 4.4.4. Large-scale networks swollen with THF.

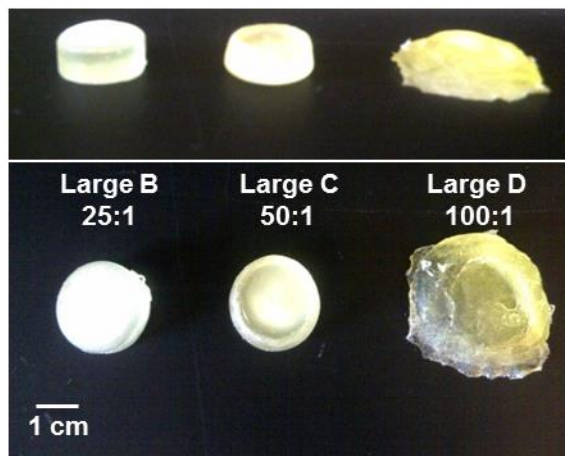


Figure 4.4.5. Large-scale networks are shown after purification and drying.

The NMR spectra of the a poly(DODT) network was acquired by swelling a 50:1 network to equilibrium in deuterated solvent (deuterated THF).(ER-242) The ^1H NMR spectrum shows three peaks which correspond to the poly(DODT) units (Figure 4.4.6). In THF their shifts have changed, but their positions relative to one another are consistent with poly(DODT). The sulfur adjacent protons (C) appear at 4.80 ppm. Peaks from the

central methylene protons (A) and the oxygen adjacent protons (B) still appear close to one another at 5.49 ppm and 5.60 ppm , respectively. Peaks at 4.36 ppm and 3.62 ppm most likely arise from THF in the deuterated solvent. Other peaks were too broad and too small to be confidently assigned. While the semi-solid state caused large signal broadening in the ^1H NMR spectrum (Figure 4.4.6), the ^{13}C spectrum (Figure 4.4.7) shows three well defined peaks corresponding to the DODT units in the networks sample. Peaks at 71.24 ppm, 70.49 ppm and 39.71 ppm) follow the same assignments described previously for poly (DODT) (Section 4.1).

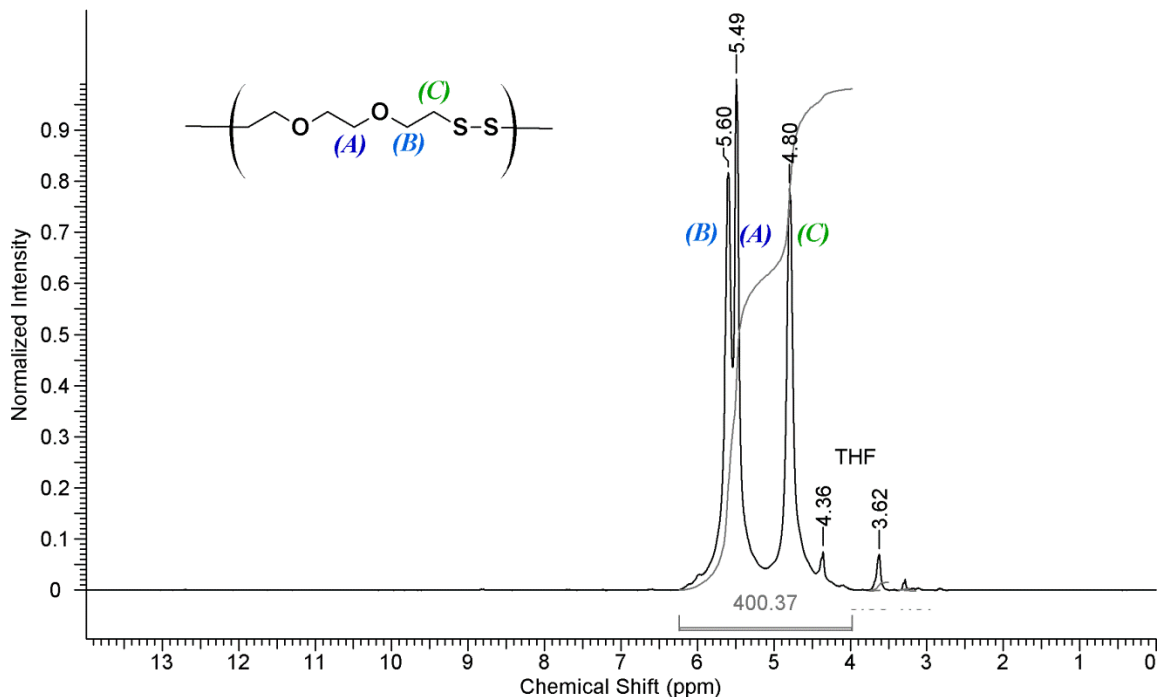


Figure 4.4.6. ^1H NMR spectrum of swollen poly(DODT) network with 50:1 crosslinker ratio (10 s relax; 128 trans.; THF- d_8 ; 300 MHz;).

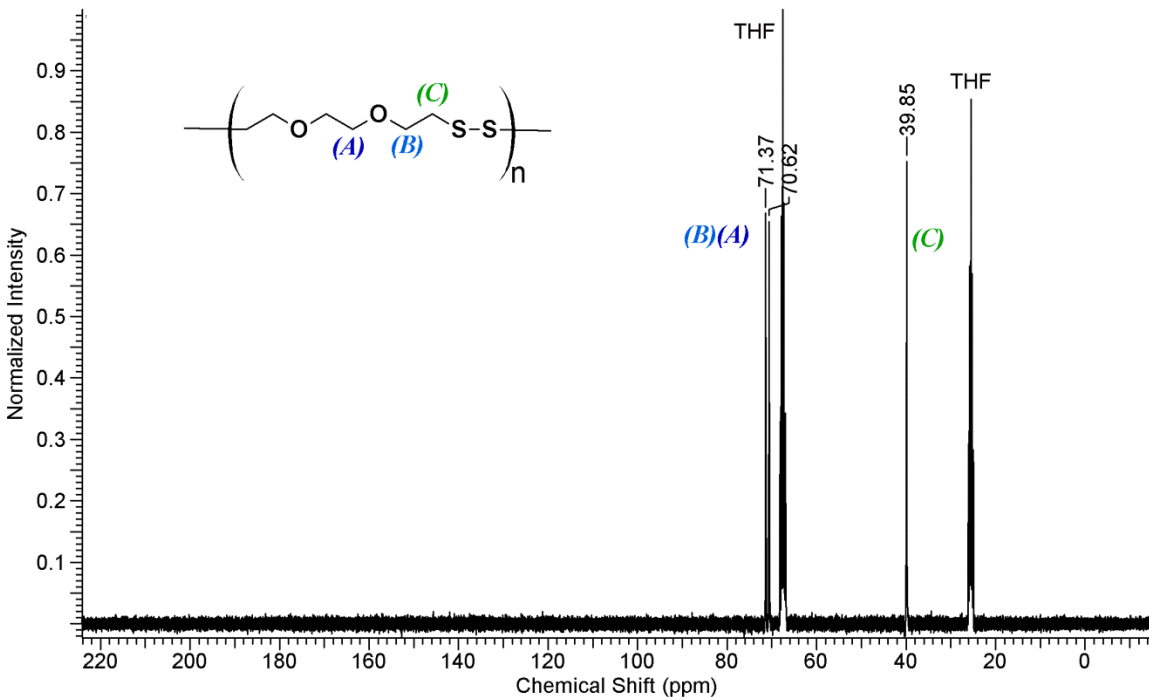


Figure 4.4.7. ^{13}C NMR spectrum of swollen poly(DODT) network with 50:1 crosslinker ratio. (THF-d₈; 300 MHz; 6 s relax; 4096 trans.)

Networks with higher crosslinker ratio (6:1 and 25:1) did not swell sufficiently for NMR using this method. Because the 50:1 network did not show strong peaks useful to elucidating the network structure, the 100:1 network was not analyzed by this method in the gel state. Instead, the ^{13}C NMR of the 100:1 network in the solid state was run. The spectrum displayed the 3 peaks characteristic of poly(DODT). Figure 4.4.8 shows the solid state spectrum of the 100:1 network.

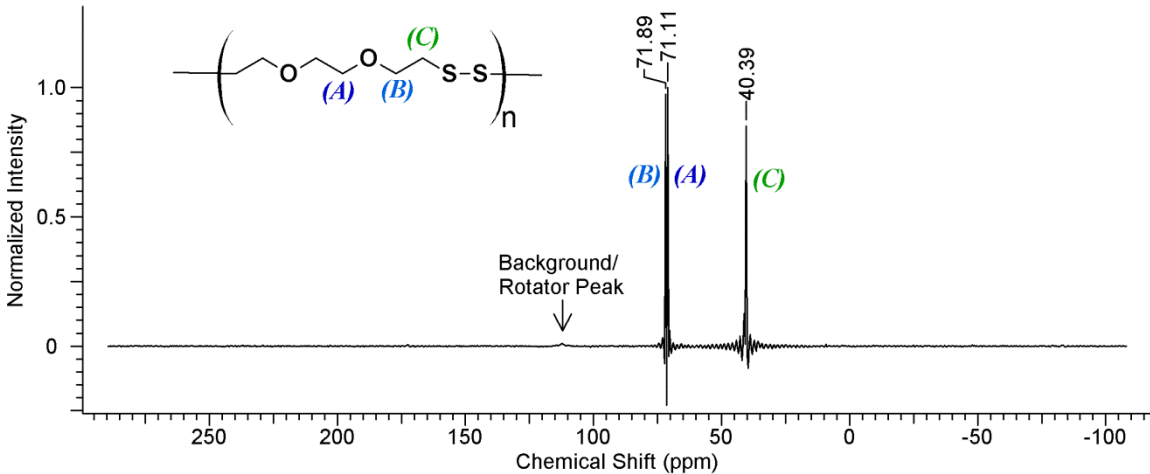


Figure 4.4.8. Solid-state, ^{13}C NMR of 100:1 network (1024 s; 400 MHz)

Diffuse reflectance infrared Fourier transform spectroscopy (DRIFTS) was used to compare the networks with 1:6 and 1:100 crosslinker ratios, and the spectra are shown in Figure 4.4.9. Because spectra collected from DRIFTS are significantly different from those collected from FTIR, a network with a 1:1 ratio was synthesized and analyzed in DRIFTS in order to elucidate peaks corresponding to the TMPTMP crosslinker (shown in grey, Figure 4.4.9). All spectra showed a broad band around 3000 cm^{-1} that is characteristic of C-H stretching. The strong peak at 1146 cm^{-1} (**a**) in the 1:1 network spectrum corresponds to the $\text{CH}_2-\text{C(O)-O}$ from the ester groups in TMPTMP. This signal appeared as a weaker band in the two other spectra as well. The band which appears between 1734 and 1745 cm^{-1} (**b**) corresponds to the carbonyl (C=O) stretch from TMPTMP. A shoulder at 1773 cm^{-1} (**c**) is only visible in the 1:100 network spectrum and originates from the ether bond stretching of DODT. Another band at 1930 cm^{-1} (**d**) is stronger in the 1:100 network spectrum, but its origin is unclear and may be an artifact of the uneven sample surface. Importantly, there are no sharp bands seen near 2552 cm^{-1} that would indicate S-H stretching.

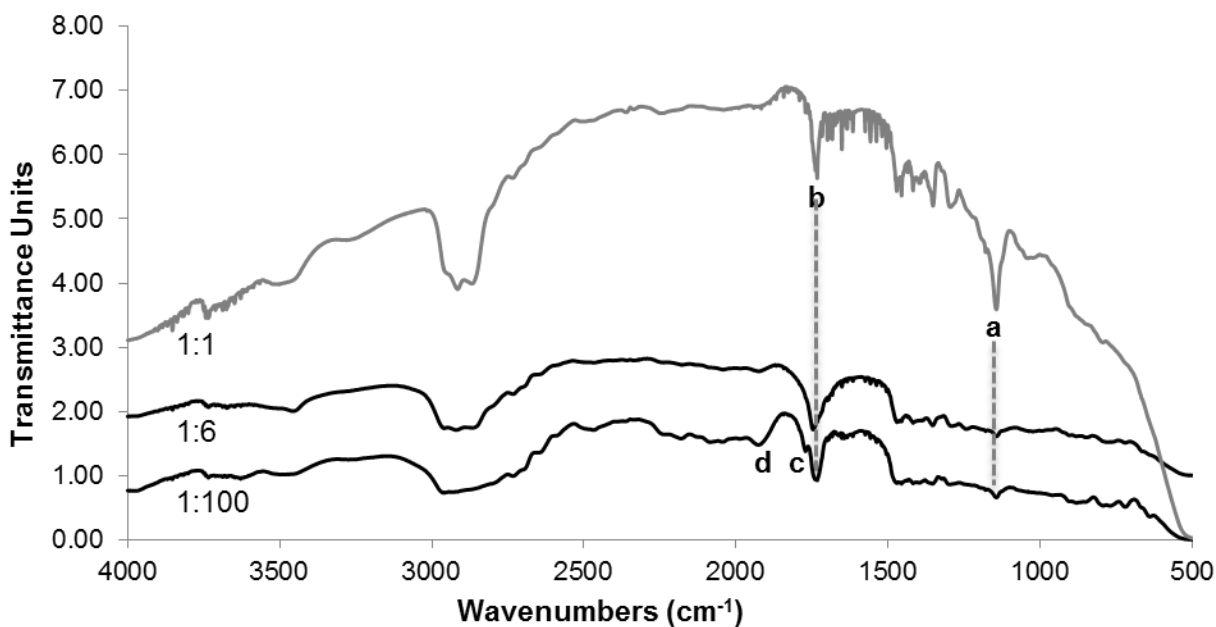


Figure 4.4.9. DRIFTS spectra for three networks with three different crosslinker ratios.

4.4.3. Swelling and crosslink density

The DODT networks were swollen in a range of organic solvents including, acetone, THF and chloroform. However they did not swell in hexane, nor did they swell in water. Figures 4.4.10 and Figures 4.4.11 show the percent mass gain and propagated error calculated from mass measurements for each network in THF and DI H₂O respectively. The equations used for error propagation are shown in Equations 4.2 and 4.4. The was used in calculate the propagated error. Each initial dry mass (m_I) measurement was assumed to have an uncertainty (σ_I) of ± 0.0002 g which was based on the precision of the analytical balance. The standard deviation of averaged swollen mass measurements was used for the uncertainty of swollen measurements (σ_S). Covariance terms were taken to be zero.⁹⁷

$$mass\ gain = m_g = m_s - m_l \quad \text{Eq. 4.1}$$

$$error_{mass\ gain} = \sigma_g \approx \sqrt{m_l^2 \sigma_l^2 + m_s^2 \sigma_s^2} \quad \text{Eq. 4.2}$$

$$\% gain = \left(\frac{m_g}{m_l} \right) * 100 \quad \text{Eq. 4.3}$$

$$error_{\% gain} = \sigma_{\% g} \approx \frac{m_g}{m_l} \sqrt{\left(\frac{\sigma_g}{m_g} \right)^2 + \left(\frac{\sigma_l}{m_l} \right)^2} \quad \text{Eq. 4.4}$$

The numerical data is presented in Table 4.4.6 and Table 4.4.7. All network samples swelled over 300% in THF. The sample with the highest DODT to crosslinker ratio (100:1) swelled the most with 463% mass gain, while the 25:1 and 6:1 showed similar swelling at with 320% and 312% mass gain. The greatest water uptake was seen in the 6:1 sample with 9% mass gain. The uptake in the other samples was about 1% and is less than the calculated propagated error value. The error bar values were calculated using the error propagation.

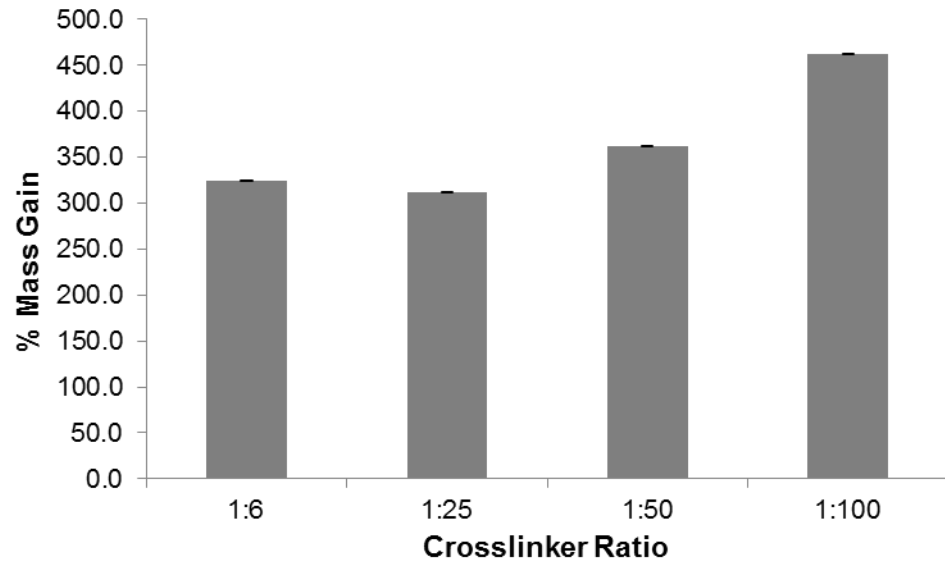


Figure 4.4.10. Mass gain for networks swollen in THF (error bars are propagated error values).

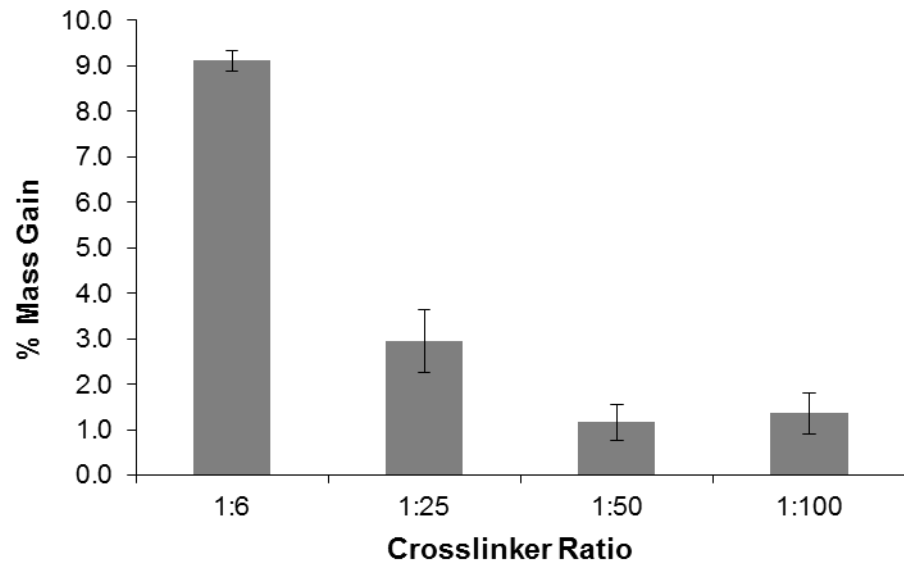


Figure 4.4.11. Mass gain for networks swollen in DI H₂O (error bars are propagated error values).

Table 4.4.5. Results from THF swelling study using small samples from optimized recipe.

DODT:TMPTMP	Initial Mass (g)	Swollen Mass (Average of 5) (g)	Mass Gain (g)	% Mass Gain	Calculated Propagated Error
A 6:1	0.0539	0.2286	0.1747	324.2 %	1.0 %
B 25:1	0.0471	0.1941	0.1470	312.1%	1.0 %
C 50:1	0.0664	0.3065	0.2401	361.5 %	0.6 %
D 100:1	0.0558	0.3140	0.2582	462.8 %	0.6 %

Table 4.4.6. Results from DI H₂O swelling study using small optimized samples.

DODT:TMPTMP	Initial Mass (g)	Swollen Mass (Average of 5) (g)	Mass Gain (g)	% Mass Gain	Calculated Propagated Error
A 6:1	0.1001	0.1092	0.0091	9.1%	0.2 %
B 25:1	0.0556	0.0572	0.0016	2.9%	0.7 %
C 50:1	0.0671	0.0679	0.0008	1.2%	0.4 %
D 100:1	0.0589	0.0597	0.0008	1.4%	0.5 %

THF was a good swelling solvent for the networks, and THF-swollen networks were used to calculate the M_n between crosslinks (or M_c). The solubility parameter (δ_p) for poly(DODT) was calculated using Eq. 2.4. Three well-known researchers have published molar attraction constants for chemical groups (Small, Hoy and van Krevelen).^{45,46,44} The total for a DODT repeat unit was calculated using each of their parameters. Table 4.4.7 lists each group and its contribution according to Small, Hoy or van Krevelen.

Table 4.4.7. Group molar attraction constants (F) and DODT repeat unit molar attraction constant.

Group	F (MPa ^{1/2} •cm ³ •mol ⁻¹)			No. of groups per unit	ΣF (MPa ^{1/2} •cm ³ •mol ⁻¹)		
	F _{Small}	F _{Hoy}	F _{van Krevelen}		Small	Hoy	van Krevelen
-CH ₂ -	272	269	280	6	1632	1614	1680
-O-	143	235	256	2	286	470	512
-S-S-	920	856	920	1	920	856	920
DODT Totals:					2838	2940	3112

The molar volume may also be calculated using a group contribution method,⁴⁵ or it can be determined by dividing the molar mass by the density of the compound. Because the density of poly(DODT) was determined experimentally, the molar volume was calculated both ways. The two methods gave similar results (Table 4.4.8). The solubility parameter was then calculated for a poly(DODT) repeat unit in all 6 possible combinations of ΣF and V. The values were all within a reasonable variation of each other, and the average value was 19.01 ± 1.11 MPa^{1/2}. Another experimental method of estimating the solubility parameter is to swell a crosslinked polymer in a variety of solvents and use the solubility parameter of the solvent in which it swells the most. The solubility parameter of THF (a good solvent for poly(DODT)) is 19.4 MPa^{1/2} and agrees well with our estimated value for poly(DODT).

Table 4.4.8. Solubility parameter (δ) calculated 6 different ways for the poly(DODT) repeat unit.

Molar Volume		δ (MPa) ^{1/2}		
(cm ³ •mol ⁻¹)		ΣF Small	ΣF Hoy	ΣF van Krevelen
V	150.22	18.89	19.57	20.72
V _m	161.84	17.54	18.17	19.23

From the solubility parameters, χ was calculated using Eq. 2.3. Because the solvent and polymer are so similar, the entropic term (0.34) dominates the value of the interaction parameter, χ . The calculated value of χ was 0.34001. The calculated average molecular weight between crosslinks (M_c) values are displayed in Table 4.4.9. The networks with 6:1 and 25:1 DODT:TMPTMP ratio had very similar M_c values of approximately 3,700 g/mol, while the largest M_c (7,200 g/mol) was derived from the polymer with the largest monomer to crosslinker ratio (100:1).

Table 4.4.9. M_c calculated from Flory-Rehner Equation (Chapter 2, Eq. 2.1).

Crosslinker Ratio	DODT
A 6:1	3,867 g/mol
B 25:1	3,618 g/mol
C 50:1	4,684 g/mol
D 100:1	7,232 g/mol

Knowing the M_c, the natural question is: What would M_n and M_w be if no crosslinker were added? To answer this question, DODT homopolymer was synthesized under the same conditions as the networks (1:1 DODT:triethylamine ratio; with THF and ethyl acetate). As the DODT polymerization progressed in the top organic emulsion layer

of the reaction, a droplet began to grow and hang from the top layer polymer product. Eventually, this droplet fell and formed an oblong bead at the bottom of the reaction vial (Figure 4.4.12). After 4 days, the two polymers were soaked separately in acetone and dried in a vacuum oven.

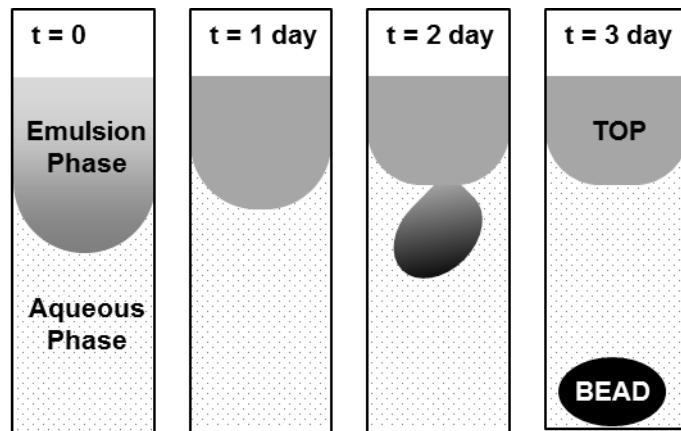


Figure 4.4.12. Cartoon of DODT polymerization with organic solvent mixture used in network synthesis.

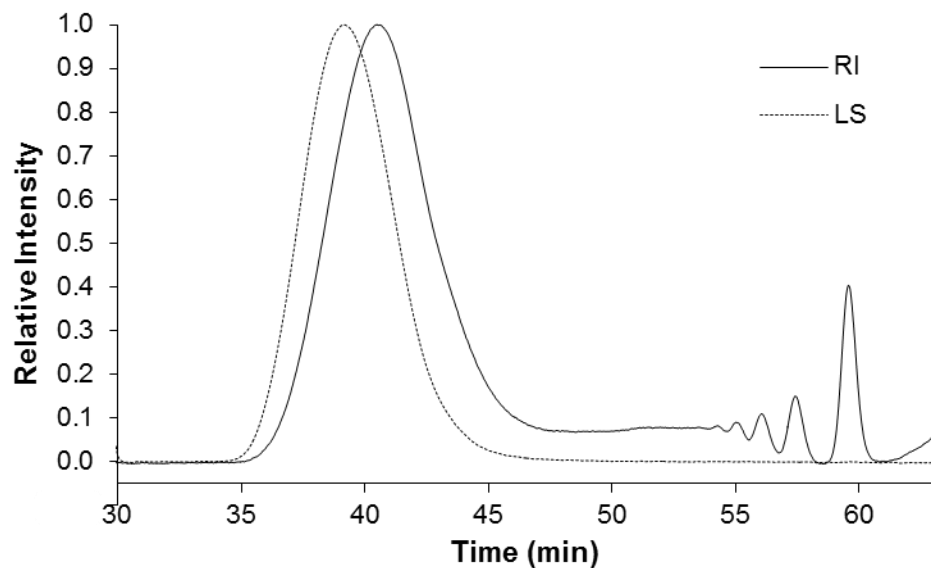


Figure 4.4.13. RI and LS traces from poly(DODT) polymer sample Top.

Table 4.4.11. SEC results for poly(DODT) using network system without TMPTMP.

Sample	M_n	M_w	M_n/M_w	R_{gz} (nm)	R_{hw} (nm)	$[\eta]_w$ (mL/g)
Top	85,400	163,000	2.00	21.2	12.4	87.5
Bead	103,500	199,500	1.93	26.7	14.1	102.6

The dry samples were analyzed by SEC. Both samples displayed about the same molecular weight distribution of 1.9-2.0, which slightly elevated over what has been observed in the polymerization system without the addition of organic solvents. The SEC results are shown in Table 4.4.11. The bead had somewhat higher M_n (103,500 g/mol) than the polymer in the top layer (85,400 g/mol). The low molecular weight fraction of the sample shows peaks at 59.6 min, 57.4 min, 56.1 min and 54.3 min. Their estimated peak molecular weights are 150 g/mol, 340 g/mol, 550 g/mol and 1060 g/mol respectively, corresponding to cyclic oligomers as seen in MALDI-ToF analysis. The M_n of the high molecular weight fraction in both samples is less than the M_n from 2 hr reaction 10-120-55.

The proton and carbon NMR spectra are shown in Figures 4.4.14 and 4.4.15 respectively. The 1H NMR spectrum shows the three peaks characteristic of poly(DODT) at 3.75 ppm (**b**; triplet), 3.64 ppm (**a**; singlet) and 2.90 ppm (**c**; triplet). In addition to these peaks, there is a small singlet signal at 3.67 ppm and a small triplet signal at 2.97 ppm. Part of a peak is visible at 3.78 ppm, and a very small triplet peak is seen at 1.25 ppm. In the ^{13}C NMR, strong peaks characteristic of poly(DODT) appear at 70.35 ppm (B), 69.68 ppm (A) and 38.41 ppm (C). Small peaks near to the characteristic peak are seen at 70.48 ppm, 69.55 ppm, 39.19 ppm; 38.81 ppm and 38.65 ppm (very small).

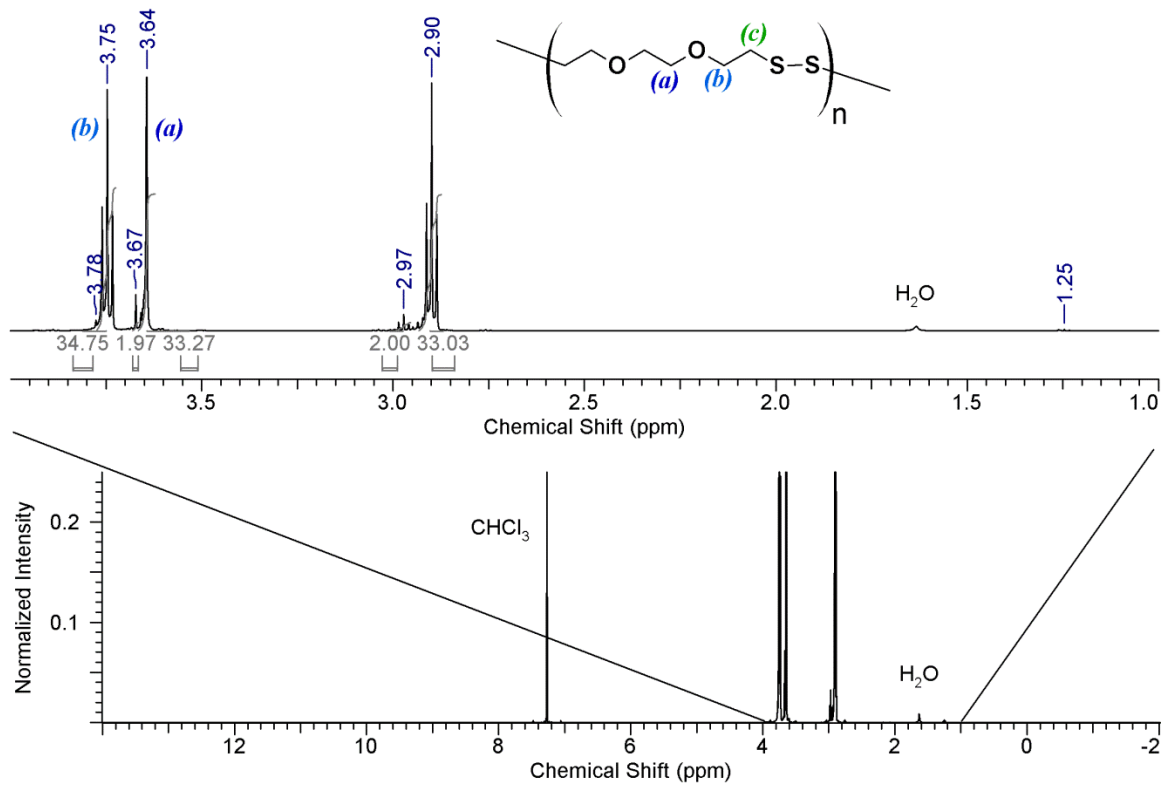


Figure 4.4.14. ^1H NMR of Top polymer sample (12 s relax.; 128 trans.; 500 MHz; CDCl_3)

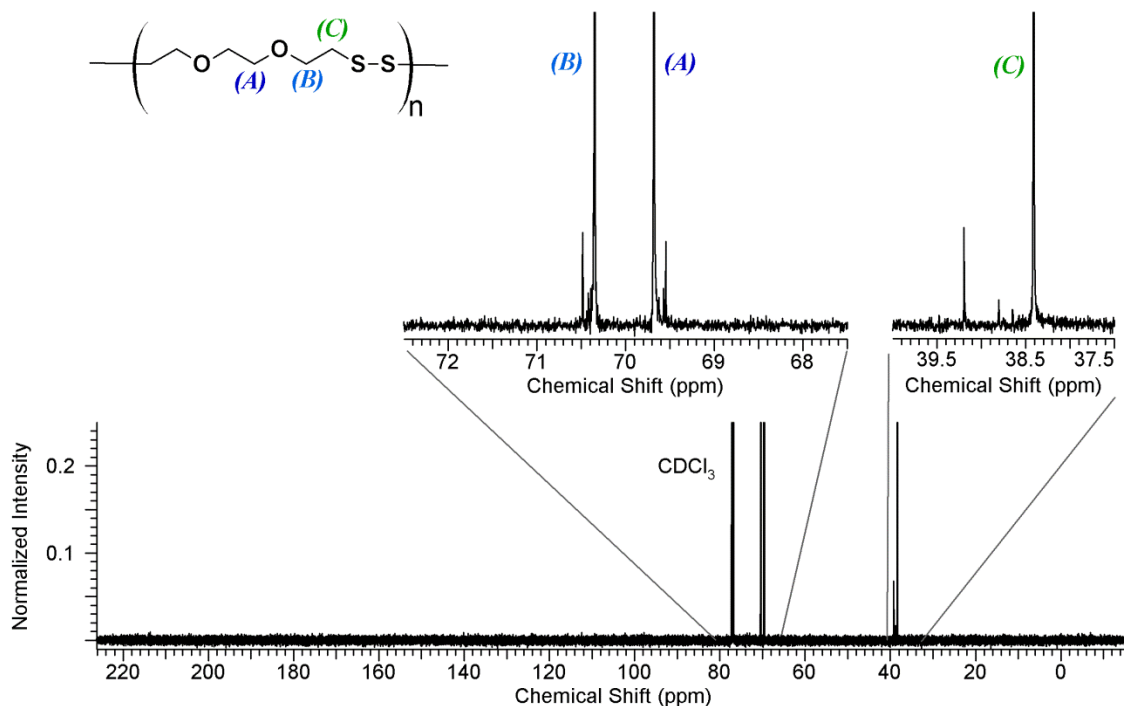


Figure 4.4.15. ^{13}C NMR of Top polymer sample (1 s relax.; 1024 trans.; 500 MHz; CDCl_3)

The spectra do not indicate the presence of thiol groups, as there is no peak in the ^{13}C spectra near 24 ppm. The origin of the smaller peaks may be from the high concentration of oligomers in the sample. Cyclic oligomers, particularly dimers, may show slightly different shifts from the polymers. Additionally, it should be noted that because these reactions were performed in capped vials, it is very likely that glue or wax in the vial cap began to degrade after 4 days in contact with THF, ethyl acetate and triethylamine.

4.4.4. Reduction of DODT networks

4.4.4.1. Dithiothreitol

A 100:1 network sample exposed to 50 mM dithiothreitol (DTT) solution in THF degraded completely within 48 hrs. Unlike poly(DODT) which degraded back to its monomeric form when exposed to DTT in a solution of THF *and* H₂O, the network exposed to DTT/THF/H₂O solution for one week did not degrade but instead swelled slightly.

4.4.4.2 Aqueous environments

The networks were tested for degradation in a range of aqueous environments. Samples soaked in 50 mM glutathione buffer solution (pH = 5.2) at 37°C were weighed twice a week for 6 weeks. Acetate buffer was used to mimic lysosomal conditions and to prevent base-catalyzed glutathione (GSH) oxidation to oxidized glutathione (GSSG). To a series of 4 vials, 3.0 mL of the GSH solution was added followed by the network sample. The samples became opaque white, as seen in the water-swelling studies, but no significant change in mass was observed. Table 4.4.11 shows three example measurements from the experiment and the dry mass of the sample after 42 days of exposure to GSH. Very little mass losses were observed.

Table 4.4.11. Results from GSH (Aq) degradation in acidic buffer (pH = 5.2).

Sample	Initial Dry Mass (g)	Swollen Mass (g)			Final Dry Mass (g)	% Difference
		11 days	14 days	42 days		
1:6	0.1001	0.1019	0.1018	0.1009	---	---
1:25	0.0556	0.0563	0.0563	0.0562	0.0549	-1.26%
1:50	0.0671	0.0676	0.0676	0.0676	0.0661	-1.49%
1:100	0.0589	0.0599	0.0598	0.0600	0.0583	-1.02%

To model conditions in the digestive system, networks were exposed to three different solutions at 37°C. An aqueous solution of HCl with pH = 2.09 was used to model the stomach conditions and two aqueous mixtures of bile acids with concentrations of 4.15 mg/mL (pH = 7.23) and 200 mg/mL (pH = 6.50) were used model conditions in the small intestines. Average bile salt concentration in contents of the duodenum (gut immediately following stomach) and jejunum (small intestines) after a standard meal is about 4.15 mg/mL(REA-45) but varies depending on the health of the patient. A network sample with a 1:50 crosslink ratio was selected for testing in all three solutions. After 5 days only the small mass gain attributed to water uptake was recorded. The samples in the bile salts solution did take on the brownish color of the solution and a tacky feel, but no change in shape or size was observed. Photographs of the networks before and after exposure to the bile salts are shown in Figure 4.4.16. Mass change results are listed in Table 4.4.12.

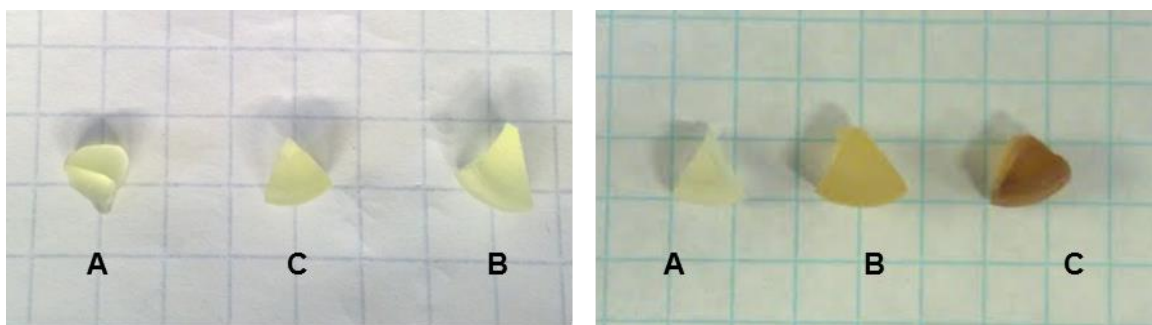


Figure 4.4.16. Network samples before and after exposure to HCl (A) and bile salt solutions (B = 4.5 mg/mL and C = 200 mg/mL).

Table 4.4.12. Results from poly(DODT) network exposure to digestive system models.

Digestive Model	Initial Mass (g)	Mass after 5 days 5 days exposure(g)	% Difference
Stomach (HCl; pH = 2)	0.0888	0.0906	2.03
Small Intestines (Bile salts; 4.15 mg/mL)	0.1597	0.1632	2.19
Small Intestines (Bile salts; 2% wt)	0.1161	0.1199	3.27

The complete degradation of the network in DTT/THF verified THF that the networks are connected by disulfide bonds and may be degraded under reductive conditions. However, under acidic aqueous conditions, including those containing a disulfide reducing agent (GSH), the networks are stable within the time tested. While a change in the appearance of the networks was observed, but it did not translate into significant mass change. In fact, the change in color when exposed to bile salts suggests that the salts are penetrating into the network even if little water is able to do so. A slow rate of water intrusion into the networks indicates that they might eventually degrade following a surface eroding mechanism. While not ideal for an oral drug delivery

system, they merit further investigation as a flexible implant designed to degrade over years.

4.4.5. Effect of Sodium Pyrophosphate on Network Conversion

A network series was synthesized according to the optimized method except that a freshly prepared 0.110 M solution of $\text{Na}_4\text{P}_2\text{O}_7$ in H_2O_2 (Aq; 3% by wt) was used in place of H_2O_2 alone because sodium pyrophosphate has been shown to stabilize solutions of H_2O_2 .[ER-234] Figure 4.4.17 compares the conversions of networks synthesized with and without sodium pyrophosphate at 4 days.

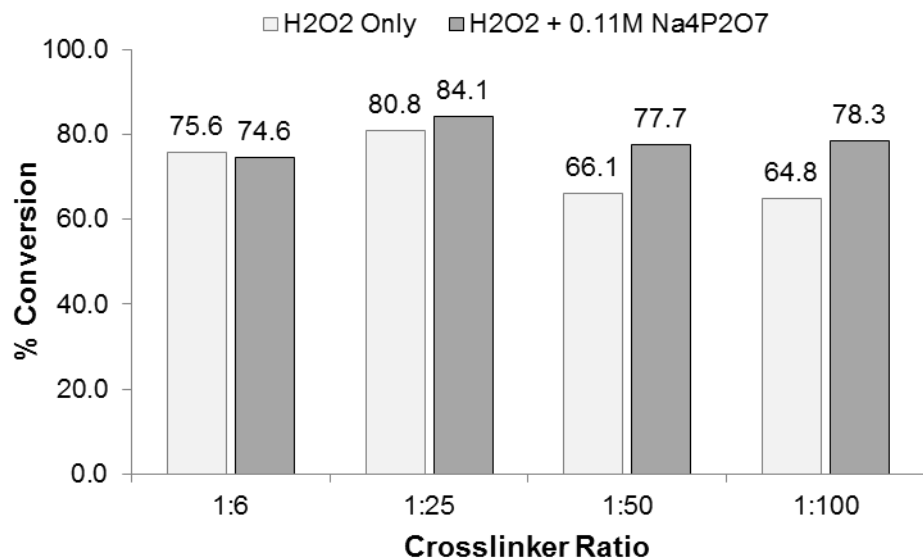


Figure 4.4.17. Network conversions at 4 days with and without sodium pyrophosphate.

The addition of $\text{Na}_4\text{P}_2\text{O}_7$ had no significant effect on the conversion of networks with 6:1 or 25:1 DODT:TMPTMP ratios, but did improve the conversion for samples with 50:1 and 100:1 monomer to crosslinker ratios.

Network conversion with time was studied using the same 0.110 M Na₄P₂O₇/H₂O₂ solution. A series of network samples were prepared with a 1:25 crosslinker ratio. At specified times, the reactions were stopped by removing the networks from the reaction vial and soaking them in acetone for 4 days. The networks were then dried and massed before soaking in THF for an additional 4 days and drying again. A plot of the network reaction conversion with time is shown in Figure 4.58. After one day of reaction time over 60% conversion was reached. The conversion continued to slowly increase for the next 3 days and only increased 4% over the next four days. The final conversion after 8 days was 90.6%. Because Na₄P₂O₇ has little effect on network conversion with 25:1 DODT:TMPTMP ratio, we believe that a similar time v. conversion plot would be observed for H₂O₂ solution alone. Additionally, the conversion data is in good agreement with the previous observation that a reaction time of at least 4 days was required to make networks which maintained their shape after purification by swelling THF.

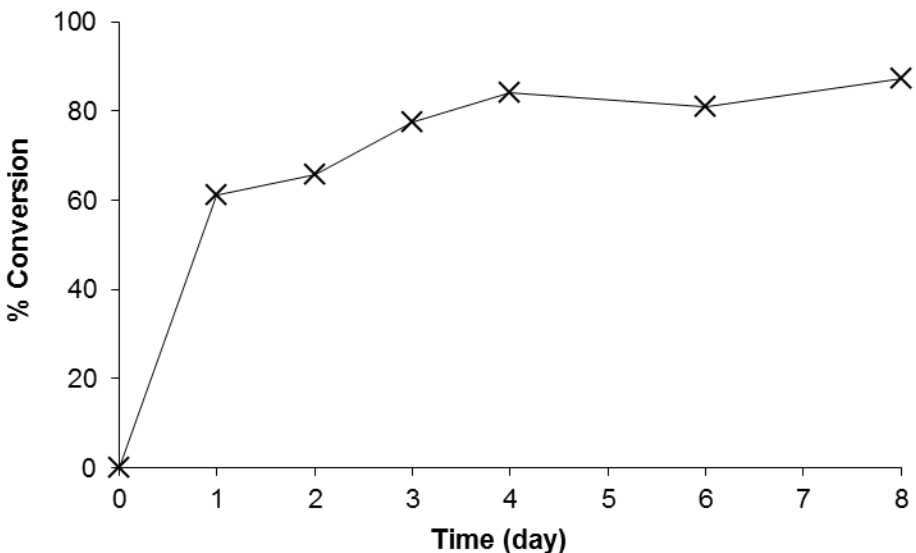


Figure 4.4.18. Poly(DODT) network conversion with time using the $\text{Na}_4\text{P}_2\text{O}_7/\text{H}_2\text{O}_2$ system.

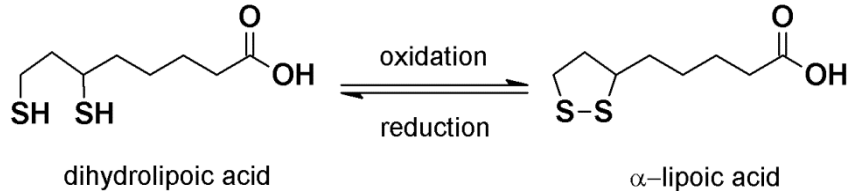
Poly(disulfide) polymer networks from DODT and TMPTMP were synthesized in a one-pot process. Conversions of up to 90% were reached after 8 days. Consistent, solid networks were formed after 4 days with conversions between 65% and 80%. The reaction proceeded in a two-phase system with an aqueous oxidizing phase and an organic rich emulsion phase. Empirically, we found that organic solvent mix which maintained a two phase system was needed to form consistent networks. Additionally we have observed that interfacial area compared to the depth of each phase plays an important role in synthesizing networks with a uniform texture.

The networks show a range of swelling characteristics and textures depending on reaction conditions. The networks swell well in THF, but do not swell well in H_2O . Networks which swelled the most in H_2O had the highest content of crosslinking agent, TMPTMP. It is thought that hydrophilicity of the ester groups present TMPTMP units

allow these samples to absorb more water. Degradation by DTT confirms the presence of disulfide bonds, yet the networks are resistant to degradation under a variety of biological conditions including acidic conditions, basic conditions and reducing conditions.

4.5. Polymerization of α -lipoic acid and synthesis of α -lipoic acid derivatives.

Dihydrolipoic acid is a natural dithiol biochemical (see Figure 4.5.1), and was identified as a potential, healthy monomer for our new oxidative polymerization method. However, the use of dihydrolipoic acid was impractical because its preferred state is the cyclized, oxidized form called α -lipoic acid. Instead, the cyclic disulfide, α -lipoic acid (α -LA), was explored as a healthy monomer for biodegradable poly(disulfide) polymers. Upon degradation, it is anticipated that polymer would return to its cyclic disulfide form, which is a necessary nutrient and powerful antioxidant.



Scheme 4.5.1. Redox pathway between dihydrolipoic acid and α -lipoic acid.

4.5.1. Characterization of α -lipoic acid (α -LA)

Two forms of α -LA are available commercially—the racemic mixture of enantiomers, (DL)- α -LA, and the *R* enantiomer, R- α -LA. The ^1H NMR spectra of the two compounds are compared in Figure 4.5.1

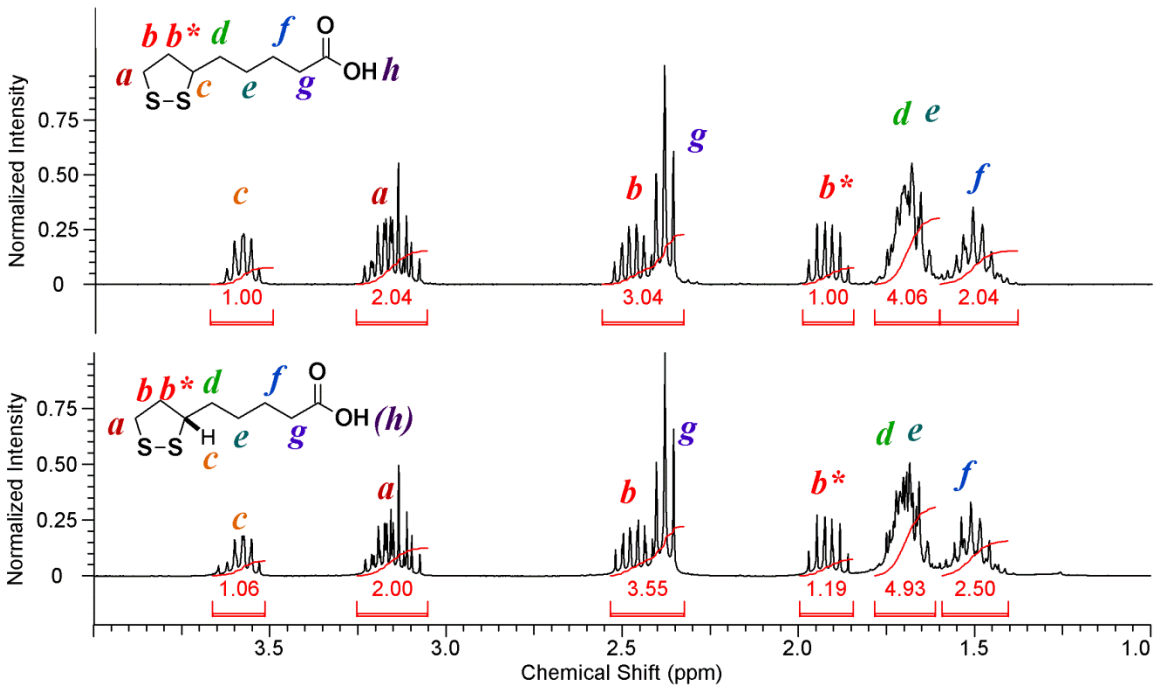


Figure 4.5.1. ^1H NMR spectra of DL- α -LA (top) and R- α -LA (bottom) (3s relax; 128 scans; 500 MHz; CDCl_3).

The acidic proton (*h*) was not seen in either spectrum. The signal of methylene protons adjacent to the carbonyl group (*g*) appears as a triplet because it is only split by two neighboring hydrogen atoms. Signals from the aliphatic hydrogens (*d,e,f*) displayed multiplet splitting patterns because they are affected by neighboring methylene protons and methylene neighbors once removed. The methyne proton signal (*c*) appears as a quintuplet because it is split by 4 neighboring hydrogen atoms. The signals from the diastereotopic methylene protons (*b* and *b**) in the thiolane ring appear at 2.45 and 1.92 ppm. Each displays quintuplet splitting pattern. The signal from the methylene group in the thiolane ring adjacent to the sulfur atom (*a*) appears as a multiplet and its splitting pattern is complicated by the two neighboring diastereotopic protons (*b/b**). Both spectra show the same peaks and splitting patterns, although the proton integrations

from the R-enantiomer deviate from what is predicted. It is possible that some impurities remain after recrystallization, for example R- α -LA dimers or trace amounts of the recrystallization solvents (hexanes and pentanes).

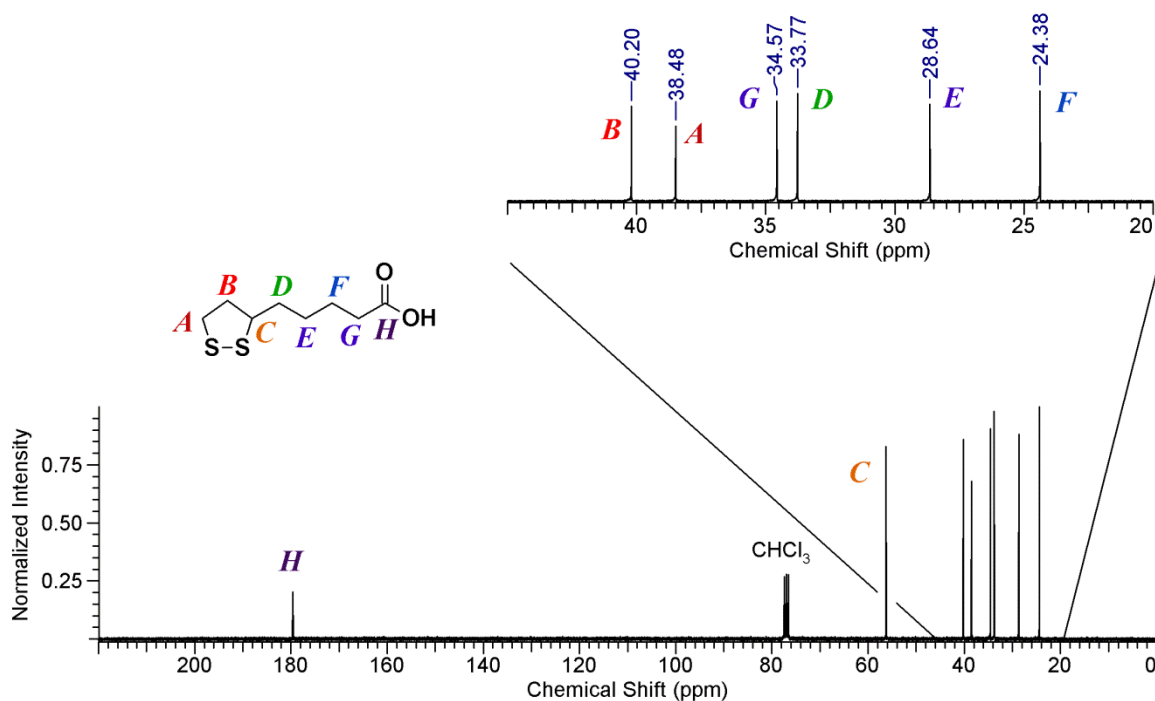


Figure 4.5.2. ^{13}C spectrum of R- α -LA (2s relax; 8192 scans; 500 MHz; CDCl_3 ;

The two forms of α -LA show the same ^{13}C NMR spectra. The ^{13}C NMR spectrum of the *R* enantiomer is shown in Figure 4.5.2. The carbonyl carbon signal from the highly de-shielded carboxylic acid group (*H*) appears at 179.59 ppm. The tertiary carbon (*C*) appears next at 56.26 ppm. Peaks corresponding to the two methylene carbons in the thiolane ring appear at 40.20 ppm (*B*) and 38.48 ppm (*A*). Farther up field the aliphatic carbon signals are seen starting with *G*, which is in the de-shielded α -position to the carbonyl, at 34.57 ppm. The most shielded aliphatic carbons (*E* and *F*) appear farthest upfield at 28.64 ppm and 24.38 ppm respectively.

In DSC thermal analysis, the two forms of α -LA were subjected to a heating cycle in which the two compounds (crystalline solids) were heated from 25°C to 105°C, cooled from 105°C to 25°C and heated again to 105°C at a rate of 2.5°C/min. It is known that thermal transitions in DSC measurements are rate dependent. A relatively slow heating/cooling rate was used in the analysis of R- α -LA and DL- α -LA so that differences between the two compounds would be more easily distinguished. In the first heating cycle the T_m was seen as a strong peak endothermic peak. The R- α -LA displayed a melting point onset of 47.35°C with a melting peak of 49.45°C, while DL- α -LA showed a melting point onset of 57.66°C with a melting peak of 60.61°C. The results are in good agreement with literature values for both compounds.⁸⁴ In the cooling cycle, neither compound displayed a crystallization peak, and neither compound displayed a T_m peak in the second heating cycle (Figure 4.5.3).

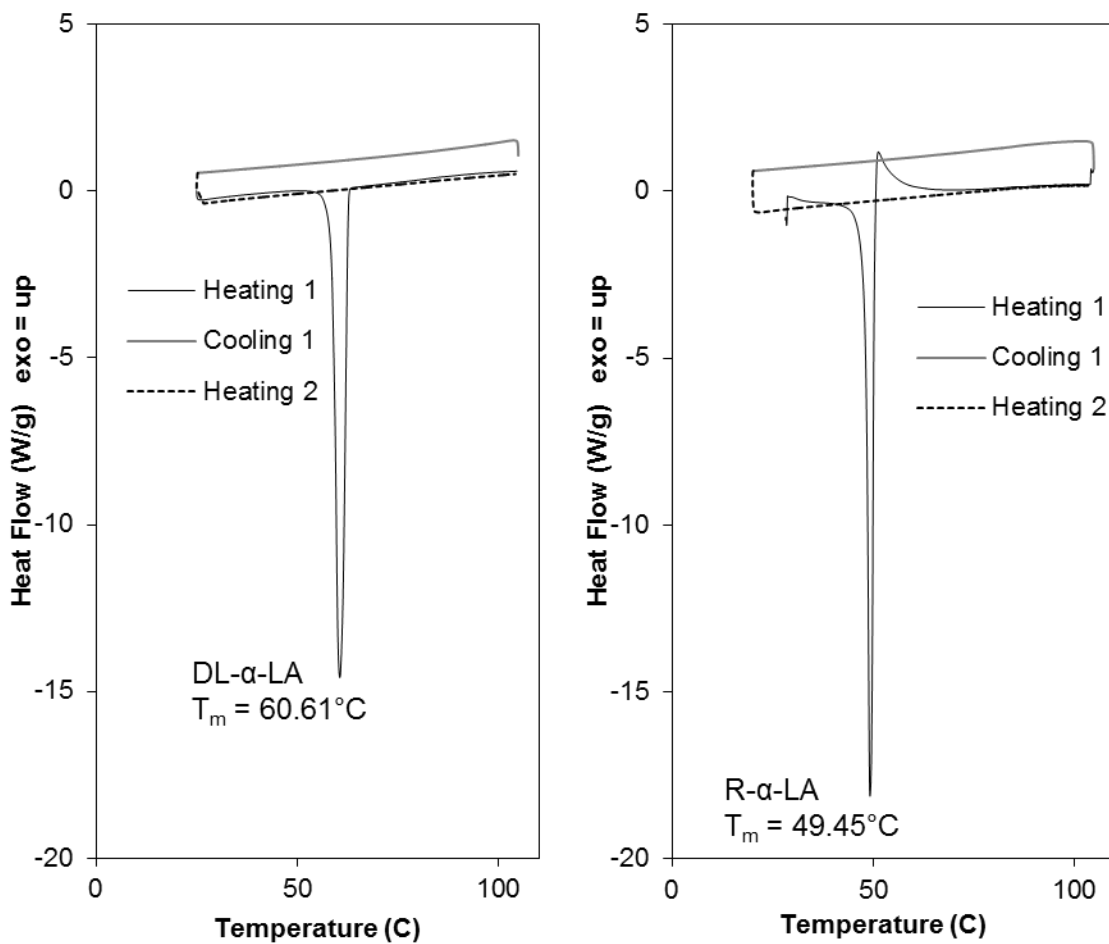


Figure 4.5.3. Full DSC heating cycles for DL- α -LA and R- α -LA; Heating rate: $2.5^\circ\text{C}/\text{min}$.

Table 4.5.1. Thermal transitions of R- α -LA and DL- α -LA.

		T_m ($^\circ\text{C}$)	
		Onset	Peak
DL- α -LA	1st Heating	57.66	60.61
	2nd Heating	n/a	n/a
R- α -LA	1st Heating	47.35	49.45
	2nd Heating	n/a	n/a

Thermal analysis of the two compounds shows that both compounds undergo a thermal polymerization reaction that eliminates the crystallinity of the polymers within

the range of analysis. From a biomaterials perspective, R- α -LA is the more interesting of the two compounds as it is naturally occurring.

4.5.2. Polymerization of α -LA

4.5.2.1. Polymerization of R- α -LA using triethylamine and H₂O₂.

R- α -LA was polymerized following the developed method for the oxidative polymerization of dithiols. First R- α -LA was added slowly to triethylamine and mixed. Because the monomer was a crystalline solid, instead of a liquid like DODT, DI H₂O was added to the triethylamine during the pre-mixing step to allow the mixture to stir. The mixture was a viscous liquid. Without the addition of water, the R- α -LA/triethylamine became a thick, gummy mass and the stir bar became immobilized. Aqueous H₂O₂ was then added to the monomer/triethylamine mixture. The R- α -LA slowly mixed into the aqueous H₂O₂. After two hours, the reaction formed a single-phase clear solution. Upon coagulation with HCl, a white polymer with the texture of taffy separated from the reaction mixture. During precipitation of R-Ox-23 into ether, the polymer fell and adhered quickly to the bottom of beaker, whereas, R-Ox-0 required overnight flocculation in the freezer (-20°C) before excess solvent could be decanted from the polymer phase. The conditions and conversion of two reactions are listed in Table 4.5.2. The samples are labeled by their monomer (R for R enantiomer and DL for racemic mixture), “Ox” for oxidative polymerization, and then the temperature of the reaction.

Table 4.5.2. Reaction conditions and conversions the polymerization of R- α -LA using triethylamine and aqueous H₂O₂.

Sample	Temp. (°C)	[R- α -LA] (mol/L)	[Et ₃ N] (mol/L)	[H ₂ O ₂] (mol/L)	% Conv.
R-Ox-23	23	0.304	0.399	0.758	34.3
R-Ox-0	0	0.333	0.399	0.758	53.6

R-Ox-23

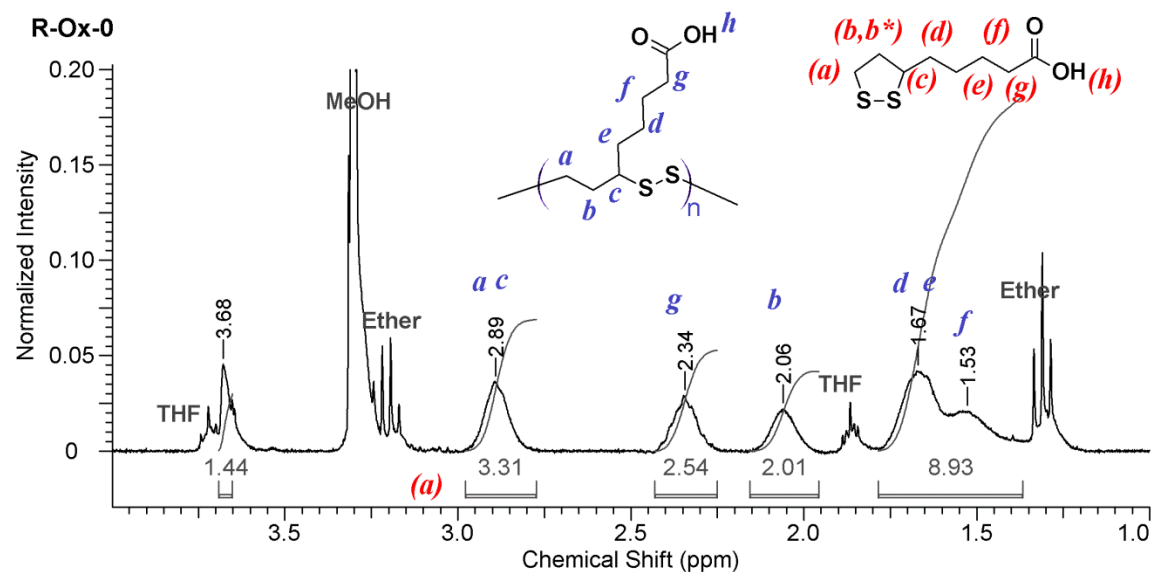
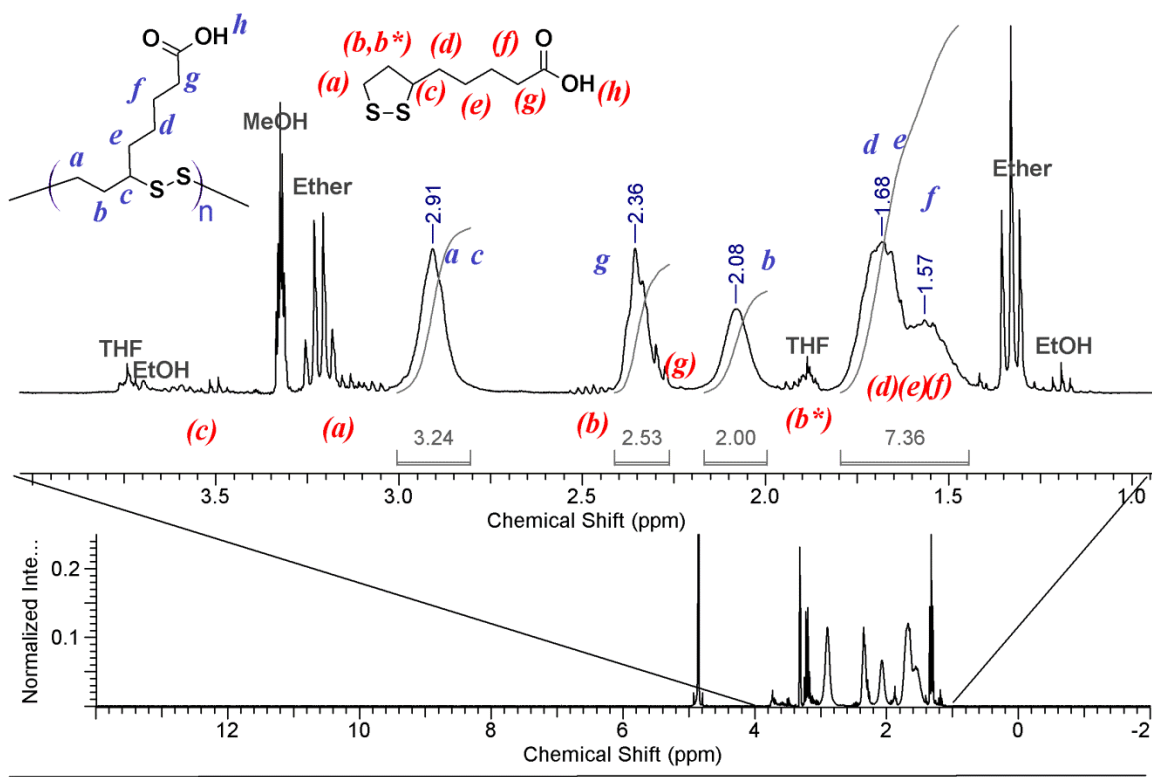


Figure. 4.5.4. ^1H NMR of R-Ox-23 (12 s relax.; 128 scans; methanol-d₄; 300 MHz).

The ^1H NMR spectrum of R-Ox-23 shows peaks from the monomer and polymer product. Signals from methylene protons, *a*, and methyne proton, *c*, of the polymer

overlap to form one peak at 2.91 ppm. The shift between the two germinal protons,(*b*) and (*b**), has narrowed in in the polymer product, and they form one peak, *b*, at 2.08 ppm. Protons in the α -position, *g*, are broad after polymerization and have lost the characteristic triplet splitting pattern. They also show a downfield shift to 2.41 ppm and partially obscure the monomer peaks that correspond to the same protons in the monomer. In methanol-d₄ the acidic protons (*h*) were not seen. A small peak, which may be a triplet appears at 1.41 ppm whose origin is uncertain, but is in the correct range to correspond to a methylene adjacent thiol proton. Also present are small peaks from THF and ethanol in which the polymer was dissolved, and strong peaks from the precipitation solvent, ether, despite spending 1 week in a vacuum oven. R-Ox-0 was much less soluble in deuterated methanol than R-Ox-23 at room temperature. At the temperature with in the NMR instrument(35°C), it was soluble enough to obtain decent ¹H spectrum. The ¹H NMR spectrum displayed the same peaks at 2.89 ppm, 2.34 ppm, 2.06 ppm, 1.67 ppm and 1.53 ppm but with increased broadening. An additional peak appears at 3.68 ppm which is too large to attribute to ethanol impurity. The integration value of this peak relative to *b* would be approximately 1.4. A peak with a similar shift was attributed to the sulfur adjacent methyne proton by Kisanuki *et al.* where a-LA was polymerized through the formation of thioester bonds.⁷⁹

One reason for peak broadening, particularly with respect to protons in the thiolane ring, is possibility of head-to-head; tail-to-tail, or tail-to-head bonding. Figure 4.5.5 displays the three possible monomer configurations in the polymer backbone.

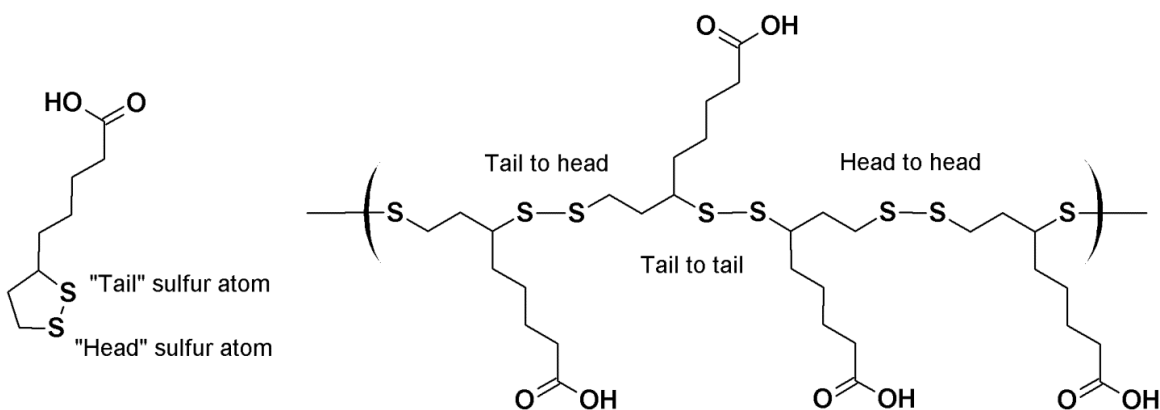


Figure 4.5.5. Possible monomer configurations in polymer backbone of poly(α -LA).

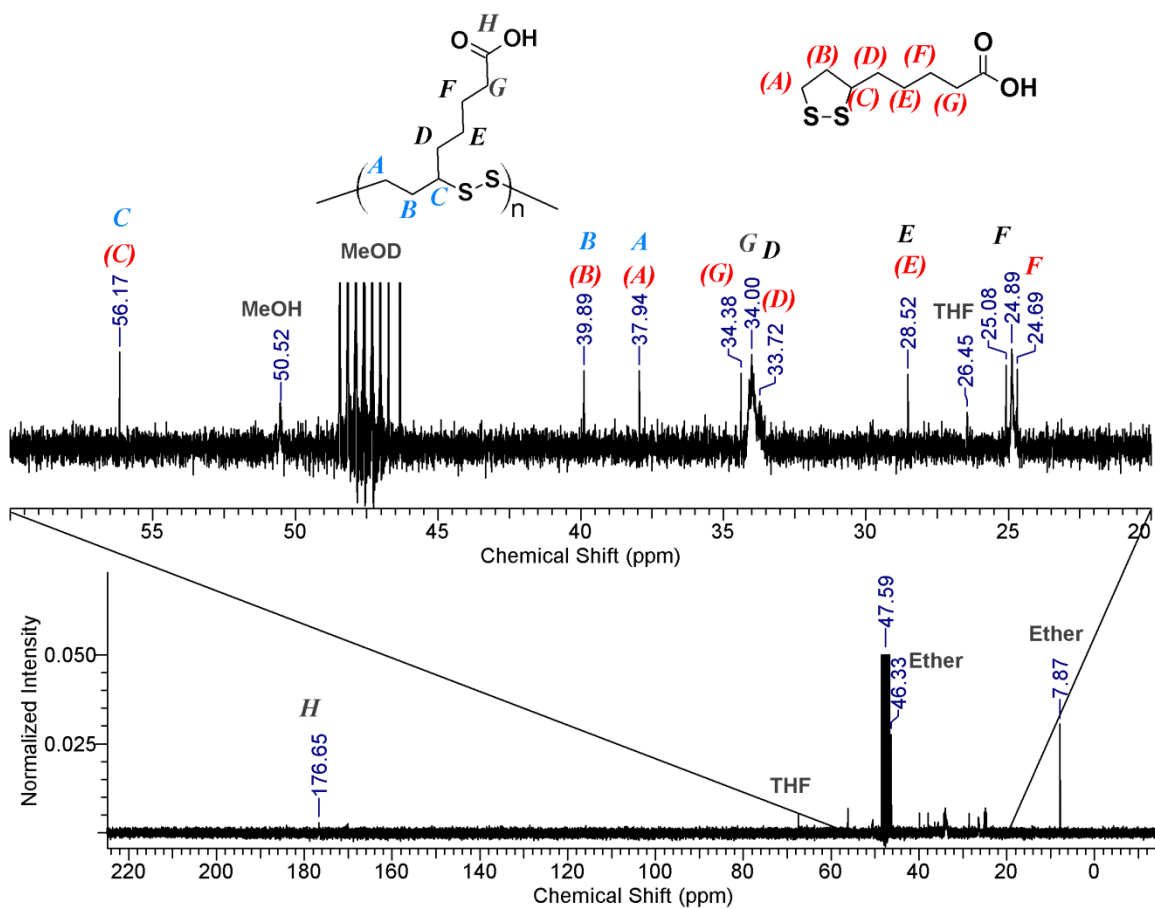


Figure 4.5.6. ^{13}C NMR of R-Ox-23 (300 MHz; 12 s relax.; 2400 scans; methanol-d₄).

In the ^{13}C NMR spectrum (Figure 4.5.6), most of the peaks which correspond to the polymer overlap the peaks from the monomer. Broadening of the peaks corresponding to carbons D, F and G is also seen. The origin of a sharp peak shown at 25.08 ppm is unclear. This range is characteristic of thiol-adjacent carbons, as well as the aliphatic carbon F. If it does arise from thiol adjacent carbon it would be an indication that the monomer may polymerize through the disulfide bond, but also through the formation of a thioester which has been reported in the literature (see Figure 2.4.3).

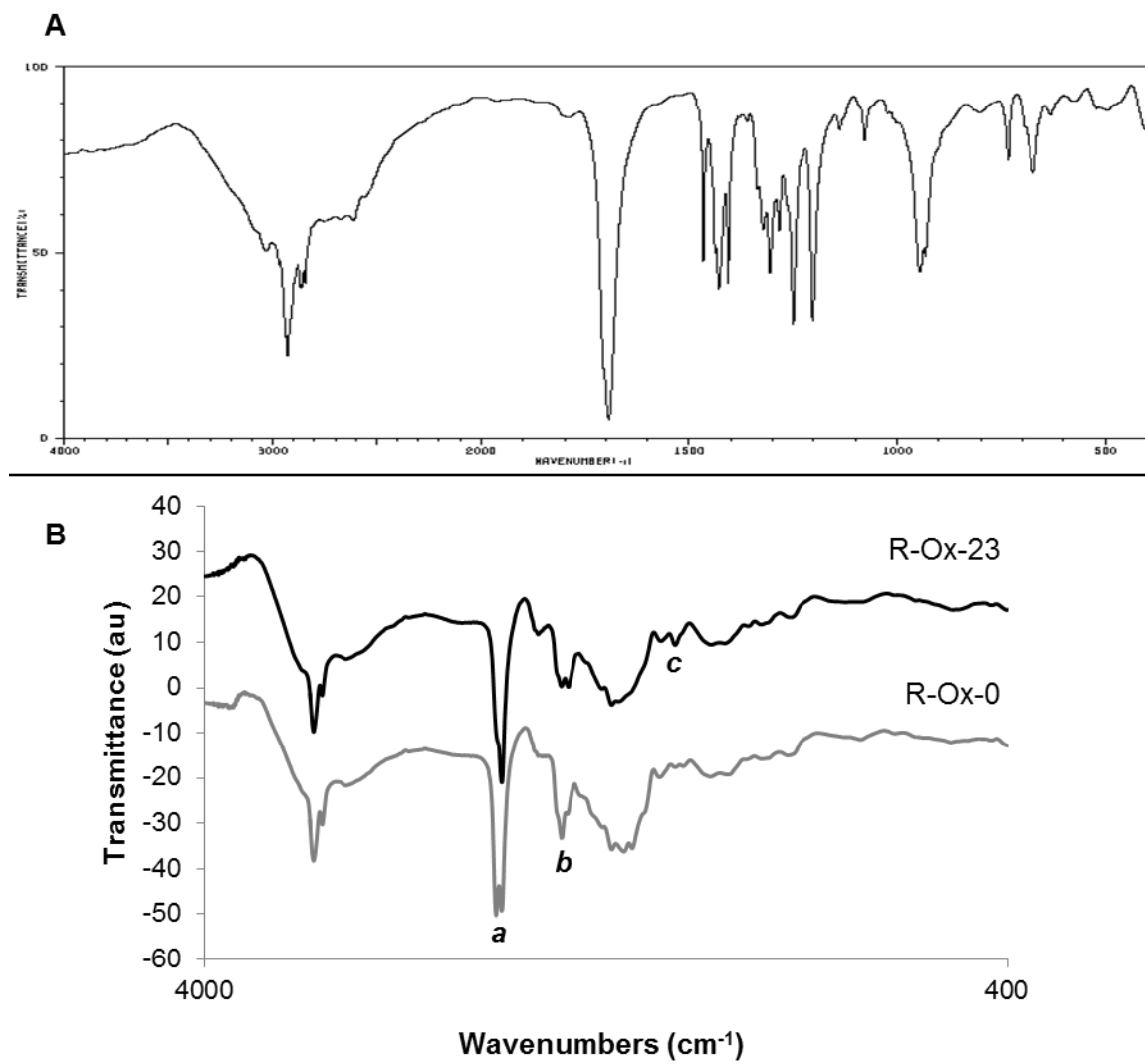


Figure 4.5.7. A) FTIR spectrum α -lipoic acid from SBDS* B) FTIR spectra of R-Ox-23 and R-Ox-0. (64 scans)

The FTIR spectrum of both polymerization products are compared in Figure 4.5.7. Both spectra show similarities to the monomer spectrum found in the Spectral Database. Two sharp peaks between 2930 and 2860 from $\text{C}-\text{H}$ stretching overlay the broad $\text{O}-\text{H}$ stretch. A strong carbonyl stretching band ($>\text{C}=\text{O}$) appears at 1699cm^{-1} in

the literature spectrum and at 1707 cm^{-1} in the experimental spectra. In the fingerprint region, the sharp bands shown in the monomer spectrum become broad and weak.

The most noticeable differences between the two spectra are indicated by **a**, **b**, and **c**. The strong carbonyl peak (1707 cm^{-1}) shows a shoulder in the R-Ox-23, which appears as another peak in the R-Ox-0 spectrum (1731 cm^{-1}). In R-Ox-0, the peak at 1437 cm^{-1} , which corresponds to C-H bending vibrations in cyclic alkanes, is stronger than it appears in R-Ox-23. Conversely, the peak at 1037 cm^{-1} , which corresponds to -OH absorption is stronger in the R-Ox-23 spectrum than it is in the R-Ox-0 spectrum. The differences between the two spectra suggest that R-Ox-0 contains more residual monomer than R-Ox-23.

DSC analysis showed that both polymers had a glass transition at -14°C . No other transitions were seen. The DSC trace of R-Ox-0 is shown in Figure 4.5.8.

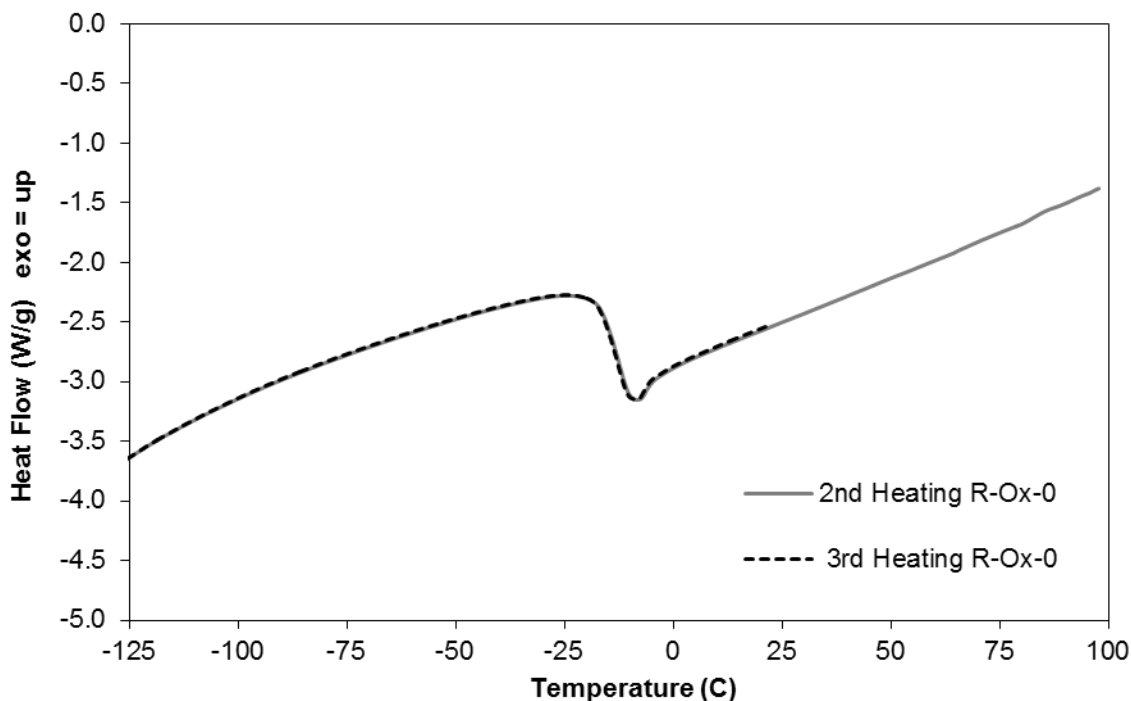


Figure 4.5.8. DSC chromatograms of 2nd and 3rd heating cycles for sample R-Ox-0 (heating rate = 10°C/min).

4.5.2.2. Thermal polymerizations of α -LA

The thermal polymerization of α -LA has been reported in the literature,^{77,78,83} but no comparison between polymers of R- α -LA and DL- α -LA have been made. Here, both forms α -LA were polymerized thermally in bulk conditions under reduced pressure (80 mtorr). The conditions and conversion of several thermal polymerizations under vacuum are listed in Table 4.37. Samples are named by the monomer (enantiomer (R), or racemic mixture (DL)), T for “Thermal” and then by the temperature of the reaction. For example, in sample R-T-90, the R-enantiomer was thermally polymerized at 90°C. In the sample R-T-100, α -LA was added to the reaction flask in solution with ethanol. The

flask was kept open at 100°C for 2 hrs to evaporate all ethanol, and for 80 min under vacuum.

After thermal polymerization, the resultant products were sticky, yellow, tough solids. The products could not be “poured” from the reaction flask as reported by Kisanuki and coworkers,⁸³ instead it was required to dissolve the material for removal from the reaction flasks. Precipitation into water produced a yellow polymer, some of which would form a film at the air-water interface. Precipitation into chloroform yielded an off-white polymer, while precipitation in diethyl ether produced a tough, white polymer mass which adhered tightly to the bottom of the glass precipitation beaker.

Table 4.5.3. Reaction conditions and conversions for the thermal polymerization of α -LA under vacuum.

Sample	Temp. (°C)	Time	% Conv.	Precipitating Solvent	Observations
DL-T-90-A	90	3 hrs	78.52	Ether	White
DL-T-90-B	90	3 hrs	59.16	Water	Yellow
DL-T-90-C	90	3 hrs	52.6%	Water CHCl_3	Yellow Off-white
R-T-80 1 st PPTN 2 nd PPTN	80	0.5 hrs	84.85	Water	Yellow
			30.60	Ether	White
R-T-90	90	3 hrs	58.96	Ether	White
R-T-100	100	2 + 1.3 hrs	32.50	Ether	White

The polymers precipitated into ether showed very little residual monomer in their ^1H NMR spectra. Figure 4.5.9 compares the ^1H NMR spectra of samples DL-T-90-A and R-T-90 which were both precipitated into ether. In contrast, precipitation into water

yielded a yellow polymer. The yellow color is characteristic of the thiolane ring, and is a good indication of the presence of residual monomer. The presence of a large amount of residual monomer is seen in the ^1H NMR spectrum of R-T-80-1st PPTN (Figure. 4.5.8).

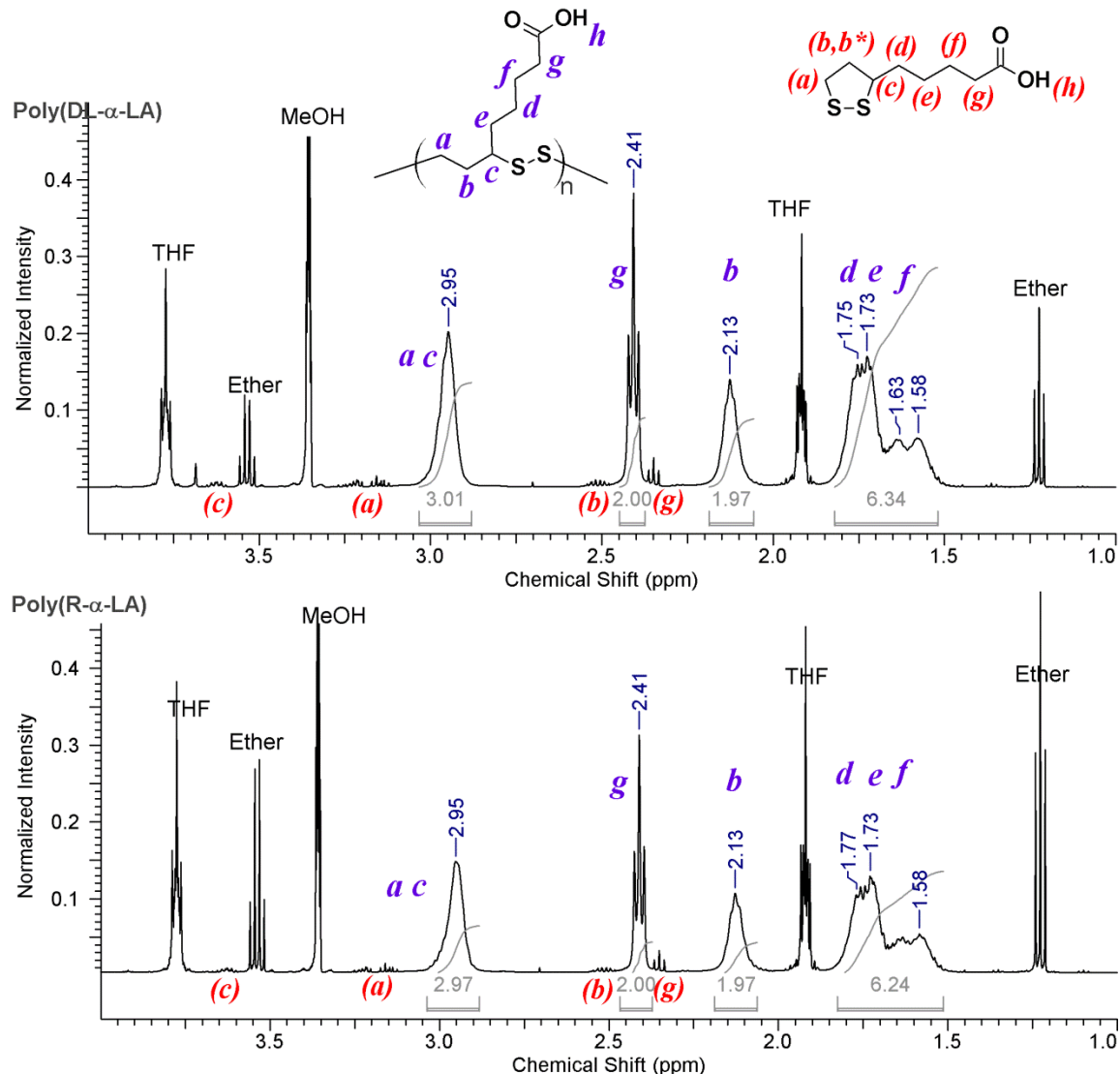


Figure 4.5.9. ^1H NMR spectra of samples DL-T-90-A and R-T-90 (10 s relax.; 512 scans; 500 MHz; methanol-d₄).

The ^1H NMR spectra from poly(DL- α -LA), sample DL-T-90-A, and poly(R- α -LA), sample R-T-90, showed nearly identical spectra. Both show small peaks

corresponding to residual monomer which are labeled in parentheses at the bottom of the two spectra. The signals corresponding to the aliphatic methylene protons (*d,e,f*) of the monomer are overlapped by the signals in the polymer and are not labeled. The signals from the *d*, *e* and *f* in the polymers did not shift significantly but did become broader and lose the definition of their splitting patterns. The peaks corresponding to protons in the thiolane ring shifted after polymerization, become much broader and lost all resolution of the monomer splitting pattern. The signals from methylene protons, *a*, and methyne proton, *c*, form the peak at 2.95 ppm. The diastereotopic protons, *b* and *b**, form one peak at 2.13 ppm. Protons in the α -position to the carbonyl group were the least effected by polymerization; they shifted slightly downfield to 2.41 ppm and maintained their triplet splitting pattern. In deuterated methanol the acidic protons (*h*) were not seen. Also present are strong peaks from the precipitation.

The ^1H spectrum of sample R-T-80-1st PPTN shows large peaks corresponding to residual monomer (Figure 4.5.10). This is in good agreement with the color of the polymer sample, which was yellow. Additionally, in deuterated DMSO, the acidic protons are seen at 11.98 ppm.

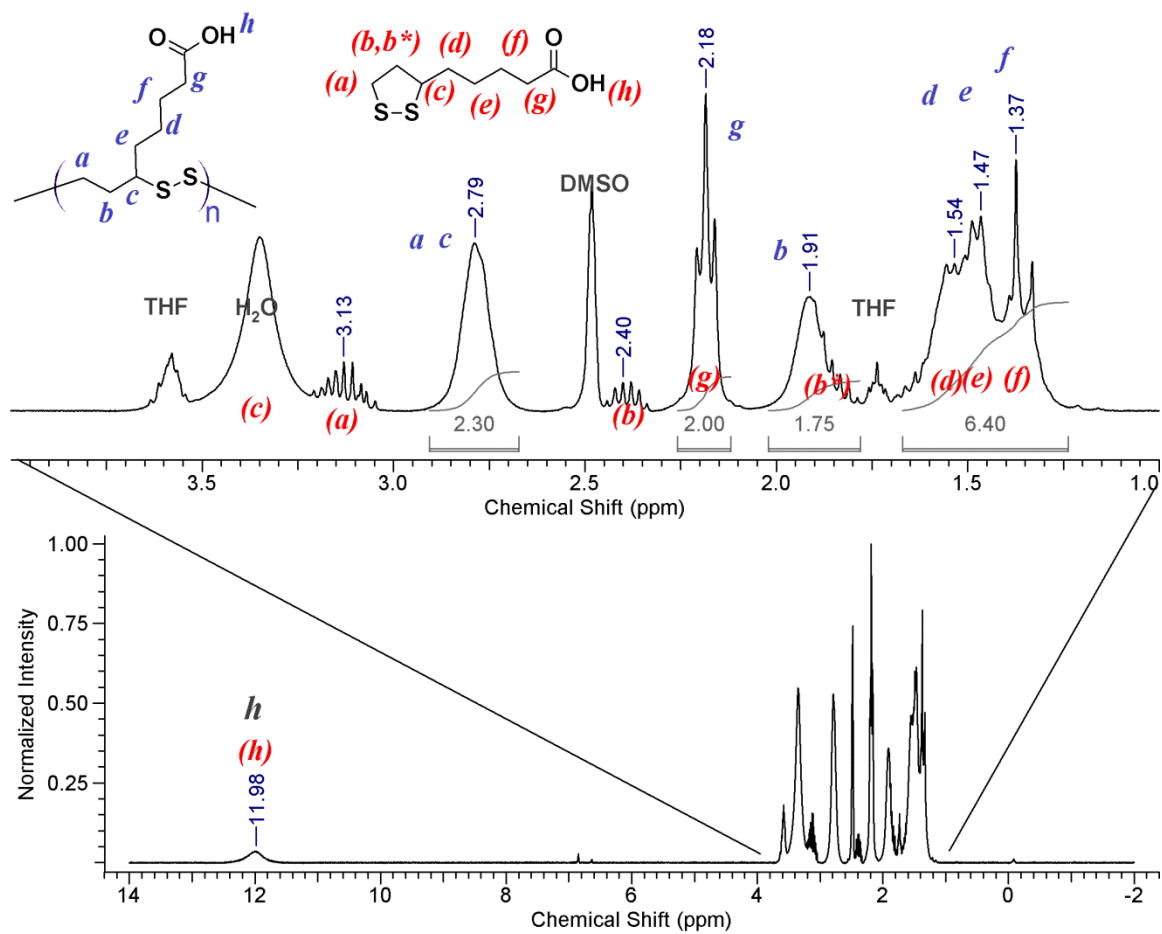


Figure 4.5.10. ^1H NMR of sample R-T-80-1st PPTN (15 s relax; 32 scans; 300 MHz; DMSO-d_6).

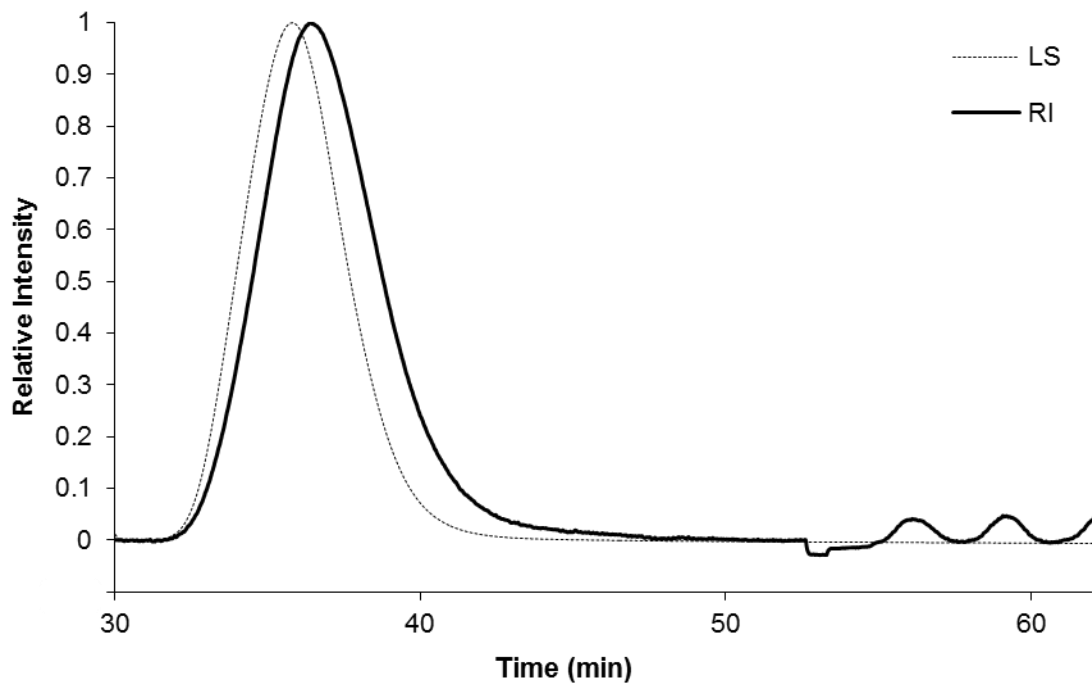


Figure 4.5.11. SEC chromatograms from R-T-100.

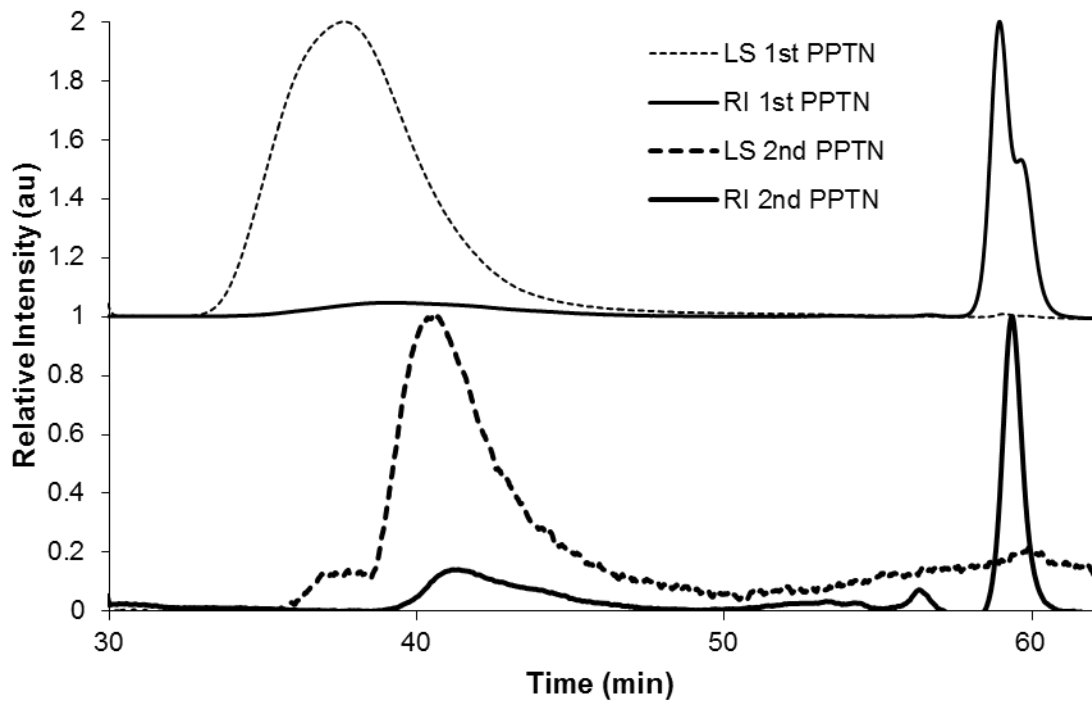


Figure 4.5.12. SEC chromatograms from R-T-80-1st PPTN (top) and R-T-80-2nd PPTN (bottom) are compared.

Table 4.5.4. Results from SEC analysis of thermally polymerized α -LA monomers.

Sample	M_n	M_w	M_n/M_w	R_{gz} (nm)	R_{hw} (nm)	$[\eta]_w$ (mL/g)
R-T-80-2 nd PPTN	161,000	226,000	1.41	18.8	10.2	31.1
R-T-100	975,000	1,534,000	1.57	65.5	36.5	223.1

The thermal polymerization of α -LA produced very high molecular weight polymers which were filtered out in SEC sample preparation. Sample R-T-100 showed the strongest RI signal with a nice distribution (Figure 4.5.11). Using this sample, the dn/dc of poly(α -LA) was calculated from 100% mass recovery to be 0.109 mL/g. This dn/dc value was used to calculate the molecular weights of all other poly(α -LA) samples. No signal was detected for DL-T-90-A nor for R-T-90. A very weak signal was seen in the high molecular weight region for R-T-80-1st PPTN, but the signal became stronger after the 2nd precipitation. Results from SEC analysis of thermal polymerizations are listed in Table 4.5.4.

The RI and LS signals for R-T-80-1st PPTN and 2nd PPTN are compared in Figure 4.5.12. The peak in the low molecular weight region was bimodal after the 1st precipitation, and it became monomodal after the 2nd PPTN. Because the polymer was white after the 2nd precipitation into ether, it is proposed that the monomer was removed but the dimer, and other oligomers remain.

4.5.2.4. Direct visualization of poly(α -LA) polymer structure using AFM

Endo and coworkers have proposed a catenane structure for poly(disulfide) polymers including thermally polymerized poly(α -LA) (Section 4.1.; Figure 4.1.30). We wanted to directly visualize the structure of the poly(α -LA) polymers using atomic force

microscopy (AFM), however, most AFM techniques do not have the resolution for single-molecule detection. To overcome the resolution limits of AFM two strategies were developed to increase the width of the poly(α -LA) polymer chains. The first strategy used post-polymerization amplification of thermally polymerized poly(α -LA). Briefly, short poly(ethylene glycol) (PEG) chains were grafted to the poly(α -LA) backbone through the pendant carboxylic acid groups to create brush-like polymers that were wide enough to visualize using AFM. The second strategy, α -LA was first conjugated to 2,000 g/mol PEG chains to make macromonomers. The macromonomers were then polymerized thermally. The resulting brush polymers were then visualized using AFM.

Figure 4.5.13 displays a cartoon of the two amplification strategies for AFM imaging.

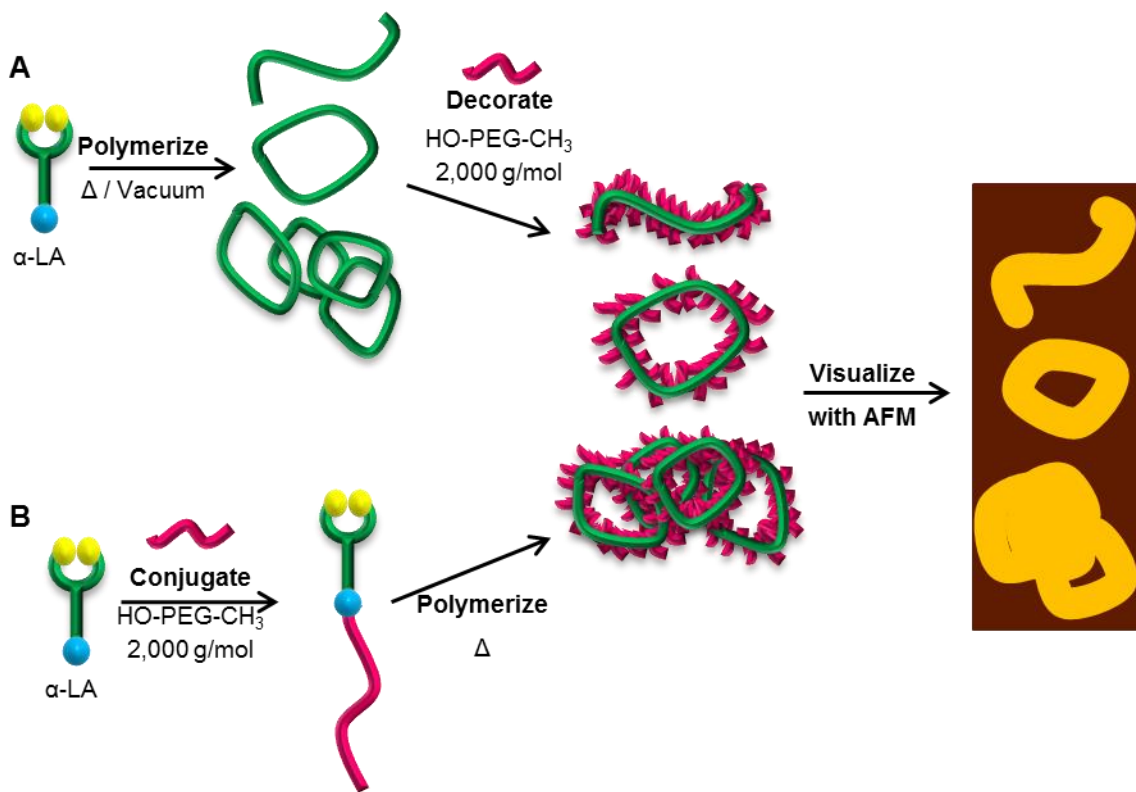


Figure 4.5.13. Amplification strategies for AFM visualization of poly(α -LA) chains.

4.5.2.4.1. Post-polymerization functionalization of poly(α -LA) with HO-PEG-CH₃

Poly(α -LA), sample R-T-100 (0.1168 g), was dissolved in THF (12.0 mL) with HO-PEG-CH₃ (1.0967g; M_n = 2,000 g/mol). The theoretical concentration of carboxylic acid groups in the solution was 46.7 mM. The concentration of HO-PEG-CH₃ in the solution was 45.8 mM. The immobilized enzyme catalyst (*Candida antarctica* lipase B on Immobead 150) was added to the solution and the reaction was placed under N₂ atmosphere at 65°C for 47.5 hours. When the reaction was removed from heat, all of the THF had evaporated. The product was in a solid state. The product was tested for solubility in several solvents. It was not soluble in isopropyl alcohol and only slightly soluble in water, acetone and THF. The product was soluble in chloroform. The product was dissolved in chloroform, filtered, dried over MgSO₄ and then the solvent was removed by rotary evaporation. The final mass of product was 0.3919g. Assuming that all poly(α -LA) starting material was in the product, this calculates to the functionalization of about 1 in every 4 acid groups.

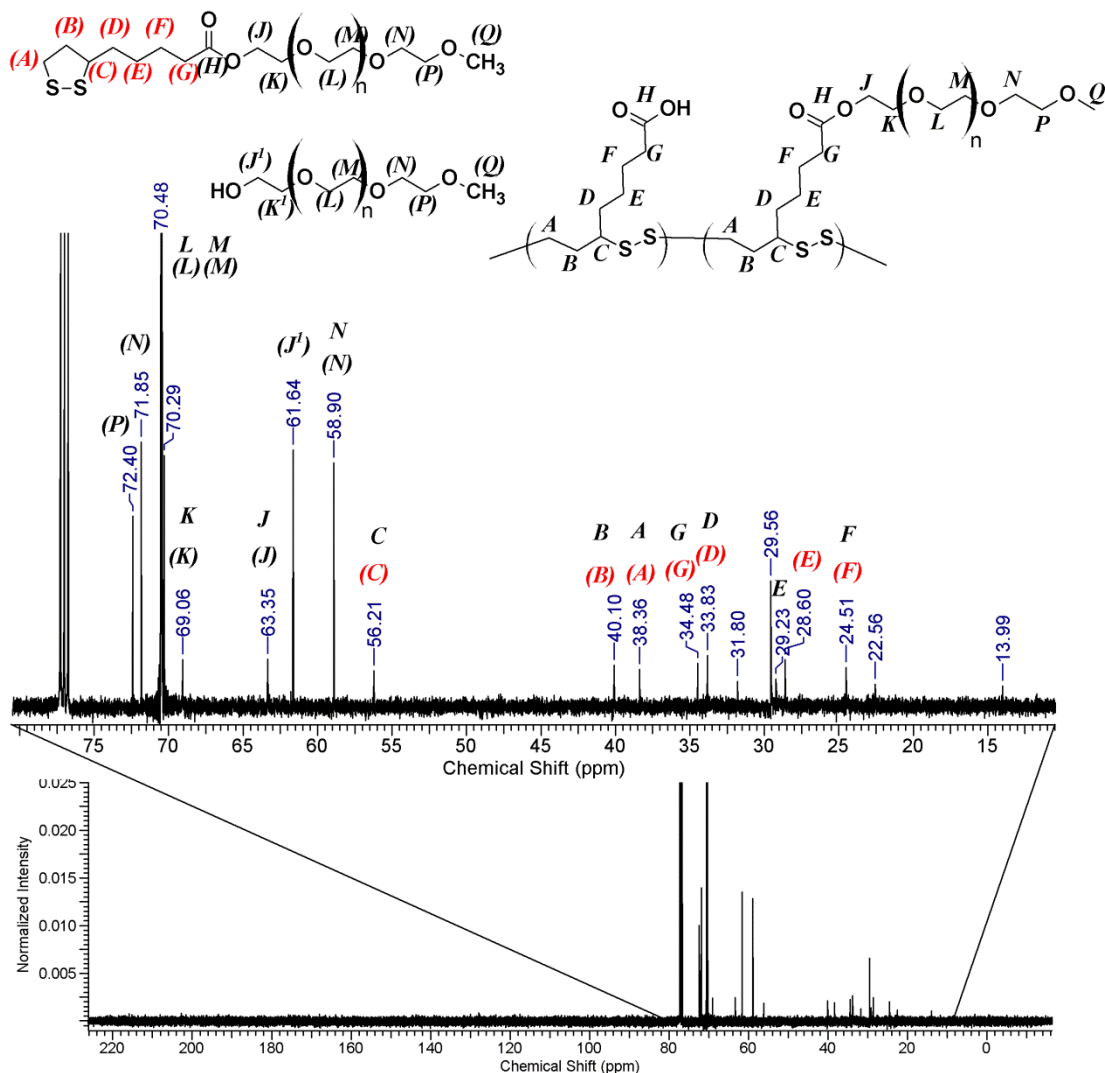


Figure 4.5.14. ^{13}C NMR spectrum of PEG-decorated poly(α -LA). (6 s relax.; 5000 scans; CDCl_3 ; 300 MHz)

The carbon NMR of the product is shown in Figure 4.5.14 show all of the peaks described previously in poly(α -LA) labeled A - H. Additional peaks corresponding to HO-PEG-CH₃ and the α -LA-PEG-CH₃ are also present with PEG peaks labeled J-N, P,Q. Peaks at 31.8 ppm, 29.56 ppm 22.56 and 13.99 ppm do not appear to correspond to the expected products or starting materials. Shifts corresponding to thiols and sulfides are

known to appear in this region. A peak corresponding to the carbonyl carbon is conspicuously missing from the spectrum. Increasing the relaxation time to 30 s with 1024 transients on the 500 MHz instrument did not reveal a carbonyl carbon signal. Further investigation into the chemical structure of the PEG-decorated poly(α -LA) is needed.

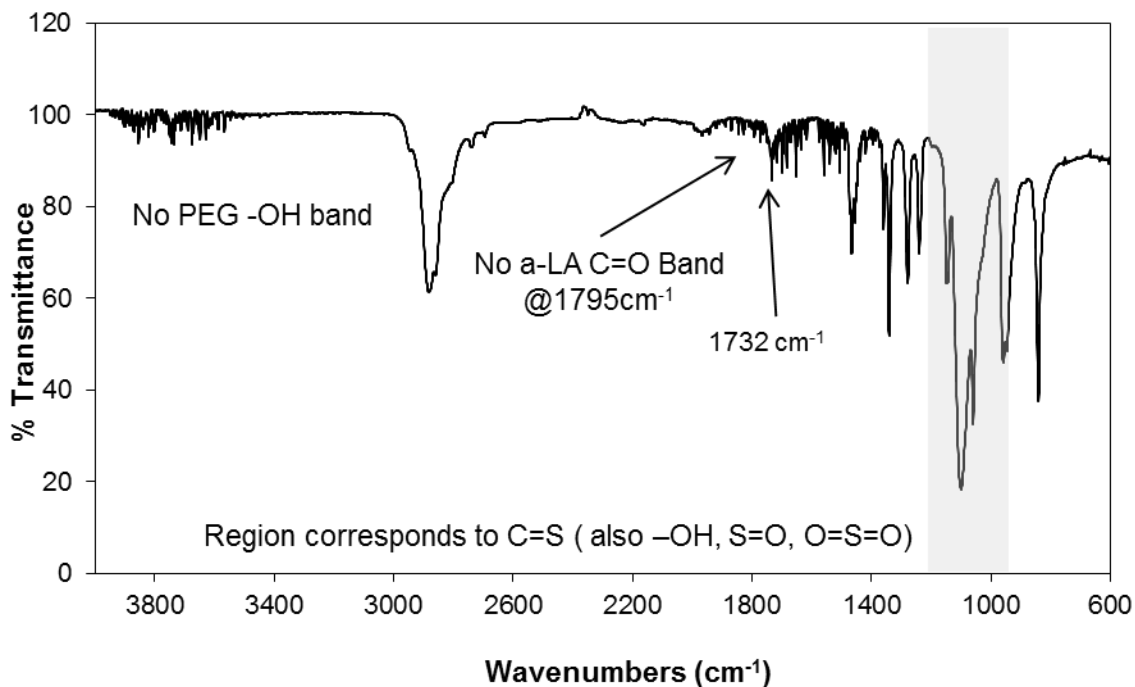


Figure 4.5.15. The FTIR spectrum of PEG-decorated poly(α -LA) product.

The FTIR spectrum of the product is shown in Figure 4.5.15. The spectrum does not show the characteristic alcohol (-O-H) stretching band. The strong carbonyl stretching band at 1795 cm^{-1} which is characteristic of α -LA is not seen. There is a band at 1735 cm^{-1} which is characteristic of ester bonds. Interestingly, strong bands appear in

the 1000 cm^{-1} to 1200 cm^{-1} region. This region corresponds to vibrations arising from thiocarbonyl, sulfoxide and sulfone functional groups.

The SEC traces (LS, RI and UV) of the product are shown in Figure 4.5.16. The RI signal in the high molecular weight region is very weak indicating that the high molecular weight product has been removed by filtration during SEC sample preparation. The in the low molecular weight region, a large peak is seen. Using the 0.068 mL/g as the dn/dc value, which is literature value for the dn/dc of PEG in THF the M_n is measured to be $2,000\text{ g/mol}$ with M_w/M_n of 1.04 . These values correspond well with unreacted PEG starting material. MALDI-ToF analysis of the sample revealed two PEG distributions one corresponding to the unreacted PEG, and a smaller distribution corresponding to the α -LA-PEG conjugate.

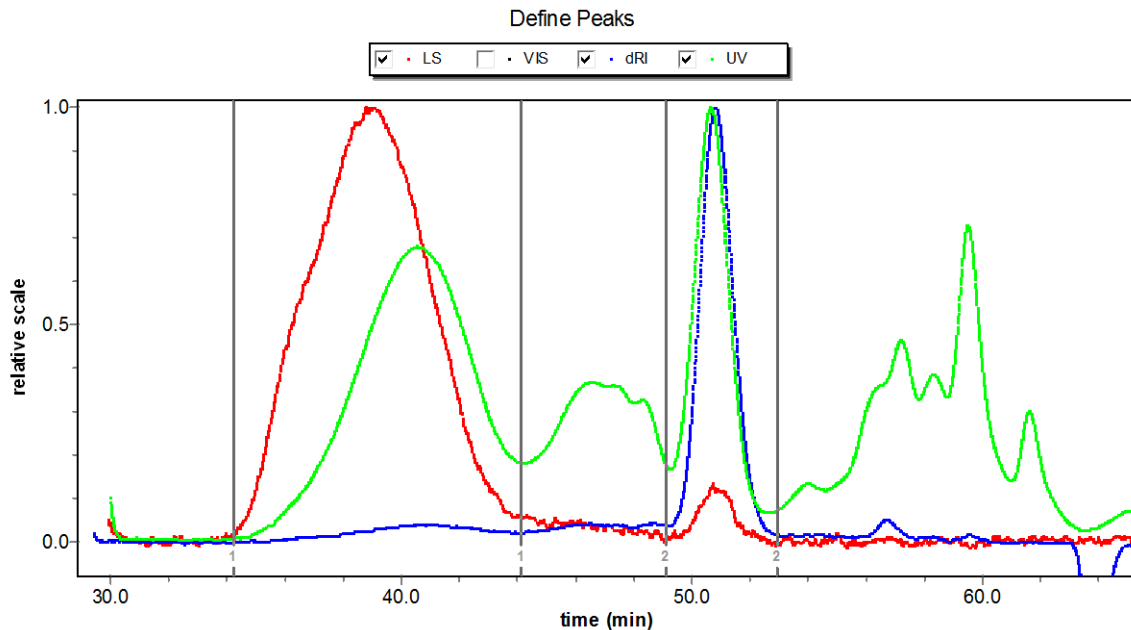


Figure. 4.5.16. The LS (red), RI (blue) and UV (green) traces from SEC analysis of the poly(α -LA)-PEG product are shown.

The product was dissolved in chloroform (0.11 mg/mL) and spun-cast onto freshly cleaved mica substrates. The product was then analyzed using AFM. The AFM images collected are shown in Figures 4.5.17 and 4.5.18.

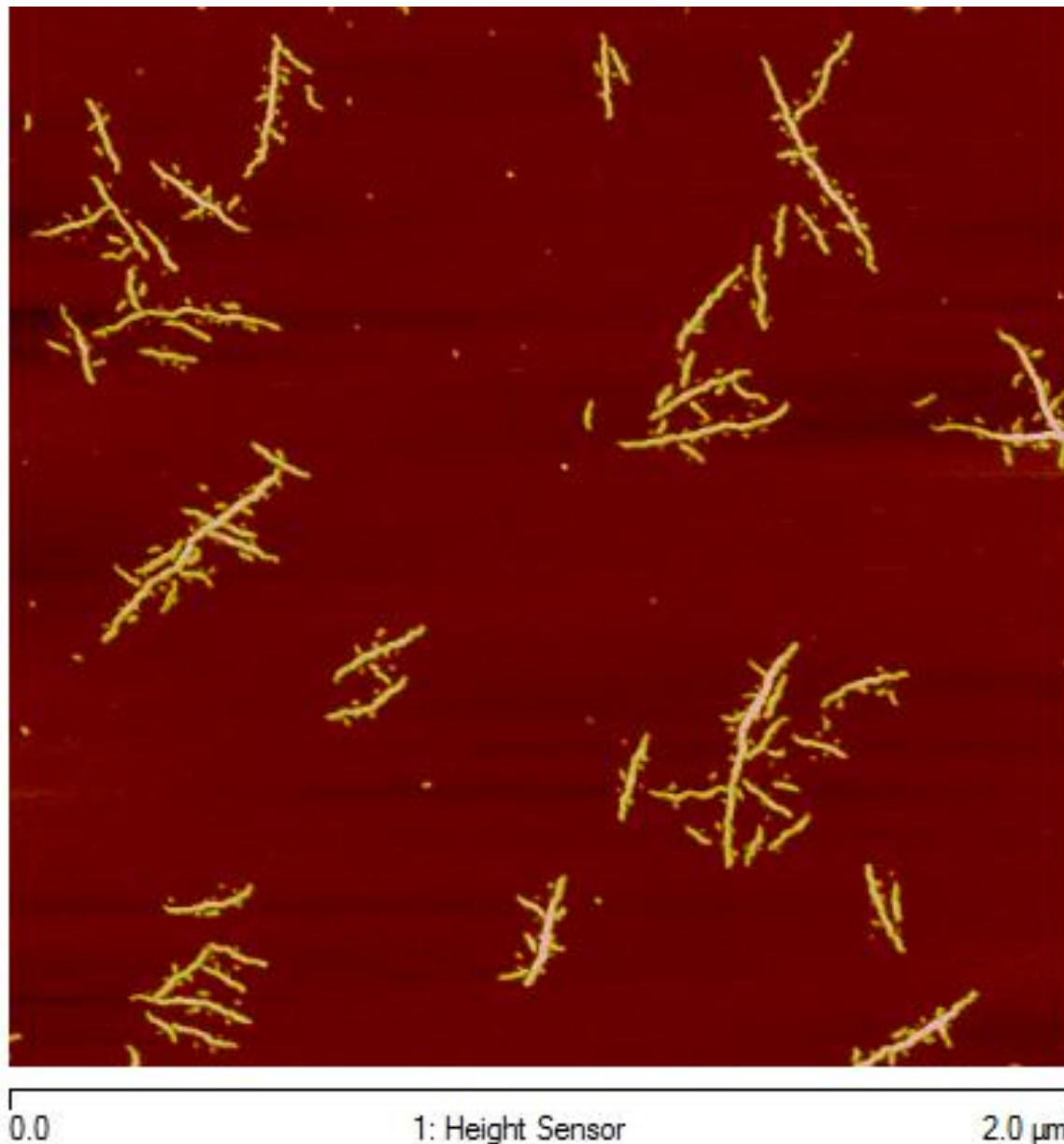


Figure 4.5.17. AFM image of a 0.11mg/mL solution of poly(α -LA) sample R-T-100 decorated with 2000 g/mol PEG in chloroform spuncast onto mica.

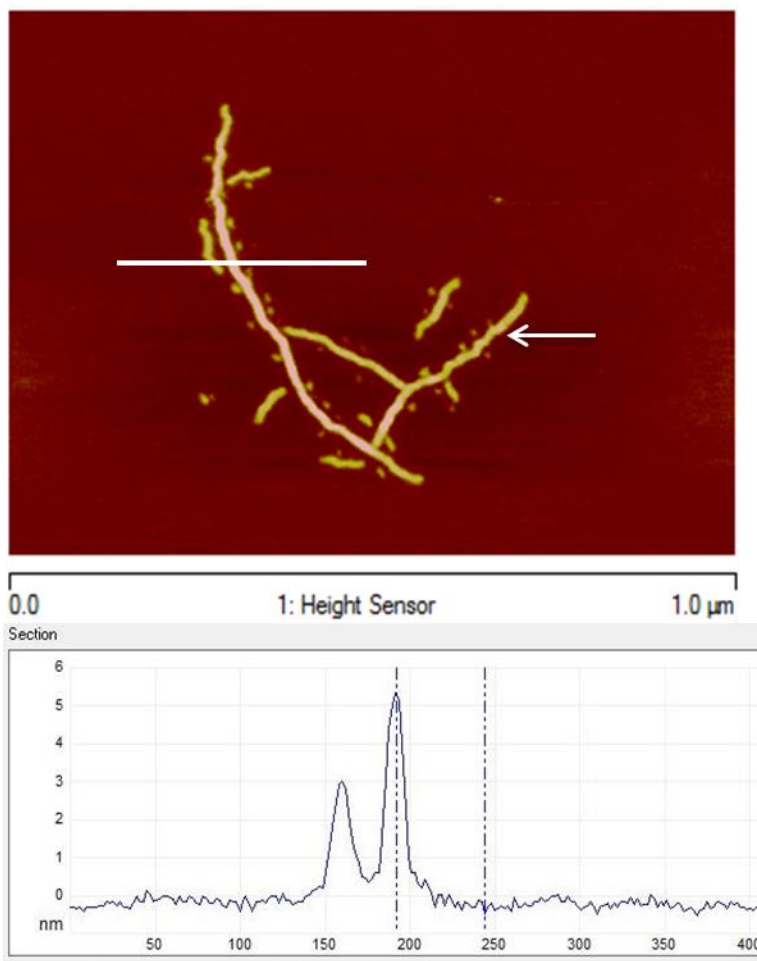


Figure 4.5.18. Detail of AFM image of a 0.11mg/mL solution of poly(α -LA) sample R-T-100 decorated with 2000 g/mol PEG in chloroform spuncast onto mica. Height profile taken from area indicated by white horizontal line. Branch indicated by arrow is 290 nm long.

The AFM images of the decorated poly(R- α -LA) show branch-like structures. Cyclic structures were not observed. The height of the imaged species was between 3 to 5 nm above the surface of the mica surface. The height profile shows that the approximate width of each branch is 20 nm, however, tip error causes this number to be artificially large. The approximate length of the branch indicated in Figure 4.5.18 is

290 nm. Using 0.164 nm ($(4 \times 0.154) + 0.205)/5 = 0.164$ nm) as the average bond length in a poly(α -LA) repeat unit and 706 g/mol as the average M_n per repeat unit ($((3 \times 206.3) + 2,206.3)/4 = 706$ g/mol) 290 nm back calculates to an approximate molecular weight of 307,000 g/mol.

4.5.2.4.2. Synthesis and polymerization of α -LA- PEG-CH₃ macromonomers.

To make the α -LA-based macromonomers for second strategy, CALB-catalyzed conjugation of R- α -LA to methoxy-PEG ($M_n = 2,000$ g/mol) was carried out in bulk conditions, at 60°C under reduced pressure (80 mTorr). The reaction progress was followed by taking samples at timed intervals. The samples were then analyzed by MALDI-ToF. The MALDI-ToF spectrum from the sample taken at 1 hr is shown in Figure 4.5.19 and the MALDI-ToF spectrum from the sample taken after 24 hrs reaction time is shown in Figure 4.5.20. The reaction progression was calculated by comparing the maximum peak intensity in the product spectrum to the maximum peak intensity in starting material. A plot of reaction completion against time is shown in Figure 4.5.21.

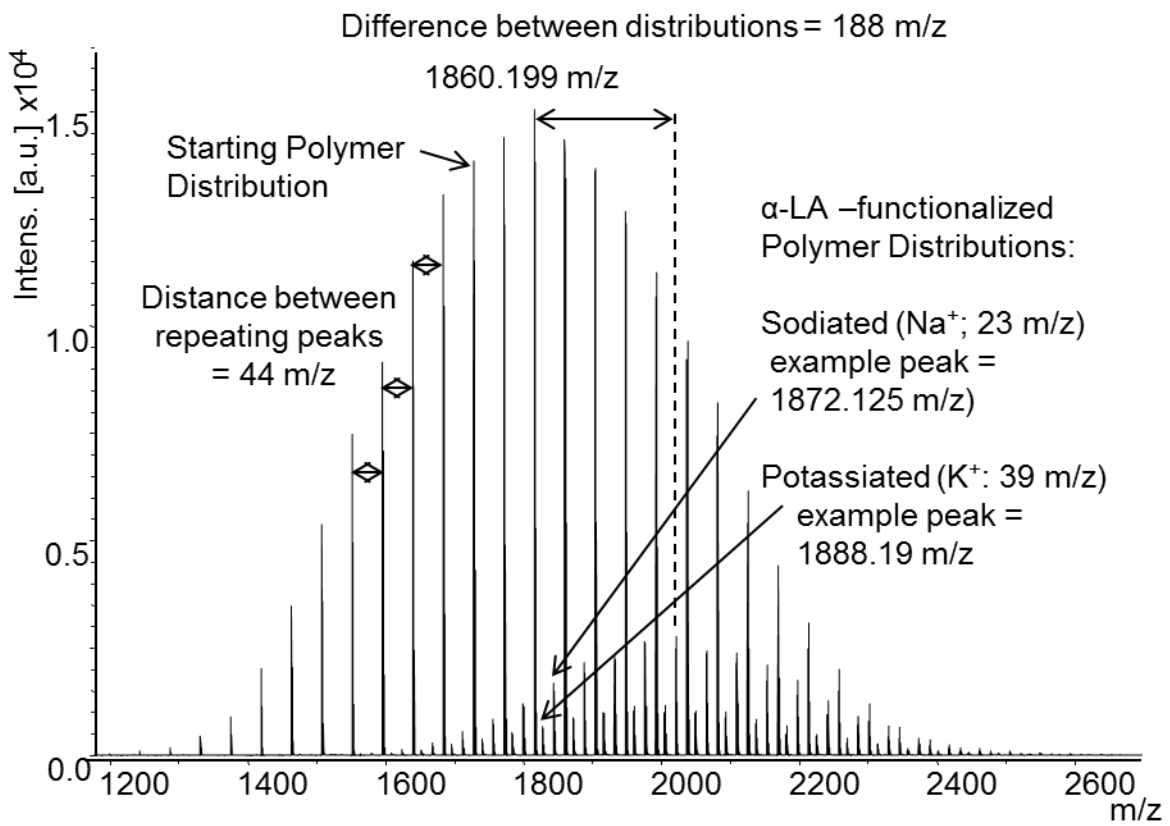


Figure 4.5.19. MALDI-ToF MS spectrum of CALB-catalyzed PEG- α -LA conjugation reaction at 1 hr.

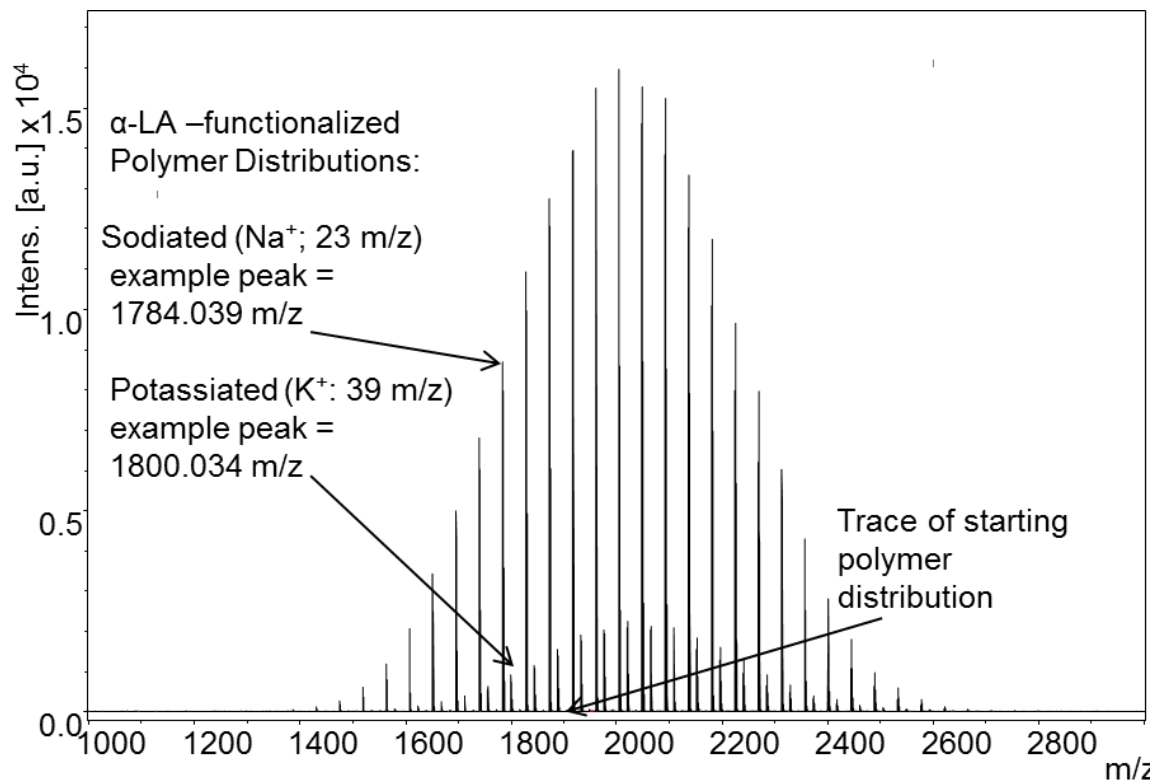


Figure 4.5.20. MALDI-ToF MS spectrum of CALB-catalyzed PEG- α -LA conjugation product at 24 hrs.

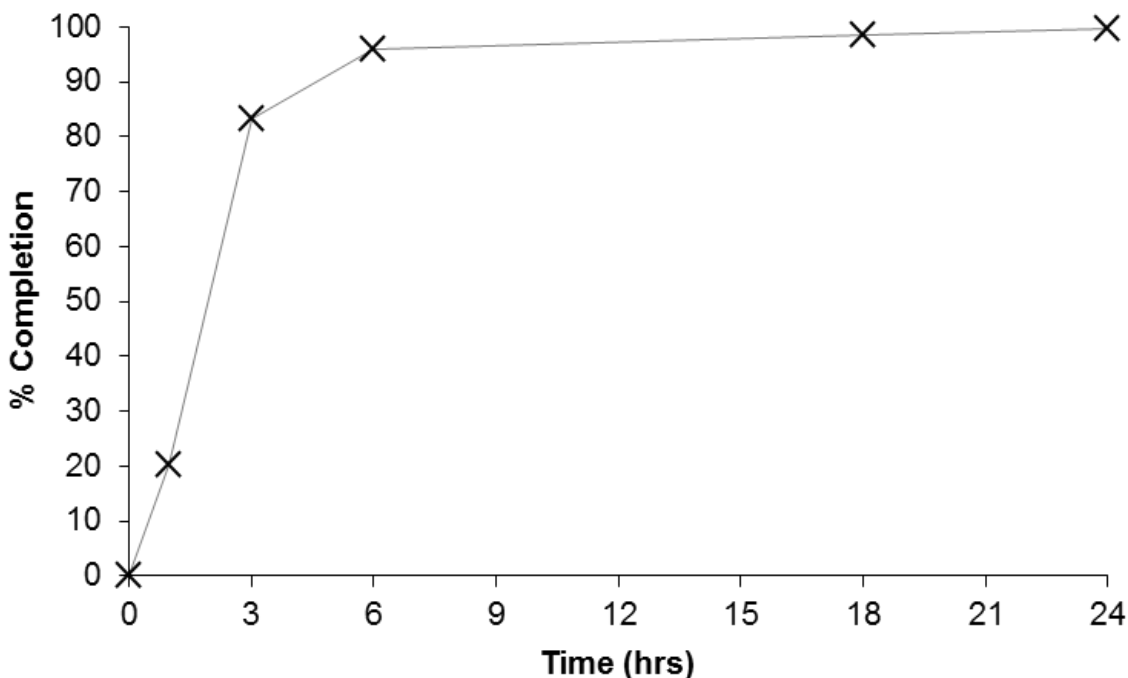


Figure 4.5.21. The progression for CALB-catalyzed PEG- α -LA conjugation at 60°C under vacuum.

The MALDI-ToF spectrum of the aliquots showed that the reaction reached 95.8 % completion in the first 6 hrs and slowly progressed to 99.7 % completion by 24 hrs. There was a shift in the MALDI spectrum of 188 m/z units from the starting polymer to the conjugated product. This is equal to the expected change upon formation of the lipoate conjugate. A reaction which was performed under the same conditions but in the absence of CALB showed only trace conjugation after 24 hrs. A detail of the MALDI-ToF mass spectrum is shown in Figure 4.5.22. The principal distribution corresponds to the PEG starting material. A very small secondary distribution is seen which could pertain to α -LA conjugated PEG chains.

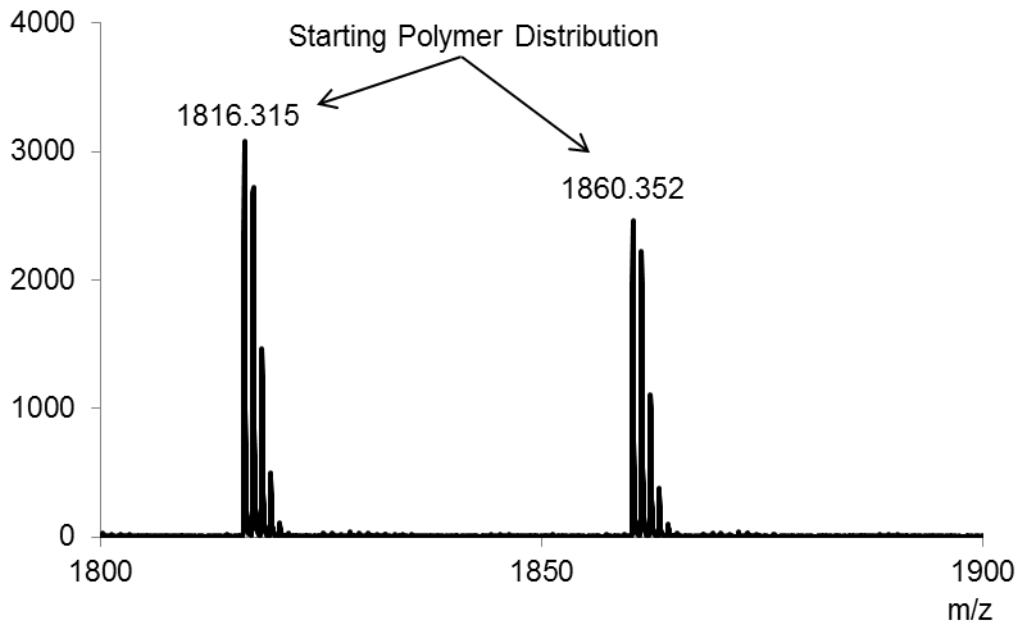


Figure 4.5.22. Detail of MALDI-ToF MS spectrum of from uncatalyzed reaction of α -LA and PEG at 24 hrs shows only trace amounts of conjugated product.

The macromonomer was then homopolymerized at 90°C under reduced pressure (80 mTorr) for 3 hrs. The macromonomer was also copolymerized with R- α -LA in a 1:4 (α -LA-PEG: α -LA) molar ratio also with heat under reduced pressure for 3 hrs. After purification by dissolution in THF followed precipitation in ether. The purified products could not be dissolved thoroughly in THF, and were not characterized by SEC. The poly(α -LA-PEG) and poly(α -LA-co- α -LA-PEG) samples were then characterized using AFM. The AFM images showed no branch-like structures. Instead, small curved structures were visualized (see APPENDIX C). With the decreased concentration of α -LA in each reaction, it is possible that the thiolane rings were not in close enough proximity with one another to form long polymer chains.

4.5.2.3. Compression molding of α -LA as a model for industrial manufacturing processes.

Powdered polymer feedstock is often used in industrial manufacturing methods, like injection and compression molding. For example, a powdered polymer feedstock may be added to the hopper of an injection molding machine, melted and then used to fill the mold cavity. Alternatively, powdered polystyrene mixed with blowing agents is added to compression molds as a solid and heated then to make expanded polystyrene.

After noticing that reduced pressures were not necessary for the thermal polymerization of α -LA, it was hypothesized that solid α -LA (monomers) could be used as in the same way as powdered polymer feedstocks. In this way the powdered monomer would be polymerized in the mold. Here the compression molding of R- α -LA and DL- α -LA was investigated. Table 4.5.5 shows molding conditions for compression molding trials. Weak RI signals in SEC prevented measuring the molecular weights of the resulting polymers.

Table 4.5.5. Molding conditions for α -LA monomers and observations.

Sample	Molding Temp (°C)	Time	Annealed	Observations of
DL-CM-95	95	2 hrs	Yes	Opaque pale yellow with holes
DL-CM-90	90	2 hrs	Yes	Opaque pale yellow
R-CM-100	100	5 min	No	Transparent bright yellow
R-CM-90	90	2 hrs	Yes	Transparent yellow with opaque patches

Compression molding of DL- α -LA at 95°C produced an opaque, pale yellow polymer sheet (sample name DL-CM-95). The sample showed several holes in the

otherwise smooth, tough sheet. To avoid sheet defects in subsequent compression molding trials, the monomers were melted thoroughly in the mold before placing them in the compression press. Photographs of two compression molded samples are shown in Figure 4.5.23. Sample R-CM-90 (A) was tough, smooth and not sticky. Sample R-CM-90 (B) was perfectly transparent when it was removed from the mold, but opaque regions grew after 3 days. The sample was slightly sticky and had an elastic give when touched.

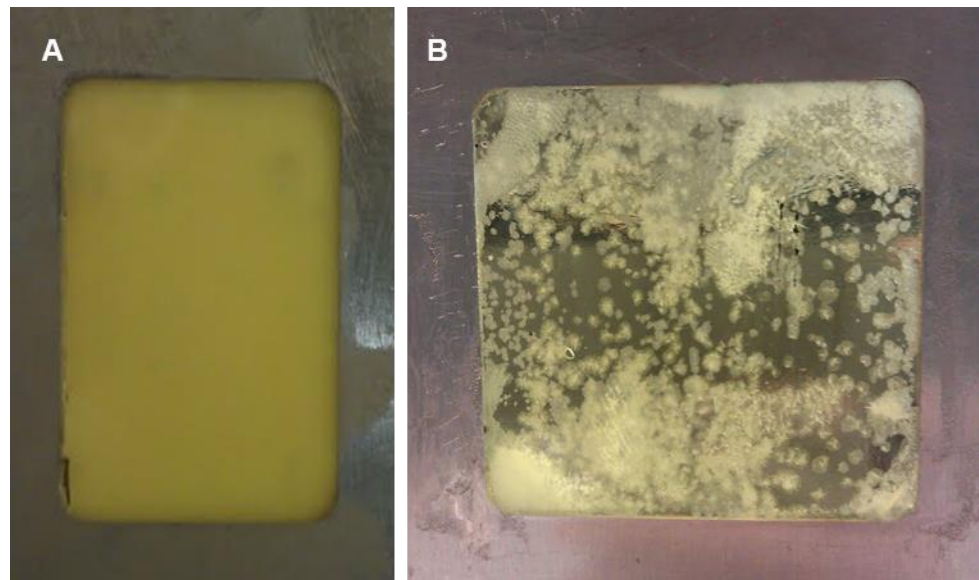


Figure 4.5.23. Compression molded sheets of DL-CM-90 (A) and R-CM-90 (B).

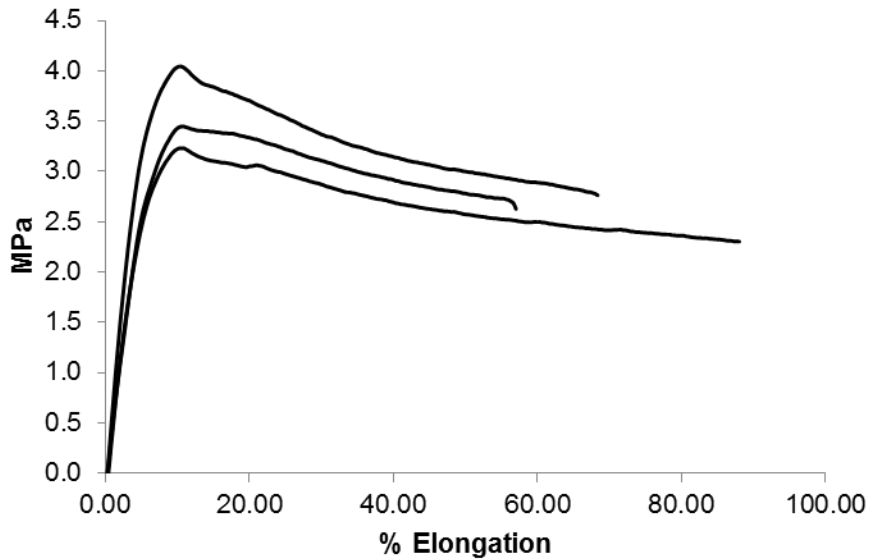


Figure 4.5.24. Tensile curves from sample DL-CM-95 (extension rate = 500 mm/min).

The tensile curves from DL-CM-95 are shown in Figure 4.5.24. Three micro tensile bars were die-cut from the molded sheet, measured, and pulled on a tensiometer at an extension 500 mm/min at room temperature. Showed a Young's modulus is 0.066 GPa and the highest ultimate tensile strength reached (UTS) was 4.02 MPa. The average UTS of the three measurements was 3.55 MPa. Because sample DL-CM-95 was opaque, it was not possible to see any internal defects.

A sample of DL-CM-95 was placed in 50 mM GSH in sodium acetate buffer solution (pH = 5.2) and incubated at 37°C. A plot of sample mass loss with time is shown in Figure 4.5.25. Degradation appeared to slow after 21 days, and fresh GSH solution was added. From the slope of the lines, complete degradation after 400-425 days was calculated.

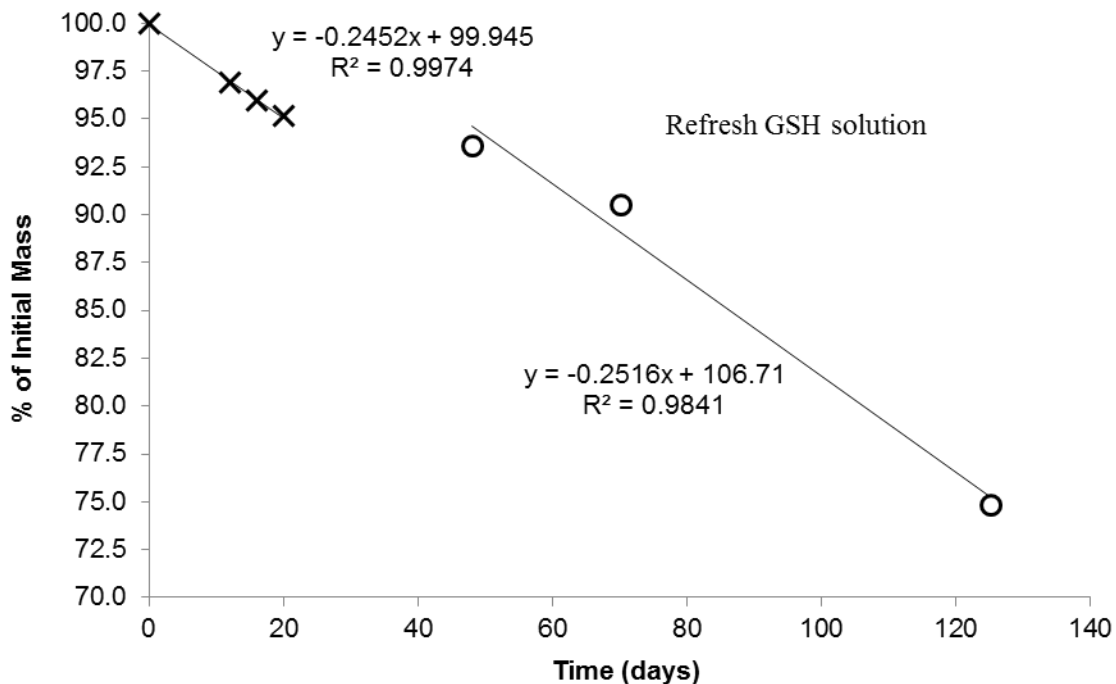


Figure 4.5.25. The degradation of DL-CM-95 by GSH(50 mM in acetate buffer; pH = 5.2; 37°C) with time is shown.

When sample DL-CM-95 was incubated with aqueous GSH at 37°C it became transparent. When a small sample of DL-CM-95 was placed in the oven alone and it also became translucent. The loss of opacity was thought to indicate a loss of crystallinity. Because crystallinity often adds strength to elastomers, the tensile strength of compression molded α -LA was tested at 37°C.

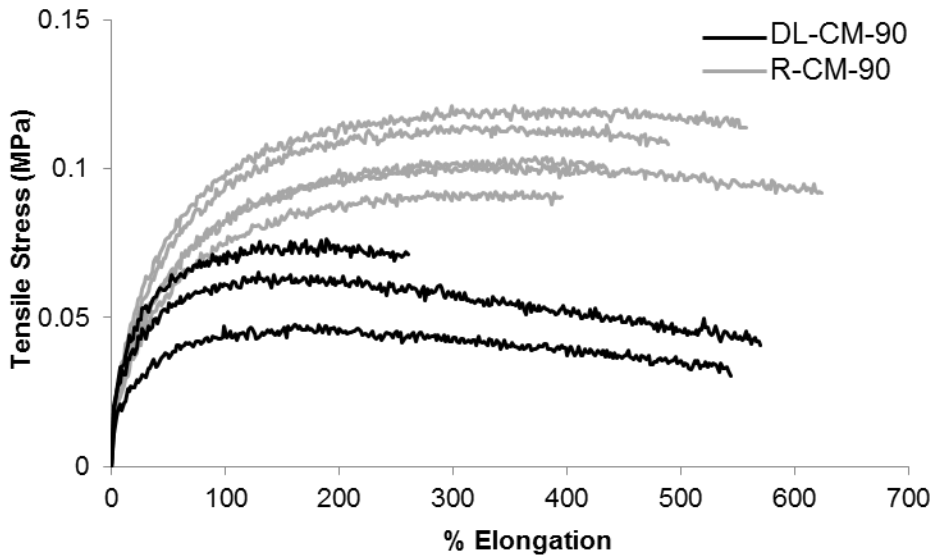


Figure 4.5.26. Tensile curves from samples DL-CM-90 and R-CM-90 at 37°C (extension rate = 500 mm/min).

The tensile curves from DL-CM-90 and R-CM-90 are shown in Figure 4.5.26.

The samples were measured on a tensiometer with a temperature-control chamber set to 37°C. Sample DL-CM-90 showed an UTS of 0.060 MPa (average of 3 measurements), while R-CM-90 had a UTS of 0.105 MPa (average of 5 measurements). The tensile properties of compression molded DL- α -LA at 37°C are much lower than at room temperature.

4.5.1.3. Polymerization of R- α -LA at air/water interface.

It was observed that polymeric films would form at the air/water interface when a solution of α -LA was dropped onto the surface of water. The formation of α -LA polymers at the air/water interface was further investigated. A 0.500 M solution of α -LA in THF was prepared. Using a syringe, 0.50 mL of the solution was dropped onto the

surface of water at three temperatures (25, 65 and 100°C). The off-white products which formed at the air/water interface was collected and dried in a vacuum oven. These samples are named by the monomer, R enantiomer, PPTN (precipitation) and by the temperature of the water. The conversion of each reaction is shown in Table 4.5.5.

Table 4.5.6. Yield and conversion data for the three precipitation polymers.

Sample	DI H ₂ O Temp (C)	Mass Product (g)	% Conv. of α-LA
R-PPTN-25	25	0.0279	47.9
R-PPTN-65	65	0.0241	41.3
R-PPTN-100	100	0.0218	37.4

In the SEC analysis, polymers were dissolved in THF and filtered through a 0.45 μm PTFE filter. R-PPTN-100 went through the filter without difficulty. R-PPTN-65 was more difficult to push through the filter, and sample R-PPTN-25 was the most difficult. The results from R-PPTN-65 and R-PPTN-100 are shown in Table 4.5.6. SEC data for R-PPTN-25 is not available because not enough polymer remained in solution after sample preparation, and RI signals were very weak.

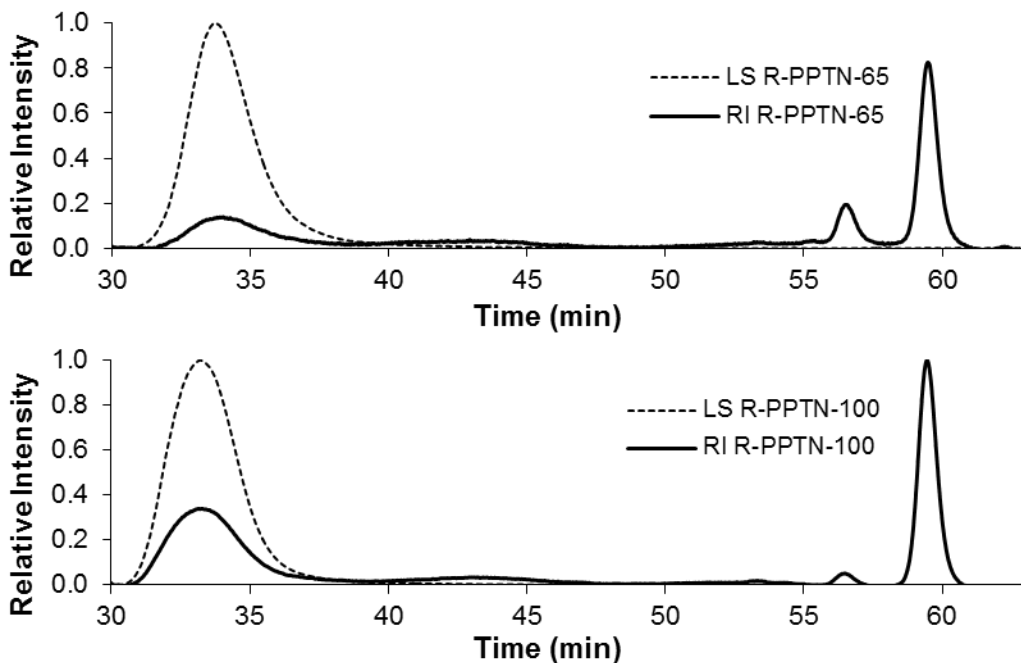


Figure 4.5.27. SEC traces (LS and RI) from poly(α -LA) samples R-PPTN-65 and R-PPTN-100.

Table 4.5.7. SEC data for polymers synthesized by precipitation ($dn/dc = 0.109 \text{ mL/g}$).

Sample	M_n (g/mol)	M_w (g/mol)	M_w/M_n	R_{gz} (nm)	R_{hw} (nm)	$[\eta]_w$ (mL/g)
R-PPTN-65	2,672,000	3,414,000	1.28	92.0	56.6	354.7
R-PPTN-100	4,207,000	4,583,000	1.09	111.5	69.8	489.4

The SEC traces for the two products are shown in Figure 4.5.19. In addition to the peak in the high molecular weight region, both SEC traces show large peaks in the low molecular weight region of the chromatogram. The high molecular weight products from R-PPTN-65 and R-PPTN-100 reach M_n well over 1,000,000 g/mol, which is the upper detection limit of the instrument.

While the thermal polymerization of α -LA acid has been reported in the literature, polymerization of α -LA by water represents a new, and particularly green method for the synthesis of poly(α -LA). As described here previously the poly(α -LA) is collected from the air/water interface. During this process, it is also possible to create polymer filaments which are pulled from the interface. Figure 4.5.28. shows a polymer fiber pulled from the same system used in R-PPTN-25. A patent disclosure has been submitted to the University regarding this new method of polymerization and fiber processing.



Figure 4.5.28. Poly(α -LA) filament is pulled from R- α -LA precipitated onto H₂O at 25°C.

4.6. Synthesis of monofunctional α -LA derivatives via enzymatic catalysis.

The polymers of α -LA are not water soluble. Water-soluble α -LA-based polymers may also be of use, particularly in biomedical applications, like hydrogels. Also, the reduction of poly(DL- α -LA) by glutathione (GSH) under aqueous conditions was shown to be relatively slow. Increasing the water intrusion rate of α -LA-based polymers, by increasing the water solubility of the monomers, may also increase the rate of degradation by water soluble reducing agents like GSH. With this in mind the use of enzymatic catalysis in the synthesis of water soluble α -LA-based monomers was investigated.

4.6.1. Synthesis of α -LA-DEG-CH₃

The esterification reaction of diethylene glycol methyl ether (DEG) with R- α -LA was catalyzed using *Candida antarctica* lipase B. Three concentrations of DEG were investigated. The reactions were performed at 55°C in covered test tubes under normal atmosphere. The reagent concentrations and yields of the reactions are shown in table 4.43. Reactions are labeled by the concentration of DEG starting material. Dry THF was used as the solvent in the LA-DEG-1.0 and LA-DEG-0.5 reactions.

Table 4.6.1. Conversion results from reaction of CH₃-DEG and α -LA after 14 hours at 55°C.

Sample	[R- α -LA]	[DEG]	% Conv.
R-LA-DEG-Bulk	0.50 mol/L	8.49 mol/L	97.0
R-LA-DEG-1.0	0.50 mol/L	1.00 mol/L	91.6
R-LA-DEG-0.5	0.50 mol/L	0.48 mol/L	85.3

The ESI mass spectrum of each reaction is shown in Figure 4.6.1. The ^1H NMR spectrum of the bulk reaction is shown if Figure 4.6.2 and is representative of the other two reactions.

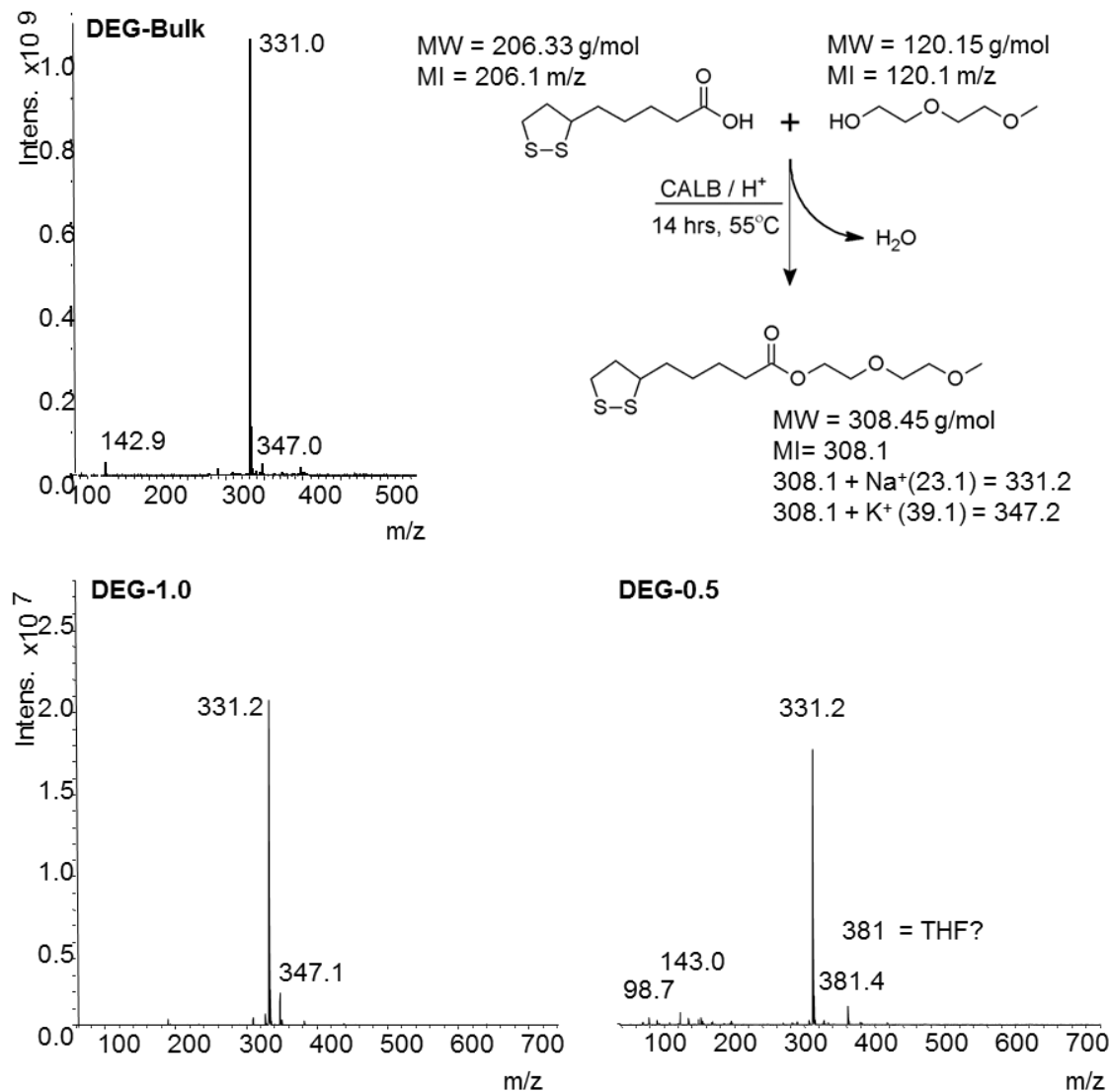


Figure 4.6.1. ESI mass spectra for the products of α -LA and DEG esterification.

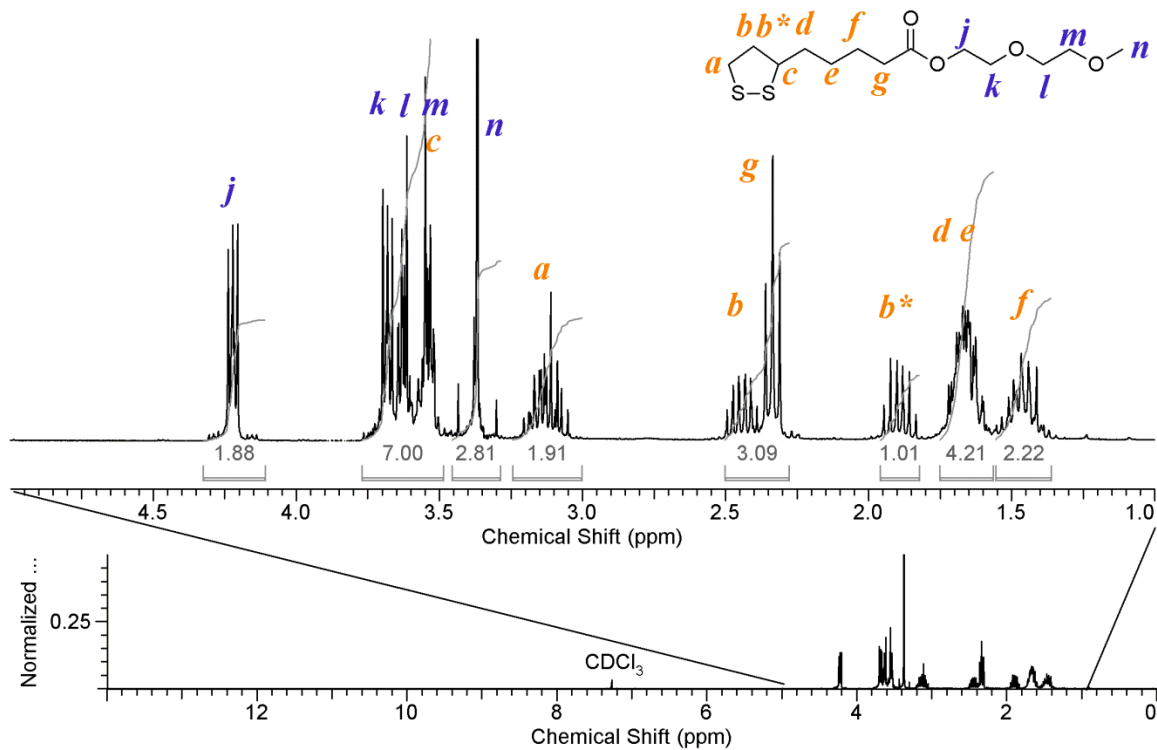


Figure 4.6.2. ^1H NMR spectrum of sample DEG-LA-Bulk (3 s relax.; 64 scans; 500 MHz; CDCl_3).

The yield of the CH_3 -DEG- α -LA conjugate was improved by increasing the concentration of DEG-CH_3 . The bulk reaction returned 97.0% of the desired CH_3 -DEG- α -LA product. All three samples show a strong peak at 331 m/z which corresponds to the molecular weight of the desired product plus the sodium counter ion ($308+23 = 331$). None of the ESI spectra show unreacted α -LA (no peak at 229 m/z ($206+23 = 229$)) indicating that all α -LA was converted to CH_3 -DEG- α -LA. The spectra from R-LA-DEG-Bulk and R-LA-DEG-0.5 reactions each show a small peak at 143 m/z. This peak does not appear in the MS-MS spectra of the molecular ion peak, and is attributed to trace amounts of residual CH_3 -DEG-OH ($120 + 23 = 143$).

4.6.2. Synthesis of α -LA-TEG-OH and α -LA-HEG-OH

The CALB-catalyzed esterification reactions of R- α -LA with TEG and with HEG were performed in bulk under a N₂ atmosphere at 55°C. Reactions were stopped after 4 hrs. The ESI mass spectra of the products are show in Figure 4.6.3 and 4.6.4. The 1H NMR spectra for the two products are shown in Figure 4.73.

Table 4.6.2. Reagent concentrations and conversions for α -LA-TEG-OH and α -LA-HEG-OH synthesis.

Sample	[R- α -LA]	[DEG-CH ₃]	% Conv.
R-LA-TEG	0.25 mol/L	5.25 mol/L	77.6
R-LA-HEG	0.25 mol/L	3.99 mol/L	100.0

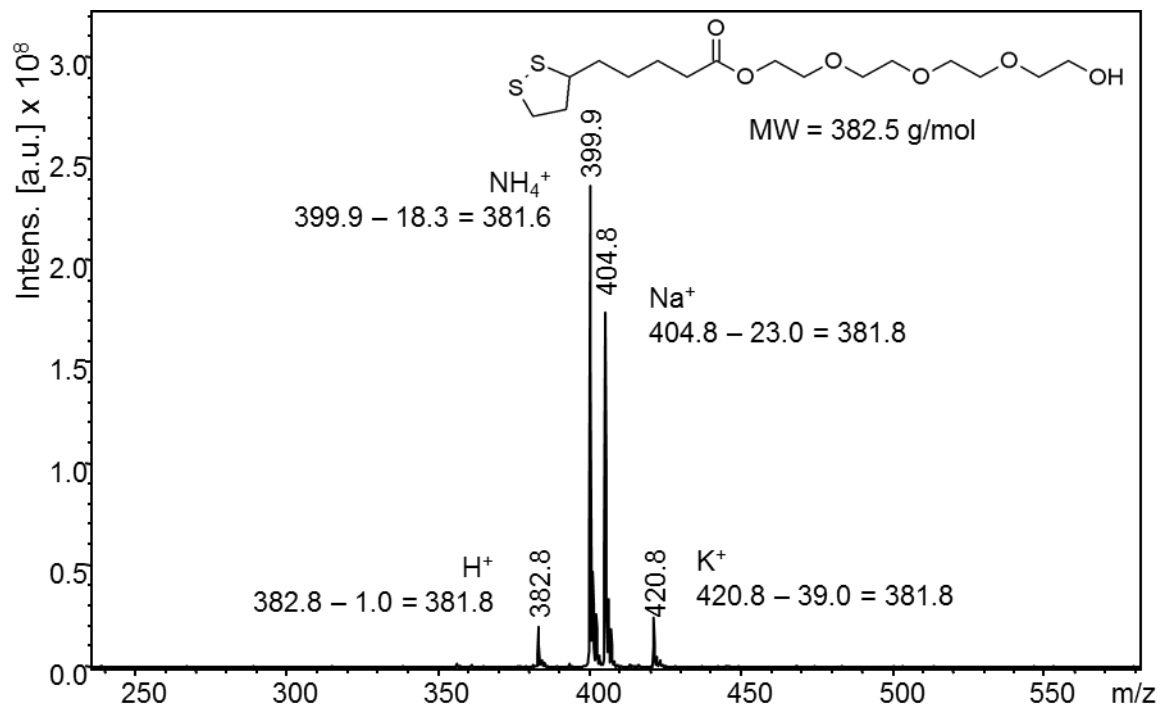


Figure 4.6.3. ESI mass spectrum from the product of α -LA and TEG esterification in bulk.

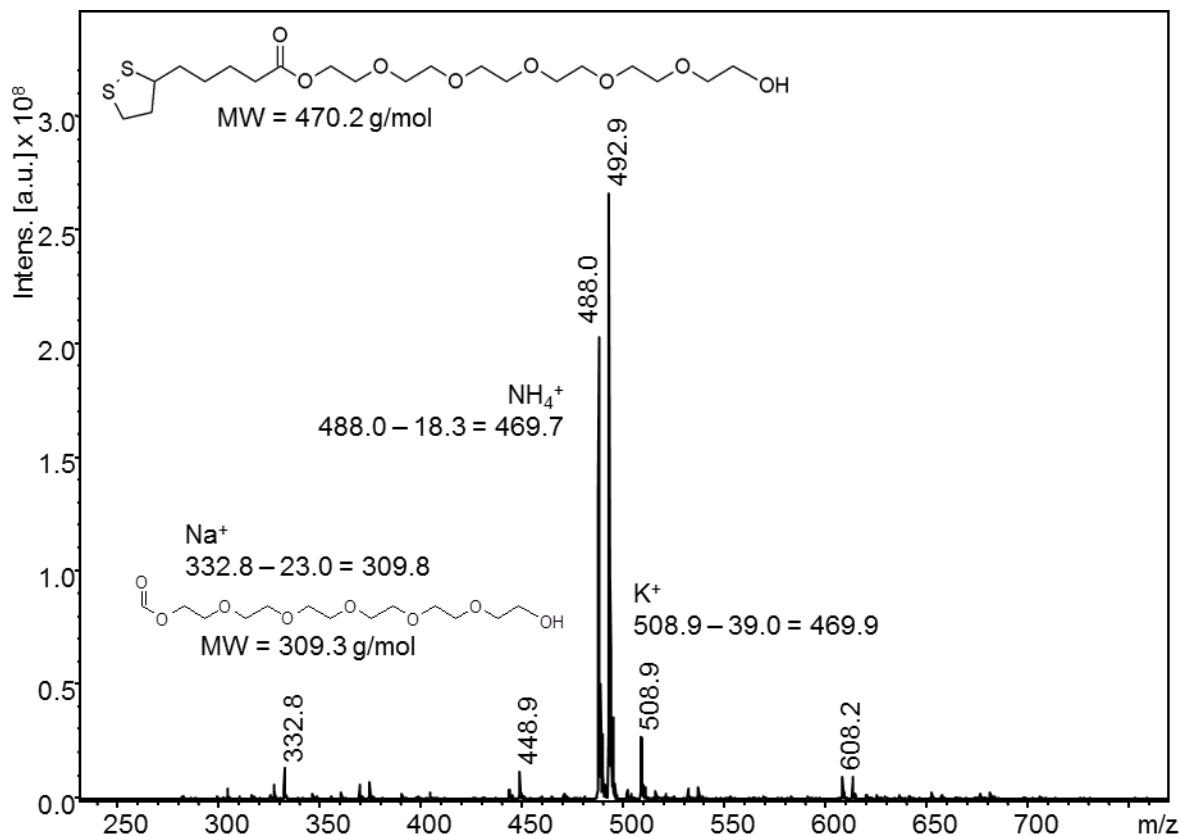


Figure 4.6.4. ESI mass spectrum from the product of α -LA and HEG esterification.

Figures 4.6.3 and 4.6.4 show the ESI results for the product of α -LA conjugation with TEG and HEG respectively. The ESI results for both glycols indicate that the monofunctional products were produced. To peaks corresponding to starting materials are not present in the spectra. Additionally, peaks corresponding to the difunctionalized glycols are not seen. The desired lipoate conjugate accompanied by an NH_4^+ counter ion appears in both spectra one of the dominant species.

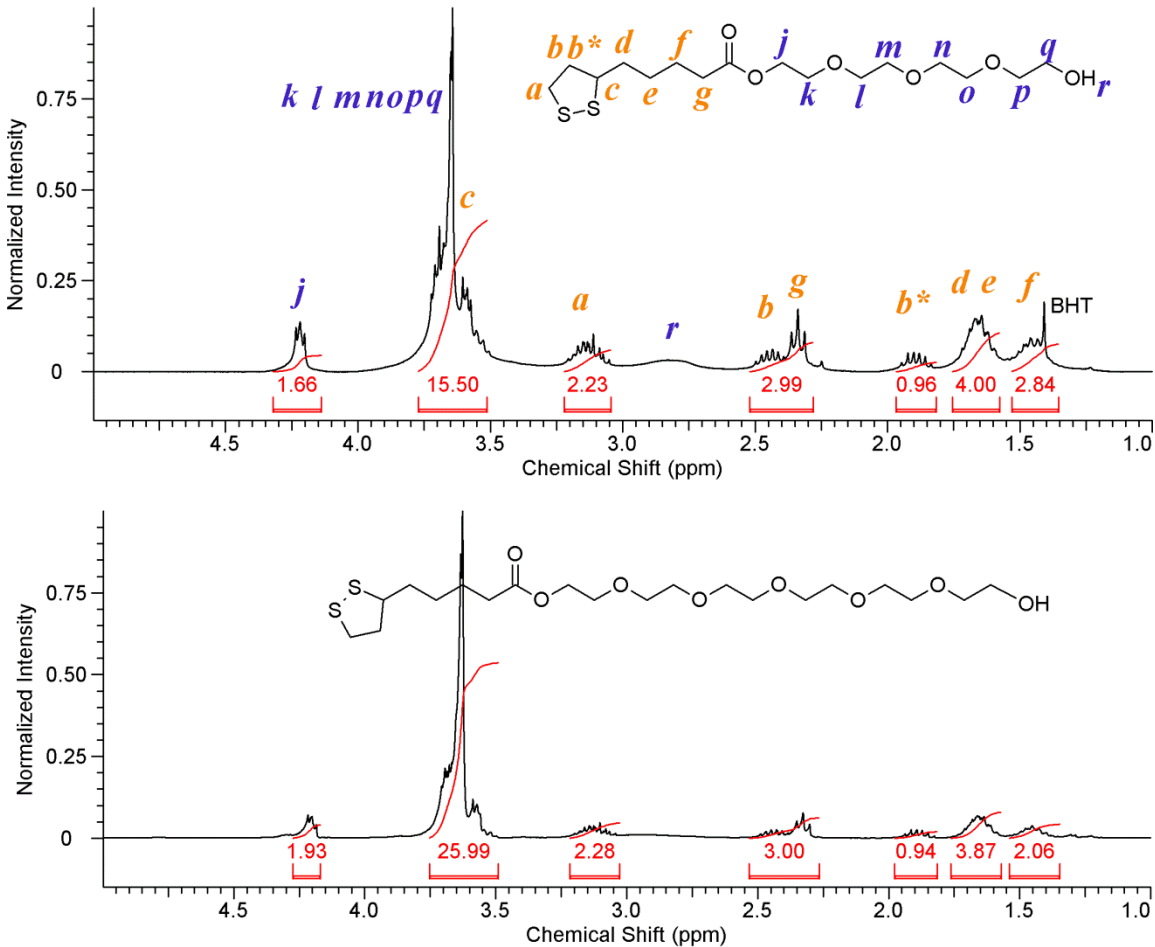


Figure 4.6.5. Proton NMR spectra are compared for the TEG and HEG product. (3 s relax, 64 scans in CDCl_3).

The results from the conjugation of α -LA to DEG, TEG, HEG and PEG (Section 4.5) show that CALB-catalyzed esterification is an effective method of synthesis. The α -LA-glycol conjugates may serve as monomers in future work, and have already been used in our group to functionalize poly(isobutylene) polymers.

CHAPTER V

CONCLUSIONS

Poly(disulfide) polymers are among the oldest synthetic polymers, and yet academic investigation into these unique polymers has been limited and sporadic over the past 90 years. Industrial investigation into poly(disulfide) polymers lead to their use in niche markets such as roofing, adhesives and solid rocket propellants. However, as a biologically active covalent bond, the disulfide group has found new commercial applications in the biomedical field. The disulfide bond is readily cleaved under reducing conditions found within organisms, particularly in the cytosol. The disulfide bond is also readily synthesized under oxidizing biological conditions. These mild oxidizing conditions lend themselves to the development of new synthetic strategies that follow a green chemistry approach. With green chemistry practices in mind, we set out synthesize disulfide-bonded polymers and networks for anticipated use in biodegradable biomedical applications.

Here, new methods of poly(disulfide) polymer synthesis were presented. The first new method presented was developed to polymerize dithiol monomers, DODT and ED, in an oxidative mechanism. At the beginning of the reaction, two phases were present—an organic phase, made up of the monomer and triethylamine, and an oxidizing aqueous phase, which was made up of dilute H₂O₂. This two phase system produced DODT polymers with M_n> 250,000 and with molecular weight distributions as low as 1.15.

Maintaining a two phase system was critical to producing high molecular weight polymers. When the reaction temperature was maintained below the lower critical solution temperature of triethylamine and water (~18°C) only oligomers (dimer, trimer and tetramer) were produced, and the reaction mixture formed a stable emulsion. Reaction systems which were started at 0°C, but reached temperatures above 18°C during the reaction (exothermic), produced polymers ($M_n > 110,000$ g/mol in 25 min) with a high content of oligomers (40-60%). Reactions which were started at room temperature (ie. above the LCST) and reached a maximum temperature of 55°C produced the highest molecular weight polymers ($M_n > 250,000$ g/mol in 2 hrs) with a low concentration of oligomers. Room temperature polymerizations which reached a maximum temperature of 70°C produced high molecular weight polymers (48,000 g/mol in 2 hrs) with a low concentration of oligomers. MALDI-ToF analysis showed that all oligomers were cyclic. NMR analysis of the polymers showed the absence of thiol end groups in all polymers except for those that reached 70°C.

In addition to the effect of reaction temperature, the effect of triethylamine concentration (on reactions started at room temperature) was investigated. Triethylamine plays two seemingly opposed roles in the new polymerization mechanism. First, it creates an organic phase which is immiscible with the aqueous phase. Second, it ionizes the thiol groups which makes the monomer soluble in the oxidative aqueous phase. Changing the concentration of triethylamine greatly affected the kinetics of polymerization reaction. At the low extreme of triethylamine concentration investigated (0.833 M or 1:1 molar ratio with DODT), the maximum conversion reached was 50 % and the M_n v. conversion plot resembled that of a step polymerization with low molecular weights at low

conversions. When triethylamine was present in 2:1—2.5:1 molar ratio with DODT conversions reached over 90% and the M_n v. conversion plot looked more like a controlled radical polymerization., with M_n increasing almost linearly with conversion. At the high concentration extreme, with triethylamine in a 6:1 molar ratio with DODT, conversion reached about 80%, and the M_n v. conversion plot looked more like an uncontrolled radical polymerization, with high M_n reached at low conversions. The chain extension experiment demonstrates the system also has living character.

Hydrogen peroxide concentration greatly affects the molecular weight of the resulting polymers. Under otherwise identical conditions, a reduction in the H_2O_2 concentration by $\frac{1}{2}$ (from 0.751 M to 0.375 M) lead to a $\frac{9}{10}$ reduction in M_n , from 52,000 g/mol to 5,000 g/mol. Mechanical stirring (high shear) also lead to reduced molecular weights. The M_n of magnetically stirred copolymers was 263,000 g/mol while the M_n of mechanically stirred copolymers was 42,000 g/mol. Under high shear conditions, the interface between organic and aqueous phases was disrupted and the two phases are forced to mix which increased the number of reacting species and decreased the polymer molecular weight. In support of this suggestion, the mechanically stirred polymers had a broader molecular weight distribution.

From our experimental results we propose a mechanism for poly(disulfide) polymer synthesis that combines chain-growth and step-growth pathways. Figure 5.1. shows a cartoon of our proposed mechanism. The first step is monomer activation. The dithiol is prepared for oxidation by the creation of the dianion by triethylamine (represented by the triangle). The dianion is then oxidized (by hydrogen peroxide) to produce the active diradical monomer species. The active species quickly couple to form

the dormant cyclic dimer. The dimer may be reactivated by another diradical and undergo a chain growth, ring-opening polymerization that successively adds dormant dimers to the polymeric ring. In the two-phase polymerization system (at T>18.7°C) this mechanism appears to dominate leading to high molecular weights and molecular weight distributions that correspond to radical coupling. In the step-growth pathway, the dimer may react with another diradical and form the dormant trimer. In turn the trimer may be reactivated by another radical species to form at tetramer and so on. In a single-phase polymerization (at T<18.7°C), this pathway appears to dominate and because conditions are dilute, only oligomeric species are formed.

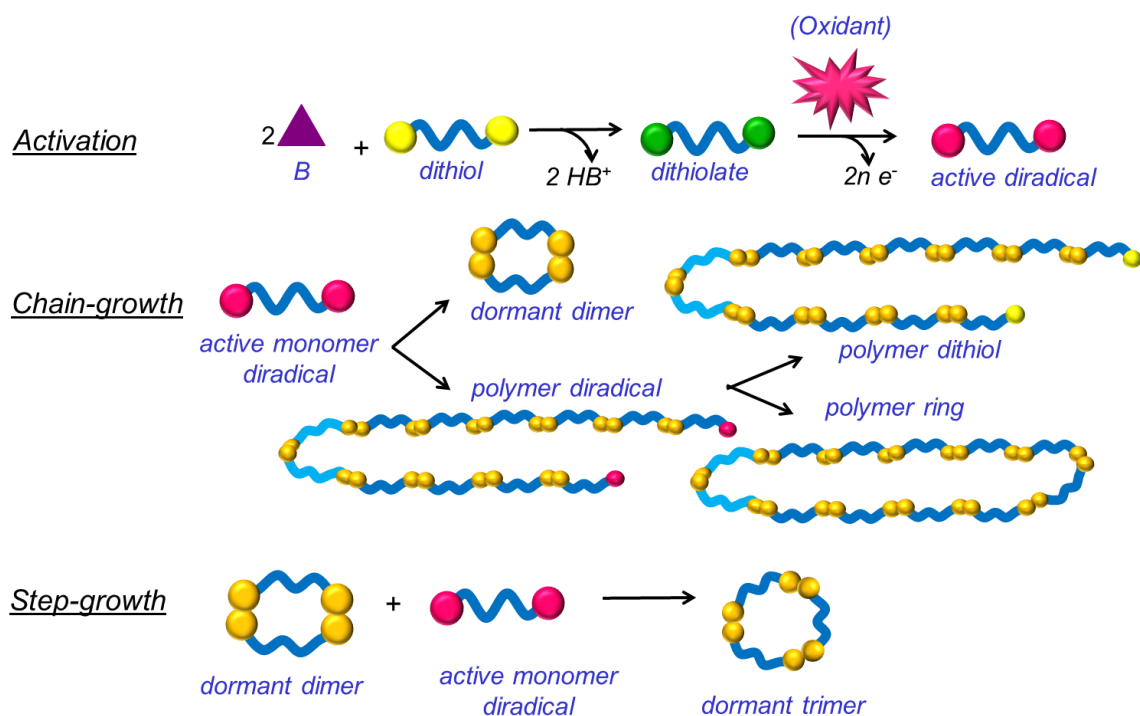


Figure 5.1. Proposed mechanism for new method of oxidative dithiol polymerization includes both chain-growth and step-grow pathways.

It is hoped that work reported here on dithiol polymerization and poly(disulfide) polymers will encourage further investigation into the mechanism and structure of polymers. Further investigation into the solution dynamics and rheological properties are needed to elucidate the structure of the high molecular weight polymers. From a chemical engineering perspective, another interesting avenue of investigation would be the development of a continuous batch process for this new oxidative polymerization system. Empirically it was found that the scale of the reaction also affects the polymers produced, which follows logically from the importance of both temperature and mixing rate (or interfacial area). Further investigation into controlling the molecular weights through reaction scale would be interesting.

A variation of the new polymerization system was applied to the synthesis of poly(DODT)-based networks. Here monomer and crosslinker were reacted together in – one-pot process that, like the polymerization reactions, proceeded in a two phase system. The networks synthesized swelled in THF, chloroform and acetone (slightly), but did not swell in hexanes, or water. Swelling in THF was used to calculate the crosslink density of the networks from the Flory-Rehner equation. The network with the lowest concentration of crosslinker swelled the most and had a calculated $M_c = 7,000$ g/mol. The networks were completely degraded by DTT, indicating the exclusive presence of disulfide crosslinks, but were stable under conditions which modeled biological conditions. The networks are flexible, non-malodorous, and merit further investigation into their possible applications.

The new method of polymerization was applied to the monomer α -lipoic acid, which is a natural anti-oxidant biochemical that contains disulfide bond in its thiolane

ring. With this monomer, a two phase system was only seen at the beginning of the reaction, but after 2 hrs reaction time, a clear solution was formed. Unlike the polymerization of DODT, a polymer phase did not form during the reaction. Instead, the solution (basic pH) was neutralized to recover the polymer. The same monomer was polymerized thermally in a reaction flask under vacuum and in a compression mold to model industrial manufacturing procedures. Polymers from thermal polymerization were decorated using an enzyme-catalyzed esterification reaction and imaged with AFM to reveal branch-like structures.

Additionally, a new method of polymerization was developed for this monomer. In this new method, an organic solution of the monomer is dropped onto the surface of water and the polymer forms at the air-water interface. Filaments of the polymer may be pulled from the surface of the water. This process is truly green as the monomer may be dissolved in ethanol and because the reaction proceeds at room temperature. Any residual solvents would just be water and ethanol.

Poly(α -lipoic) acid showed slow degradation in a glutathione solution, confirming its ability to degrade under biological conditions. Using CALB-catalyzed transesterification, conjugates of α -LA were synthesized in high conversions. Conjugates synthesized include α -LA-DEG-CH₃, α -LA-TEG, α -LA-HEG, α -LA-PEG. We believe this polymer and polymers from derivatives of this polymer have great potential as biomaterial.

It is interesting that the two new methods of polymer synthesis presented rely on multi-phase systems. While multiphase systems are employed in organic synthesis, we, as chemists, often have a habit of first looking to solution-state chemistry. It is hoped

that this work will also foster renewed interest into multi-phase reaction systems, their application to geener synthetic strategies.

REFERENCES

- 1 Anastas, P. T.; Warner, J. C. *Green Chemistry: Theory and Practice*, Oxford University Press: New York, **1998**, p.30.
- 2 Odian, G. *Priciples of Polymerization, 4th Ed.* Hoboken, NJ: John Wiley & Sons, Inc.; **2004**.
- 3 Patrick, J.C. Method of Making Plastic Substances and Products Obtained Thereby. US Patent 1,890,191. Dec.6, 1932.
- 4 Patrick, J.C. Polysulfide Polymer. US Patent 2,553,206. May 15, 1951.
- 5 Patrick, J.C.; Mnookin, N.M. Method of Making Plastic Substances and Products Obtained Thereby. US Patent 1996486, April 2, 1935.
- 6 Fettes, E.M.; Jorczak, J.S. Polysulfide Polymers. *Industrial and Engineering Chemistry*, **1950**, 42, 2217-2223.
- 7 Kishore, K.; Ganesh, K. Polymers containing disulfide, tetrasulfide, diselenide and ditelluride linkages in the main chain. *Advances in Polymer Science*, **1995**, 121, 83-121.
- 8 Ramakrishnan, L.; Sivaprakasam, K. Synthesis, characterization, thermal degradation, and comparative chain dynamics studies of weak-link polysulfide polymers. *Journal of Polymer Research*, **2009**, 16, 623-635.
- 9 Kalaei, M.R.; Famili, M.H.N.; Mahdavi, H. Synthesis and characterization of polysulfide rubber using phase transfer catalyst. *Macromolecular Symposium*, **2009**, 277, 81-86.
- 10 Oae, S. *Organic Sulfur Chemsitry: Structure and Mechanism*. Ann Arbor, MI: CRC Press, **1991**.
- 11 Danehy, J.P.; Noel, C.J. *Journal of the American Chemical Society*, **1960**, 82, 2511-2515.
- 12 Ballinger, P.; Long, F.A. *Journal of the American Chemical Society* **1960**, 82, 795-798.

- 13 Marvel, C.S.; Olson, L.E. Polyalkylene Disulfides. *Journal of the American Chemical Society*, **1957**, 79, 3089-3092.
- 14 Bonsignore, P.V.; Marvel, C.S.; Banerjee, S. Polyalkylene disulfides and polysulfides containing silicon. *Journal of Organic Chemistry*, **1960**, 25, 237-240.
- 15 Whistler, R.L.; Hoffman, D.J. Preparation and polymerization of a sugar dithiol. *Journal of Polymer Science: Part A-1*, **1967**, 5, 2111-2117.
- 16 Meng, Y.Z.; Hllil, A.R.; Hay, A.S. Synthesis of macrocyclic aliphatic disulfide oligomers from dithiols by oxidative coupling with oxygen using a copper-amine catalyst. *Polymers for Advanced Technology*, **2004**, 15, 564-566.
- 17 Meng, Y.Z.; Tjong, S.C.; Hay, A.S. Synthesis of cocylic(arylene disulfide)oligomers and their adhesion properties as heating-melt adhesive. *Polymer*, **2001**, 42, 5215-5224.
- 18 Song, L.N.; Xiao, M.; Shu, D.; Wang, S.J.; Meng, Y.Z. Mechanical and thermal properties of poly(arylene disulfide) derived from cyclic(4,4'-oxybis(benzene)disulfide) via ring-opening polymerization. *Journal of Materials Science*, **2007**, 42, 1156-1161.
- 19 Choi, W.; Sanda, F.; Kihara, N.; Endo, T. A novel one-pot oxidation polymerization of dithiols obtained from bifunctional five-membered cyclic dithiocarbonates with amines. *Journal of Polymer Science: Part A: Polymer Chemistry*, **1998**, 36, 79-84.
- 20 Cerritelli, S.; Velluto, D.; Hubbell, J.A. PEG-SS-PPS: Reduction-sensitive disulfide block copolymer vesicles for intracellular drug delivery. *Biomacromolecules*, **2007**, 8, 1966-1972.
- 21 Ishida, H.; Kisanuki, A.; Endo, K. Ring-opening polymerization of aromatic 6-membered cyclic disulfide and characterization of the polymer. *Polymer Journal*, **2009**, 41, 110-117.
- 22 Goethals, E.J.; Sillis, C. Oxidation of dithiols to polydisulfides by means of dimethylsulfoxide. *Macromolecular Chemistry and Physics*, **1968**, 119, 249-251.
- 23 Meng, Y.Z.; Liang, Z.A.; Lu, X.Y.; Hay, A.S.; Aromatic disulfide polymers back to macrocyclic disulfide oligomers via cyclo-depolymerization reaction. *Polymer*, **2005**, 46, 11117-11124.

- 24 Wang, X.-L.; Jensen, R.; Lu, Z.-R. A novel environmental-sensitive biodegradable polydisulfide with protonatable pendants for nucleic acid delivery. *Journal of Controlled Release*, **2007**, *120*, 250-258.
- 25 Sun, Z.; Geng, Y.; Li, J.; Jing, Xiabin, J. Wang, F. Chemical polymerization of aniline with hydrogen peroxide as oxidant. *Synthetic Metals*, **1997**, *84*, 99-100.
- 26 Ikeda, R.; Tanaka, H.; Uyama, H.; Kobayashi, S. *Macromolecules*, **2000**, *33*, 6648-6652.
- 27 Augustine, R.L., Ed. Oxidation: Techniques and Applications in Organic Synthesis, Vol 1. New York: Marcel Dekker, Inc., **1969**, 247-248.
- 28 Pascal, I.; Tarbell, D.S.; The kinetics of the oxidation of a mercaptan to the corresponding disulfide by aqueous hydrogen peroxide. *Journal of the American Chemical Society*, **1957**, *79*, 6015-6020.
- 29 Supale, A.; Gokavi, G. Oxidation of thiols to disulfides using H_2O_2 catalyzed by recyclable chromic potassium sulphate at room temperature. *Catalysis Letters*, **2008**, *93*, 141-148.
- 30 Hanhela, P.J.; Mazurek, W. Thermal stability of sealants for military aircraft: Modification of polysulfide prepolymers with ether and thioether monomers. Australian Patent AD-A264 079, February 1993.
- 31 Tatsuma, T.; Yokoyama, Y.; Buttry, D.A.; Oyama, N. Electrochemical polymerization and depolymerization of 2,5-dimercapto-1,3,4-thiadiazole. QCM and spectroscopic analysis. *Journal of Physical Chemistry B*, **1997**, *101*, 7556-7562.
- 32 Endo, K.; Bu, H.-B. Synthesis of disulfide polymer by electrochemical polymerization. *Polymer*, **2001**, *42*, 3915-3198.
- 33 Endo, K.; Bu, H.-B. Electrochemical polymerization of 1,10-decanedithiol in CH_2Cl_2 and additive effect of benzylmercaptan. *Journal of Electroanalytical Chemistry*, **2001**, *506*, 155-161.
- 34 Mason, T.J. Ultrasound in synthetic organic chemistry. *Chemical Society Reviews*, **1997**, *26*, 443-451.
- 35 Garcia Ruano, J.L.; Parra, A.; Aleman, J. Efficient synthesis of disulfides by air oxidation of thiols under sonication. *Green Chemistry*, **2008**, *10*, 706-711.

- 36 Hisano, N.; Morikawa, N.; Iwata, H.; Ikada, Y. Entrapment of islets into reversible disulfide hydrogels. *Journal of Biomedical Materials Research* **1998**, *40*, 115-123.
- 37 Shu, X. Z.; Liu, Y.; Palumbo, F.; Prestwich, G. D., Disulfide-crosslinked hyaluronan-gelatin hydrogel films: a covalent mimic of the extracellular matrix for in vitro cell growth. *Biomaterials* **2003**, *24*, 3825-3834.
- 38 Yoshida, H.; Klinkhammer, K.; Matsusaki, M.; Möller, M.; Klee, D.; Akashi, M. Poly(γ -glutamic acid) nonwovens as reduction-responsive scaffolds. *Macromolecular Bioscience*, **2009**, *9*, 568-574.
- 39 Koo, H.; Jin, G.; Lee, Y.; Mo, H.; Cho, M. Y. Synthesis of Poly(ethylene oxide sulfide) with Large Molecular Weight by O₂ Gas Oxidation. *Bulletin of the Korean Chemical Society*, **2005**, *26*, 2069-2071.
- 40 Koo, H.; Jin, G.-W.; Kang, H.; Lee, Y.; Nam, H.Y.; Jang, H.-S.; Park, J.-S. A new biodegradable crosslinked polyethylene oxide sulfide (PEOS) hydrogel for controlled drug release. *International Journal of Pharmaceutics*, **2009**, *274*, 58-65.
- 41 Ding, Z. Y.; Aklonis, J. J.; Salovey, R. Model filled polymers. VI. Determination of the crosslink density of polymeric beads by swelling. *Journal of Polymer Science: Part B Polymer Physics*, **1991**, *29*, 1035-1038.
- 42 Peacock, A. J.; Calhoun, A. *Polymer Chemistry: Properties and Applications*; Hanser Gardner: Cincinnati, **2006**.
- 43 Zeng, W.; Du, Y.; Xue, Y.; Frisch, H. L. Chapter 16: Solubility Parameters. In *Physical Properties of Polymers Handbook*, 2nd Ed.; Springer: New York, **2007**, 289-303.
- 44 Small, P. A. Some factors affecting the solubility of polymers. *Journal of Applied Chemistry*, **1953**, *3*, 71-80.
- 45 van Krevelen, D. W.; te Nijenhuis, K. *Properties of Polymers*, 4th Ed.; Elsevier: Amsterdam, **2009**.
- 46 Hoy, K. L. New values of solubility parameters from vapor pressure data. *Journal of Paint Technology*, **1970**, *42*, 76-118.
- 47 Shirley, B.A., Ed. Protein stability and folding: Theory and practice. New York: Humana Press, **1995**.

- 48 Bindoli, A.; Rigobello, M.P.; Scutari, G.; Cabbiani, C.; Casini, A.; Messori, L. Thioredoxin reductase: A target for gold compounds acting as potential anticancer drugs. *Coordination Chemistry Reviews*, **2009**, 253, 1692-1707.
- 49 Jacob, C.; Knight, I.; Winyard, P.G.; Aspects of biological redox chemistry of cysteine: from simple redox responses to sophisticated signaling pathways. *Biological Chemistry*, **2006**, 10, 1385-1397.
- 50 Yano, Y.; Ohshima, M. Sutoh, S.; Nakazato, M. Flavin mimics possessing remarkably high oxidizing power: 6,8-diazaflavins. *Chemical Communications*, **1984**, V, 1031-1032.
- 51 Yano, Y.; Oshima, M.; Yatsu, I.; Sutoh, S. High oxidizing activity of 3, 10-dimethyl-8-azaalloxazine (8-azaflavin) and its synthetic application as a turnover redox catalyst under aerobic conditions. *Journal of the Chemical Society, Perkins Translations 2*, **1985**, 6, 753-758.
- 52 Holden, J.W.; Main, L. The kinetics and mechanism of the oxidation of mercaptoethanol by riboflavin. *Aust. J. Chem.* **1997**, 30, 1387-1391.
- 53 Holmgren, A.; Bjornstedt, M. Packer, L.; Ed. Biothiols, Part B, Glutathione and Thioredoxin: Thiols in signal transduction and gene regulation. *Methods in Enzymology*, **1995**, 252, 199-301.
- 54 Faris, R.J.; Wang, H.; Wang, T. Improving the digestibility of soy flour by reducing disulde bonds with thioredoxin. *Journal of Agricultural and Food Chemistry*, **2008**, 56, 7146-7150.
- 55 Mustacich, D.; Powis, G. Thioredoxin reductase. *Biochemistry Journal*, **2000**, 346, 1-8
- 56 Rosenthal-Kim, E. Q.; Puskas, J. E.; *Pure and Applied Chemistry*, **2012**, 84, 2121-2133.
- 57 Randall, L.O. Reaction of thiol compounds with peroxidase and hydrogen peroxide. *Journal of Biological Chemistry*, **1946**, 164, 521-527.
- 58 Faber, K. Biotransformations in Organic Chemistry, 5th Ed. New York: Springer-Verlag, **2004**.
- 59 Packer, L.; Witt, E. H.; Tritschler, H. J., Alpha-lipoic acid as a biological antioxidant. *Free Radical Biology and Medicine*, **1995**, 19, 227-250.

- 60 Alleva, R.; Nasole, E.; Di Donato, F.; Borghi, B.; Neuzil, J.; Tomasetti, M., alpha-Lipoic acid supplementation inhibits oxidative damage, accelerating chronic wound healing in patients undergoing hyperbaric oxygen therapy. *Biochemical and Biophysical Research Communications* **2005**, *333*, 404-410.
- 61 Ramachandran, L.; Krishnan, C.V.; Nair, C.K.; Radioprotection by alpha-lipoic acid palladium complex formulation (POLY-MVA) in mice. *Cancer Biother Radiopharm.* **2010**, *4*, 395-339.
- 62 Akram, M.; Stuart, M. C.; Wong, D. K. Y., Direct application strategy to immobilise a thioctic acid self-assembled monolayer on a gold electrode. *Analytica Chimica Acta* **2004**, *504*, 243-251.
- 63 Wang, H.; Chen, S.; Liu, L.; Jiang, S. Improved method for the preparation of carboxylic acid and amine terminated self-assembled monolayers of alkanethiolates. *Langmuir*, **2005**, *21*, 2633-2636
- 64 Langry, K. C.; Ratto, T. V.; Rudd, R. E.; McElfresh, M. W., The AFM measured force required to rupture the dithiolate linkage of thioctic acid to gold is less than the rupture force of a simple gold–alkyl thiolate bond. *Langmuir*, **2005**, *21*, 12064-12067.
- 65 Dijksma, M.; Boukamp, B. A.; Kamp, B.; van Bennekom, W. P., Effect of Hexacyanoferrate(II/III) on Self-Assembled Monolayers of Thioctic Acid and 11-Mercaptoundecanoic Acid on Gold. *Langmuir*, **2002**, *18*, 3105-3112.
- 66 Karamanska, R.; Mukhopadhyay, B.; Russell, D. A.; Field, R. A., Thioctic acid amides: convenient tethers for achieving low nonspecific protein binding to carbohydrates presented on gold surfaces. *Chemical Communications (Camb)* **2005**, *26*, 3334-3336
- 67 Wang, Y.; El-Boubou, K.; Kouyoumdjian, H.; Huang, X.; Zeng, X. Lipoic acid glyco-conjugates, a new class of agents for controlling nonspecific adsorption of blood serum at biointerfaces for biosensor and biomedical applications. *Langmuir*, **2010**, *26*, 4119–4125.
- 68 Dixit, V.; Van den Bossche, J.; Sherman, D. M.; Thompson, D. H.; Andres, R. P., Synthesis and Grafting of Thioctic Acid–PEG–Folate Conjugates onto Au Nanoparticles for Selective Targeting of Folate Receptor-Positive Tumor Cells. *Bioconjugate Chemistry*, **2006**, *17*, 603-609

- 69 Abdelghani-Jacquin, C.; Abdelghani, A.; Chmel, G.; Kantlehner, M.; Sackmann, E., Decorated surfaces by biofunctionalized gold beads: application to cell adhesion studies. *European Biophysics Journal*, **2002**, *31*, 102-110.
- 70 Song, S.-J.; Kim, K. S.; Kim, K. H.; Li, H. J.; Kim, J.-H.; Jeong, M. H.; Kim, B. H.; Ko, Y. M.; Cho, D. L., Preparation of a biocompatible stent surface by plasma polymerization followed by chemical grafting of drug compounds. *Journal of Materials Chemistry*, **2009**, *19*, 3248-3252.
- 71 Zhang, W. J.; Frei, B. Alpha-lipoic acid inhibits TNF- α -induced NK- $\kappa\beta$ activation and adhesion molecule expression in human aortic endothelial cells. *Federation of American Societies for Experimental Biology Journal* **2001**, *15*, 2423-2432.
- 72 Meng, F.; Hennick, W.; Zhong, Z. Reduction-sensitive polymers and bioconjugates for biomedical applications. *Biomaterials*, **2009**, *30*, 2180–2198
- 73 Saito, G.; Swanson, J.A.; Lee, K.-D. Drug delivery strategy utilizing conjugation via reversible disulfide linkages: role and site of cellular reducing activities. *Advanced Drug Delivery Reviews*, **2003**, *55*, 199-215.
- 74 Li, Y.-L.; Zhu, L.; Liu, Z.; Cheng, R.; Meng, F.; Cui, J.-H.; Ji, S.-J.; Zhong, Z., Reversibly Stabilized Multifunctional Dextran Nanoparticles Efficiently Deliver Doxorubicin into the Nuclei of Cancer Cells. *Angewandte Chemie Int'l Ed.* **2009**, *48*, 9914-9918.
- 75 Dodrer, N.; Regen, S. L., Polymerized liposomes designed to probe and exploit ligand-receptor recognition at the supramolecular level. *Journal of the American Chemical Society*, **1990**, *112*, 2829-2830
- 76 Balakirev, M.; Schoehn, G.; Chroboczek, J., Lipoic acid-derived amphiphiles for redox-controlled DNA delivery. *Chemistry and Biology* **2000**, *7*, 813-819.
- 77 Reed, L. J.; Niu, C.-I. Syntheses of DL- α -lipoic acid. *Journal of the American Chemical Society*. **1955**, *77*, 416-419.
- 78 Thomas, R.C.; Reed, L.J. Disulfide polymers of DL- α -lipoic acid. *Journal of the American Chemical Society*. **1956**, *78*, 6148-6149.
- 79 Nambu, Y.; Endo, T.; Okawara, M., Ring opening polycondensation of lipoic acid with tributylphosphine. *Die Makromolekulare Chemie, Rapid Communications*, **1980**, *1*, 603-607

- 80 Kobayashi, S.; Chow, T. Y.; Saegusa, T. Spontaneous alternating copolymerization of six-membered cyclic phosphonites with lipoic acid. *Polymer Bulletin*, **1983**, 9, 588-592.
- 81 Endo, K.; Yamanaka, T. Copolymerization of lipoic acid with 1,2-dithiane and characterization of the copolymer as an interlocked cyclic polymer. *Macromolecules*, **2006**, 39, 4038-4043
- 82 Yamanaka, T.; Endo, K., Network formation of interlocked copolymer obtained from copolymerization of 1,2-dithiane and lipoic acid by metal salt. *Polymer Journal* **2007**, 39, 1360-1364.
- 83 Kisanuki, A.; Kimpara, Y.; Oikado, Y.; Kado, N.; Matsumoto, M.; Endo, K., Ring-opening polymerization of lipoic acid and characterization of the polymer. *Journal of Polymer Science Part A: Polymer Chemistry*, **2010**, 48, 5247-5253.
- 84 Ikuta, N.; Sugiyama, H.; Shimosegawa, H.; Nakane, R.; Ishida, Y.; Uekaji, Y.; Nakata, D.; Pallauf, K.; Rimbach, G.; Terao, K.; Matsugo, S., Analysis of the enhanced stability of R(+)-alpha lipoic acid by the complex formation with dycloextrins. *International Journal of Molecular Sciences* **2013**, 14, 3639-3655.
- 85 Puskas, J.E.; Rosenthal, E.Q. *New Method for the Synthesis of Poly(Disulfide) Polymers and Gels*. US Patent 8,552,143. **2013**
- 86 Rosenthal, E. Q., Puskas, J.E.; Wesdemiotis, C. Green polymer chemistry: Living dithiol polymerization via cyclic intermediates. *Biomacromolecules*, **2011**, 131, 154-164.
- 87 Bevington, P.R.; Robinson, D. K. Data Reduction and Error Analysis for the Physical Sciences, 3rd ed. McGraw-Hill:Boston. **2003**.
- 88 Patiny, L.; Borel, A., ChemCalc: A Building Block for Tomorrow's Chemical Infrastructure. *Journal of Chemical Information and Modeling* **2013**, 53, 1223-1228.
- 89 Wyatt Technologies. "Molecular conformation" Online October 18 2013
<http://www.wyatt.com/products/software/molecular-conformation.html>
- 90 Brown, S.; Szamel, G. Structure and dynamics of ring polymer. *Journal of Chemical Physics*, **1998**, 108, 4705-4714.

- 91 Fu, C.; Ouyang, W.; Sun, Z.; An, L., Influence of molecular topology on the static and dynamic properties of single polymer chain in solution. *Journal of Chemical Physics*, **2007**, *127*, 44903.
- 92 Brink, K.S.; Yang, P.J.; Temenoff, J.S. Degradative properties and cytocompatibility of a mixed-mode hydrogel containing oligo[poly(ethylene glycol)fumarate] and poly(ethylene glycol)dithiol. *Acta Biomaterialia*, **2009**, *5*, 570-579.
- 93 Thioplastics. *The Infrared Spectra Atlas of Monomers and Polymers*, Philadelphia,PA: Sadtler Research Laboratories, **1980**, 262-266.
- 94 Silverstein, R.M.; Webster, F.X.; Kiemle, D.J. Spectrometric Identification of Organic Compounds, 7th Ed. Hoboken, NJ: John Wiley & Sons, Inc., **2005**.
- 95 Shaw, J.E.; Oxidation dimercaptans to organic disulfide polymers. US Pat 5464931. Philips Petroleum Company. November 7, 1995.
- 96 Bertozzi, E. R.. Davis. F. O.; Fettes, F. M.; Disulfide interchange in polysulfide polymers. *Journal of Polymer Science* **1956**, *19*, 17-27.
- 97 Bevington, P.R.; Robinson, D. K. Data Reduction and Error Analysis for the Physical Sciences, 3rd ed. McGraw-Hill:Boston. **2003**.

APPENDICES

APPENDIX A

THIOKOL MONOMERS

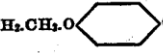
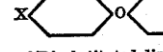
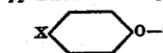
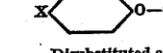
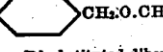
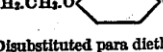
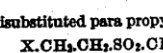
A list of the many monomers polymerized and copolymerized is shown if the figure below which was taken directly from US Patent 2,363,614 issued in 1944 to J.C. Patrick of the Thiokol Corporation.

Figure A1.1. List of monomers polymerized at Thiokol.

polymer, per se, possesses hardness and brittleness.

B. Compounds producing the extensible (R'S₂) type of polymer.—Any of the compounds listed in Tables VII, VIII and IX below can be substituted for the BB' disubstituted ethyl ether of Example 7 above.

TABLE VII

CH ₂ .CHX.O.CHX ₂ .CH ₂ .	10	CH ₂ .O.CH.CH ₂ .O.CH ₂ .CH ₂ .O.CH ₂ .CH ₂ .O.CH ₂ .
AA' disubstituted ethyl ether		X X ₁
X.C ₂ H ₄ .O.C ₂ H ₄ .X ₁ .		Disubstituted dimethoxy tetra ethylene glycol
BB' disubstituted ethyl ether	5	CH ₂ .CH ₂ .CH ₂ .O.CH ₂ .CH ₂ .CH ₂ .
X.CH ₂ .O.CH ₂ .X ₁ .	15	X X ₁
Disubstituted methyl ether		AA' disubstituted propyl ether
X.C ₂ H ₄ .O.C ₂ H ₄ .O.C ₂ H ₄ .X ₁ .		CH ₂ .CH ₂ .CH ₂ .O.CH ₂ .CH ₂ .CH ₂ .
Disubstituted ethoxy ethyl ether		X X ₁
X.C ₂ H ₄ .S.C ₂ H ₄ .X ₁ .	20	Gamma gamma disubstituted propyl ether
Disubstituted thio ethyl ether		CH ₂ .CH ₂ .CH ₂ .O.CH ₂ .CH ₂ .CH ₂ .
X.CH ₂ .S.CH ₂ .X ₁ .		X X ₁
Disubstituted thio methyl ether		BB' disubstituted propyl ether
X.CH ₂ .O.CH ₂ .C.CH ₂ .O.CH ₂ .X ₁ .	25	CH ₂ .CH ₂ .CH ₂ .O.CH ₂ .CH ₂ .CH ₂ .
Disubstituted 1,3 methoxy, 2,2 dimethyl propane		X X ₁
X.CH ₂ .CH ₂ .CH ₂ .O.CH ₂ .O.CH ₂ .CH ₂ .X ₁ .	30	Alpha beta disubstituted propyl ether
Disubstituted dipropyl formal		CH ₂ .CH ₂ .CH ₂ .O.CH ₂ .CH ₂ .CH ₂ .
X.CH ₂ .CH ₂ .O.CH ₂ .O.CH ₂ .CH ₂ .X ₁ .		X X ₁
Disubstituted diethyl formal		Alpha gamma disubstituted propyl ether
X.CH ₂ .O.CH ₂ .CH ₂ .O.CH ₂ .	35	CH ₂ .CH ₂ .CH ₂ .CH ₂ .O.CH ₂ .CH ₂ .CH ₂ .
Disubstituted dimethoxy ethane		X X ₁
X.CH ₂ .CH ₂ .O  O.CH ₂ .CH ₂ .X ₁ .	40	Alpha alpha disubstituted butyl ether
Disubstituted para diethoxy benzene		CH ₂ .CH ₂ .CH ₂ .O.CH ₂ .CH ₂ .CH ₂ .
X.CH ₂ .O.CH ₂ .CH ₂ .O.CH ₂ .X ₁ .	45	X X ₁
Disubstituted dimethoxy ethane		Beta beta disubstituted butyl ether
X.CH ₂ .CH ₂ .CH ₂ .S.CH ₂ .CH ₂ .CH ₂ .X ₁ .		CH ₂ .CH ₂ .CH ₂ .CH ₂ .O.CH ₂ .CH ₂ .CH ₂ .
Disubstituted dipropyl thio ether		X X ₁
X  O  X ₁ .	50	Gamma gamma disubstituted butyl ether
pp' Disubstituted diphenyl ether		CH ₂ .CH ₂ .CH ₂ .CH ₂ .O.CH ₂ .CH ₂ .CH ₂ .
X  O-CH ₂ X ₁ .	55	X X ₁
Disubstituted anisole		Delta delta disubstituted butyl ether
X  CH ₂ .O.CH ₂  X ₁ .	60	X.CH ₂ .CH=CH  CH ₂ .X ₁ .
Disubstituted dibenzyl ether		Disubstituted 3 tolyl propene 2
X  O 	65	X.CH ₂ .CH=CH.CH ₂ .CH ₂ .X ₁ .
aa' Disubstituted diphenyl eth		Disubstituted pentene 2
X  CH ₂ .O.CH ₂  CH ₂ .X ₁ .	70	X.CH ₂ .CH=CH.CH ₂ .CH ₂ .X ₁ .
Disubstituted para propyl dibenzyl ether		Disubstituted hexene 2
X.CH ₂ .CH ₂ .SO ₂ .CH ₂ .CH ₂ .X ₁ .		X.CH ₂ .CH ₂ .CH=CH.CH ₂ .CH ₂ .X ₁ .
Disubstituted diethyl sulphone		1,7 disubstituted heptene 3
X.CH ₂ .CH ₂ .CH ₂ .SO ₂ .CH ₂ .CH ₂ .CH ₂ .X ₁ .		X.CH ₂ .CH ₂ .CH=CH.CH ₂ .CH ₂ .X ₁ .
Disubstituted dipropyl sulphone		1,6 disubstituted hexene 3
		H ₂ C.CH=CH.CH ₂ .CH ₂ .
		X X ₁
		1,4 disubstituted pentene 2
		H ₂ C.CH ₂ .CH=CH.CH ₂ .CH ₂ .
		X X ₁
		1,6 disubstituted heptene 3

65 All of the above compounds have two carbon atoms separated by and joined to intervening structure characterized by ether linkage or the grouping



and all of these compounds produce polymers which, per se, have not only elasticity but also elongation as an outstanding characteristic thereof. Such properties can, for the purposes of

APPENDIX B

MEASUREMENT OF DN/DC FOR POLY(DODT) IN THF

Dilute solutions of sample 10-120-55 were prepared. The concentration of each solution is shown in Table A.2.1.

Table A.2.1. Concentration of each sample used in dn/dc measurement
($\rho_{\text{THF}} = 0.8892 \text{ g/mL}$)

Solution	Flask (g)	+ Sample (g)	Sample (g)	+ THF (g)	Vol. THF (mL)	Conc. (mg/mL)
1	21.2314	21.2641	---	43.2351	24.7087	1.3234
2	20.3572	29.4356	0.0135	42.8220	25.2641	0.5348
3	14.0788	15.8297	0.0026	22.7415	9.7421	0.2675
4	13.8468	14.7990	0.0014	22.5392	9.7755	0.1450
5	13.5337	14.3828	0.0005	22.3231	9.8846	0.0517

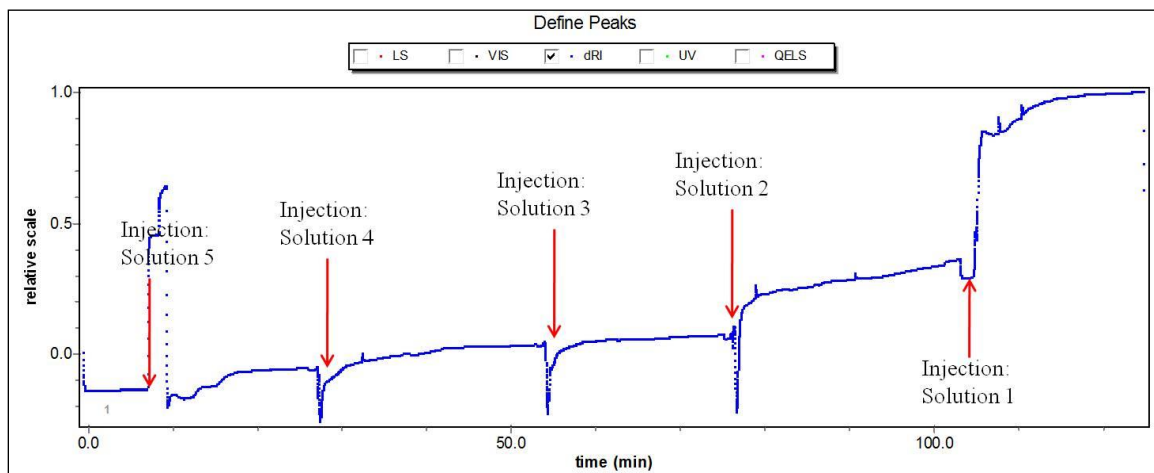


Figure A.2.1. Signal from RI detector plotted with time.

Starting with the least concentrated sample, the samples were injected in the detector using a syringe pump. The RI detector was allowed to stabilize, and take static measurements for about 10 minutes for each sample. There was an increasing signal drift in all samples and the median of the signal plateau was calculated.

Table A2.2. Voltage readings from each polymer solution and baseline

Solution	Start	End	Median	% Variance
0	---	---	-0.0085	
1	0.0490	0.0540	0.0515	9.71
2	0.1130	0.1180	0.1155	4.33
3	0.1450	0.1511	0.1481	4.12
4	0.3100	0.3440	0.3270	10.40
5	0.8180	0.8243	0.8212	0.77

$$C = \frac{dn}{dc} \cdot \frac{dc}{dV} = \frac{dn}{dV} = \frac{n_{solution} - n_{solvent}}{V_{solution} - V_{baseline}} \quad [A1]$$

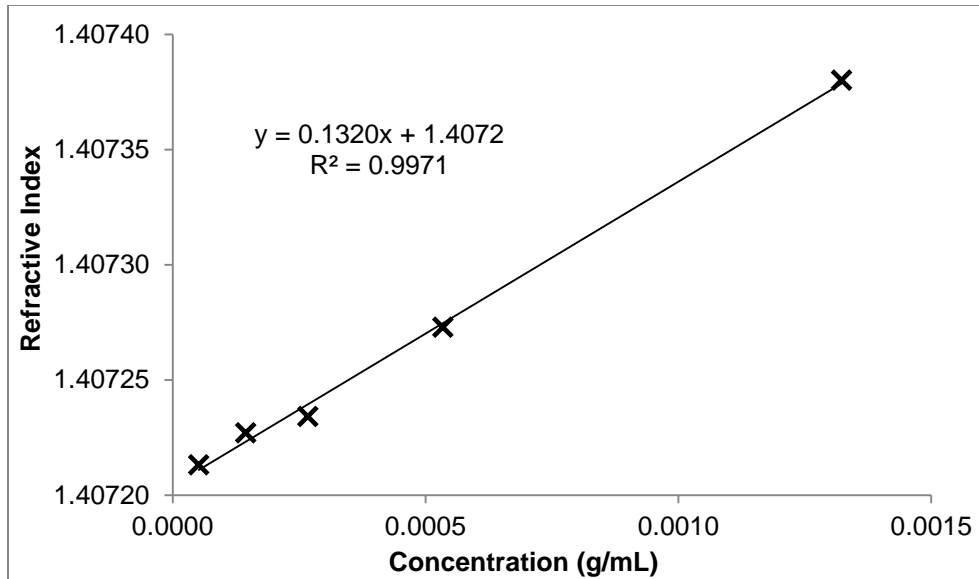


Figure A2.2. Plot of Equation A1 using RI voltage readings.

From the median voltage readings, the known calibration constant of the instrument and the literature value for the refractive index of THF, the dn/dc value of the polymer was determined by plotting Equation A1. The calibration constant (C) of the instrument was calculated previously using a sodium chloride solution and is 2.1701×10^{-4} and the refractive index of THF is 1.4072 (from Aldrich). Using the experimental values for $V_{solution}$ and $V_{baseline}$, we are able to calculate the refractive index of the solution ($n_{solution}$). The values are then plotted against concentration. The slope of the resulting line is the refractive index of the polymer in THF.

APPENDIX C

AFM IMAGES OF POLY(α -LA-PEG) and POLY(α -LA-PEG-*co*- α -LA)

An α -LA-PEG macromonomer was synthesized (described in Section 4.5.2.4.2) from the esterification of α -LA and 2,000 g/mol PEG. The macromonomer was then heated under vacuum to make a polymer from the opening of the thiolane ring. The polymer product was then sent to Polyinsight for AFM imaging. A dilute solution of the polymer in chloroform was spun cast onto mica chips and imaged using AFM. An AFM image of the polymer is shown in Figure A3.1. The high PEG content of the polymers lead to the adsorption of atmospheric water leading to fuzzy images. Linear and round structures with widths of approximately 40 nm are seen.

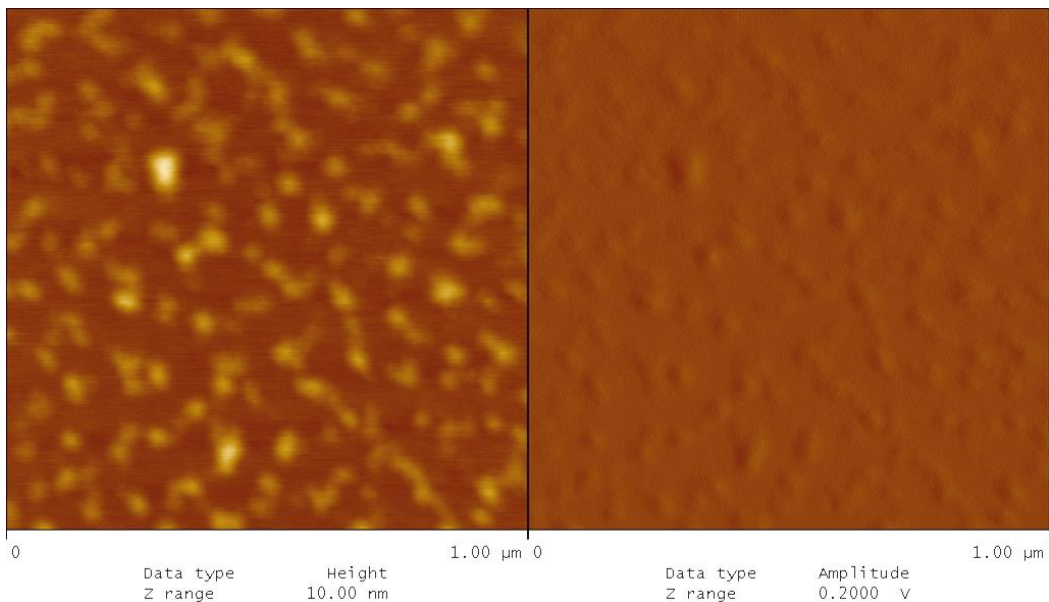


Figure A3.1. AFM images of dilute solution of poly(α -LA-PEG) spun cast onto mica and imaged in tapping mode.

The α -LA-PEG macromonomer was copolymerized with α -LA by heating under vacuum to make a copolymer from the opening of the thiolane ring. The polymer product was then sent to Polyinsight for AFM imaging. A dilute solution of the polymer in chloroform was spun cast onto mica chips and imaged using AFM. An AFM image of the polymer is shown in Figure A3.2. Again, the high PEG content of the polymers lead to the adsorption of atmospheric water leading to fuzzy images. Here, linear structures are generally longer (200 nm) than those seen in the homopolymer, however the approximate width of the structures 40 nm is the same.

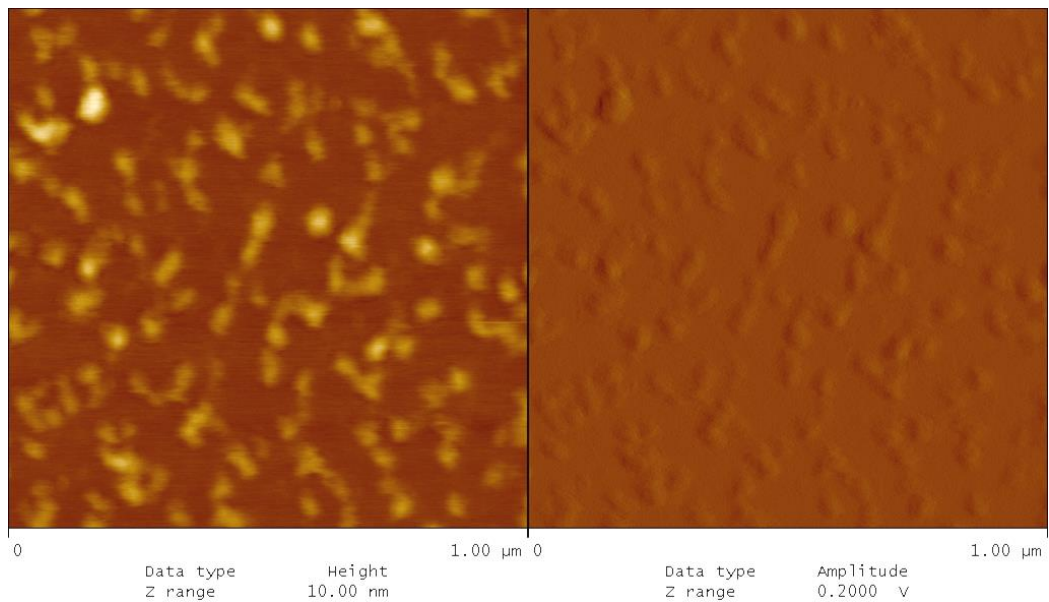


Figure A3.2. AFM images of dilute solution of poly(α -LA-PEG-co- α -LA) spun cast onto mica and imaged in tapping mode.